



Natural Resources
Canada

Ressources naturelles
Canada



EARTH SCIENCES SECTOR
GENERAL INFORMATION PRODUCT 61

**Consequences of climatic changes on
contamination of drinking water by nitrate
on Prince Edward Island**

Savard, M M; Somers, G

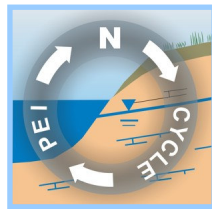
2007

Originally released as: Consequences of climatic changes on contamination of drinking water by nitrate on Prince Edward Island, Savard, M M (ed.); Somers, G (ed.); 2007; 142 pages (ESS Cont.# 20060676)

©Her Majesty the Queen in Right of Canada 2007

Canada

“Consequences of climatic changes on contamination of drinking water by nitrate on Prince Edward Island”



Report Prepared by

Martine M. Savard, George Somers, Daniel Paradis, Eric van Bochove, Harold Vigneault, René Lefebvre, Georges Thériault, Reinder De Jong, Yefang Jiang, Budong Qiang, Jean-Marc Ballard, Rim Cherif, Noura Ziadi, John MacLeod, Odile Pantako, Jingyi Y. Yang

Edited by Martine M. Savard & George Somers

**EARTH SCIENCE SECTOR
GEOLOGICAL SURVEY OF CANADA**



and



Agriculture and Agri-Food Canada Agriculture et Agroalimentaire Canada



Environment, Energy and Forestry

**Presented March 20, 2007
to**

**NATURAL RESOURCES CANADA
CLIMATE CHANGE ACTION FUND: IMPACTS & ADAPTATION
Contribution Agreement A881/A843**



**Natural Resources
Canada**

**Ressources naturelles
Canada**

**Geological Survey
of Canada**

**Commission géologique
du Canada**

Contributing authors

Natural Resources Canada

Martine. M. Savard* & Daniel. Paradis

Geological Survey of Canada, 490 de la Couronne, Québec, QC, G1K 9A9, Canada

Agriculture and Agri-Food Canada

Eric van Bochove, Georges Thériault, Rim Cherif & Noura Ziadi

2560 Bld Hochelaga, Québec (Sainte-Foy), QC, G1V 2J3, Canada

Reinder De Jong & Budong Qiang

Eastern Cereal and Oilseed Research Centre, 960 Carling Ave., Ottawa, ON, K1A 0C6, Canada

John MacLeod

440 University Ave, Charlottetown, PEI, C1A 4N6, Canada

Jingyi Y. Yang

Greenhouse & Processing Crops Research Centre, 2585 County Rd 20, Harrow, ON, Canada, N0R 1G0, Canada

Institut national de la recherche scientifique - Eau, Terre et Environnement

Harold Vigneault, Jean-Marc Ballard, René Lefebvre & Odile Pantako

490 de la Couronne, Québec, QC G1K 9A9, Canada

Prince-Edward Island Department of Environment, Energy & Forestry

George Somers* & Yefang Jiang

11 Kent St., C.P. 2000, Charlottetown, PEI, C1A 7N8, Canada

*** Corresponding authors:**

msavard@nrcan.gc.ca

Ghsomers@gov.pe.ca

Executive Summary

Prince Edward Island land use, water supply infrastructure and water management policies have all evolved under historical assumptions regarding sustainability. With the recent focus on climate change and the great reliance the Province places on groundwater, these areas are re-evaluated, with particular emphasis on nitrate contamination of groundwater resources. A team sharing expertise in agriculture, geology, geochemistry, hydrogeology and numerical modelling has studied the specific impacts of climate change on groundwater. The study integrates a watershed scale investigation of the nitrogen export from agricultural soils to groundwater under current and potential future practices. At the Provincial scale, modelling predicts the potential nitrate levels which would result from various climate change and some associated agricultural adaptation scenarios.

At the watershed scale, characterization of N inputs and geochemical modelling confirm the important contribution of agricultural N inputs, especially chemical fertilizers, on groundwater nitrate concentrations. Moreover, significant seasonal differences in the main N sources and fluxes include the products of year-round nitrification. This change in main seasonal sources has important implications for the development of remedial measures. Leaching of chemical fertilizers from soils to the aquifer dominates the summer N fluxes, whereas the release of N by nitrification of plant residual material dominates during winter. It appears that winter contributes a significant part of the annual total N load. Numerical modelling using two independent approaches predicts continued increases in groundwater nitrate concentrations under current land use practices. This modelling also suggests that substantial reductions in N inputs to the aquifer will be necessary if the regulatory authorities want to reverse the current trend and reduce groundwater nitrate contents to more acceptable levels. Modelling on an Island-wide scale of future agriculture and climate shows that climate change alone is unlikely to effect groundwater nitrate levels. However, the effects of one potential adaptation scenario by the agricultural sector to climate change could result in significant increases in groundwater nitrate, an average increase of 11% for the province as a whole, and an increase ranging from 5% to 30% for individual watersheds.

An examination of current water supply infrastructure shows that the brunt of groundwater nitrate cost has fallen on the shoulders of domestic well owners, through the replacement of wells or installation of water treatment devices. Increases in the number of wells with excessive nitrate levels will only add to this burden. To date, only a few municipal supplies have been adversely affected by elevated nitrate levels, with relatively modest cost implications, as alternate water sources have been available. Should treatment of municipal water become necessary, the costs of producing water for distribution could as much as double.

Key recommendations based on these research activities are: (1) to develop effective strategies aimed at reduction of N leaching to groundwater which need to focus not solely on optimizing fertilizer application rates but also on management of residual plant material; (2) to maintain current monitoring activities and assess N transfer processes from agricultural soils to groundwater in various watershed settings; and (3) to accelerate actions on a comprehensive, ecosystem based, strategic plans for the sustainable development of the agricultural sector with respect to water resources. The way PEI addresses the current situation and adapts to climate change will determine the sustainability of the Province's groundwater resources.

Sommaire exécutif

L'histoire récente de l'Île-du-Prince-Édouard montre que l'aménagement du territoire, l'infrastructure d'approvisionnement en eau et les politiques de gestion de l'eau ont évolué sur la base de présomptions en ce qui a trait à la durabilité de la ressource en eau. Vu l'intérêt récent pour le changement climatique et la grande dépendance de la province pour l'eau souterraine, ces aspects sont réexaminés en mettant l'accent sur l'enjeu critique de la contamination en nitrate des ressources en eau souterraine. Une équipe composée d'experts en agriculture, géochimie, géologie, hydrogéologie et modélisation numérique a étudié les impacts spécifiques des pratiques actuelles et du changement climatique sur l'eau souterraine. Cette large initiative intègre une investigation à l'échelle du bassin-versant du transfert de l'azote des sols vers l'eau souterraine, en considérant les pratiques actuelles et d'éventuelles pratiques pour le futur. À l'échelle de la province, une étude modélise les concentrations potentielles de nitrate qui seraient produites suivant diverses conditions climatiques et des scénarios d'adaptation des pratiques agricoles qui leurs seraient associés.

À l'échelle du bassin-versant, la caractérisation de l'afflux en azote et la modélisation géochimique de celui-ci confirment l'importance de l'apport agricole aux teneurs totales en nitrate de l'eau souterraine, particulièrement sous forme de fertilisants chimiques. De plus, les sources principales d'azote et ses flux diffèrent significativement d'une saison à l'autre et les charges répertoriées incluent les produits d'une nitrification effective tout au cours de l'année. Le changement de sources dominantes en cours d'année a d'importantes implications pour le développement de mesures correctives concernant les excès en nitrate. La perte des sols en nitrate dérivé des engrais chimiques domine la charge de l'aquifère de la saison estivale, alors que le nitrate provenant de la dégradation de résidus de plantes domine la charge hivernale. Il apparaît que le produit hivernal de la nitrification constitue une part significative de la charge annuelle de nitrate. La modélisation numérique par deux approches indépendantes prédit une augmentation continue du contenu en nitrate des eaux souterraines en considérant l'utilisation actuelle du territoire. La modélisation suggère que des réductions substantielles du transfert d'azote vers l'aquifère seraient nécessaires si les groupes à vocation réglementaire souhaitent renverser l'actuelle tendance à la hausse des teneurs en nitrate des eaux souterraines et réduire ces teneurs à des valeurs non critiques. À l'échelle de la province, la modélisation des modifications anticipées de pratiques agricoles combinées au changement climatique montre que le futur climat à lui seul aura très peu d'effet sur le contenu en nitrate des eaux. Cependant, les effets possibles d'un scénario d'adaptation du secteur agricole au changement climatique pourraient entraîner une hausse substantielle des concentrations provinciales moyennes en nitrate de 11%, et des augmentations individuelles de 5 à 30% pour les bassins versants.

L'examen des infrastructures d'approvisionnement en eau révèle que le poids financier généré par les excès en nitrate est encouru en grande partie par les propriétaires de puits domestiques, de par l'obligation de forer de nouveaux puits ou d'acquérir des systèmes de traitement. Des hausses du nombre de puits avec teneurs élevées en nitrate ne feraient qu'accroître ces coûts. Jusqu'à maintenant, seules quelques infrastructures municipales ont été affectées par des teneurs excessives en nitrate; les implications monétaires dans ce cas ont été modestes puisque des sources d'eau alternatives étaient disponibles. S'il advenait que le traitement des eaux

municipales soit nécessaire, les coûts d'approvisionnement en eau potable de la province pourraient doubler.

Les recommandations découlant de ces diverses activités de recherche incluent : (1) de développer des stratégies efficaces visant à réduire le transfert de nitrate des sols vers les eaux souterraines, ces stratégies devraient cibler non seulement l'optimisation du taux d'application des fertilisants chimiques mais aussi la gestion des résidus de plantes; (2) de poursuivre les activités de surveillance de la qualité des eaux et de caractériser les processus de transfert de l'azote des sols agricoles vers l'eau souterraine dans des types variés de bassin-versants; et (3) d'accélérer la mise-en-oeuvre de stratégies intégrées, basées sur les écosystèmes, pour le développement durable du secteur agricole en regard aux ressources en eau. La durabilité des ressources en eau de l'Île-du-Prince-Edouard dépend entièrement de la manière dont les preneurs de décisions aborderont la situation actuelle et de l'adaptation du secteur agricole au changement climatique.

Acknowledgements

This multidisciplinary and multi-institutional project addressing the climate change issues at the scale of the PEI province was supported by the Climate Change Impact & Adaptation program (NRCan), whereas the pilot investigation of the Wilmot watershed was also supported by the groundwater program of the Earth Science Sector (NRCan), and the GAPS program of AAFC. Crucial logistic support, fieldwork investigation as well as historical data were kindly provided by the Prince Edward Island department of Environment, Energy and Forestry. The authors would like to acknowledge the sustained dynamic participation of Dr. Christine Rivard to group discussions on modelling during the two first years of the CCAI project. The valuable advice and discussions on the adaptation scenario with Drs. Huffman, MacGregor, Junkins, Ileka and Mr. Holmstrom are gratefully acknowledged. Many thanks to Barry Thompson for providing land use data. The entire initiative benefited from constructive discussion with A. Rivera and skilful administrative support of C. Laberge, F. Bolduc, A. Desbarats, B. Lavender, G. Laplante and S. Chalifoux.

We sincerely thank scientists, technicians and students from NRCan, Agriculture and Agri-Food Canada and PEI-EEF: G. Bégin, G. Bordeleau, S. Côté, C. Deblonde, F. Dechmi, I. Destroismaisons, N. Goussard, S. Hill, V. Kirkwood, S. Liao, M. Luzincourt, M.L. McCourt, S. Michaud, B. Murray, J. Mutch, B. Potter, J., A. Smirnoff and J. Zaakar. The authors would also like to acknowledge the assistance of staff from the Cities of Charlottetown and Summerside, the Towns of Stratford and Cornwall, and the Island Regulatory and Appeals Commission in providing data. The complete report benefited from the constructive reviews of Dr. Alfonso Rivera from Natural Resources Canada and Dr. John MacLeod from Agriculture and Agri-Food Canada. GSC contribution number: 20060676.

Table of contents

Executive Summary	3
Sommaire exécutif.....	4
Acknowledgements	6
Table of contents	7
Detailed table of contents.....	8
List of figures	11
List of tables	13
1 Purposes and approach of the research project on climate change impacts on nitrate contamination of Prince Edward Island groundwater	14
2 Nitrogen Leaching from agricultural soils at the watershed scale	21
3 Sources and seasonal dynamics of Nitrate in the Wilmot watershed/aquifer system of Prince Edward Island.....	29
4 Numerical Modelling of Nitrate Transport in the Wilmot Watershed Using Field Specific N-inputs	41
5 Watershed-scale numerical modelling of nitrate transport using spatially uniform averaged N inputs	52
6 Modelling four Climate Change scenarios for Prince Edward Island.....	66
7 Modelling of Nitrogen leaching in Prince Edward Island under Climate Change scenarios.....	76
8 Numerical modelling of the evolution of groundwater nitrate concentrations under various Climate Change scenarios and agricultural practices for Prince Edward Island.....	93
9 Impacts of Climate Change on the water supply infrastructure in Prince Edward Island	110
10 General implications of Climate Change on contamination of groundwater by nitrate on Prince Edward Island	121
11 References	128
ANNEX – Map of sample location for the nitrate characterization and Tables of analytical results.	140

Detailed table of contents

Executive Summary	3
Sommaire exécutif.....	4
Acknowledgements	6
Table of contents	7
Detailed table of contents	8
List of figures	11
List of tables	13
1 Purposes and approach of the research project on climate change impacts on nitrate contamination of Prince Edward Island groundwater	14
1.1. Introduction	14
1.2. The Nitrogen cycle	14
1.3. The nitrate problem in Prince Edward Island and potential climate change impacts	16
1.3.1. Prince Edward Island context.....	16
1.3.2. Potential effects of climate change.....	18
1.3.3. Present water supply infrastructure and agricultural practices.....	18
1.4. Purpose of the research	18
1.5. Methodology	19
1.6. Concluding comments.....	20
2 Nitrogen Leaching from agricultural soils at the watershed scale	21
2.1 Introduction	21
2.2 Methodology	22
2.2.1 Characterization of the study areas	22
2.2.2 Soil N flux estimation	23
2.2.3 Percolation water sampling and analysis	24
2.2.4 Soil N transformation	24
2.3 Results and discussion.....	25
2.3.1 Available soil N at the watershed scale.....	25
2.3.2 N in drainage water at Harrington experimental farm	26
2.3.3 Soil N.....	27
2.4 Conclusions	28
3 Sources and seasonal dynamics of Nitrate in the Wilmot watershed/aquifer system of Prince Edward Island.....	29
3.1 Introduction	29
3.2 Sampling and analytical methods.....	30
3.3 Results	31
3.4 Interpretation and Discussion.....	33
3.4.1 Seasonality of nitrate loads transferred to GW	33
3.4.2 Sources of nitrate in the Wilmot aquifer	35
3.5 Conclusions	39

4	Numerical Modelling of Nitrate Transport in the Wilmot Watershed Using Field Specific N-inputs	41
4.1	Introduction	41
4.2	Hydrogeology of the Wilmot River watershed	41
4.3	Groundwater flow modelling	43
4.4	Nitrate transport modelling	46
4.5	Conclusions	51
5	Watershed-scale numerical modelling of nitrate transport using spatially uniform averaged N inputs	52
5.1	Introduction	52
5.2	Conceptual Model of the Groundwater Flow System	53
5.2.1	Regional context	53
5.2.2	Hydrogeology	54
5.2.3	Groundwater and Wilmot River Interaction	56
5.3	Numerical Modelling of Groundwater Flow and Nitrate Transport	56
5.3.1	Aquifer discretization	57
5.3.2	Hydrogeological Parameters	57
5.3.3	Boundary conditions	58
5.3.4	Recharge	58
5.3.5	Soil nitrogen available for leaching	58
5.3.6	Fractured porous media mass transport	60
5.4	Assessment of the impact of agricultural practices	61
5.5	Conclusion	64
6	Modelling four Climate Change scenarios for Prince Edward Island	66
6.1	Introduction	66
6.2	Data and Methodology	67
6.2.1	Data bases – sources of weather data	67
6.2.2	Stochastic weather generation	68
6.3	Development of daily climate scenarios	69
6.4	Projected changes in future climate scenarios	70
6.5	Summary	74
7	Modelling of Nitrogen leaching in Prince Edward Island under Climate Change scenarios	76
7.1	Introduction	76
7.2	Methodology	77
7.2.1	Residual Soil Nitrogen (RSN)	78
7.2.2	Water balance calculations and nitrogen leaching	79
7.2.3	Input data	81
7.2.4	Simulation runs	82
7.3	Results and discussion	83
7.3.1	Baseline (1971 - 2000) scenario	83
7.3.2	Climate change (2040 - 2069) scenarios	84
7.3.3	Climate change coupled with agricultural management change	88
7.4	Conclusion	92
8	Numerical modelling of the evolution of groundwater nitrate concentrations under various Climate Change scenarios and agricultural practices for Prince Edward Island	93
8.1	Introduction	93
8.2	Conditions representative of Prince Edward Island	94

8.2.1	Land use	94
8.2.2	Climate and hydrology	96
8.2.3	Hydrogeology	97
8.2.4	Climate change scenarios	98
8.2.5	Residual Soil Nitrogen	99
8.3	Model description and calibration	99
8.3.1	HELP model	100
8.3.2	FEFLOW model	100
8.4	Assessment of the impact of climatic changes (CC) and agricultural practice changes (APC)	106
8.4.1	CC impact assessment	106
8.4.2	APC impact assessment	107
8.5	Conclusion	109
9	Impacts of Climate Change on the water supply infrastructure in Prince Edward Island	110
9.1	Introduction	110
9.2	Water supply infrastructure in PEI	111
9.2.1	Current Infrastructure	111
9.2.2	Water Use	112
9.3	Value of water supply infrastructure	115
9.3.1	Value of the current water supply infrastructure	115
9.3.2	Cost implications of elevated nitrate levels	116
9.4	Discussion	117
9.5	Conclusion	120
10	General implications of Climate Change on contamination of groundwater by nitrate on Prince Edward Island	121
10.1	Introduction	121
10.2	Principle factors to consider in relation to the N cycle at the watershed scale	122
10.3	Main aspects to consider in relation to climate change and its impacts on the N cycle at the Island scale	124
10.4	Conclusions & Recommendations	126
11	References	128
ANNEX – Map of sample location for the nitrate characterization and Tables of analytical results.		140

List of figures

Figure 1.1. - Conceptual diagram of the nitrogen cycle adapted to the context of Prince Edward Island and Wilmot watershed.....	16
Figure 1.2. - Mean nitrate concentrations for the main watershed of Prince Edward Island arranged in four compositional groups	17
Figure 2.1. - Conceptual model inputs and outputs to estimate the potentially available soil N for leaching from forested and cropped lands of Wilmot watershed	24
Figure 2.2. - Nitrate and ammonium activities from IEM buried in soils receiving four different fertilization treatments	27
Figure 3.1. - Map showing the location (a) and outline (b) of the Wilmot river watershed as well as the distribution of the sampling sites.	31
Figure 3.2. - Seasonal results obtained for the Nitrogen and Oxygen isotopes of nitrate dissolved in GW from private wells	32
Figure 3.3. - Average per season of isotopic results obtained for GW collected from private wells of the Wilmot watershed compared with isotopic fields for potential sources of nitrate.....	33
Figure 3.4. - (a) Daily average of seasonal N-NO ₃ ⁻ transfer from.....	34
Figure 3.5. - Source apportionment of nitrate per season for the Wilmot aquifer.....	37
Figure 3.6. - Source apportionment ranges of nitrate for summer (a) and winter (b) in the Wilmot watershed	40
Figure 4.1. - Model domain for ModFlow simulations – Wilmot Watershed, showing location of transect A-A’	43
Figure 4.2. - Vertical discretization and boundary conditions for ModFlow simulations - Wilmot watershed	44
Figure 4.3. - Comparison of separated and simulated base flows at the Wilmot River gauging station	45
Figure 4.5. - Simulated concentration (mg/L) contour of NO ₃ -N in groundwater along the Confederation Tail transect, illustrating distribution of nitrate in response to variable N-inputs based on local land use	49
Figure 4.6. - Simulated NO ₃ -N concentrations over time at various aquifer depths.	50
Figure 5.1. - Location of Prince Edward Island and the Wilmot River Watershed.....	53
Figure 5.2. - Conceptual model of the groundwater flow system and discretization of the numerical	55
Figure 5.3. - Historical nitrogen mass applied over the Wilmot River watershed	59
Figure 5.4. - Nitrogen input scenarios and corresponding simulated average nitrate concentrations that would be present in model layers.....	62
Figure 5.5. - Model average nitrate concentrations for scenario #1 in relation to nitrate concentration measured in domestic wells for the period of 2002-2004.....	63
Figure 6.1. - Eleven meteorological stations and 23 Soil Landscape of Canada (SLC) polygons on PEI	69
Figure 6.2. - Historical/current (1971-2000) growing season mean Tmax, Tmin and non-growing season mean Tmax and Tmin	71
Figure 6.3. - Changes in growing season mean Tmax and Tmin for 2040-2069 to the present (1971-2000), projected by CGCM2 A2 and CGCM2 B2	72
Figure 6.4. - Changes in non-growing season mean Tmax and Tmin for 2040-2069 to the present (1971-2000), projected by CGCM2 A2 and CGCM2 B2	73
Figure 6.5. - Historic and 2040-2069 growing season and non-growing season precipitation totals projected by CGCM2 A2 and CGCM2 B2	74
Figure 7.1. - Flow chart of the RSN modeling system.....	78
Figure 7.2. - Simulated nitrogen leaching with historic management and the baseline climate (a) and projected changes with CGCM2 A2 (b), CGCM2 B2 (c), HadCM3 A2 (d) and HadCM3 B2 (e).	86
Figure 7.3. - Probability curves of estimated nitrogen leaching in SLC polygons 535001 and 536013	87
Figure 7.4. - Simulated residual soil nitrogen (300 yr averages) using (a) historic management practices and (b) the adaptation scenario; (c) relative differences between historic management and the adaptation scenario	89
Figure 7.5. - Simulated nitrogen leaching with the adaptation and climate change scenarios	92

Figure 8.1. - Location of Prince Edward Island and distribution of its 48 main watersheds.....	95
Figure 8.2. - Schematic representation of the water balance in PEI and the conceptual model for the numerical simulation.....	98
Figure 8.3. - FEFLOW model for Prince Edward Island with mesh detail showing the eight layers, the triangular surface elements and the boundary conditions.....	101
Figure 8.4. - Evolution of nitrate concentrations applied at the model surface for the Rainer Creek, the Mill River and the Poplar Point River watersheds from 1959 to 2069.....	103
Figure 8.5- Model calibration with the average groundwater nitrate concentrations measured in domestic wells for 2002-2005	104
Figure 8.6. - Class distribution of simulated mean nitrate concentrations per watershed and histogram of the number of watersheds in each class for present day (2001) (a), year 2050 with today's nitrate loading (b), and the four CC scenarios (c, d, e and f).....	104
Figure 8.7. - Class distribution of simulated mean nitrate concentrations per watershed and histogram of the number of watersheds in each class for present day (2001) (a), year 2050 with today's nitrate loading (b), and the four CC scenarios involving APC (c, d, e, f).....	105
Figure 9.1. - The percentage of PEI water use by sector of activities	113
Figure 9.2. - Population trends for selected communities with central water infrastructure	114
Figure 9.3. - Current distribution of nitrate concentrations in domestic wells and distribution predicted under climate change adaptation scenarios: a) Island-wide statistics, b) Wilmot watershed and surrounding area.....	119

List of tables

Table 2.1. - Agriculture and forest areas in Wilmot River watershed (PEI) for a typical 3-year rotation period estimated from Landsat-7 images, and total available soil N by hectare of agricultural and forest land by season estimated from a conceptual model	26
Table 2.2. - Nitrate-N and ammonium-N and total dissolved nitrogen (TDN) concentrations in water samples from agricultural and forest soils of Harrington experimental farm (PEI).....	27
Table 3.1. - Dates of sampling of the 8 seasons of investigation and number of collected samples	31
Table 3.2. - Model conditions for source apportionment and solution to the 3 equations/3 unknowns problem	36
Table 3.3. - Mass balance calculations of main nitrate source contribution to the total load based on agricultural practices in the Wilmot watershed	38
Table 4.1. - Hydraulic properties used in the Wilmot River watershed groundwater model	45
Table 5.1. - Main characteristics of the Wilmot River Watershed	54
Table 5.2. - Weather and water balance for the Wilmot River Watershed.....	54
Table 5.3. - Field-based and calibrated hydraulic properties of the Wilmot River aquifer model	57
Table 5.4. - Estimates of historical Soil Nitrogen Available to Leaching (SNAL) and equivalent nitrogen flux and concentration over the Wilmot Watershed	59
Table 6.1. - Climate normals (1971-2000 means) for 11 PEI stations	67
Table 6.2. - Climate change scenarios for 2040-2069 compared to 1971-2000 means at Charlottetown (PEI).....	70
Table 7.1. - Aggregated crop coefficients (K_{ij}) at the SLC polygon scale for different phenological periods	80
Table 7.2. - Meteorological stations and their associated SLC polygons.....	83
Table 7.3. - Province-wide average components of the nitrogen balance (kg N ha^{-1}) as simulated with historic crop and animal husbandry practices and with an adapted agricultural management scenario	83
Table 7.4. - Province-wide average components of the soil water balance and nitrogen leaching as simulated with baseline climate data and with climate change scenario data, with no changes in crop and animal husbandry practices.....	85
Table 7.5. - Summary of province-wide averages of nitrogen related parameters under different climate and different agricultural management scenarios	90
Table 8.1. - Main characteristics of Prince Edward Island.....	96
Table 8.2. - Weather for the Prince Edward Island	96
Table 8.3. Streamflow characteristics of selected Rivers in Prince Edward Island.....	97
Table 8.4. - Summary of the change in temperature, precipitation, evapotranspiration, runoff and recharge for the historical period and the four CC scenarios for the entire Prince Edward Island	99
Table 8.5. - Field-based and calibrated hydraulic properties of the Prince Edward Island aquifer model	102
Table 8.6. - Classification of nitrate concentrations for each watershed and % change compare to 2001 in mean nitrate concentration for the entire PEI for scenarios 1 to 9	108
Table 9.1. - The Main Characteristics of Wells in the PEI.....	111
Table 9.2. - The Current Water Supply Infrastructure of the main PEI Municipalities	111
Table 9.3. - Estimated Annual Water Use by Sector in PEI.....	113
Table 9.4. - Book Value and Estimated Replacement Costs of Municipal Water Supply Infrastructure	115
Table 9.5. - Estimated overall value of the water supply infrastructure.....	116

1 Purposes and approach of the research project on climate change impacts on nitrate contamination of Prince Edward Island groundwater

Martine M. Savard, George Somers, Reinder De Jong, Daniel Paradis & Eric van Bochove

1.1. Introduction

While Canada has a relative abundance of water, development of the resource has historically occurred under the assumption of essentially un-limited availability. Even now, water management decisions are made on the basis of historical conditions both with respect to quantity and quality. Given the potential impacts of climate change on water availability, it is becoming increasingly important to evaluate the variations in hydrologic conditions that may occur in light of potentially different climatic conditions. Moreover, the adequacy of water supply systems must be evaluated under changing climatic conditions. The majority of the Canadian population (78%) relies on surface water resources (Natural Resources Canada, 2005a), but groundwater (GW) is used by the majority of the rural population. Systems relying on GW have several unique characteristics that set them apart from surface water supplies, with important implications regarding their vulnerability to climate change. In particular, GW systems often have limited storage and water treatment facilities, and may be vulnerable to contaminants not easily removed by the conventional treatment processes used by surface water systems. Moderate to severe seasonal water shortages in many parts of the country have resulted from drought, infrastructure problems and increased water consumption (Environment Canada, 2001), thus some shortages relate directly to climatic influences, while others relate to the status of water supply infrastructure and/or water demand. It is clear from this picture that studies generating timely scientific results that can be used to inform decision makers are required in order for Canada to develop strategies on adaptation to climate change and protection of the water resources.

Prince Edward Island (PEI) residents are 100% dependent on GW for potable uses and for the vast majority of industrial and commercial water uses (Natural Resources Canada, 2005b; Piggott *et al.*, 2001). At the same time, a large part of the provincial economy is based on the intense agricultural activities on the island, posing a potential threat to GW quality. For that reason the Province of PEI represents a priority for the evaluation of the impacts of climate change and is the focus of this multidisciplinary and inter-institutional investigation.

1.2. The Nitrogen cycle

It is perhaps instructive to briefly review the main processes of the Nitrogen (N) cycle to provide a context for the work that follows. Nitrogen moves from atmosphere to biosphere and hydrosphere through organic and inorganic processes (Fig. 1.1). This element is a very important nutrient which is crucial for many animal life processes. It composes parts of both proteins and nucleic acids such as DNA and RNA. In plants, much of N is used in chlorophyll molecules, essential for photosynthesis and further growth.

The atmosphere is the largest nitrogen reservoir on earth (78% as nitrogen gas - N₂), followed by the hydrosphere and the biosphere (sedimentary rocks are excluded as they are part of a much longer cycle). Nitrogen fixation or nitrification combines nitrogen with oxygen to create nitrate (NO₃⁻), the most readily consumable N form to plants. Lightning, industrial processes such as

fertilizer production, bacterial free nitrogen-fixing in soils, as well as bacterial nitrogen-fixation in legume roots all fix N (Mackenzie, 1998). Microbial soil nitrification uses two oxygen from water and one oxygen from air to produce NO_3^- . Later on, plants or animals (which eat plants or animals that have eaten plants) use up nitrate. After being used by plants and animals, nitrogen is disposed of in decay and wastes. Decomposers use the detritus from plants and animals and change N into ammonia (nitrogen with 3 hydrogen atoms - NH_3) which is toxic for plants or animals. Some bacteria in soils can turn ammonia into nitrite (nitrogen with two oxygen - NO_2) whereas some other bacteria change nitrite into nitrate (hand lens, Fig. 1.1). Under low oxygen conditions, microbes can convert nitrate into nitrogen gas through the process of denitrification.

Some plants get nitrogen from the soil by absorption at their roots in the form of either nitrate or ammonium. All nitrogen consumed by animals comes from eating of plants at some stage of the food chain. Nutrient-poor soils can be planted with legumes to enrich them with nitrogen. Agricultural practices can also involve spreading of chemical or organic fertilizers to aid crop growth (Fig. 1.1). A large part of N is taken up by the living forms in the biosphere and can be removed from agricultural regions through harvest. Septic waste, manures and chemical fertilizers constitute the main sources of nitrate in agricultural regions. In these regions, if NO_3^- is in excess of plant requirements in soils, leaching can export this nitrate to aquifers and runoff can transport it to streams. Nitrate can become a contaminant of water if its concentration (N-NO_3^-) is above the natural ambient level, or a pollutant if its concentration exceeds 10 mg/L (see further). Once nitrate is in the hydrosphere, it is bound to reach large water bodies, ultimately the ocean (Fig. 1.1).

Elevated nitrate concentrations in drinking water are of concern because of their links to adverse human health effects and of their role in nutrient loading and eutrophication in ecosystems. In drinking water, the most commonly reported adverse effect is methaemoglobinaemia (blue baby syndrome), affecting bottle fed infants. Various other adverse health effects of elevated nitrate levels have been postulated, including suggestive evidence for an association between gastric cancer and moderate levels of nitrate in drinking water. In consequence, a health based guideline has been established for nitrate at 45 mg/L (10 mg/L $\text{NO}_3\text{-N}$) and this guideline is intended to apply to both children and adults (Health Canada, 1987).

There is also a growing appreciation for the role that the discharge of high nitrate GW (base flow) plays in the transport of N to aquatic ecosystems. A guideline of 2.9 mg/L $\text{NO}_3\text{-N}$ has been established for the protection of freshwater aquatic life, based on toxicity to fish (CCME 2005). In addition the discharge of nitrate through GW contributes to the overall nutrient loading and resulting eutrophication in estuarine environments, where nitrogen is generally cited as being the limiting nutrient (Somers *et al.*, 1999). Considering the very significant base-flow contribution (GW discharge) to total stream flow in the PEI (see Chapter 8), and GW nitrate concentrations typically well in excess of aquatic health guideline values (see further), GW nitrate levels could have real implications for the health of the province's surface water ecosystems.

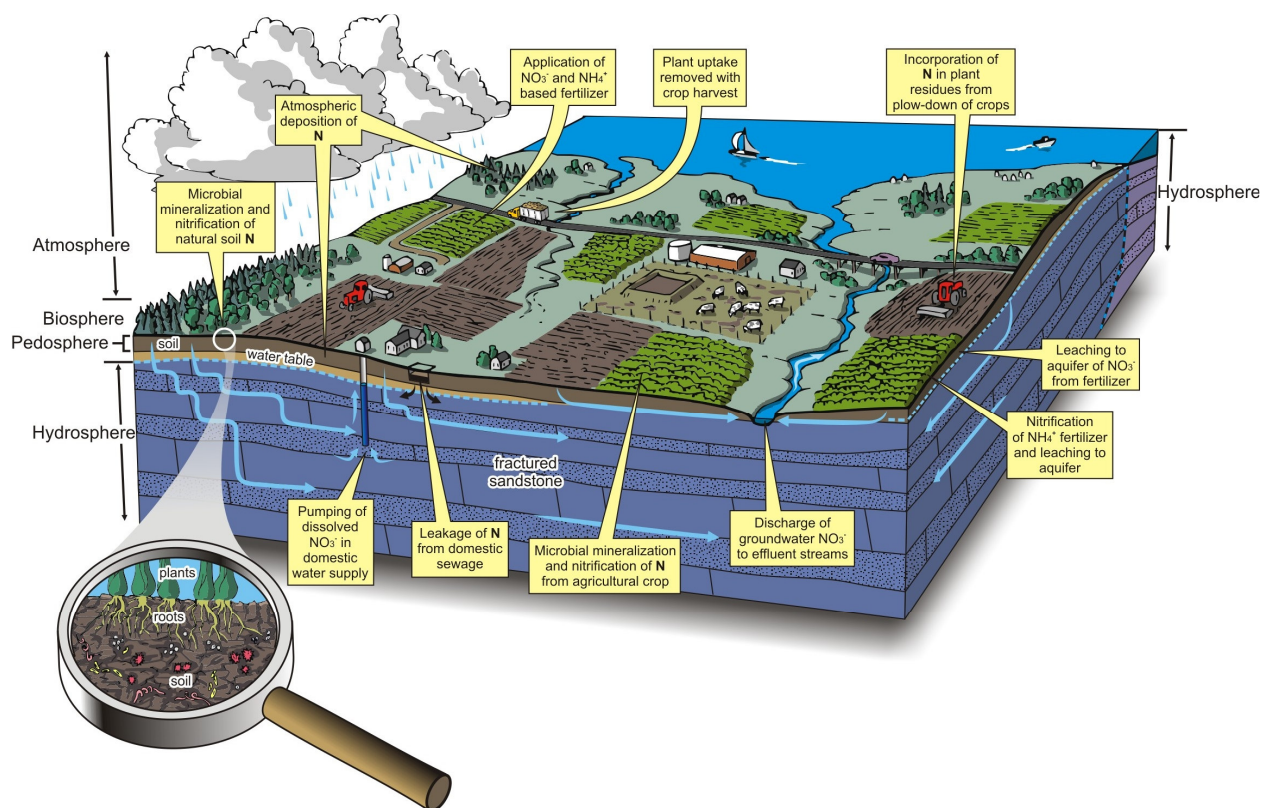


Figure 1.1. Conceptual diagram of the nitrogen cycle adapted to the context of Prince Edward Island and Wilmot watershed.

1.3. The nitrate problem in Prince Edward Island and potential climate change impacts

1.3.1. *Prince Edward Island context*

Prince Edward Island GW derives entirely from a suite of sedimentary rocks of Upper Pennsylvanian to Middle Permian strata that underlie the entire Island. These formations host a number of discrete GW flow systems with boundaries generally similar to those of surface watershed divides. The hydrogeological characteristics and general behaviour of these systems is similar throughout the Province because of its relatively uniform physiographic, geological and climatic conditions. For water quality, water extraction as well as water budget considerations, watersheds and aquifers have been studied together, and managed on an individual basis. Groundwater discharge (i.e. base flow) also accounts for a high proportion of fresh surface water flow, with significant water quantity and quality implications for Island streams, rivers and estuarine environments.

The domestic water needs for slightly over half of the population are met by private wells, with the balance of the population being supplied by municipal drinking water systems, also utilizing the GW sources. Traditionally, source water quality for municipal supplies is such that water treatment is not required (except for disinfection).

Many areas in PEI are characterized by agricultural activity including intensive potato cultivation, which has potentially significant impacts on drinking water quality, with nitrate

contamination creating perhaps the most significant water quality impact in rural areas. Groundwater nitrate concentrations in most regions of the Province are significantly above natural background levels. The island-wide average nitrate concentration is 3.8 mg/L but nitrate levels are not evenly distributed geographically (Fig. 1.2). Typically watersheds with few anthropogenic sources have mean nitrate concentrations of less than 2 mg/L, whereas mean concentrations are in excess of 5 mg/L in those watersheds with intensive agricultural activities. In some of these cases, as much as 20% of wells produce water exceeding the 10 mg/L drinking water guideline for nitrate. Historical data (1965-2005) indicate an empirical relationship between nitrogen (N) input in the watershed and base flow nitrate concentration of the Wilmot River (see chapters 4, 5, 8). We selected the Wilmot watershed for a pilot study because its cropping practices are typical of PEI's agricultural regions. The hydrogeological conditions of the Wilmot watershed-aquifer system are representative of most of PEI. The watershed is also ideally suited to the study of nitrate transfer from soils to aquifer due to the intensity of agricultural production, availability of wells for sampling and accessibility of records for GW and SW quantity and quality. The Wilmot River basin is located in west central PEI, and is approximately 5km wide and 17km long (Fig. 1.2).

In PEI, there is evidence to suggest that nitrate levels are continuing to rise in both GW and fresh surface water fed by GW (Somers *et al.*, 1999, Young *et al.*, 2002). While the biggest impact of nitrate contamination has been experienced by private wells, nitrate problems have already adversely impacted municipal water supplies in some areas of the province. For instance, the municipality of Borden has had to abandon wells in one location in favour of a new well field location and the community of Victoria has reconstructed its municipal wells to overcome problems with high nitrate levels in wells previously supplying their municipal water system.

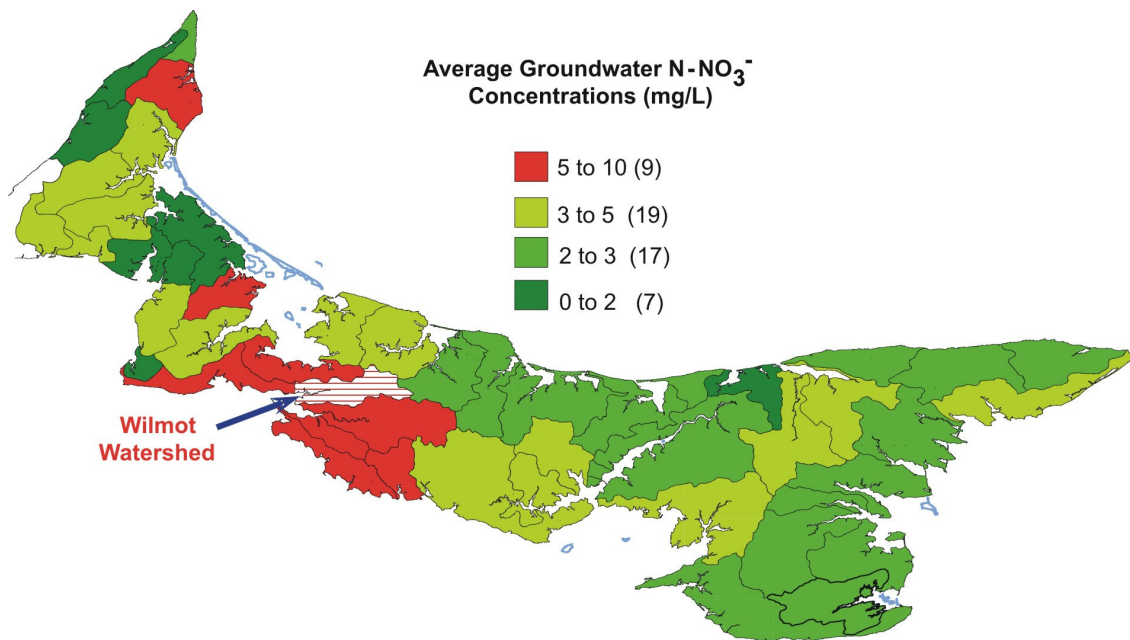


Figure 1.2. Mean nitrate concentrations for the main watersheds of Prince Edward Island arranged in four compositional groups (PEI-EEF). Location of the Wilmot Watershed selected for a pilot study of the N cycle (see Chapters 2-5).

1.3.2. Potential effects of climate change

The global average surface temperature relative to 1990 is expected to increase by 1.4 to 5.8°C by 2100 whereas the Canadian mean temperature could increase by 5 to 10°C over the next century. Furthermore, there will be more frequent extremes of high temperatures and fewer cold extremes, and more precipitation will fall over shorter periods (IPCC, 2001; McCulloch *et al.*, 2001).

Any changes in amplitude and timing of precipitation or in the snowpack resulting from increased temperatures would be expected to have implications for the timing or the amount of GW recharge, water table elevations and base flow to surface water bodies, and ultimately for the fate and transport of nitrogen species in GW and surface water. In addition, some predicted climatic conditions (Bootsma *et al.*, 2005a) could possibly generate increased risks of GW contamination on PEI due to longer crop-growing season, acceleration of soil N mineralization and potentially more inputs of N fertilizers. Any increase in the frequency or magnitude of contamination of aquifers by nitrate would have direct consequences on the quality of drinking water and surface water, and would ultimately increase eutrophication of coastal waters. In addition to human and ecological health, all of these factors have associated socio-economic implications related to the cost of water, as well as the health of the fisheries and tourism sectors.

1.3.3. Present water supply infrastructure and agricultural practices

The existing water supply infrastructure and water management practices in PEI have evolved under current climatic conditions and water characteristics, and have not been developed with consideration of potential future water quantity or quality scenarios. The use of essentially “raw” water for potable purposes, and absence of municipal water treatment facilities is of particular significance. Similarly, agricultural practices are also based on the current field conditions.

1.4. Purpose of the research

At the present time, no study or analysis of current water supply infrastructure, or water management and land use policies exist that will allow assessment of the impact of Climate Change (CC), especially for ecosystems where agricultural production has a strong impact on the quality of GW. Moreover, we do not know the consequences of potential intensification of agricultural production under higher temperature and precipitation regimes on the vulnerability, quality and quantity of drinking water. The purpose of the research is to provide answers to these questions in order to support decision making relative to potential CC impacts and associated adaptive measures for the sustainability of GW resources and agriculture development in PEI.

Objectives

1. In a pilot watershed-scale study of the Wilmot river, (i) estimate the soil-to-aquifer rate of nitrate transfer, (ii) evaluate the source apportionment of GW nitrate, (iii) evaluate the seasonal load of nitrate transferred from agricultural soils to the aquifer; (iv) model the transport of nitrate under current land use practices.

2. Evaluate the impact of doubling the atmospheric concentration of carbon dioxide ($2\times\text{CO}_2$), the so called greenhouse effect, on climate and on the contamination of drinking water by nitrogen (N), in terms of nitrate (NO_3^-) on PEI.
3. Evaluate the implications of climate change on the current water supply infrastructure on PEI, particularly with respect to nitrate levels and water treatment.
4. Discuss the implications of research results for the development of strategies to mitigate nitrate GW contamination, and to help water resource managers maintain the drinking water capacity on PEI.

1.5. Methodology

The research team includes scientists of the Geological Survey of Canada/Natural Resources Canada (GSC-NRCan), Agriculture and Agri-Food Canada (AAFC) PEI-Environment, Energy & Fisheries (PEI-EEF) and Institut de recherche scientifique–Eau, Terre, Environnement (INRS-ETE). The goal of the team is to combine field characterization of soils and modelling of Residual Soil Nitrogen (RSN) and over winter soil-nitrogen leaching, with field-based hydrogeological and hydrogeochemical surveys as well as modelling of GW flow and contaminant transport, to predict the impact of $2\times\text{CO}_2$ climate change (CC) scenarios on the contamination of GW by nitrate.

Field characterization of soil N properties is presented for the AAFC Harrington Experimental Farm of Charlottetown which is representative of the crop rotation of intensive potato cropping systems (Chapter 2) as well as overall physiographic and hydrogeological characteristics of the Province. Modelling of the soil-N export, the isotopic characterization of GW nitrate and modelling of flow and transport of nitrate are presented for the Wilmot watershed, a watershed/aquifer system to the west of Charlottetown which is also hydrogeologically representative of most of the province (Chapters 2-5). It should be noted, that while the watershed belongs to the group of most intensively cultivated watersheds containing the highest average nitrate concentrations in the Province (5-10 mg/L; [Fig. 1.2](#)), the general nature of cropping practices in the Wilmot watershed is valid for the Province as a whole.

Data from the General Circulation Models developed at the Canadian Centre for Climate Modelling and Analysis (McFarlane *et al.*, 1992) and at the Hadley Centre for Climate Prediction and Research (Gordon *et al.*, 2000) are used for various aspects of predictive modelling of $2\times\text{CO}_2$ climate change scenarios. During the first annual workshop of the project held in September 2004 in Québec City (Chapter 6), the research team selected the specific climatic conditions to be used in the model simulations.

The RSN and nitrogen leaching models calculate the annual nitrogen and water budgets by comparing inputs and outputs and reporting on the difference. RSN includes inputs in the form of nitrogen fertilizer, manure and nitrogen fixation by leguminous plants such as alfalfa, and outputs in the form of nitrogen in the harvested portion of the crops. The residual soil nitrogen (RSN) is the difference between inputs and outputs, or the amount of nitrogen which is not used by the crop, and which is left in the soil at the end of the growing season. Depending upon soil and climatic conditions, this nitrogen potentially leaches over winter from the soil profile (Chapter 7).

The availability of water resources under 2xCO₂ scenarios is evaluated and 3-D advective transport models using FEFLOW serve to simulate nitrate transport on a watershed scale, and GW and surface flow modelling under CC and RSN assessment at the scale of the Island (Chapter 8).

The infrastructure study involved identifying, inventorying and valuating municipal, industrial and private water supply infrastructure. The overall availability of GW, general water demand considerations and the relative proportions of water used by key sectors is assessed. Finally the current direct costs associated with nitrate contamination are estimated, and the potential CC consequences on these costs are discussed briefly. The results provided by this step are intended to facilitate an assessment of the vulnerability of current drinking water supply infrastructure under different CC scenarios (Chapter 9).

1.6. Concluding comments

In light of the potential effects of climate change, regulators and water managers need to consider the potential impacts on source water quality, and the associated engineering and financial implications for the water supply infrastructure. An assessment of the impact of climate change on the hydrological cycle, the nitrate levels in GW and the implications for economics of water supply presented here will aid in this evaluation. Awareness and knowledge on the various facets and dimensions of the problem will help direct how to best invest in strategies to minimize impacts on source water quality.

2 Nitrogen Leaching from agricultural soils at the watershed scale

Eric van Bochove, Georges Thériault, Rim Cherif, Noura Ziadi & John MacLeod

ABSTRACT

The characterization of Nitrogen leaching from agricultural fields of PEI shows that substantial amounts of nitrate are present at the end of the crop season and are available to reach aquifers afterwards. A conceptual model estimates that approximately 200 tons of N are available for leaching every year at the Wilmot watershed (PEI) scale for 1998-2001. This represents an averaged annual concentration of $5.6 \text{ mg NO}_3\text{-N L}^{-1}$ in the leaching water reaching the aquifer. A substantial portion of this N, representing 80 to 90% of the annual N balance, is available for leaching at the end of the crop season. Nitrate concentrations in drainage water samples are higher after the potato-rotation year than during other crop seasons. Low nitrate concentrations are measured in leachate at spring thaw indicating that most of nitrate available from the preceding potato crop season is likely leached at the end of fall or during winter. The results obtained from early spring ionic exchange membrane sampling show a high availability of nitrate in soil possibly throughout winter as well, resulting from soil N mineralization and nitrification over the winter period.

2.1 Introduction

Nitrogen is the most abundant element in the atmosphere as molecular N (N_2). However, only the reactive forms of nitrogen such as ammonium (NH_4^+) and nitrate (NO_3^-) support the growth of plant and microbes (Galloway *et al.*, 2003). In the last century, anthropogenic activities have more than doubled the global rate of reactive forms of nitrogen production (Vitousek *et al.*, 1997), and fertilizer N production is one of the major contributors. When available N exceeds the nitrogen requirement of crops, the mobile NO_3^- is easily leached to the groundwater (GW), especially in areas with well-drained soils and shallow aquifers (Mitchell *et al.*, 2003; Levallois *et al.*, 1998). As a result, agricultural activities such as livestock production and crops do have an impact on GW quality.

Groundwater plays an active role in the nitrogen cycle by being a pathway for transportation of the various dissolved N-bearing molecules. Groundwater is also normally a medium for chemical and biogeochemical transformations of these same molecules. Well water and, to some extent, surface waters used for water consumption by animals and humans are replenished by GW. Transfer of N by GW to surface water may also contribute to nutrient loading and subsequent eutrophication of surface waters. Consequently, GW contamination by nitrate can have direct consequences on human and animal life and aquatic health.

The shallow aquifers of Prince Edward Island (PEI) constitute the only source of freshwater for its population, agriculture and industry. In many areas, such as in the Wilmot River watershed, nitrate in GW is significantly exceeding the natural background. The present level of understanding of the N cycle in the Wilmot River watershed is that excess nitrate in soils due to intensive potato production moves with the GW flow to private wells and main rivers without much natural attenuation because the oxygen level in the aquifer does not favour bacterial nitrate reduction. This unconfined aquifer is composed of fractured sandstone with minor siltstone beds

overlain by a thin sandy till layer. Its upper part is strongly fractured and constitutes a fast path layer for GW flow. The water table shows typical seasonal responses to climate for the region, including a major spring recharge due to snowmelt, a summer water-table decline, a moderate autumn recharge and several significant recharge events caused by partial melting of snow during mild winter days.

Nitrate originates from fertilizers and from the soil organic N pool following mineralization (a process during which organic nitrogen is transformed into ammonium, a more simple mineral nitrogen form) and nitrification (a process during which ammonium is transformed in nitrate). Bacterial soil N mineralization and nitrification leading to labile nitrate in fertilized agricultural soils have been reported to take place during summer and to a minor extent during fall in northern regions (Alexander, 1977). Although, it has been demonstrated that denitrifying bacteria, converting nitrate into two gaseous forms of nitrogen, the water-soluble nitrous oxide (N_2O) and the water-insoluble molecular nitrogen (N_2), are active in snow covered agricultural fields near freezing point (van Bochove *et al.*, 2000; Wagner-Riddle & Thurtell, 1998), very few studies have investigated the soil N transformations over winter (Savard *et al.*, 2005) and their impacts on GW quality.

The objective of this study is to estimate the seasonal soil N flux from the unsaturated zone (vadoze zone) of agricultural soils to the aquifer at the watershed scale from experimental field monitoring by: (1) developing a conceptual model for the Wilmot watershed; (2) sampling soil drainage water in an equivalent context (Harrington Farm); and (3) using ionic exchange membranes to evaluate soil ammonium-N and nitrate-N fluxes related to soil N mineralization and nitrification at the Harrington Farm, respectively.

2.2 Methodology

The available N is estimated with a conceptual model for the Wilmot watershed. In addition, drainage water samples from different cropped experimental plots at the Harrington Farm and from an adjacent woodland lot are collected and analyzed periodically to determine the transfer magnitude and seasonality of different soil N forms to GW. Ionic exchange membranes are periodically buried within the first 20 cm of surface soil and subsequently sampled and analyzed to determine the occurrence of soil N mineralization and nitrification throughout the year.

2.2.1 Characterization of the study areas

Two study sites were used in this project. The Wilmot River basin situated in east central PEI and, the Harrington experimental farm (property of Agriculture and Agri-Food Canada) located approximately 30 km east of the Wilmot watershed. Data on landuse and agricultural practices in the Wilmot watershed were modelled, supported by site-specific data on nitrogen transfer dynamics in the soil from experimental plots at the Harrington Experimental Farm. The Wilmot River basin was chosen on the basis of manageable size, long period of record for hydrometric data and availability of wells to sample. The Harrington Experimental Farm choice is based on similar physiographic, soil and climatic conditions, and the availability of well established test plots under controlled conditions, with collection of detailed agricultural practices and more sophisticated sampling apparatus.

The Wilmot River basin (87 km²) is characterized by an unconfined, mixed-porosity sandstone aquifer covered by permeable till. The basin is also characterized by intense potato cropping activity. Similar physiographic, hydrogeological and soil conditions exist at both sites and are representative of much the Province.

All drainage water samples were collected at the AAFC Harrington experimental farm site. The farm is mainly sited on an Orthic Humo-Ferric Podzol mapped as a Charlottetown fine sandy loam common to the potato growing areas of PEI. This gently sloping site (1-3%) was considered representative of the pedo-climatic characteristics of the Wilmot River basin and offered excellent permanent facilities to collect drainage water. A 3-year rotation cropping management (potato-barley-red clover) has been applied on the plots since 1993. Hence in 2004, plots were cropped with potato and with barley in 2005. Three fertilization treatments were applied in triplicate: spring solid manure, spring liquid manure and mineral fertilization. Forest soil water samples were captured on the upper section of the slope in a wooded area next to the experimental plots.

2.2.2 Soil N flux estimation

A conceptual model was developed to estimate the soil N amounts leached from cropped fields and forested areas to the aquifer in the Wilmot River watershed. This model is based on a global balance sheet between seasonal N contributions (system inputs) and N removals (system outputs). Six modelling assumptions were that: (1) the vadoze zone is defined herein as the first meter of surface soil; (2) the vadoze zone (soil) N outputs, except for losses of ammonia (NH₃) from volatilization and denitrification, are the aquifer N inputs; (3) nitrate and nitrous oxide represent most of the N leached to the aquifer; (4) all potato fields within the watershed are uniformly following a three-year rotation plan (potato-cereal-red clover); (5) one third of hay was legumes and the remaining was considered grass hay; and (6) the undefined category from the Landsat-7 image analysis was considered to be legumes to avoid overestimation of N fertilizer application in the watershed.

The conceptual model uses agronomic and climatic data to determine the excess N during two periods starting in April of each year: spring-summer-early fall (April to November) and fall-winter (December to March). [Figure 2.1](#) illustrates the conceptual model inputs which are defined as N contribution to the ecosystem, and outputs defined as N removal from the ecosystem. The data used for fertilizer type, fertilization recommendations and crop yields were provided by the PEI Dept. of Agriculture, Fisheries and Aquaculture. Three major crops are considered for the fertilizer input calculation: potato (177kg N ha⁻¹), grain (55kg N ha⁻¹) and hay (112kg N ha⁻¹). The crop N removal coefficients used to calculate the N removed at crop harvest are taken from CFI (Canadian Fertilizer Institute, 2001). The precipitation data were provided by the Meteorological Service of Canada-Environment Canada. A value for N deposition (4.5kg ha⁻¹ yr⁻¹) was taken from Aber *et al.* (2003). N gaseous emission (1.25 % of total N) was taken from the report of the International Panel of Climate Change (IPCC, 1997). The Wilmot forested and potato-, grain- and hay-cultivated areas were estimated using the watershed contours and a GIS tool (ArcView 9.0) and two Landsat-7 images (1998 to 1999) and both Landsat-7 images and aerial photography for 2000. Legume area was derived as mentioned above in the fourth assumption of the conceptual model. Seasonal N amounts remaining in soil and potentially

available for leaching were calculated for each crop and per hectare of agricultural land in the Wilmot watershed.

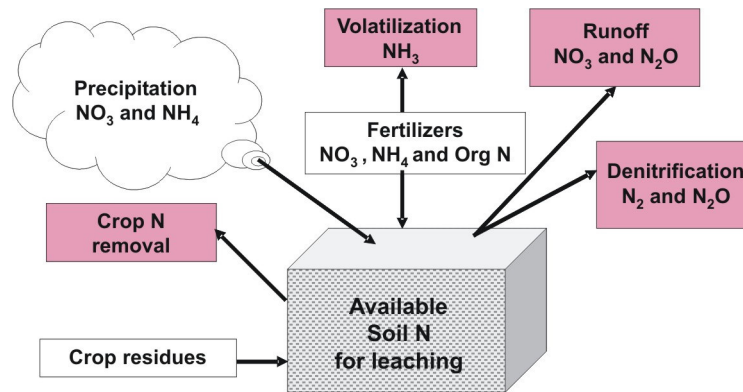


Figure 2.1. Conceptual model inputs (white boxes) and outputs (shaded boxes) to estimate the potentially available soil N for leaching from forested and cropped lands of Wilmot watershed.

2.2.3 Percolation water sampling and analysis

Nitrate, nitrite (NO_2^-), nitrous oxide, ammonium and total nitrogen concentrations are estimated from historical drainage-water data (1989 to 2003), tile drainage system, pan lysimeters and from soil ionic exchange resins data (2004 to 2005) sampled at Harrington experimental farm under the different rotation cropping systems.

A 3.4 ha ten-plot contiguous tile drainage system (Milburn and MacLeod, 1991; Milburn et al., 1992) was used in this study to collect drainage water from agricultural soils. Tile drains collected percolating water from independent plots and channelled it to a central collector system. Three pan-lysimeters buried at 80-cm depth were used to collect percolating water from forest soil. A detailed description of the pan-lysimeters can be found in (Caron *et al.*, 1999). Drainage and lysimeter water samples were collected during a three-day interval following two hydrological events for each sampling season (autumn, winter and spring). Colorimetric Flow Injection Analysis (FIA) and ion chromatographic methods were used to analyse the different soluble nitrogen species (dissolved N_{total} , NO_3^- , NH_4^+) on drainage and lysimeter water samples. A headspace equilibration technique (Kampbell *et al.*, 1989) followed by gas chromatography was used to analyse the dissolved nitrous oxide in the water samples.

2.2.4 Soil N transformation

To determine mineral nitrogen availability, anionic (positively charged) and cationic (negatively charged) exchange membranes, called hereafter ionic exchange membranes (IEM) were used *in situ* as a soil testing method (Qian *et al.*, 2007; Ziadi *et al.*, 2006) during 2004 and 2005. All details regarding the *in situ* use of these membranes are based on the study of Ziadi *et al.* (1999). Briefly, four anionic and four cationic membranes are periodically buried at a predetermined spot within the plots (4-m² area surrounding the spot) into the surface horizon (0-20cm). A total of eight 2-week periods of IEM cycle was carried out: two in the fall of 2004 and six from April to July 2005. In addition, one 145-day period was done in winter 2004-2005 (November 24-April 19) to evaluate fall and winter N mineralization. After each contact period, collected membranes

are first washed with distilled water in the field to remove any adhering soil particles and placed in individual tubes containing a solution of NaCl (anionic exchange membranes) or hydrochloric acid (cationic exchange membranes) and analyzed in the laboratory for NO_3^- by ion chromatography and NH_4^+ by colorimetric FIA, respectively.

2.3 Results and discussion

2.3.1 Available soil N at the watershed scale

N potentially available for leaching from forested and cropped soils to the aquifer within the Wilmot watershed is estimated for two yearly periods using the conceptual model. The spring-summer period started from planting and seeding in April until the end of November after harvest. The fall-winter period ran from December to March. The conceptual model estimations show that 199 to 221 Mg of N per year was available for leaching at the Wilmot watershed scale from 1998 to 2001. Table 2.1 shows inter-annual variations in crop areas reflecting crop rotation practices on the agricultural land of the Wilmot watershed, as well as total soil N available for leaching per hectare of agricultural and forest lands for the two yearly periods. The land use for 2000-2001 is very accurate and is determined from both 2000 aerial photograph and a Landsat-7 image, while on the other hand, land uses for 1998-1999 and 1999-2000 are determined from Landsat-7 images only. Initially, the Landsat-7 image analysis focussed primarily on potato crops and all other information from the Landsat-7 scene may well underestimate agricultural land use although their potato estimates is within 85% accurate. This could explain the relative increase of forest and total land use which does not give a good comprehension of the deforestation activity for agriculture benefit during the last decade. For example, in 1990, the forested land area in the Wilmot watershed was covering 1122 ha. Therefore during the last decade, the forest area was reduced by more than 15% and this area was mainly converted into agricultural land. The potential underestimation of agricultural land use from the Landsat-7 images for 1998-1999 and 1999-2000 leads inevitably to an underestimation of the available soil N assessment.

A significant 80 to 90% of N representing the annual soil N balance is available at the end of the crop season. Atmospheric N deposition in precipitation, as of NO_3^- and NH_4^+ forms, is a major and variable input to soil N representing 58 to 86 Mg (millions of kg) of the total annual N amounts from 1998 to 2001. Moreover, soil N available from agricultural lands throughout winter is assumed to originate only from precipitation accounting for 29% to 39% of annual atmospheric N deposition and is proportional to cultivated areas. Although, concomitant results from nitrate isotope measurements in GW (Savard *et al.*, 2005), drainage water and exchange membranes sampled in winter and early spring (Table 2.1, Fig. 2.2) indicate evidence of over-winter soil N transformations, these inputs were not included in the conceptual model because more data is needed to properly quantify winter transfer. The N budget calculations for different crops show that potatoes and hay were the major contributors to soil N available for leaching at the end of the crop season. In fact, these crops present an average contribution of 81% to the total N amount for the three-year period of 1998-2001. The estimated quantity of N available for leaching from agricultural land shown in Table 2.1 agrees well with the mean annual aquifer recharge (410 mm) and the nitrate concentration range of 4 to 7 mg $\text{NO}_3\text{-N L}^{-1}$ found for the Wilmot aquifer (Paradis *et al.*, 2006). Considering the more accurate values for 2000-2001 in Table 2.1, the calculation gives an annual concentration of 5.6 mg $\text{NO}_3\text{-N L}^{-1}$ in the leachate that would reach the aquifer.

Table 2.1. Agriculture and forest areas in Wilmot River watershed (PEI) for a typical 3-year rotation period estimated from Landsat-7 images, and total available soil N by hectare of agricultural and forest land by season estimated from a conceptual model.

Year	Landuse area (ha)						Available soil N (kg N ha ⁻¹)	
	Forest	Grain	Grass Hay	Potatoes	Legumes	Total	Spring-Summer (April-November)	Fall-Winter (December-March)
1998-1999	635	2306	1193	1918	596	6648	26.1	4.0
1999-2000	773	1993	1128	1860	1065	6819	25.9	6.5
2000-2001*	946	2107	1140	2238	716	7147	25.1	2.8

* The corresponding estimated value of 5.6 mg NO₃-N L⁻¹ is obtained as follow:

$$[(25.1+2.8) \text{ kg NO}_3\text{-N}\cdot\text{ha}^{-1} \times 7147 \text{ ha} \times 1 \times 10^6 \text{ mg NO}_3\text{-N}\cdot\text{kg}^{-1} \text{ NO}_3\text{-N}] \div [410 \text{ mm} \times 1 \times 10^{-3} \text{ m}\cdot\text{mm}^{-1} \times 8700 \text{ ha} \times 1 \times 10^4 \text{ m}^2\cdot\text{ha}^{-1} \times 1 \times 10^3 \text{ L}\cdot\text{m}^{-3}]$$

Note that the total mg of NO₃-N is calculated with the forest and agricultural land area, while the total volume of recharge with the watershed area

2.3.2 N in drainage water at Harrington experimental farm

Long-term (1989-2003) drainage data from the Harrington experimental farm show that the potato year within the rotation practice induces yearly average nitrate concentrations in water two to three times higher than those of barley and red clover years (MacLeod *et al.*, 2002a). [Table 2.2](#) shows that nitrate concentrations in drainage water samples are significantly higher for December 2004 after the potato-rotation year than for December 2005 after the barley – red clover rotation year. Low nitrate concentrations are measured at spring thaw of 2005 (April 5) indicating that most of the nitrate available from the preceding potato crop season is likely leached at the end of fall or during winter. The forest lysimetric water samples show systematically lower nitrate contents. Spring thaw of 2005 was also characterized by higher water ammonium concentrations (0.43 mg L⁻¹) in the agricultural treatments than in December 2004 and 2005 showing that soil N mineralization was taking place very early at snow melt or occurred over winter. It is noteworthy that total dissolved nitrogen (TDN) content follows a tendency similar to the one of nitrate concentration, and that their concentrations are only slightly higher. This implies that the nitrate species constitutes most of the dissolved N forms.

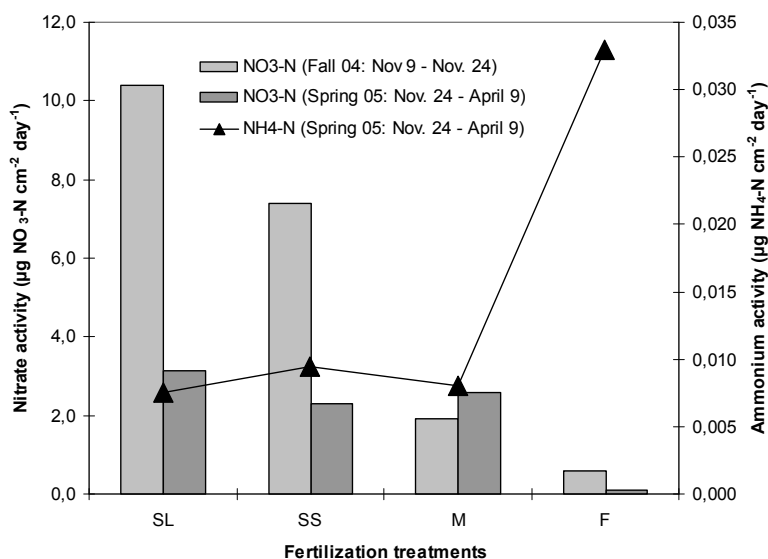


Figure 2.2. Nitrate and ammonium activities from IEM buried in soils receiving four different fertilization treatments: SL = spring liquid manure; SS = spring solid manure; M = fractionated mineral fertilizers; and F = no fertilizer in forest soil.

Table 2.2. Nitrate-N and ammonium-N and total dissolved nitrogen (TDN) concentrations in water samples from agricultural and forest soils of Harrington experimental farm (PEI). All agricultural plots (n=9) were cultivated in potato in 2004 and barley – red clover in 2005.

Sampling Date	N-NO ₃ (mg L ⁻¹)		N-NH ₄ (mg L ⁻¹)		TDN (mg L ⁻¹)	
	Agricultural ^a	Forest ^b	Agricultural	Forest	Agricultural	Forest
----- Mean (CV%)-----						
Dec. 1, 2004	29.4 (29)	6.9 ^c	0.14 (116)	nd ^d	33.2 (24)	7.7 ^c
April 5, 2005	9.0 (22)	no value	0.43 (66)	no value	10.3 (18)	no value
April 27, 2005	19.5 (18)	0.5 (71)	0.46 (91)	0.04 (71)	20.7 (19)	1.1 (12)
May 10, 2005	19.2 (22)	1.3 (39)	0.84 (72)	0.02 (31)	21.8 (21)	1.8 (27)
Dec. 1, 2005	6.7 (7)	no value	0.13 (60)	no value	7.1 (8)	no value

a) 27 samples = 3 daily samples of 3 treatments (spring liquid, spring solid, mineral) in triplicate

b) 9 samples = 3 daily samples of 1 treatment in triplicate. Adjacent forest soil (Deciduous forest).

c) One sample only.

d) not detected.

2.3.3 Soil N

In fall 2004, IEM were buried for 15 days (November 9 to November 24) and in spring 2005, for 136 days (November 24 to April 9) in cropped and forested plots. Nitrate activities measured from anionic exchange membranes at the end of fall 2004 and at spring 2005 are substantially higher in agricultural soil treatments than in the forest soil (Fig. 2.2). This indicates that the soil N cycling differs between these ecosystems. The nitrate activities are two to three times higher in fall 2004 than in spring 2005 for all treatments, with the exception of the fractionated mineral fertilizer treatment (M). In spring, liquid manure (SL) and spring solid manure (SS) treatment

plots are similar for the fractionated mineral fertilizers treatment (M) plots. These results suggest that nitrates are produced in soil over winter and trapped by the exchange membranes. In contrast, ammonium activities measured from cationic exchange membranes in spring 2005 are much higher in forest than in agricultural fields indicating that mineralization of soil organic N is present in the forest litter and that plant and microbial uptake of ammonium may reduce the quantity of substrate available for nitrification (Zak *et al.*, 1990).

The results obtained from drainage water analysis show that excess nitrate is likely leached to GW at the end of a potato cropping season and exchange membranes measurements indicate a possible nitrate production in soil over winter. These findings suggest that soil N mineralization and nitrification are occurring together in agricultural fields and as a consequence, additional nitrate is potentially produced and leached during winter rainfalls on snow and partial snow melts. This hypothesis is confirmed by the analyses of natural abundance of nitrate isotopes in GW sampled in the Wilmot watershed between 2003 and 2005 by Savard *et al.* (2005) and Savard *et al.* (2004).

2.4 Conclusions

This chapter presents essentially an annual estimation of N available from the agricultural fields and forested lots for leaching to the aquifer of the Wilmot River watershed at PEI. Even though only atmospheric N deposition is accounted for the winter season estimates (December to March), it appears that substantial amounts of nitrate are present at the end of the crop season and are available to contaminate the aquifer afterwards. Drainage water and exchange anionic and cationic membrane analyses confirm that nitrate is available at the end of crop season and is produced over winter or at the end of winter. These findings are corroborated by the nitrate O isotope ratios measurements in GW showing that nitrate having a specific cold weather isotopic pattern is leached to the aquifer during winter months. More than 200 Mg of N per year was available for leaching at the Wilmot watershed scale from 1998 to 2001. Considering a mean annual aquifer recharge of 410mm for the Wilmot watershed, the amount of N available for leaching corresponds to $5.6 \text{ mg NO}_3\text{-N L}^{-1}$ potentially reaching the aquifer annually. These estimated N amounts are of the same magnitude than those simulated by hydrogeological models or measured in GW of the top aquifer units. However, one has to keep in mind that N does not reach the aquifer uniformly during the year. Recharge events, especially in fall and spring season are likely periods of more NO_3 -concentrated leaching water.

3 Sources and seasonal dynamics of Nitrate in the Wilmot watershed/aquifer system of Prince Edward Island

Martine M. Savard, George Somers & Daniel Paradis

ABSTRACT

The general opinion is that bacterial nitrification leading to labile nitrate in fertilized agricultural soils of Northern regions is greatly diminished during winter and that the main contributors to excess N in these regions are chemical fertilizers. We have carried out seasonal sampling of groundwater over two years with the aim of assessing the fate of nitrate in the Wilmot aquifer which is rapidly responding to recharge events. Nitrogen and oxygen isotope results indicate that nitrification occurs all year long and that winter nitrate production is high. The main sources of nitrate contributing to the total load in groundwater are chemical fertilizers during summer (~64% of the total summer load) and residual crop material during winter (~62% of winter load). The significant nitrification of crop residues during the cold seasons has important implications for the development of strategies to protect water resources.

3.1 Introduction

Contamination of groundwater (GW) by nitrate is a widely recognized problem globally, and while there are many sources of N-bearing molecules, elevated nitrate levels are most often attributed to the impacts of intensive agricultural activities, principally as a result of fertilizer or manure inputs. Other sources of N of varying importance locally, include atmospheric deposition, and domestic and industrial wastewater discharges. The identification and quantification of nitrate types in regions where the N-NO_3^- concentrations exceed the recommended health threshold of 10 mg/L constitutes a key step in supporting informed decisions for protecting GW resources. The Wilmot river watershed on Prince Edward Island (PEI) is an area of intense agricultural activity, dominated by potato cropping, where nitrate levels locally exceed the health threshold (Chapter 1). For these reasons the Wilmot watershed has been selected to conduct a pilot investigation on nitrogen (N) dynamics between soils and aquifer (see also Chapter 2).

Soil processes affecting N-bearing components of the N cycle play a complex and significant role in the ultimate fate of N in the environment. GW investigations have frequently focused primarily on leaching and denitrification of N present in soils in excess of crop requirements. In addition, the literature on the significance of nitrification during the non-growing season is sparse, yet such soil process may contribute a significant proportion to the overall release of N to GW. Key processes affecting the GW load of nitrate and its isotopes have been discussed thoroughly in previous works (e.g. Kendal & Aravena, 2000; Savard *et al.*, 2007). The inorganic and organic sources of N commonly used to fertilize agricultural soils show distinct nitrogen isotope characteristics ($\delta^{15}\text{N}$ values): -2‰ for urea, 0‰ for chemical fertilizers, and >10 ‰ for manures. However, as suggested by greenhouse experiments on maize, $\delta^{15}\text{N}$ of plants might not always be a good indicator of N sources applied to fields (Choi *et al.*, 2002), and the overlap between $\delta^{15}\text{N}$ fields of different source types makes this tracer alone of limited use in identifying nitrate sources in GW. Classical papers have demonstrated that the $\delta^{15}\text{N}$ - $\delta^{18}\text{O}$ combination can be useful for fingerprinting the sources of nitrate dissolved in GW of various settings (e.g. Aravena *et al.*, 1993; Heaton 1983; Fukada *et al.*, 2004, Moore *et al.*, 2006). In some cases, it has been suggested

that the effects of microbial denitrification taking place under anaerobic conditions obliterates the isotopic specificity of the nitrate sources. The GW of the Wilmot aquifer is well oxygenated and for that reason denitrification cannot alter the original isotopic ratios, and the dual isotope approach in this setting may allow fingerprinting nitrate from manures and N-bearing chemical fertilizers.

The concept of discrimination of seasonal GW nitrate using $\delta^{18}\text{O}$ ratios has been previously recognized (Wassenaar, 1995) and used to separate atmosphere and soil nitrate in forested areas (Spoelstra *et al.*, 2001). However, stable isotopes of N and O, combined with a program of seasonal sampling have seldom been used to shed additional light on the sources and dynamics of N in soils and aquifers under temperate climatic conditions. Here we analyse nitrate isotopes in GW to investigate the processes involved in the seasonal transfer of soil nitrate to the rapidly responding Wilmot aquifer, and to evaluate the relative contribution of various sources to seasonal N loads. Our specific objectives are to: (1) understand the dominant seasonal processes involved in transferring nitrate from the agricultural soils to the regional aquifer, and (2) estimate the proportions of nitrate in GW coming from chemical fertilizers, manures and crop residues for the growing and non-growing periods of the year. Particular attention is paid to the importance of mineralization of N-bearing molecules in crop residual materials and to the release of N from inorganic fertilizers in overall N cycling.

3.2 Sampling and analytical methods

Water samples obtained for $\delta^{15}\text{N}$ and $\delta^{18}\text{O}$ analyses were collected from private wells distributed throughout the Wilmot watershed (Fig. 3.1). The wells have an average depth of 18m in the aquifer, are of open hole construction and are generally cased down to the overburden-rock contact. The water level is generally below the casing, in the rock formations. GW samples were obtained using outdoor taps devoid of treatment systems. Prior to sampling, the systems were purged until temperature, pH and conductivity stabilized. The samples were filtered using a 0.45 μm filter to remove particulate matter and then analysed by spectrophotometer to estimate the concentrations of NO_3^- and other ions in order to determine how much GW would subsequently be needed for ion resin exchange extraction. Samples were collected once every season during the 2003-2005 period (Table 3.1).

All isotope analyses were performed at the Delta-Lab of the Geological Survey of Canada (Québec). Nitrate was extracted using modified cation and anion-exchange resins and silver-nitrate precipitation protocols proposed by the USGS (Chang *et al.*, 1999; Silva *et al.*, 2000). The extraction is followed by analyses of the $\delta^{15}\text{N}$ and $\delta^{18}\text{O}$ ratios, using on-line combustion and pyrolysis-IRMS systems, respectively. Average precision obtained on sample duplicates (n=86, 161) is 0.1‰ for $\delta^{15}\text{N}$ and 0.2‰ for $\delta^{18}\text{O}$.

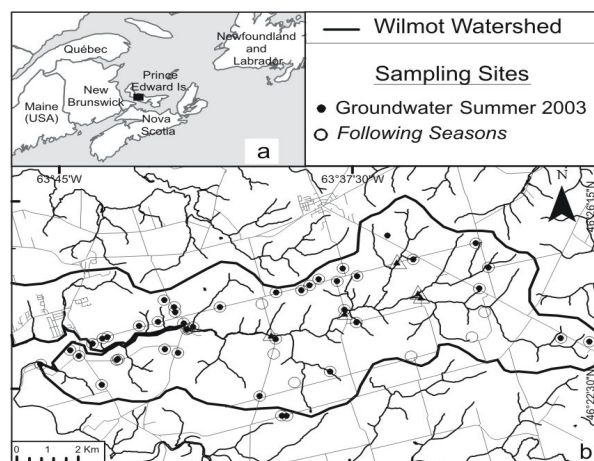


Figure 3.1. Map showing the location (a) and outline (b) of the Wilmot river watershed as well as the distribution of the sampling sites.

Table 3.1. Dates of sampling of the 8 seasons of investigation and number of collected samples.

Season	Sampling Period		GW	
	From	To	n	#
Summer	08-07-2003	04-08-2003	41	1
Autumn	28-09-2003	02-12-2003	20	2
Winter	02-03-2004	10-03-2004	20	3
Spring	31-03-2004	03-06-2004	20	4
Summer	06-07-2004	16-09-2004	49	5
Autumn	29-09-2004	19-12-2004	25	6
Winter	13-01-2005	10-03-2005	25	7
Spring	05-04-2005	05-05-2005	27	8

indicates the number attributed to the respective season of sampling
n: number of samples.

3.3 Results

Average GW nitrate concentrations varied little throughout the 8 seasons of sampling: 7.2, 6.5, 6.4 and 5.5 mg/L throughout summer, fall, winter and spring of 2003-2004, and 8.1, 6.9, 7.1 and 7.4 mg/L for summer, fall, winter and spring of 2004-2005, respectively (Liao *et al.*, 2005). The same is true for the $\delta^{15}\text{N}$ values obtained for nitrate dissolved in the GW samples (Fig. 3.2a). In contrast, the $\delta^{18}\text{O}$ values show important seasonal trends, with the difference between summer-fall and winter-spring periods presenting an average downshift of 10.0 ‰ for 2003-2004, and of 1.3‰ for 2004-2005 (Fig. 3.2b).

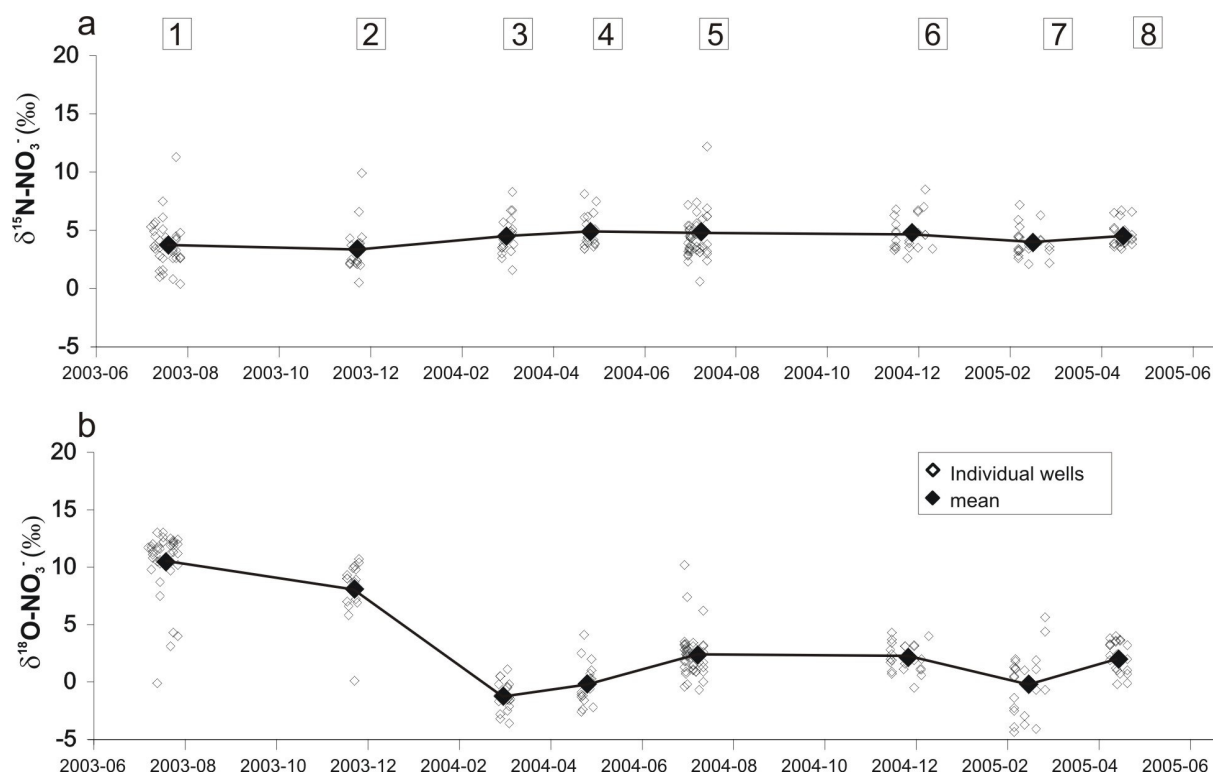


Figure 3.2. Seasonal results obtained for the Nitrogen and Oxygen isotopes of nitrate dissolved in GW from private wells (see Table 1 for sampling dates and season number; see Figure 1 for distribution of samples).

The average 2003-2004 and 2004-2005 GW values plotted in the $\delta^{18}\text{O}-\delta^{15}\text{N}$ space relative to a compilation of domains of various potential nitrate sources are all circumscribed by the field of plant residues (Fig. 3.3). The summer and fall averages appear near the upper left limit of the plant field drawn from the literature, whereas the winter and spring values for that year show much lower $\delta^{18}\text{O}$ values but slightly higher $\delta^{15}\text{N}$ ratios (Fig. 3.3a). The average results obtained for 2004-2005 all cluster in the lower left quarter of the plant residue field, with the summer and fall values showing slightly higher $\delta^{18}\text{O}$ and $\delta^{15}\text{N}$ ratios than the two other seasons (Fig. 3.3b).

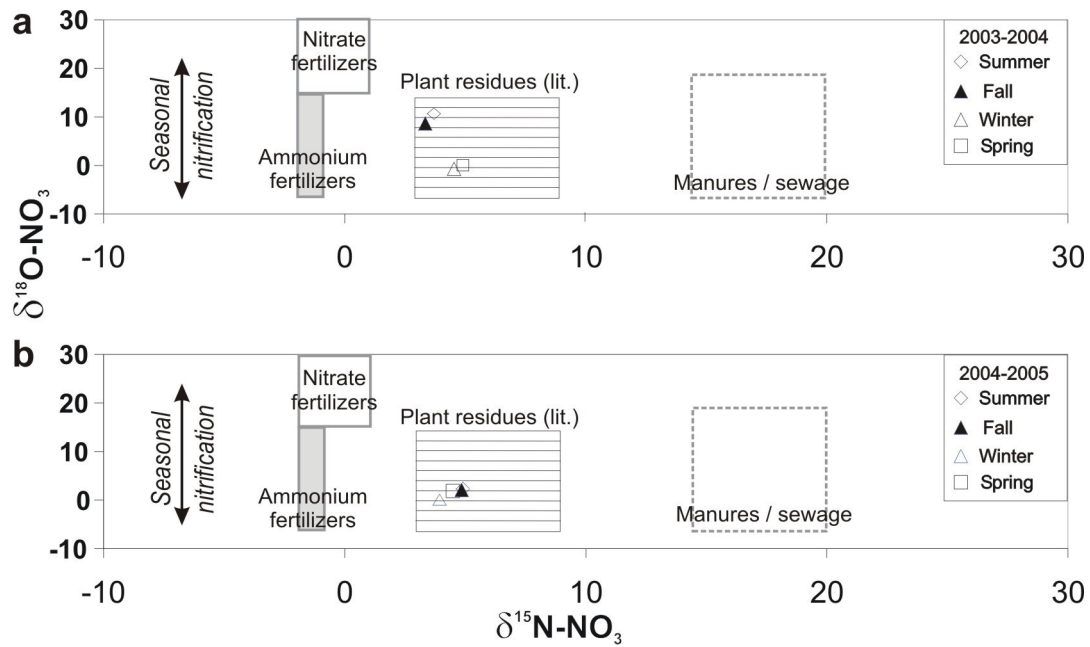


Figure 3.3. Average per season of isotopic results obtained for GW collected from private wells of the Wilmot watershed compared with isotopic fields for potential sources of nitrate.

3.4 Interpretation and Discussion

3.4.1 Seasonality of nitrate loads transferred to GW

Savard *et al.* (2006, 2007) demonstrated that denitrification does not affect the GW load of nitrate on the basis of the relation between nitrate concentration and $\delta^{15}\text{N}$ values, and suggested that mixtures of shallow, NO_3^- -rich water with deeper, NO_3^- -poor GW generated various degrees of dilution of nitrate in GW of the private wells. Therefore the nitrate concentration measured at the top of the aquifer can be used to estimate transfer rate of nitrate from soils to GW. Here, daily nitrate loads reaching the aquifer were calculated for the eight seasons investigated (Fig. 3.4a) using the estimated daily average volume of recharge to the aquifer and the average concentrations in GW (Savard *et al.*, 2007). This daily load constitutes a minimum because the sampled wells yield composite GW samples carrying nitrate concentrations lower than nitrate levels in soil leachates prior to their dilution at the top of the aquifer (leachate concentrations from sampling points covering the study area are not available; see chapter 2). Here we only need to compare relative averages of nitrate transfer on a daily basis and there is no need for absolute load values. The estimated daily N transferred to the entire aquifer ranges from 0.17 to 2.46 tonnes/d (Fig. 3.4a), corresponding to fluxes of 7 to 103 Kg/ha/y, respectively. These calculations show that the highest N-loads (0.90 to 2.46 tonnes/d; or 38 to 103 Kg/ha/y) are released during the cold seasons of the two yearly cycles in the Wilmot watershed (seasons 3, 4, 7 and 8).

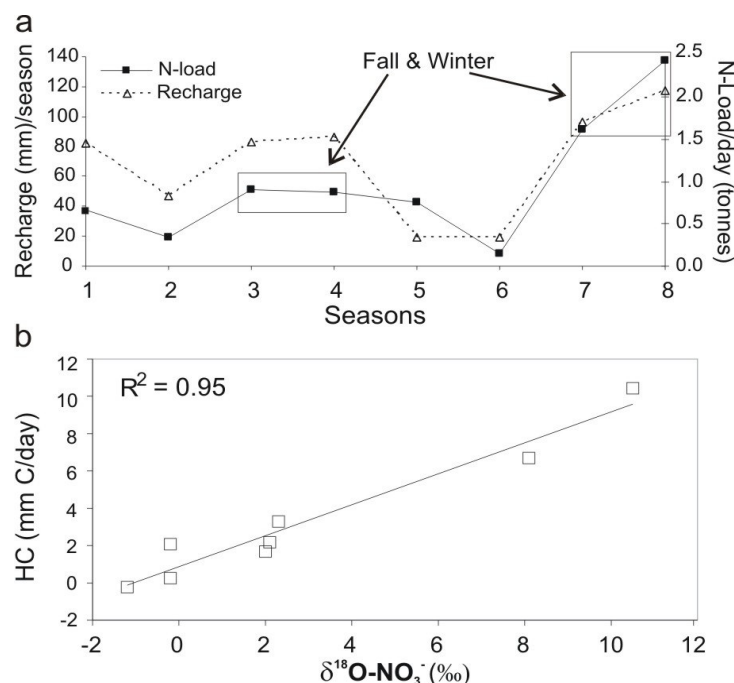


Figure 3.4. (a) Daily average of seasonal N-NO_3^- transfer from soils to the aquifer, compared to the cumulative recharge for each season. (b) Hydroclimatic index plotted against average $\delta^{18}\text{O}$ values for each investigated season.

In terms of seasonality, GW $\delta^{18}\text{O}_{\text{NO}_3^-}$ downshifts appear universally in the regional compilation of GW results for individual well samples (Annex), which represent a mixture of waters from various aquifer depths. In soil processes leading to nitrification, nitrate contains two oxygen atoms from soil water and one atom from free O_2 in soil (Andersson and Hooper, 1983; Kumar *et al.*, 1983; Hollocher, 1984). Given that oxygen of atmospheric O_2 has a $\delta^{18}\text{O}$ value of +23.5 ‰, and that soil water originating from local precipitation carries $\delta^{18}\text{O}$ values reflecting seasonal temperature influences as reported in Savard *et al.* (2006, 2007), the isotopic ratios of nitrate expected to have resulted from microbial activities during the periods of interest can be calculated and used to interpret the observed $\delta^{18}\text{O}$ trends. It is suggested that the differences between the $\delta^{18}\text{O}_{\text{NO}_3^-}$ values of the summer-fall and winter-spring periods are determined by the points in time when nitrate is produced and subsequently transferred to the Wilmot aquifer, and by the quantity of nitrate reaching the aquifer at these times.

The range of $\delta^{18}\text{O}$ values of 2003-2004 summer-fall and winter-spring precipitation vary from -8.4 to -5.4‰ (average -6.5) and from -26.4 to -7.8‰ (average -16.7‰), respectively (Savard *et al.*, 2007). According to the Atlantic Fertilizers Institute (Jacques Whitford Environment Ltd, 2001), the proportions of nitrate fertilizers and other N-bearing commercial products used in PEI are 24 and 76%, respectively. Note that the non-nitrate N-species have to be bacterially transformed into nitrate. If nitrifying bacteria utilize soil waters with summer-fall characteristics, assuming the above noted proportions of fertilizers are valid for the Wilmot watershed, and taking into account the high $\delta^{18}\text{O}$ values for nitrate fertilizers (+30.0‰; Annex), regional estimates for the summer-fall nitrate mixture would be between +8.9 and +10.4‰ (average +9.9‰). This range of values covers the observed GW summer and fall averages for private wells

(Fig. 3.2a). If nitrifying bacteria utilize soil waters with winter and spring characteristics, assuming there is a residual of 5% of fertilizer nitrate (+30‰) in the soil mixture, the estimated $\delta^{18}\text{O}$ range for winter and spring nitrate is between -7.7 and +4.0‰ (average -1.6‰); covering the average values for these two seasons (Fig. 3.2a). Therefore the $\delta^{18}\text{O}_{\text{nitrate}}$ values for the summer-fall and winter-spring periods of 2003-2004 suggest active nitrification during all four seasons and rapid transfer of nitrate to the aquifer.

We also conclude that the seasonal $\delta^{18}\text{O}$ trends in GW imply that precipitation is largely controlling the oxygen isotopic ranges in the soil water and in turn, the values of bacterially mediated nitrate. Under field conditions, the exact proportions of leachates and their $\delta^{18}\text{O}$ characteristics in mixtures will be controlled by local hydrogeological properties, as well as climatic conditions, such as the amount of recharge and air temperature which greatly influences the oxygen isotope fractionation during precipitation. These climatic conditions can vary considerably and it is therefore expected to find significant nitrate $\delta^{18}\text{O}$ variations from year to year during specific periods of sampling, correlating to differences in these climatic parameters. To illustrate this point, we have calculated a hydro-climatic index (HC) which takes into account variations in temperature and recharge conditions for the various precipitation events between the sampling periods. The index equals the daily average recharge multiplied by daily average air temperature, divided by the number of days between sampling sessions (Savard *et al.*, 2007). The correlation between the HC and average nitrate- $\delta^{18}\text{O}$ values found in seasonal GW explains 95% of the $\delta^{18}\text{O}$ variations (Fig. 3.4b). This empirical relationship expresses a solid co-variation throughout the eight seasonal sampling periods, supporting our assumption that the hydro-climatic conditions largely control the average $\delta^{18}\text{O}$ values of nitrate produced by biologically mediated process and transferred to the aquifer on a regional scale. The calculated minimal daily N-load transferred to the aquifer constitutes an estimate also reflecting the importance of seasonal nitrate fluxes (Fig. 3.4a). This evaluation combined with the $\delta^{18}\text{O}_{\text{NO}_3^-}$ characteristics indicates that winter and spring provide the highest rate of transfer during the two yearly cycles covered for the Wilmot watershed and that recharge is a crucial factor controlling the rate of transfer.

3.4.2 Sources of nitrate in the Wilmot aquifer

The Wilmot watershed receives approximately 100Kg/ha of applied N annually, and also receives ~7 Kg/ha/year of atmospheric N which is among the highest rates in North America (Jacques Whitford Ltd, 2001; Environment Canada data). The $\delta^{15}\text{N}$ and $\delta^{18}\text{O}$ ratios for the potential sources of nitrate in GW were compiled from various studies around the world (Fig. 3.3; compiled from Kendall and Aravena, 2000). The graphical positions of average results for the Wilmot aquifer as presented in (Fig. 3.3b) can be attributed to: (1) plant residues, (2) mixtures of manures and chemical fertilizers, or (3) mixtures of chemical fertilizers, plant residues and manures. To estimate the contribution from each source, we pose a problem of three equations and three unknown fractions:

$$1 = F_{\text{pr}} + F_{\text{m}} + F_{\text{cf}} \quad (\text{eq. 1}),$$

$$\delta^{18}\text{O}_{\text{mea}} = F_{\text{pr}} \times \delta^{18}\text{O}_{\text{pr}} + F_{\text{m}} \times \delta^{18}\text{O}_{\text{m}} + F_{\text{cf}} \times \delta^{18}\text{O}_{\text{cf}} \quad (\text{eq. 2}), \text{ and}$$

$$\delta^{15}\text{N}_{\text{mea}} = F_{\text{pr}} \times \delta^{15}\text{N}_{\text{pr}} + F_{\text{m}} \times \delta^{15}\text{N}_{\text{m}} + F_{\text{cf}} \times \delta^{15}\text{N}_{\text{cf}} \quad (\text{eq. 3}).$$

In these equations, F stands for fractions of nitrate from the 3 sources identified with the subscripts *pr*, *m* and *cf* for plant residues, manures and chemical fertilizers, respectively. The average nitrate isotopic characteristics measured in GW and the ratios for potential sources ([Annex](#)) are used in equations 2 and 3, and designated using the same subscripts ([Table 3.2](#)). The solution to the three equations obtained for summer 2003 suggests that manures contribute 22% to the summer load, plant residues, 13%, and chemical fertilizers, 65%. During winter 2004, the proportions are 15, 62 and 23% for manures, plant residues and chemical fertilizers, respectively ([Table 3.2](#)). If we assume that the wet and dry atmospheric input of nitrate deposited on PEI is 5% of the annual load, and that there are no important seasonal changes to that input, the proportions, in the same order become 21, 12 and 62% for summer 2003, and 14, 59 and 22% for winter 2004.

Table 3.2. Model conditions for source apportionment and solution to the 3 equations/3 unknowns problem.

Season	1	3
	‰	‰
GW $\delta^{15}\text{N}_{\text{measured}}$	3.7	4.5
* $\delta^{15}\text{N}_{\text{pr}}$	3.0	3.0
$\delta^{15}\text{N}_{\text{m}}$	19.1	19.1
$\delta^{15}\text{N}_{\text{cf}}$	-1.3	-1.3
** GW $\delta^{18}\text{O}_{\text{measured}}$	11.3	-1.2
$\delta^{18}\text{O}_{\text{pr}}$	5.0	-3.5
$\delta^{18}\text{O}_{\text{m}}$	16.9	5.0
$\delta^{18}\text{O}_{\text{cf}}$	10.7	1.0
	%	%
F_{m}	22	15
F_{pr}	13	62
F_{cf}	65	23

Note 1 : an input of 5% from the atmosphere is taken into consideration, we therefore assume a 95% contribution from the 3 other sources (distributed as the program calculates; F_{pr} , F_{m} , F_{cf}).

Note 2: GW measured values are averages for samples from private wells distributed regionally.

* Average for natural soil is 4.3‰; fertilized soils are generally less enriched (Kendall & Aravena, 2000).

** Value takes into account the fact that dilution by GW in wells reduce the true signal of soil water.

As mentioned above, the average $\delta^{15}\text{N}$ values only vary moderately over the 8 seasons studied, whereas the $\delta^{18}\text{O}$ results show significant changes during the same period, and even within a single season ([Annex](#)). For this reason we have performed a sensitivity test on our model for this variable. Sensitivity of the solutions is evaluated for GW-average $\delta^{18}\text{O}$ values covering a range of 2‰, adding and subtracting two increments of 0.5 ‰ from the original average value ([Fig. 3.5a](#)). Following this test for summer 2003, the proportion of nitrate contributed from chemical fertilizers changes by as much as 20% (~5% per increment), but chemical fertilizers remain the dominant source. For the same test, winter proportions for plant residues vary between 40 and 80% (~10% per increment), but crop residues continue to be the dominant source within the $\delta^{18}\text{O}$ range tested.

The source apportionment exercise does not aim to provide precise values for the contribution of various sources, but rather at assessing which source contributes most significantly to the seasonal loads during the period of investigation. With the sensitivity test validating the model, we have solved the three equations for all seasons investigated ([Fig. 3.5b](#)). Note that the average

recharge during summer and fall 2004 (20mm) is significantly lower than during the 6 other seasons (85mm; Fig. 3.4a). In such a case, the mere GW average $\delta^{18}\text{O}$ values cannot be used to solve the equations because a dilution effect (greater proportion of deeper, low nitrate water as a result of very limited recharge) may have significantly affected this signal. We have therefore used the maximum $\delta^{18}\text{O}$ values measured for summer and fall 2004.

The proportions obtained through the source apportionment calculations suggest that chemical fertilizers are the dominating source of nitrate during summer, but that plant residues dominate the nitrate loads of most other seasons in the Wilmot Watershed (Fig. 3.5b).

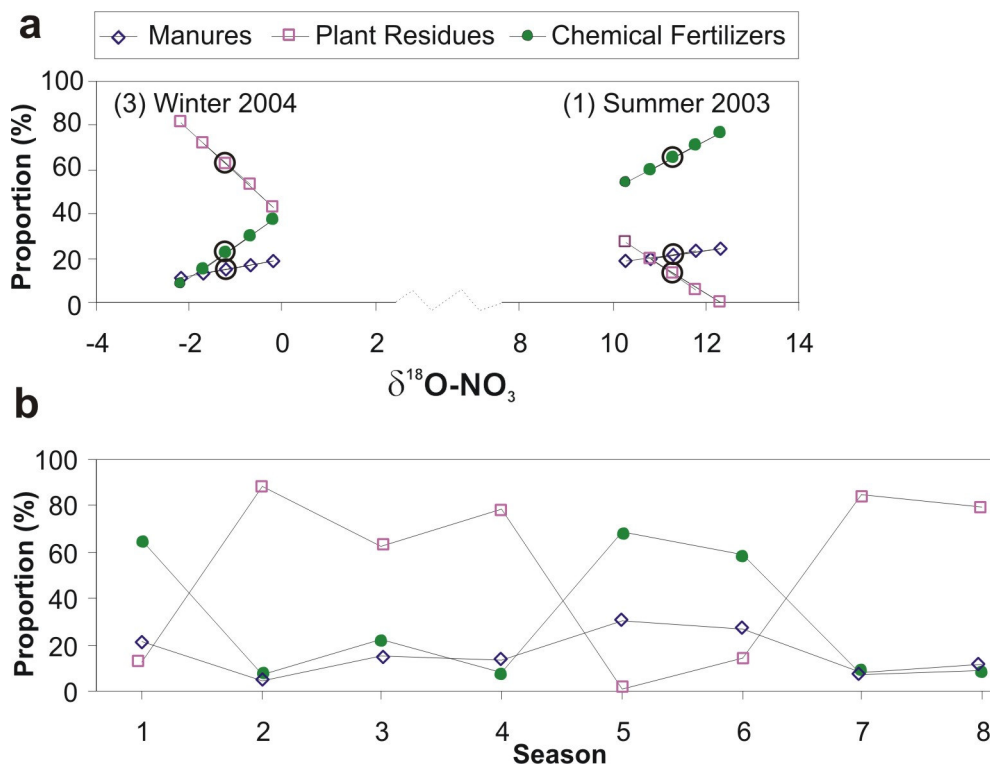


Figure 3.5. Source apportionment of nitrate per season for the Wilmot aquifer. (a) Sensitivity of model solution of nitrate proportions from the three main potential sources relative to a total average $\delta^{18}\text{O}$ variation of 2 ‰, for seasons 1 and 3. Circled points indicate the original $\delta^{18}\text{O}$ values used for calculations of proportion in Table 3.2. (b) Proportions of manures, plant residues and chemical fertilizers obtained for the 8 seasons of sampling (see text for details). The legend above stands for the two graphs.

As a check on the results suggested by the calculations based on isotopic ratios described above, a simple mass balance estimation of the proportions of various sources, was made based on agricultural practices typical of the Wilmot area (Table 3.3). Information on the relative proportions of different land use, typical manure and fertilizer application rates, and estimated N contents of different crop fractions were used to calculate theoretical contributions of different N sources (Atlantic Agri-Tech, 2006; Jacques Whitford Ltd, 2001).

Table 3.3. Mass balance calculations of main nitrate source contribution to the total load based on agricultural practices in the Wilmot watershed.

N sources (inputs + residual)	Growing Season		Non-growing season	
	kg/ha	%	kg/ha	%
inorganic fertilizers	68	66	0	0
Manure	12	12	12	27
mineralization of plant residues	18	18	29	63
direct atmospheric deposition	3	3	4	8
residential sewage	1	1	1	2
<i>N sources (inputs + residual)</i>	<i>102</i>	<i>100</i>	<i>46</i>	<i>100</i>
total N inputs to system				
inorganic fertilizers	68	73	0	0
manure	12	13	12	50
fixation of N by legumes	8	8	8	31
direct atmospheric deposition	4	4	4	14
residential sewage	1	1	1	5
<i>total N inputs to system</i>	<i>93</i>	<i>99</i>	<i>25</i>	<i>100</i>

First, an estimation of annual nitrogen contributions was created, which was subsequently subdivided into discrete periods representing the summer/fall period and winter/spring period. The mass balance estimations show some discrepancies relative to calculations based on seasonal isotope characteristics of nitrate (Table 3.2). This is perhaps partly due to the nature of the mass balance calculation. For example, while some carry over of inorganic fertilizer into the fall or winter (see Chapter 2) may be anticipated, in the mass balance calculation, all inorganic fertilizer is assigned to the summer period. Similarly, while the degradation of plant residues is likely to occur at some scale year round, the mass balance calculations assume that plant N is released essentially “instantly” with timing associated with major agronomic practices such as plough-down of cover crops in the spring. Also, the mass balance calculations do not take into account any of the variations in annual climatic influences described in section 3.4.1. In spite of these limitations, the mass balance calculations support the estimates provided by the calculations based on the isotopic model (Table 3.2). The relative contributions of various N sources, including the “intermediate” products of mineralization of organic N in plant residues, which is not an external input to the agricultural system, suggest this mechanism plays an important role in the cycling of N, especially in cold periods (Table 3.3a). The relative portions of external N sources to the agricultural system highlight the dominant role of inorganic fertilizers as the primary N input to the watershed regardless of intermediate steps such as mineralization of organic N in plant residues involved in the overall N-cycle (Table 3.3b). It is important to note that these calculations consider N inputs only (not N outputs), and while inputs during the summer/fall period are nearly twice those of the winter/spring period, it is suggested that this is offset by the lack of N uptake during cold periods. The end result is consistent with the idea that winter transfer of nitrate to the aquifer is highly significant in spite of the lower inputs of this period, in large part because of the importance of the mineralization of organic N in plant residues during this period.

Overall, the source apportionment exercise indicates that the dominating nitrate source depends on the nature of the N-bearing species present in the agricultural soils during a particular season, either inorganic fertilizers or plant residues (Fig. 3.6). The calculated estimates clearly stress the fact that the agricultural practices govern the annual N-cycle in the Wilmot watershed, whether from spreading of chemical fertilizers or leaving plant residues on, or in soils.

3.5 Conclusions

Overall, we infer that the GW $\delta^{18}\text{O}_{\text{nitrate}}$ cycles in the Wilmot watershed result from on-going nitrification in soils during the four Canadian seasons. This interpretation implies that soil microbial activity produces nitrate all year long including winter, either by nitrification of ammonia based fertilizers or decomposition of plant residues, and that nitrate transfer from soils to GW takes place whenever recharge is occurring. Fluctuations of precipitation, temperature and recharge to the aquifer change the seasonal proportions and isotope ratios, and thus modulate the amplitude of seasonal shifts. The direct correlation between recharge rates and fluxes of nitrate to the aquifer stresses the importance of considering recharge as a key parameter to study climate change impact on the N cycle (see also chapters 6 to 8).

It seems that the winter nitrate production is significant as our calculations show that the winter-spring periods of the two yearly cycles in the Wilmot watershed release 0.90 to 2.46 tonnes/d (38 to 103 Kg/ha/y) which represent the highest N-loads for the two years of investigation. This winter load is mostly derived from the degradation of crop residues (62% of winter load), whereas the summer loads are dominated by chemical fertilizers (64% of summer load). In both cases, the nitrate levels originate primarily from N release related to agricultural practices; the levels expected in natural settings such as forested land would be much lower (Chapter 2). Finally, our hope is that the conclusions of this research will assist in the development of remedial strategies and in assessing the implications of climate change on N contamination in PEI. In particular, it appears clear that truly effective strategies aimed at a reduction of N leaching to GW will need to focus not solely on optimizing fertilizer application rates, but will need to carefully consider the management of residual plant material. This is likely to pose special challenges, especially for production of annual crops, where it will be necessary to balance the many benefits of organic matter in soils against their contribution to N leached to the aquifer.

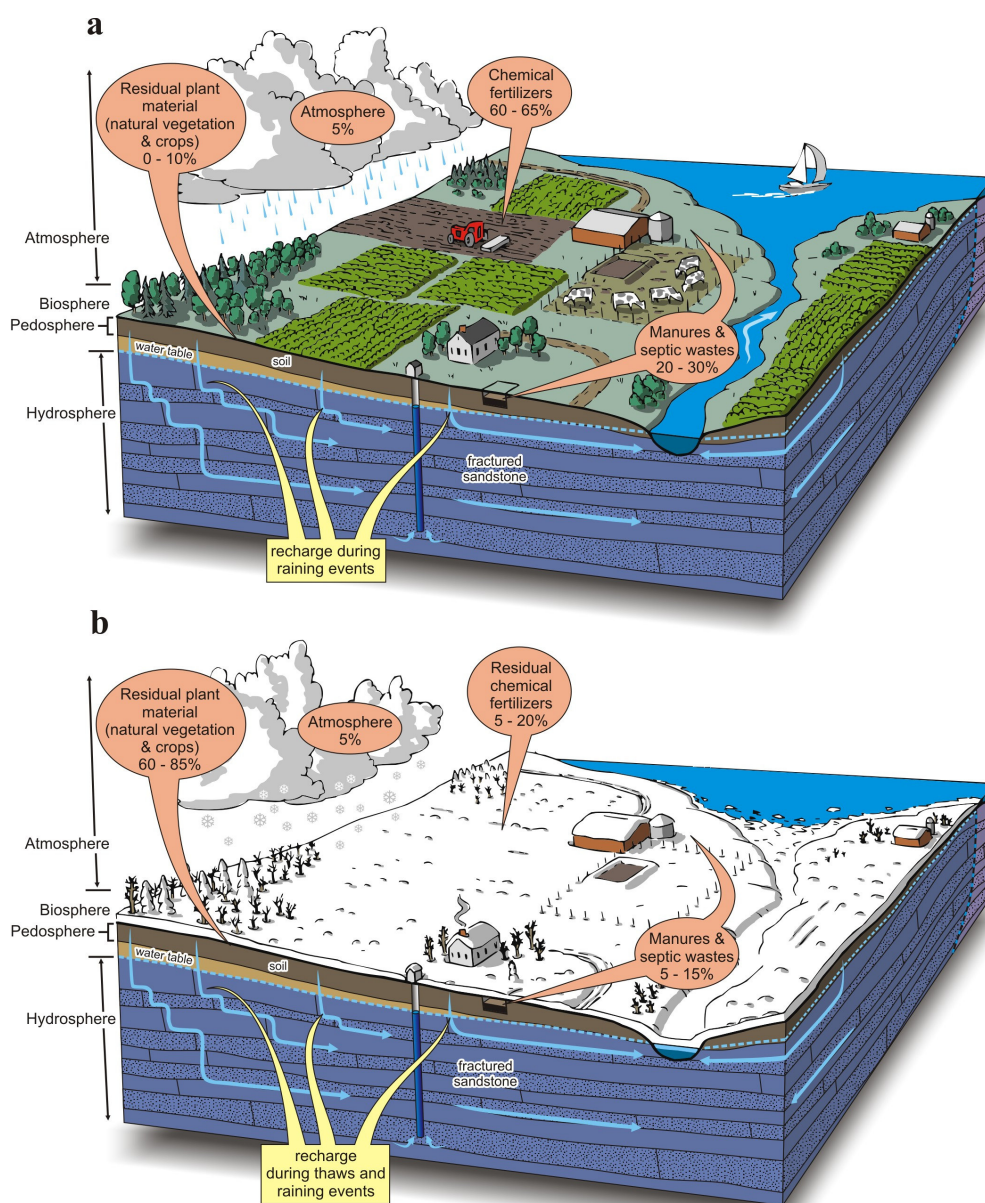


Figure 3.6. Source apportionment ranges of nitrate for summer (a) and winter (b) in the Wilmot watershed. The atmospheric N-NO_3^- input is assumed constant whereas the residual plant material, chemical fertilizer and manure input are estimated by a three equations- 3 unknowns solution and confirmed by mass balance calculations (see text for details).

4 Numerical Modelling of Nitrate Transport in the Wilmot Watershed Using Field Specific N-inputs

Yefang Jiang & George Somers

ABSTRACT

3D groundwater flow and mass transport models are developed to assess nitrate contamination in the Wilmot River watershed. Vertically, the flow model delineates multiple flow systems within the active flow zone and these systems roughly correspond to the stream network. The feature of $K_h \gg K_z$ dominates the flow pattern, and the distribution and migration of nitrate in the aquifer. The transport model shows that base flow responds rapidly to nitrate leaching and the plume in the shallow flow systems reaches quasi-steady state within a few years, with the nitrate plume front progressively moving into the deeper portions of the aquifer. Predictive simulations indicate that continuing with existing land use practices, nitrate concentrations at shallow and intermediate depths will reach 8.5 mg/L by 2010 and 2025 respectively, and for deeper groundwater levels will reach 7.1 mg/L by 2050. Only with substantial reductions in N-inputs, perhaps in the range of 50% of current levels, are significant decreases in groundwater nitrate levels predicted.

4.1 Introduction

Groundwater (GW) and surface water in many agricultural watersheds in P.E.I. exhibit nitrate ($\text{NO}_3\text{-N}$) concentrations elevated significantly above natural background levels, and in some cases, the health threshold of 10 mg/L (Somers *et al.*, 1999; Young *et al.*, 2002). Groundwater is the sole source of potable water, and river base flow (former GW) comprises a high proportion of the total annual flow. Thus elevated nitrate levels are of concern both with respect to drinking water quality and nutrient loading with associated eutrophication in estuarine environments (Somers *et al.*, 1999; Young *et al.*, 2002). Monitoring data suggests that nitrate levels in both GW and surface water are continuing to rise.

In response to this concern, a three-year collaborative project, involving the Geological Survey of Canada (GSC), PEI Department of Environment, Energy and Forestry (PEI-EEF), and Agriculture, Agri-Food Canada (AAFC), was implemented in 2003 to examine nitrate sources, fate and transport in the Wilmot River watershed. The Wilmot River watershed has been selected as representative of the hydrogeological conditions on PEI and of those watersheds at risks due to intensive agricultural activities on the island (Savard *et al.*, 2004; Chapter 1). An important aspect of the project is to assess land use impacts on GW and surface water quality, using numerical modelling, and provide input for the development of nutrient reduction strategies on PEI. Steady state simulations have been conducted to establish the GW flow regime in the study area, followed by transient simulations of mass transport processes involved in the evolution of nitrate concentrations throughout the aquifer.

4.2 Hydrogeology of the Wilmot River watershed

To illustrate the conceptual hydrogeological model for the watershed, the local geology is briefly described here and further details can be found in van de Poll (1983) and Mutch *et al.* (1992).

Field observations and drilling confirm that, hydrogeologically, the Wilmot River watershed bears strong similarities to the other parts of the island. The watershed is underlain by terrestrial sandstone formations with a total thickness of > 850m (based on logs from oil exploration boreholes and internal documents of PEI EEF). The formation consists of a sequence of Permo-Carboniferous red beds ranging in age from Carboniferous to Middle Early Permian (van de Poll, 1983). Sandstone is the dominant rock type with a texture ranging from very fine to very coarse. Regionally, the bedrock is either flat lying or dipping gently to the east, northeast or north. There has been little structural deformation of these sedimentary rocks; however, steeply dipping joints in excess of 75° are common (van de Poll, 1983). The bedrock is overlain by a thin veneer of glacial deposits (1-5m). This overburden is primarily basal till of local origin, and covers most areas of the watershed.

Characteristics of the local aquifer are drawn from field observations, drilling, pumping tests and previous work performed in the nearby Winter River watershed (~30 km east of the Wilmot area; Francis, 1989). The uppermost portion of the sandstone red bed formation forms a fractured-porous aquifer, characterized by significant fracture permeability dominated by horizontal bedding plane fractures, in addition to intergranular porosity. These features are evidenced by the apparent “semi-confined” and delayed drainage effects observed in pump tests in the watershed and elsewhere in the Province. Work performed in the Winter River watershed concluded that horizontal layering of the aquifer along with the predominance of horizontal bedding plane fractures leads to a stratified aquifer with a vertical component of hydraulic conductivity ranging from one to three orders of magnitude less than horizontal values. Multi-level slug tests in the watershed have shown that hydraulic conductivity of the aquifer generally decreases with depth (Paradis *et al.*, 2006), which agrees with previous findings by Francis (1989). From the viewpoint of water supply, the permeability of the bedrock decreases to near negligible levels at depths of 200m. Typical industrial or commercial well yields in the Province as a whole range from 300 to 2000 m³/d.

Mean annual precipitation in the study area is ~1060 mm. Most of the precipitation occurs as rain (80%) with the remaining portion as snow. The aquifer is recharged through the tills or outcropping red beds, and discharges as a combination of base flow, evapotranspiration, pumping withdrawals and seepage at the coastline. Jiang *et al.* (2004) examined the monthly recharge between 1995 and 2001, and found recharge rates in the watershed range from 300 mm/yr. to 450 mm/yr. with an average of 400 mm/yr. (35% of annual precipitation in 2001 and 34.6% in 1998 respectively) depending on the precipitation processes and soil conditions. The aquifer demonstrates rapid hydraulic response to recharge, and a major recharge event due to snow melting occurs in April followed by a recession throughout the summer and early fall. A second recharge event often occurs in October or November corresponding with fall rains and lack of evapotranspiration. Discharge mainly occurs along stream channels and fresh water wetlands. The water table configuration mimics topography. Current GW extraction within the Wilmot watershed is minimal, with the exception of the Wilmot well field at the extreme north-western end of the basin, down-gradient of the principle region of interest. Throughout the remainder of the Wilmot watershed GW extraction is essentially limited to sparsely distributed domestic wells, and will have virtually no influence on the geometry of the flow system.

Stream-aquifer interaction is one of the key processes governing GW flow regime in the watershed. The Wilmot River and its tributaries discharge GW as seepage along most segments

in the watershed. Modelling work showed base flow accounts for ~66% of annual stream flow and >80% in the late summer and fall months in many years in the watershed (Jiang *et al.*, 2004). The main stem of the stream is ~13.4 km in length and the stream width ranges from ~0.1 m at the head and 30-200m at estuary segment. Sediments, comprised of a mixture of sand, silt and clay, cover the bedrock/till streambed. Seepage meter measurements in the Winter River watershed (Francis, 1989) show a vertical hydraulic gradient exists within the streambed sediments. The streambed materials, typically ~1.0 m in thickness in the Winter River watershed, act as weakly permeable unit that retards the hydraulic link between surface water and GW.

4.3 Groundwater flow modelling

A 3-D model was developed using ModFlow Pro v.4.0 (Waterloo Hydrogeologic Inc., 2004) for the Wilmot Watershed, and steady state simulations run to establish the configuration of the local GW flow regime. The sandstone aquifer and the saturated portion of the till is simplified as a horizontally isotropic and vertically anisotropic (i.e. $K_x=K_y>K_z$), three-dimensional laminar flow system. The model domain covers the whole Wilmot River watershed, as well as portions of the adjacent Barbara Weit and Rayners Creek watersheds (Fig. 4.1).

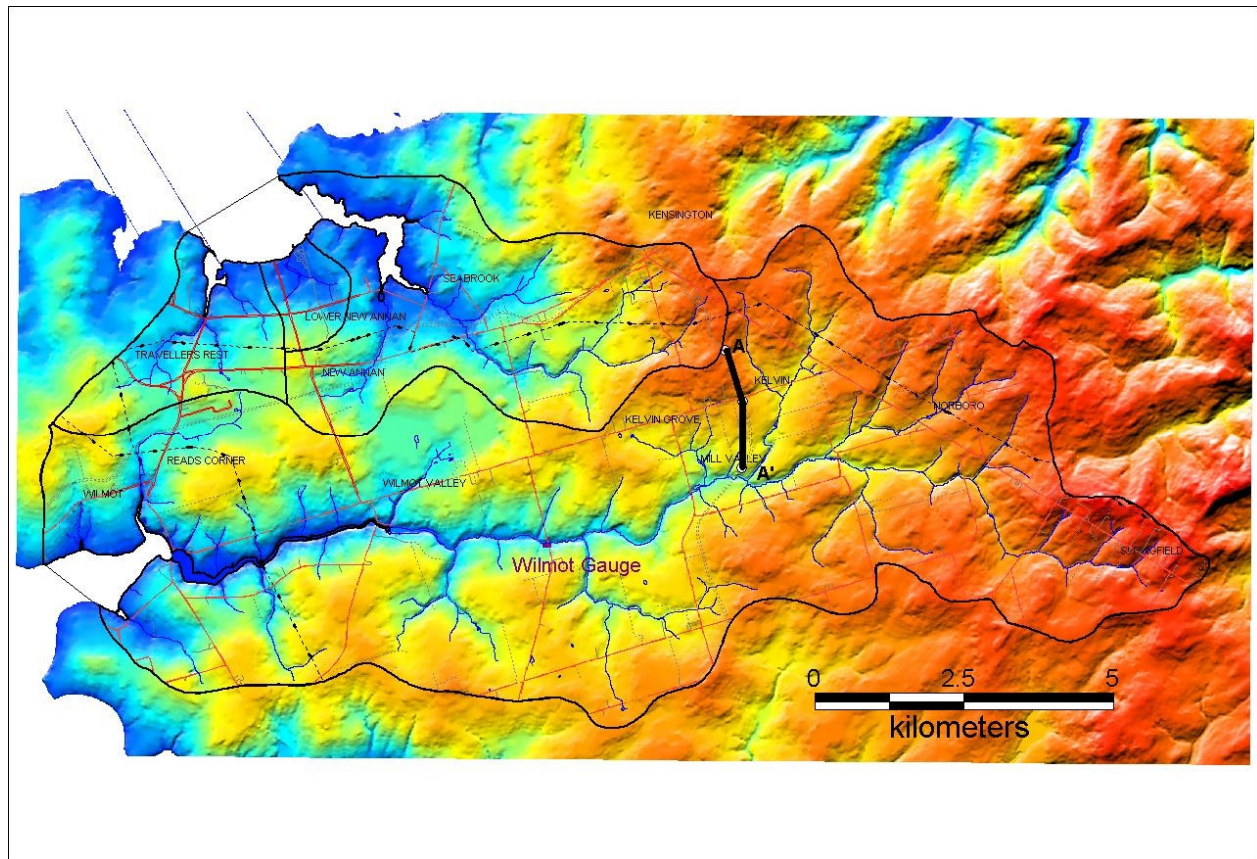


Figure 4.1. Model domain for ModFlow simulations – Wilmot Watershed, showing location of transect A-A’.

Groundwater divides along the external boundary of the model domain are assumed following surface water divides and considered impermeable. The GW divide between the Wilmot River

watershed and the adjacent Barbara Weit and Rayners Creek watersheds are similar but not completely consistent with surface water divides. Sources and sinks, consisting of precipitation infiltration, wells, stream/aquifer interaction and evapotranspiration, are included in the system.

Vertically, the model is divided into 15 layers, with thicknesses varying from 6 to 26m. Horizontal grid spacing is set at ~95 m and streams are represented as river boundaries to allow for simulation of mass transport using MT3DMS, the mass transport code used with Visual MODFLOW (Waterloo Hydrogeologic Inc., 2004). Figure 4.2 presents a schematic representation of layer discretization and delineation of boundary conditions employed in the model.

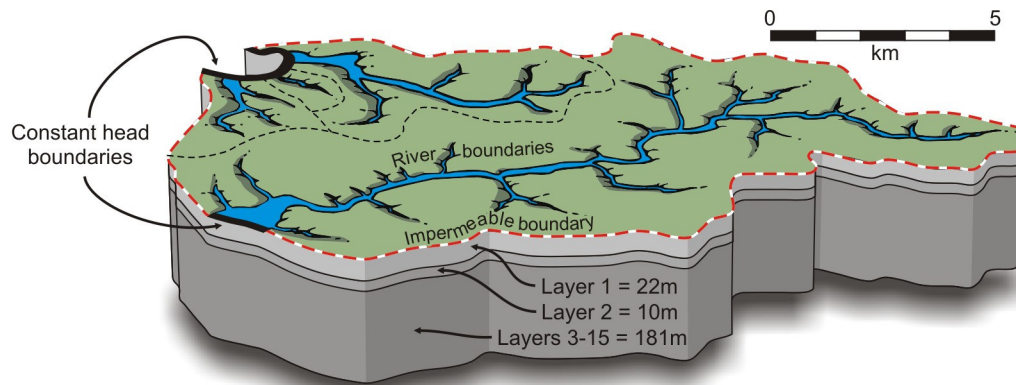


Figure 4.2. Vertical discretization and boundary conditions for ModFlow simulations for the Wilmot watershed.

The model has been calibrated based on measurements from private wells and multi-level piezometer measurements. Given 27 measurements, the calculated water levels agree with the measurements with a normalized RMS of 7% and a correlation coefficient of 0.97. The simulated heads from a transect of multi-level piezometer nests (location indicated in Fig. 4.1) compare with the measured heads with a normalized RMS of 14% and a correlation coefficient of 0.94. The model is further checked against a monthly stream base flow time series between 1995 and 2001, and the recharge used in the model is based on Jiang *et al.* (2004). By reference to Figure 4.3, one can see that the model reproduces the base flow processes with a good agreement. It is noted that the recharge used in July, August and September of the simulated hydrogeological windows usually is very low and therefore the simulated base flows essentially represent the recession processes of aquifer discharge. Specific yields determined by simulating the recession process will represent the bulk values of the watershed as a whole. The specific yields determined through the modelling range from 0.05 to 0.1. Hydraulic properties used in the model are summarized in Table 4.1.

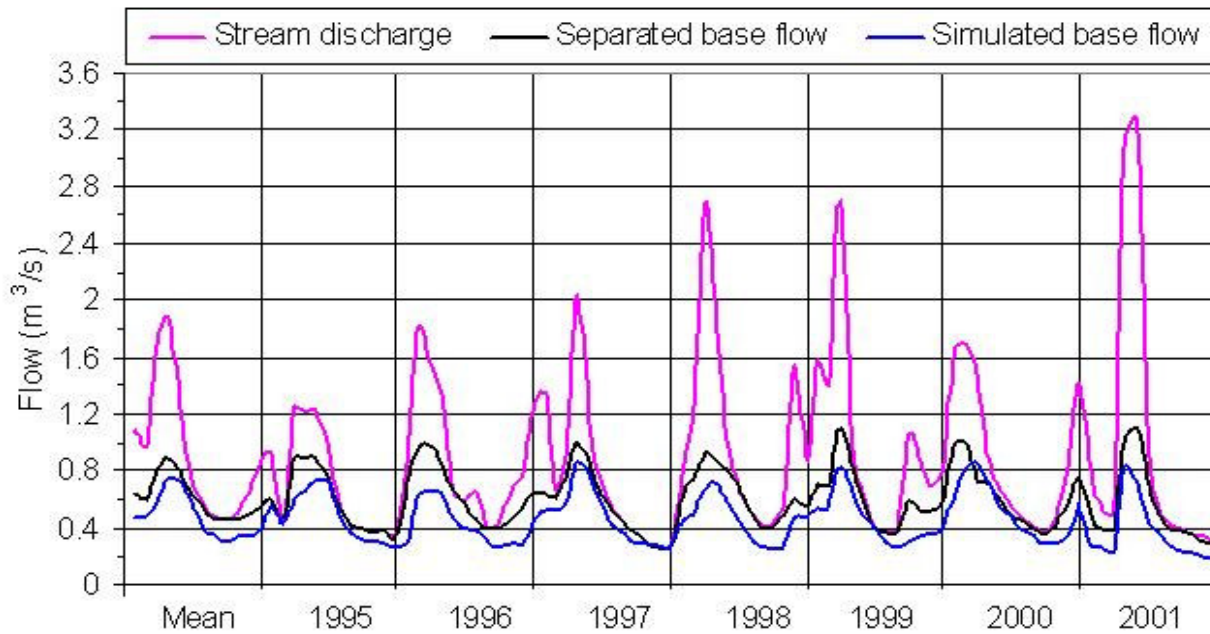


Figure 4.3. Comparison of separated and simulated base flows at the Wilmot River gauging station.

Table 4.1. Hydraulic properties used in the Wilmot River watershed groundwater model.

Layer #	Layer thickness (m)	Horizontal hydraulic conductivity (m/s)	Vertical hydraulic conductivity (m/s)	Specific yield (%) / storage (m^{-1})	Effective porosity
1 (top)	22	$2 \times 10^{-4} \sim 6 \times 10^{-5}$	$1 \times 10^{-9} \sim 2 \times 10^{-8}$	$0.05 \sim 0.1 / 1 \times 10^{-4}$	$0.05 \sim 0.07$
2	10	$1 \times 10^{-5} \sim 5 \times 10^{-4}$	$1 \times 10^{-9} \sim 1 \times 10^{-8}$	$0.07 / 1 \times 10^{-5}$	0.06
3	8	5×10^{-4}	1×10^{-8}	$0.07 / 1 \times 10^{-5}$	0.06
4	6	3×10^{-4}	5×10^{-9}	$0.07 / 1 \times 10^{-5}$	0.06
5	6	3×10^{-4}	5×10^{-9}	$0.07 / 1 \times 10^{-5}$	0.06
6	18	1×10^{-4}	5×10^{-9}	$0.05 / 1 \times 10^{-5}$	0.05
7	6	1×10^{-4}	5×10^{-9}	$0.05 / 1 \times 10^{-5}$	0.05
8	10	1×10^{-4}	1×10^{-9}	$0.05 / 1 \times 10^{-5}$	0.05
9	10	1×10^{-4}	1×10^{-9}	$0.05 / 1 \times 10^{-5}$	0.05
10	12	5×10^{-5}	1×10^{-8}	$0.05 / 1 \times 10^{-5}$	0.05
11	15	5×10^{-5}	1×10^{-8}	$0.05 / 1 \times 10^{-5}$	0.05
12	12	1×10^{-7}	1×10^{-9}	$0.05 / 1 \times 10^{-5}$	0.05
13	26	1×10^{-7}	1×10^{-9}	$0.05 / 1 \times 10^{-5}$	0.05
14	26	1×10^{-7}	1×10^{-9}	$0.05 / 1 \times 10^{-5}$	0.05
15 (base)	26	1×10^{-7}	1×10^{-9}	$0.05 / 1 \times 10^{-5}$	0.05

Three dimensional simulations and previous work elsewhere in the province (Francis 1989) suggest that horizontal hydraulic conductivity is several orders of magnitude higher than vertical conductivity. The characteristic of significant vertical anisotropy ($K_h \gg K_z$) results in laterally dominated flow in the aquifer. Because the parameters necessary to allow ModFlow to deal

explicitly with a dual porosity aquifer are not known for the study area, an approach was needed that would reproduce the effect of the very high degree of anisotropy between horizontal and vertical K, resulting from the important influence of the dominantly horizontal fracture sets in the aquifer on GW flow geometry. The use of the very low K_v has been employed to allow the model to reproduce the observed head distribution, while maintaining realistic bulk hydraulic conductivity values. It is found that vertically multiple flow systems exist, roughly corresponding to the stream network; the shallow systems, occurring from the water table to a depth of ~50m, discharge into the nearby tributaries and the boundaries of the deep flow systems (below ~50m) do not necessarily follow the surface water divides as the shallow flow systems do.

It is noted that the model is calibrated using a trial-and-error procedure and the hydraulic properties are zoned arbitrarily in the absence of sufficient geological evidence. In the Wilnot case, the aquifer is relatively homogeneous and the arbitrary zoning should not compromise confidence on the model.

4.4 Nitrate transport modelling

Transient nitrate transport simulations, using MT3DMS (Waterloo Hydrogeologic Inc., 2004), were conducted to estimate the current distribution of nitrate throughout the aquifer, and to predict GW nitrate conditions in the future, both under existing nitrogen input rates, and under several scenarios of differing N inputs. The results of the simulations shed light on the long-term implications of current land use practices, and on the degree of adjustment to these practices that may be required to effect positive water quality changes in the watershed.

Modelling of current nitrate distributions is based on historical information (Barry Thompson, personal communication) on the evolution of land use practices for the period 1965 to present. Predictive simulations, extending to 2100, begin with current estimated nitrogen distributions, with nitrogen inputs adjusted to reflect different land use scenarios including: continuation of current land use practices, a 20% increase over current N input rates, and reductions in N input rates to 1995, 1965 and pre 1965 levels.

Because a full description of the distribution of nitrate throughout the model domain under all these scenarios would be extremely lengthy, we use predicted nitrate levels at different depths, at a particular point in the watershed, to illustrate the “typical” response of the system to changes in N-inputs. The point chosen is mid-way between the watershed boundary and the discharge point of the flow system at the river (approximately corresponding to the midpoint of the transect shown on [Figure 4.1](#), representing conditions where lateral GW flow is dominant, as is expected throughout most of the model domain. Three depth intervals were chosen: shallow, (0-22m, reflecting expected base flow concentrations), intermediate (32-40m, representative of the zone tapped by most domestic wells) and deep (52-68m). It is noted that these conditions do not represent mean nitrate concentrations within the aquifer, nor do they represent those of the entire flow system, however they should reflect the average conditions prevailing throughout much of the watershed, and therefore, throughout the remainder of this work, these sites are referred to as shallow, intermediate and deep GW.

Groundwater is assumed to receive nitrate loading from fertilizer, mineralization and nitrification of soil organic nitrogen, manure, sewage, and atmospheric deposition. Land uses are grouped into

two categories, i.e. under potato production rotation and not under potato production, based on GIS data of 1995 to 2005. Spatial changes in land use practices are assumed to be fixed for the period of 1965 and 2005, with a lower N-loading rate assigned for the period prior to the 1980's to account for less intensive potato production in this period. The initial mass of nitrate leached from the polygons assigned to potato production is estimated from field-scale nitrate budget analyses based on approaches and parameters described in Delgado *et al.* (2001), Macleod *et al.* (2002a), Kraft & Stites (2003), Vet (Environment Canada, pers. com., 2005) and B. Thompson (pers. com., 2004). Both the temporal evolution of nitrogen application rates and crop rotation practices are taken into account when leaching mass is estimated. The estimated mass is then converted into recharge concentrations using a recharge rate=400mm/yr. The initial estimation is refined through model calibration.

It is assumed that the transport of nitrate in GW is controlled by advection-dispersion processes. The correct treatment of dispersivity requires knowledge of site specific parameters (α_L , α_T , D) which are not known for the Wilmot aquifer. As a result, longitudinal dispersivity has been set at 10 m and the ratios of horizontal to longitudinal dispersivity and vertical to longitudinal dispersivity are assumed to be 0.1 and 0.01 respectively. Because we are dealing principally with distributed sources of nitrate in a dominantly fast flowing system where we expect advection to be the dominant factor in mass transport, we believe that this limitation will be of minor consequence to the overall mass transport simulations. The value used for effective porosity is 0.05-0.07. Based on evidence from stable isotopes and other hydrogeochemical analyses (Savard *et al.*, 2004), nitrate is further assumed to be non-reactive, with processes such as retardation, absorption and denitrification being negligible (Chapter 3). The initial nitrate concentration in GW is set at 1.0 NO₃-N mg/L, representing background levels derived from GW base flow concentrations at that time. The transport model is calibrated against the measured nitrate levels in the Wilmot River from 1985 to 1998. The calibrated mass input is shown in [Table 4.2](#).

Table 4.2. Estimated N loading to groundwater in the Wilmot River watershed (values are averages in the rotation cycles; watershed area=112 km²).

Period	Average loading (kg/yr)	Average NO ₃ -N flux (kg/km ² .yr)	Recharge concentration (mg/l)				Crop rotation (years)
			Potato	Grain	Hay/grass	Other	
Pre-65	55115	492	1	1	1	1	-
1965-1973	185785	1659	6	5	5	1	2
1974-1988	265355	2369	12	5-6	5-6	1	2
1989-1998	333610	2979	16	6-9	5-6	1	2.5
1999-2005	387265	3458	17	9	7	1	2.5

Using historical inputs for the period 1965 to the present, predicted nitrate levels are comparable values observed in piezometers located along the transect shown in [Fig. 4.1](#), in the mid-point of the basin for shallow, intermediate and deep portions of the aquifer at 7.6, 7.0 and 4.0 mg/L respectively (Annex; wells # 11681, 11682 and 11683). Furthermore, a comparison of simulated discharge concentrations (base flow) agrees very well with long-term observations of dry-weather

flow in the Wilmot River for the period of record (Fig. 4.4). Simulated concentrations in GW cannot be as easily matched to measurements from individual private wells because of the many uncertainties with local source release processes, hydraulic properties, unknown well construction specifications, etc. In contrast, nitrate concentrations in the base flow contribution to the river should represent an integration of GW quality conditions throughout the watershed, and thus should provide an appropriate basis for comparison with modeled results.

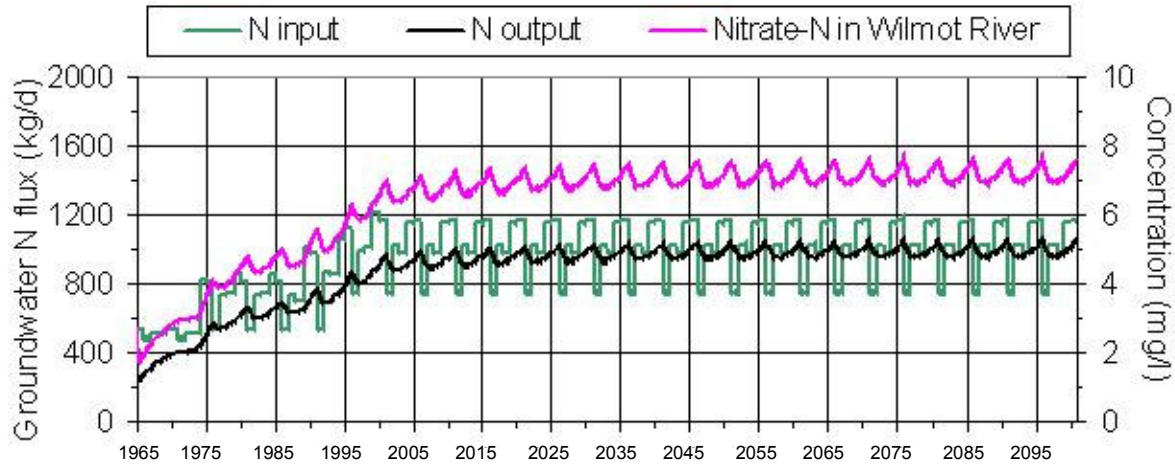


Figure 4.4. Simulated N input, output and NO₃-N concentration in the Wilmot River over time.

From the year 2000 to present, the difference between N mass input and output from the aquifer in the modelled area ($\sim 112 \text{ km}^2$) is estimated to be $\sim 100 \text{ kg N}_3\text{O-N/day}$. This surplus N is transferred to the deeper portions of the aquifer and contributes to the progressive degradation of deeper GW in the watershed. The model predicts that under these current nitrogen input conditions, shallow GW (and thus base flow to streams) responds relatively quickly to nitrate leaching from the crop lands and the nitrate reaches quasi-steady state within a few years with nitrate concentrations not exceeding 8.5 mg/L within the simulated time period. Nitrate concentrations at intermediate depths are predicted to increase for some 30 years if current practices continue, stabilizing at a concentration of approximately 8.5 mg/L. For deeper GW (52 to 68m), nitrate concentrations are predicted to rise slowly throughout the entire simulation period, reaching almost 7 mg/L by 2050, and exceeding 7 mg/L by 2100. Figure 4.5 illustrates the predicted migration of the nitrate plume through time for the transect oriented perpendicular to the basin axis, and located approximately in the mid-point of the basin (located on Fig. 4.1).

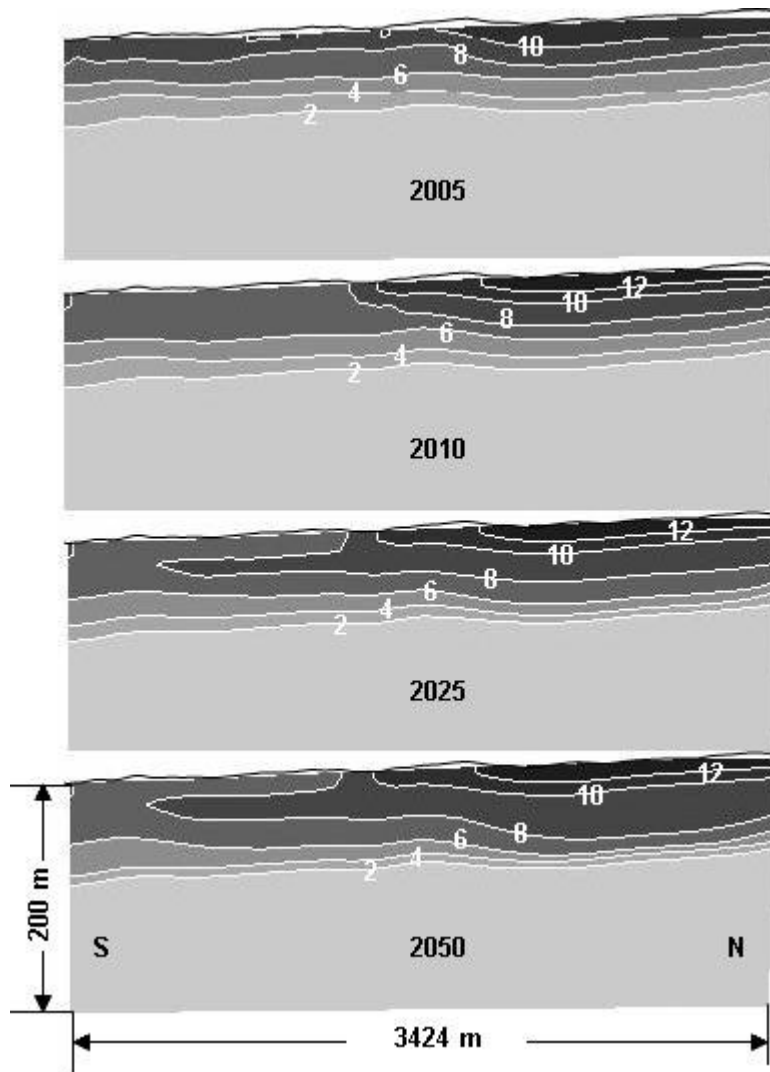


Figure 4.5. Simulated concentration (mg/L) contour of $\text{NO}_3\text{-N}$ (N input=2005 level applied from 2005 to 2050) in groundwater along the Confederation Trail transect, illustrating distribution of nitrate in response to variable N-inputs based on local land use.

For scenarios involving alternate, future land use influences, N input rates on model polygons occupied by potato crop rotations have been adjusted, and other inputs held constant. The simulations (Fig. 4.6) show little difference between the results noted above for current N-input rates, and a scenario involving a 20% increase in N loading, with the higher rate leading to a corresponding increase in steady state nitrate concentrations of approximately 1 mg/L (10 mg/L for shallow and intermediate depths, and a little more than 8 mg/L but still climbing throughout the simulation period for deep GW). The observed responses occur quickly in shallow GW (~ 5 years) whereas in intermediate and deeper zones, the majority of change in nitrate concentrations is predicted to occur over a periods of approximately 30 and 60 years respectively.

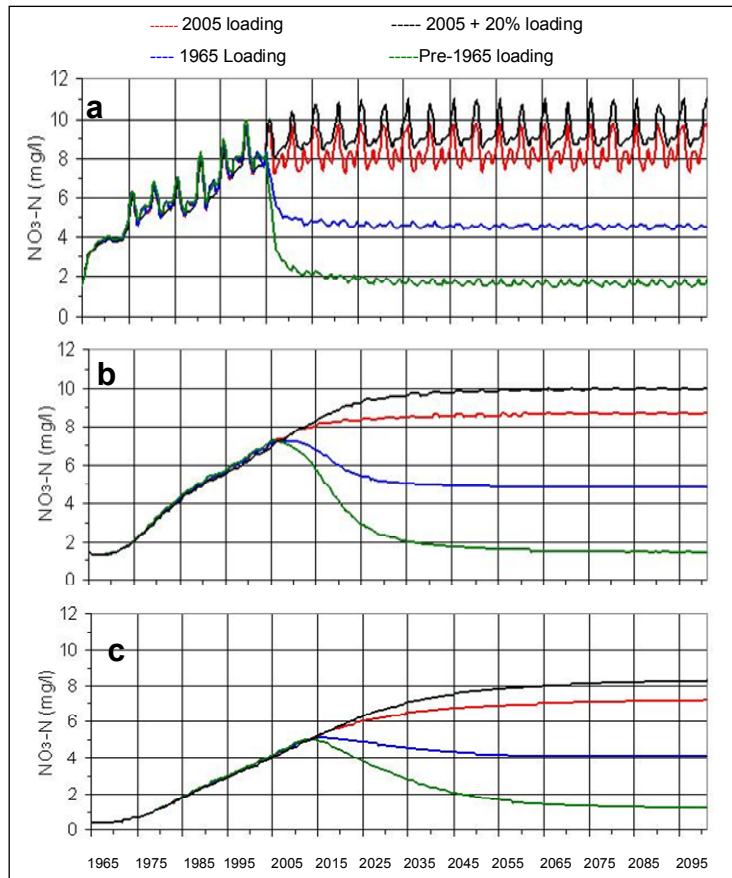


Figure 4.6. Simulated $\text{NO}_3\text{-N}$ concentrations over time at various aquifer depths (a =shallow, b = intermediate and c. = deep), under varying N-inputs.

When nitrogen inputs are reduced to 1965 levels, significant reductions in GW nitrate concentrations are observed, again occurring rapidly in shallow portions of the flow system, and more gradually in intermediate and deep portions of the aquifer. Predicted nitrate concentrations at the end of the simulation period are 5.5, 5.0 and 4.2 mg/L for shallow, intermediate and deep zones respectively under this scenario. A simulation was also run assuming a return to virtually no agricultural inputs, corresponding to essentially pristine conditions. Timing of responses again varied by depth, with nitrate concentrations at the end of the simulation period 1.5 to 2 mg/L at all depths.

4.5 Conclusions

Groundwater models are developed to assess nitrate contamination of GW in the Wilmot River watershed in the central west portion of Prince Edward Island. Vertically, the model maps out multiple flow systems within the active flow zone, roughly corresponding to the stream network. Significant vertical anisotropy ($K_h \gg K_z$) of the aquifer results in laterally dominated flow, which governs the distribution and migration of nitrate in the aquifer.

Nitrate concentrations in GW can be correlated in time with fertilizer application rates, and model simulations based on historical nitrogen inputs since 1965 result in current nitrate levels comparable to observed values for shallow, intermediate and deep portions of the aquifer. Continuing with existing (2005) rates for N input, simulations forecast that shallow and intermediate GW nitrate concentrations will both climb to the range of 8.5 to 9 mg/L, with shallow GW reaching an essentially steady state by 2010, and at intermediate depths by 2025. Nitrate concentrations in the deepest portions of the aquifer rise throughout the simulation period, reaching nearly 7 mg/l by 2050.

Simulations were also conducted to investigate the impact of different N-input rates on GW nitrate concentrations. The results indicate that if starting in 2005, nitrogen inputs were reduced to levels typical of the mid 1960's, shallow and intermediate GW will reach steady state concentrations of approximately 5 mg/L by 2010 and 2037 respectively. For the deepest portion of the flow system, nitrate levels are predicted to decline to a little over 4 mg/L by 2050. If anthropogenic N inputs were eliminated entirely (see pre-1965 N loading, [Fig. 4.6](#)), nitrate concentrations are predicted to fall to below 2 mg/L (essentially pristine conditions) by 2010, 2040 and 2053 for shallow, intermediate and deep portions of the aquifer respectively. Simulations were also conducted for nitrogen input rates representing an increase of 20% above current rates, however the results do not differ substantially from those based on current nitrogen input rates with an overall increase in nitrate concentrations of approximately 1 mg/L.

Overall, it is clear that N inputs would need to be reduced substantially below current levels before any significant change in corresponding GW nitrate levels could be expected. Reduction in N inputs should result in improvements in nitrate levels in shallow GW and associated streams within a few years and gradually reverse the trend of increasing nitrate levels in the aquifer, however for the deeper GW, including those tapped by typical domestic wells, similar reductions will take at least several decades.

5 Watershed-scale numerical modelling of nitrate transport using spatially uniform averaged N inputs

Daniel Paradis, Jean-Marc Ballard & René Lefebvre

ABSTRACT

A numerical model of groundwater flow and nitrate transport was calibrated to reproduce present-day hydraulic conditions, stream flow and nitrate concentrations in the Wilmot basin aquifer system. Available data were used to estimate the historical evolution of nitrate loadings in the watershed from 1955 to 2000. The numerical model was used to predict the potential future evolution of nitrate concentrations in the aquifer and surface water under three hypothetical future nitrate loading scenarios: constant loading, around 20% increase over 55 years and zero loading. Results show that major changes in agricultural practices would be required in the short term and maintained in the future to see improvements in groundwater quality over the Wilmot watershed. Otherwise, nitrate concentrations would continue to increase above their average present-day concentration of 6.6 mg/L, so that an even larger proportion of wells than presently would exceed the 10 mg/L maximum drinking water nitrate concentration over the watershed.

5.1 Introduction

In the context of the nitrate problem in Prince-Edward Island (PEI) presented in Chapter 1, this study aims at understanding what controlled the increase in nitrate concentrations in the aquifer and the Wilmot River recorded over the past 50 years. This research is designed to support predicting the evolution of nitrate concentrations in the aquifer system, and aquifer management decisions, especially in relation to agricultural activities.

The Wilmot watershed ([Fig. 5.1](#)) was selected for the study because it is representative of the relatively uniform geology, the typical watersheds with small streams and basins and of the hydrogeological conditions of PEI (Prest, 1973; Van de Poll, 1983; Francis, 1989). The hydrogeological general context makes the aquifers vulnerable to surface contamination. The Wilmot Watershed, representative of PEI in general, constitutes a priority in term of the nitrate problem: total dependence of its population on groundwater (GW) from private wells, vulnerable aquifer, strong link of streams to GW, and widespread agricultural activities having a vital economic role.

To achieve the cited objectives, a 3D GW flow and mass transport numerical model of the aquifer system in the Wilmot Watershed was developed. The use of a numerical model based on field-derived hydraulic properties at the watershed scale provides a unique way to integrate and explain field observations on nitrate concentrations. To support the development of that model, field work was also carried out. Other studies focussed on modelling nitrate transport through the watershed complementary to this work are presented in Chapters 4 and 8.

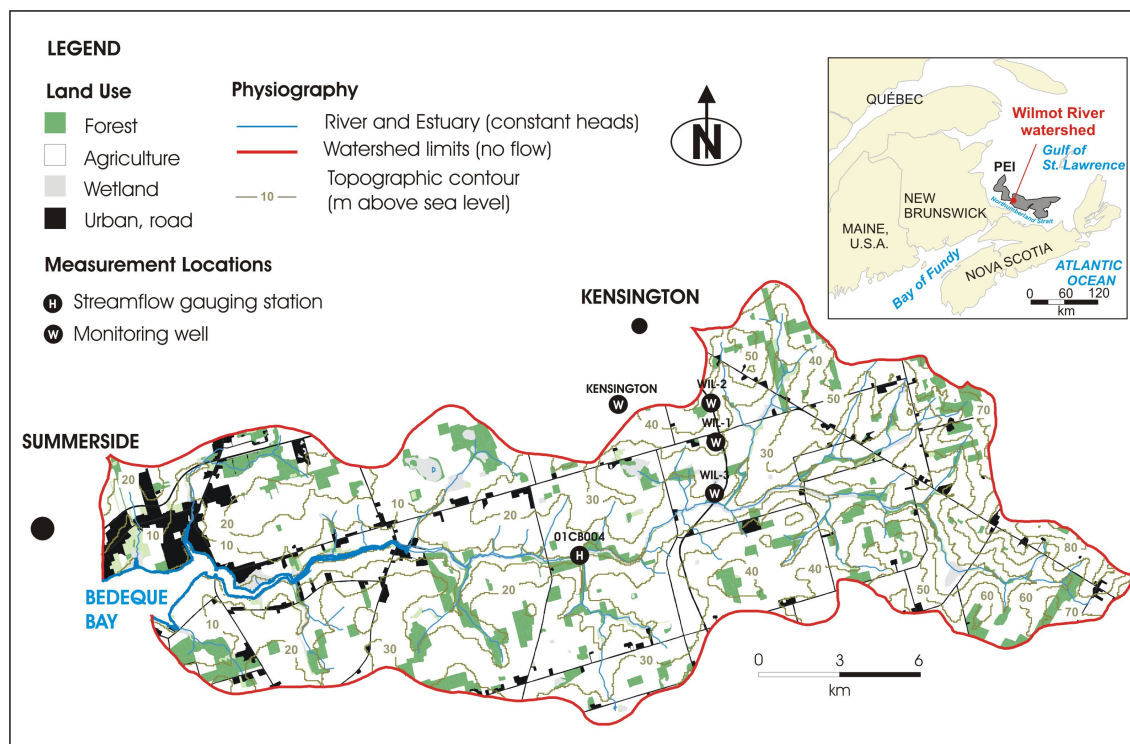


Figure 5.1. Location of Prince Edward Island (inset map) and the Wilmot River Watershed.

5.2 Conceptual Model of the Groundwater Flow System

5.2.1 Regional context

The Wilmot watershed is located in west central PEI (Fig. 5.1). The river drains an area of about 87 km² and flows south-westerly to the Bedeque Bay. The basin averages 17 km long by 5 km wide (Table 5.1). Half of the river is tidally influenced and its elevation ranges from sea level in the tidal area, to 90 masl (meter above sea level) in the headwater area.

The Wilmot watershed is predominantly rural with less than 10% of its surface dedicated to residential uses (Fig. 5.1, Table 5.1). The largest urban centre near the watershed is Summerside, with a population of 14,654 (2001 Census), located adjacent to the northwest corner of the watershed. Agricultural activities cover 76% of the watershed, small patches of forest occupy 11%, urban areas, 9%, and the rest (4%) is occupied by wetlands and recreational areas.

The climate of PEI is humid-continental, with long, fairly cold winters and warm summers. Mean annual precipitation at the Summerside meteorological Station A is 1078mm (1971-2000), most of which falls as rain (75%) (Table 5.2). The mean annual temperature is about 5.1 °C and means for monthly temperature range from minus 8.6 °C in January to 18.4 °C in July. Streamflow data for the Wilmot River have been collected at a gauging station (Water Survey of Canada station 01CB004 on Fig. 5.1) located above the tidally influenced portion of the river. At the station, the

mean annual discharge of the river is $0.92\text{m}^3/\text{s}$ (1972-1999) and the mean monthly discharge ranges from $0.45\text{m}^3/\text{s}$ in September to $1.88\text{m}^3/\text{s}$ in April, during the spring freshet.

Table 5.1. Main characteristics of the Wilmot River Watershed (Flow rates are for the 1972-1999 period recorded at the *01CB004* station located above the tidally influenced portion of the river; Land uses are based on a LANDSAT image for year 2000).

Physiography	
Area	84 km^2
Average width	5km
Average length	17km
Elevation (above sea level)	0-90m
Wilmot River Flow Rate	
Mean annual	$0.92\text{ m}^3/\text{s}$
Minimum monthly mean (Sept.)	$0.45\text{ m}^3/\text{s}$
Maximum monthly mean (April)	$1.88\text{ m}^3/\text{s}$
Land Use	
Agriculture	76%
Forest	11%
Urban, road	9%
Wetland, recreational	4%

Table 5.2. Weather and water balance for the Wilmot River Watershed (Meteorological data are for the 1971-2000 period recorded at the *Summerside A* station).

Weather	
Mean annual total precipitation	1078 mm
Mean annual rain	809 mm
Mean annual snow	269 mm
Mean annual temperature	$5.1\text{ }^{\circ}\text{C}$
Minimum mean monthly temperature	$-8.6\text{ }^{\circ}\text{C}$
Maximum mean monthly temperature	$18.4\text{ }^{\circ}\text{C}$
Water Balance	
Mean annual evapo-transpiration	438 mm
Mean annual runoff	230 mm
Mean annual recharge	410 mm

5.2.2 Hydrogeology

The Wilmot watershed area is almost entirely covered by glacial material defined as permeable unconsolidated sandy tills, a few centimetres to several meters thick (Prest, 1973). That layer is underlain mostly by fine to medium-grained fractured sandstone (80-85%) with some siltstone and claystone forming isolated lenses (Van de Poll, 1983). The sandstone is a fractured porous medium characterized by a well-developed network of fractures and a high porosity matrix (17% on average for sandstone according to Francis, 1989). The aquifer is unconfined, except in small

zones where less permeable mudstone beds alternate with sandstone to form semi-confined conditions. The water table is generally located in the first 20m of the sandstone aquifer and follows the topographic relief. A schematic hydrostratigraphic column of the aquifer is shown on Figure 5.2a.

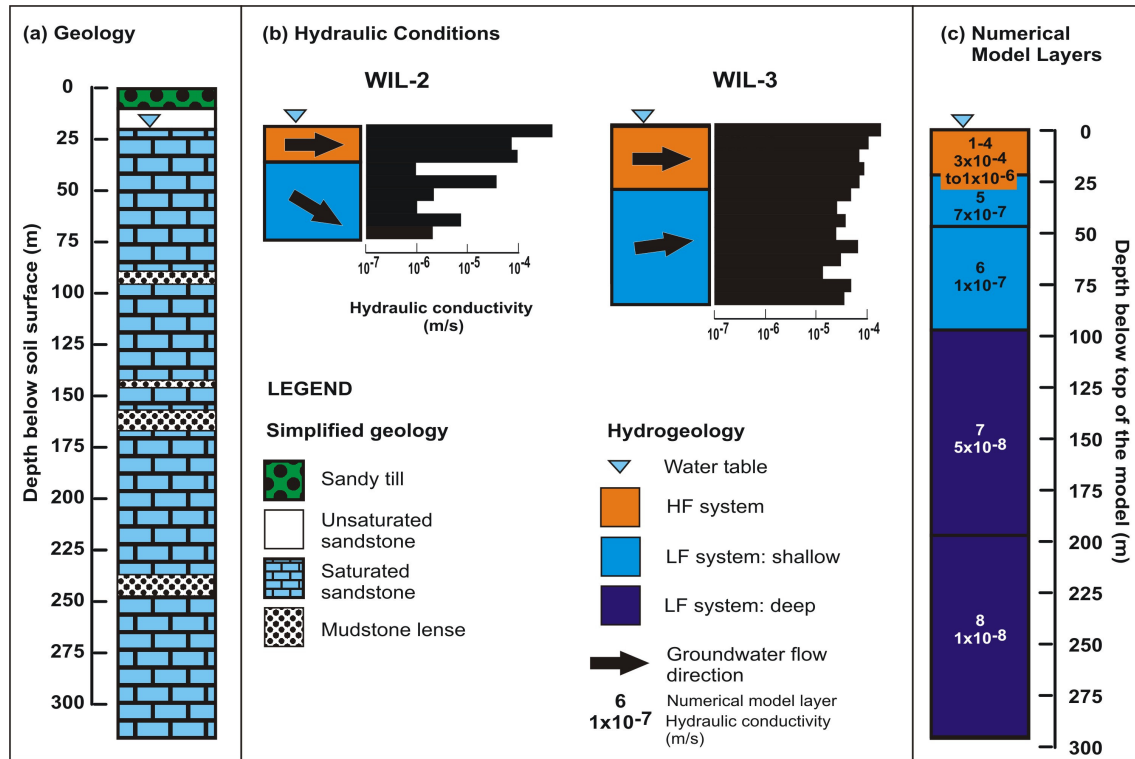


Figure 5.2. Conceptual model of the groundwater flow system and discretization of the numerical model: (a) geology; (b) hydrogeological conditions; and (c) numerical model layers.

Locations of WIL-2 and WIL-3 are shown on Figure 5.1.

To support the model development, field work was conducted to evaluate the flow properties of the aquifer. The field characterization was based on three sets of three nested piezometers installed along a transverse section through the watershed (locations of monitoring wells WIL-1, WIL-2 and WIL-3 shown on Figure 5.1). The monitoring wells reach depths between 1 to 100 m below the water table. Profiles of hydraulic conductivity, hydraulic heads, nitrate concentrations and GW age were obtained by isolating boreholes with a 6m interval double-packer.

A hydraulic conductivity measurement using multi-level slug tests for the sandstone unit range from 9×10^{-7} to 4×10^{-4} m/s. Hydraulic conductivity measured with a laboratory permeameter ranges from 10^{-8} to 5×10^{-7} m/s for sandstone and is lower than 5×10^{-10} m/s for mudstone (Francis, 1989). Comparison between field and laboratory measurements suggests that fractures play an important role in the rock permeability. Hydraulic conductivity generally decreases with depth, as a result of decreasing fracture aperture and frequency. Typically, hydraulic conductivity profiles show a strong vertical to horizontal anisotropy that ranges from 2 to 3 orders of magnitude due to alternating high and low hydraulic conductivity layers and the predominance of sub-horizontal bedding plane fractures over sub-vertical fractures.

The hydraulic conductivity profiles for monitoring wells WIL-2 and WIL-3 shown on [Figure 5.2b](#) indicate that the sandstone aquifer comprises a high flow (HF) and a low flow (LF) system. The HF system extends from the water table to a depth of 18 to 36m, the LF system being under the HF. Groundwater flow within the HF system is mostly horizontal whereas flow inside the LF system is characterized by an important vertical downward gradient near the GW divide that becomes flat toward the middle of the section and upward near the Wilmot River. Hydraulic conductivities in the HF system are always relatively high and average 1.3×10^{-4} m/s, whereas in the LF system the average conductivity is an order of magnitude lower at 3.5×10^{-5} m/s, and it is also more variable with a range between 8.4×10^{-7} and 1.7×10^{-4} m/s.

Tritium analyses on GW samples indicate an age younger than 50 years in the HF system. In the shallow LF system, Carbon-14 analyses on GW samples suggest an age between 5 000 to 7 000 years.

Based on the conceptual GW flow model ([Fig. 5.2](#)) and GW age dating, it is inferred that GW flow predominantly occurs in the HF system. The HF system is relatively shallow and in good contact with the Wilmot River as will be shown in the next section. Nitrate transported to the aquifer by infiltration of precipitation will first reach the shallow HF system. Nitrate is likely to be transported mostly in the HF system, together with the dominant GW flow. It is thus thought that nitrate found in the Wilmot River is coming predominantly from the HF system. However, it is also likely that a proportion of the nitrate transported in the HF system has also reached the underlying LF system. Considering the reduced GW flow and the mostly large GW ages encountered in the LF system, the nitrate that may be present in the LF system may not have yet reached the Wilmot River. The numerical modelling of GW flow and nitrate transport in the Wilmot Watershed will allow a verification of these hypotheses.

5.2.3 Groundwater and Wilmot River Interaction

Rivers and streams may represent a source of GW or act as a drain depending on their water level relative to the water table in the underlying aquifer. Observation of GW levels and river stages suggests that the Wilmot River gains water from the aquifer, thus acts as a drain most of the year.

Base flow represents water supplied to the river by the aquifer. The streamflow analysis with filters described by Furey and Gupta (2001) was applied to the Wilmot River, showing that base flow accounts for 63% of the mean annual streamflow (38% of the mean annual precipitation). This analysis also shows that base flow may be the only source of water to the river during summer, except immediately after precipitation events. Moreover, seasonal sampling of nitrate performed over a period of two years (2002-2004) in domestic wells (n=107) and in the Wilmot River (n=17) shows similar average nitrate concentrations as well as water and nitrate isotope properties (Savard *et al.*, 2004; this report, chapter 3). These observations indicate a highly effective connection between the aquifer and the river.

5.3 Numerical Modelling of Groundwater Flow and Nitrate Transport

The main objective of the model is to assess the impact of various scenarios of agricultural practices on the future nitrate level in the Wilmot aquifer. The three-dimensional finite element numerical simulator FEFLOW (Diersch, 2004) was used to reproduce the GW flow system and to simulate nitrate transport in the aquifer.

5.3.1 Aquifer discretization

The aquifer was divided into three main zones (Figs. 5.2c, 5.3): (1) the HF system, (2) the shallow LF system, and (3) the deep LF system. These zones were vertically divided into 8 layers, respectively 4 for HF system, and two for the shallow and two for the deep LF system (Figs. 5.2c, 5.3). The elevations of every slice (top and bottom) of each layer were set from the extrapolated potentiometric map at steady state flowing conditions. Based on the results of the multi-level hydraulic testing, the thicknesses of the first 4 layers were set respectively at 3m, 5m, 5m and 10m. The thickness of both layers 5 and 6 were set respectively at 25 and 50m and the thickness of layers 7 and 8 at 100m each. The resulting three-dimensional mesh contained 60 464 6-node triangular elements and 35,937 nodes with an average element area of 11,114m² (≈ 150 m x 150m).

Table 5.3. Field-based and calibrated hydraulic properties of the Wilmot River aquifer model (K_h and K_v are respectively horizontal and vertical hydraulic conductivity, n is total porosity and S_y is specific yield). The effective diffusion coefficient used in the model is 1×10^{-9} m²/s and longitudinal and transverse dispersivities are respectively 1 and 0.1m.

Model layer # (Depth below water table in m)	Flow System	Field K_h (m/s)	Calibrated Numerical Model			
			K_h (m/s)	K_h/K_v	S_y (%)	n (%)
1 (0-3)	HF	4.5x10 ⁻⁴ to 8.1x10 ⁻⁵	3x10 ⁻⁴	1	1	17
2 (3-8)			7x10 ⁻⁵	70	1	17
3 (8-13)			7x10 ⁻⁶	100	1	17
4 (13-23)			1x10 ⁻⁶	1000	1	17
5 (23-48)	LF	1.7x10 ⁻⁴ to 8.4x10 ⁻⁷	7x10 ⁻⁷	700	1	17
6 (48-98)	Shallow	n.d.	1x10 ⁻⁷	2	1	17
7 (98-198)	LF	n.d.	5x10 ⁻⁸	1	1	17
8 (198-298)	Deep	n.d.	1x10 ⁻⁸	1	1	17

The unsaturated zone was not simulated because water table level fluctuations resulting from infiltrated precipitation through the unsaturated zone show a lag time response of around 5 days (not shown). Furthermore, we assume that nitrate is perfectly soluble in water and that no change is occurring in the nitrate form as it leaves the root zone.

5.3.2 Hydrogeological Parameters

Initial hydraulic conductivity values of the first five layers were taken from multi-levels slug testing and adjusted during calibration (Table 5.3). The hydraulic conductivities for layers 6 to 8 were not measured in the field and are thus based on literature values ranging from 3×10^{-10} to 6×10^{-6} m/s for sandstone (Domenico and Schwartz, 1990). Fractures were not considered in the model and an equivalent porous medium was assumed. Total porosity was based on laboratory results (Francis, 1989) and an average value for sandstone of 17% was used for simulations. The implications for mass transport simulations of considering total porosity rather than only fracture porosity is discussed in section 5.3.6. The ratio of horizontal to vertical hydraulic conductivity for

each model layer was based on both the hydraulic conductivity profiles and the fracture analysis of Francis (1989).

5.3.3 *Boundary conditions*

The potentiometric map of the superficial sandstone aquifer (HF system) shows that the water table surface follows the topography (not shown). As GW flows from the highest to the lowest elevations, the area of the watershed boundaries generally coincides with the delineation of the GW flow system, with the river acting as a GW discharge zone.

The limits of the model were determined by the topographic high contour of the watershed that also corresponds to the GW divides (Fig. 5.1). The Wilmot River including the Bedeque Bay outlet were set as head boundaries with the attribution of specific heads values based on the interpolated potentiometric map. These head boundary conditions assume hydraulic connection between the river and GW. Since river stage fluctuations are small, constant heads nodes were used to represent the river in the layer 1 and the Bedeque Bay in layers 1 to 4.

5.3.4 *Recharge*

Recharge is the process by which GW is replenished by the infiltration of precipitation that reaches the aquifer. Average recharge over the watershed was estimated with streamflow analysis with filters described by Furey and Gupta (2001). Mean annual recharge calculated for 1972 to 1999 with this technique is about 410 mm/yr (Table 5.2). This recharge flux was applied uniformly over the watershed based on the relative homogeneity of the hydro-physical parameters over the area (land use, vegetation, terrain slope, soil type, precipitations).

Analysis of water table fluctuations from 1971 to 1991 indicates no trend in the mean annual water table levels (not shown). A steady-state recharge for the calibration and the prediction periods were then used in the simulation.

5.3.5 *Soil nitrogen available for leaching*

The soil nitrogen available for leaching (SNAL) is inorganic nitrogen (ammonium and nitrate) that remains in the soil at the end of the growing season. The majority of the inorganic nitrogen is nitrate, which is water-soluble and can readily be leached through the soil and enter GW. Hence, the mass of SNAL is an index of the potential for GW contamination by nitrate. To reconstruct a representative historical SNAL over the entire basin (Fig. 5.3), we have used all available pieces of information and even some values or trends available in a nearby watershed (Table 5.4). To make results more readily applicable to other areas, the nitrogen flux and concentration equivalent to SNAL are also provided in Table 5.4. The nitrogen flux is obtained by dividing SNAL by the watershed area whereas the equivalent concentration assumes dilution of the SNAL by the yearly volume of GW recharge over the area.

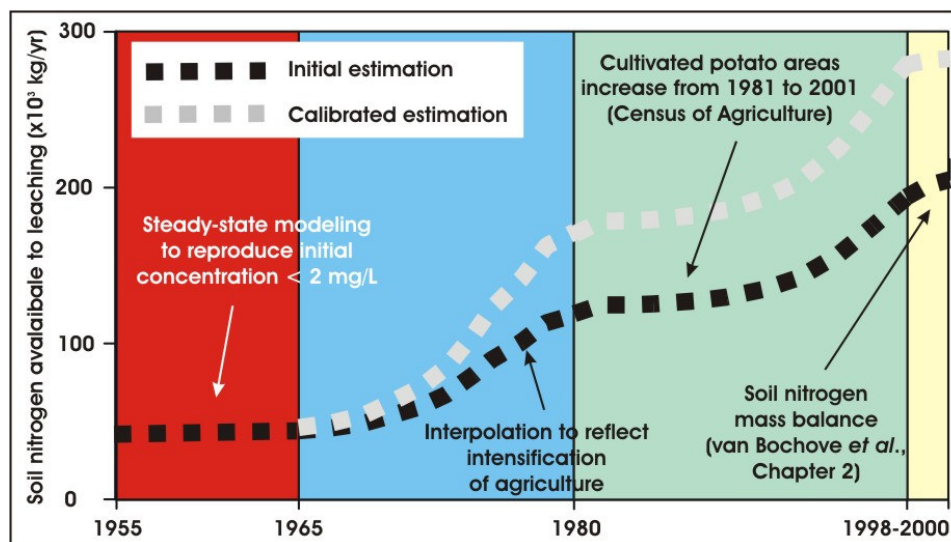


Figure 5.3. Historical nitrogen mass applied over the Wilmot River watershed based on: (1) Soil nitrogen available for leaching van Bochove *et al.* (see Chapter 2); (2) Potato farming area increase from 1981 to 2001 based on the Census of Agriculture (AAFC, 2004); (3) Steady-state modelling to represent pre-modern agricultural conditions; and (4) Interpolation between 1965 and 1980 values.

Table 5.4. Estimates of historical Soil Nitrogen Available to Leaching (SNAL) and equivalent nitrogen flux and concentration over the Wilmot Watershed. Note: calculations used a total watershed area of 87 km² and an annual recharge of 410 mm.

Period	SNAL (kg/yr)	Nitrogen flux (kg/km ² ·yr)	Equivalent concentration (mg/L)	Wilmot potato farming area (Hectare)	Source
1998-2000	207,000	2379	5.8	2000	van Bochove <i>et al.</i> (see Chapter 2)
1981	114,000	1310	3.2	1114	After PEI potato area (AAFC, 2004)
Pre-1955	41,400	476	1.2	-	Simulations

The estimate of present-day SNAL is based on van Bochove *et al.* (see Chapter 2) who used atmospheric nitrogen, crop yields, provincial fertilization recommendations and crop areas to estimate the SNAL from agricultural fields for the period of 1998 to 2000. Crop areas dedicated to potatoes, hay and grain were estimated from LANDSAT images and fertilization recommendations were used for each kind of crops. Total SNAL is around 207 000 kg/yr for the entire watershed. The second estimation of SNAL is based on the Census of Agriculture for crop areas (AAFC, 2004). It was shown that the cultivated potato area for PEI was about 25,000 hectare in 1981 and increased to almost 45,000hectares by 1996. We assumed that the same increase applies for the Wilmot watershed. Hence, the SNAL would have gone from about 114,000 kg/yr in 1981 to 207,000 kg/yr in 1998-2000, assuming that it increased proportionally to the potato crop area. The world-wide introduction of chemical fertilizers as a means to increase agricultural production occurred in 1955 (Galloway and Cowling, 2002). In PEI, it is known that

such fertilization practices began to be significant around 1965. This information allows estimation of the third historical period related to the pre-modern agricultural practices existing before 1965. For that period, the mass of SNAL was obtained from a steady-state simulation to represent nitrate concentrations in the Wilmot River. This concentration was assumed to be less than 2 mg/L, which is based on nitrate concentrations monitored in the Dunk River for that period. The Dunk River is adjacent to the Wilmot River and shows the same hydrogeological and land use characteristics. We also assume that all SNAL is nitrified and leached to the aquifer within the year. The mass of soil nitrogen available to leaching modelled was around 41 400 kg/yr for that period. Finally, the mass of SNAL was interpolated between 1965 and 1980 to reflect the intensification of agriculture and chemical fertilizer use in the 70's.

Considering that agricultural activities use 78% of the watershed and that it is fairly well distributed (Fig. 5.1), the nitrogen flux was uniformly distributed over the top slice nodes of the numerical model. Also, we first assumed that all SNAL was nitrified and leached to the aquifer within the year. However, simulations carried out to achieve nitrate concentration calibration show that 140% of the initial estimate of the nitrogen flux needs to be used to adequately reproduce nitrate concentrations observed in ground and surface waters (Fig. 5.3). This suggests that the present-day nitrogen flux estimated by van Bochove *et al.* (see Chapter 2) slightly underestimate the actual SNAL in the watershed. This underestimation could be explained as follows: (1) a 3-year crop rotation (as recommended) was assumed in Chapter 2 instead of the actual 2-2.5 year rotation observed by AAT (2005); and (2) in Chapter 2, it is assumed that the provincial fertilization recommendation was being followed, however this recommendation could be exceeded in actual agricultural practices. Isotopic data on nitrate sources suggest that chemical fertilizers are effectively found in GW during the summer (see Chapter 3), thus indicating that excessive fertilization is likely occurring due to agricultural practices.

5.3.6 Fractured porous media mass transport

The Wilmot Watershed aquifer is a fractured porous medium. There are important features related to mass transport in such a medium that need to be recognized in order to carry out meaningful simulations. In fractured porous media, GW flow transports the dissolved mass in fractures, as flow in the adjacent porous matrix is not significant due to its relatively low permeability compared to that of the fracture. However, there is also a migration of dissolved solids from the fracture into the porous matrix by diffusion. Diffusion is the movement of solute (ions or molecules) from an area of higher concentration to an area of lower concentration. In the case of the Wilmot aquifer system, the difference in nitrate concentration between the fracture and the porous matrix causes the nitrate to diffuse in the adjacent matrix. Diffusion stops when the concentrations between the fracture and porous matrix are in equilibrium. Such a process has been shown to cause retardation in the migration of dissolved organic components related to the presence of immiscible organic liquids in fractured porous media (e.g. Parker *et al.*, 1994). Jackson *et al.* (1990) also assigned to this process the persistence of Aldicarb in the sandstone aquifer of PEI. Thus, the nitrate stored in the porous matrix by chemical diffusion may have an important impact on the solute response time in PEI and must be taken into account. Another consequence of nitrate diffusion in the porous matrix is the mass storage of nitrate in the aquifer. Due to the high porosity found in PEI sandstone (typically 17%), there is a large volume available for nitrate storage in the porous matrix. This nitrate mass accumulated in the porous matrix will be “given back” to the fracture system if nitrate concentrations in the fracture system

were to decrease with time. This process implies that there could be a lag time between positive actions leading to lower nitrate mass loadings to the aquifer and improvements in GW quality resulting from such reduced nitrate loadings. It is estimated from the model that the mass of nitrate stored in the sandstone porous matrix in 2005 is 2,572,000kg. This corresponds to 39% of all the mass that has leached from the soil since 1955.

Considering the controlling effect of the porous matrix, numerical simulation of nitrate mass transport should thus focus on mass transport in the matrix rather than in the fractured medium. Simulating mass transport in the matrix allows a representation of the delay in nitrate arrival as well as the important nitrate mass storage in the aquifer system. It can also be argued that for wells completed in this aquifer, the nitrate concentration in the porous matrix will actually control in large part GW quality. Because fractures were not explicitly represented in the model, the porosity assigned to the medium in the simulator was the 'porous matrix'. This implies that simulated GW velocities will be much slower than what actually occurs in the fracture system but the modelled nitrate-mass transport will best reflect the average rate of the nitrate velocity in this porous matrix.

5.4 Assessment of the impact of agricultural practices

The model was first calibrated in steady state mode for flow modelling and in transient mode for transport modelling, then, the model was used to generate nitrate migration predictions. In the calibration process, model parameters are adjusted until simulation results are consistent with the understanding of the GW system and all the available observations. The present model was calibrated with three different kinds of data: (1) with the measured heads in domestic wells; (2) with the mean base flow recession (MBR) curve of the Wilmot River (Gburek *et al.*, 1999) and; (3) with GW and surface water nitrate concentration records. More details on the calibration results are found in Paradis *et al.* (2006).

To assess the potential impact of changes in agricultural practices over the next 55 years (from 2000 to 2055), three mass transport simulation scenarios were defined on the basis of the nitrate flux leaching to GW.

Scenario #1: Maintain the current practices in the watershed. The mass of nitrate applied over the watershed is thus kept constant at 292,000 kg/yr (140% of 207,000 kg/yr - Fig. 5.4) until 2055. This nitrate loading is equivalent to a nitrate concentration of 8.5 mg/L given the actual mean annual recharge of 410mm.

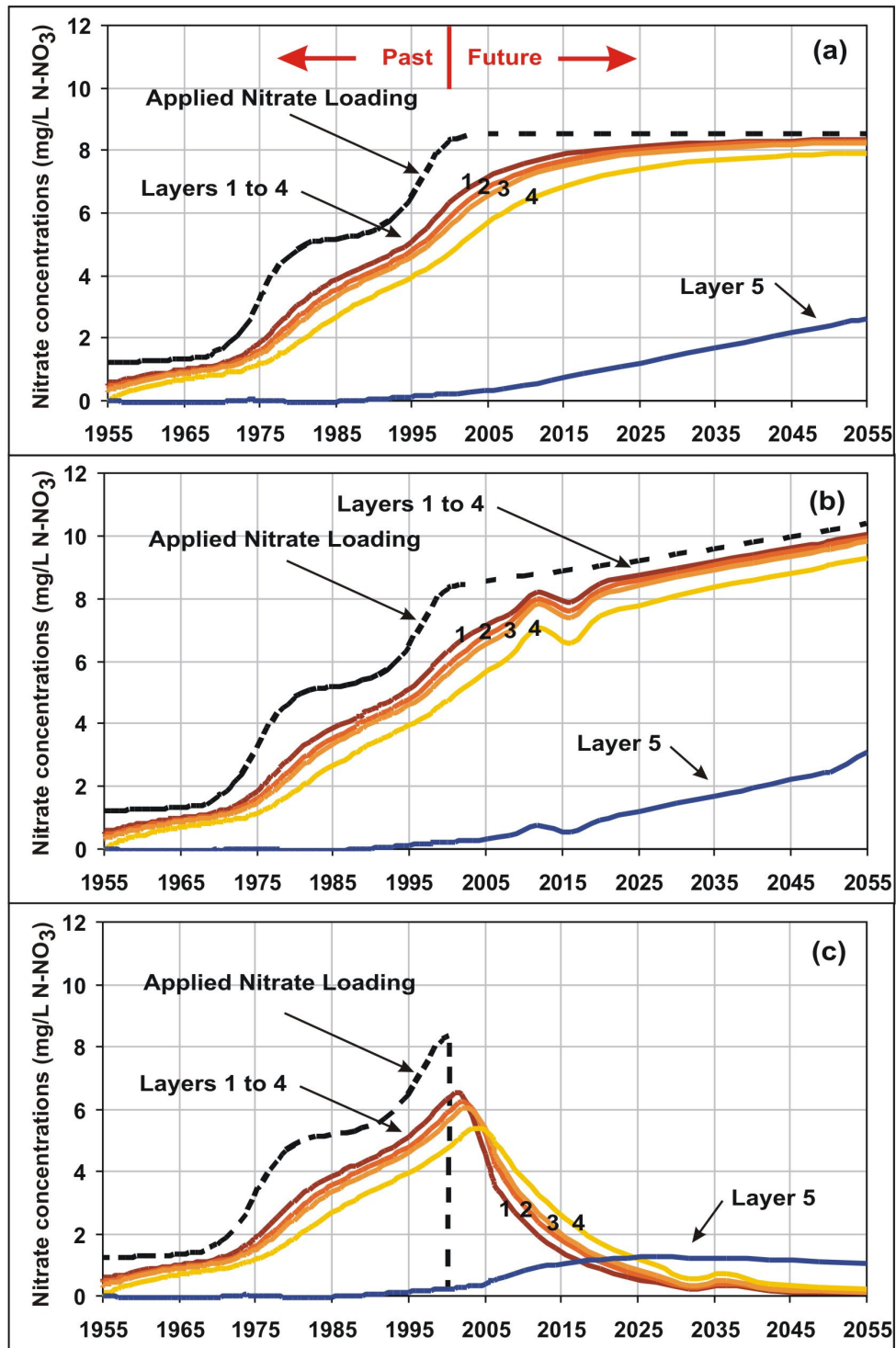


Figure 5.4. Nitrogen input scenarios and corresponding simulated average nitrate concentrations that would be present in model layers: (a) Maintain the current practices in the watershed; (b) a 23% increase in nitrogen input over 55 yrs and; (c) the mass of nitrate applied is abruptly stopped in 2000.

Scenario #2: 23% increase relative to the present-day nitrate loading. This percentage corresponds roughly to the increase observed in the last 10-15 years. The mass of nitrate applied is thus progressively increased from 292 000 kg/yr in 2000 to 360 000 kg/yr in 2055. This maximum nitrate loading of 360 000 kg/yr is equivalent to a nitrate concentration of 10.5 mg/L.

Scenario #3: No more nitrate is leaching to the aquifer. The mass of nitrate applied is abruptly stopped in 2000. This scenario is not realistic but it was simulated to more precisely determine the lag time between reductions in nitrate loadings and lower nitrate concentrations.

All the simulation scenarios were run under steady-state flow conditions and transient nitrate mass transport with 2000 nitrate concentrations used as initial conditions. Simulated average nitrate concentrations in layers 1 to 4 should be representative of concentrations found in domestic wells. [Figure 5.4](#) shows the average nitrate concentrations in the model layers for the three simulation scenarios.

Scenario #1 involving a constant nitrate loading to the aquifer set at the current load of 292 000 kg/yr leads to an increase in average nitrate concentrations from 6.6 mg/L in 2000 to constant values between 7.9 and 8.3 mg/L for layers 1 to 4 in 2055. Despite the constant nitrate loading, average nitrate concentrations kept increasing in the upper layers for about 25 years past 2000 due to the effect of nitrate mass accumulation in the porous matrix and the nitrate concentrations increase. For layer 5, the lag in response is more important and nitrate increases from 0.3 in 2000 to 2.6 mg/L in 2055, without reaching a constant concentration. Simulated results for scenario #1 are showing that the *status quo* would provide an apparently safe level of average nitrate concentration in the aquifer. Average concentrations would not exceed the 10 mg/L maximum concentration for drinking water (Health Canada, 2004). However, model results do not represent the variability in nitrate concentrations over the watershed. Knowing that today over 20% of the wells show nitrate concentrations exceeding 10 mg/L, an increase in the average nitrate concentration would lead to a higher proportion of wells exceeding that limit ([Fig. 5.5](#)).

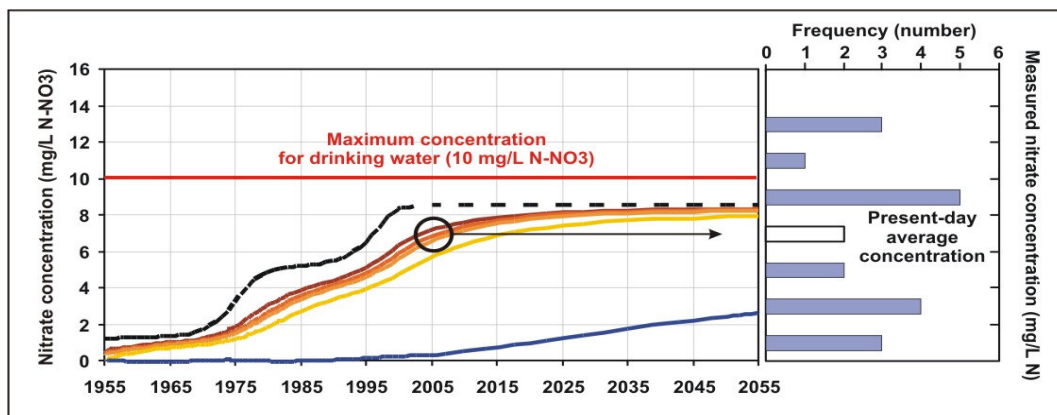


Figure 5.5. Model average nitrate concentrations for scenario #1 in relation to nitrate concentration measured in domestic wells for the period of 2002-2004. We can appreciate that present-day model and field average nitrate concentrations are similar but that field concentrations are spread around the mean.

Scenario #2 show that a 23% increase in nitrate loading would lead to average concentrations almost reaching 10 mg/L in the first four layers of the model in 2055. Under such conditions, most wells in the watershed would have nitrate concentrations near or exceeding the maximum concentration for drinking water. Groundwater would then generally be unsafe for drinking without treatment throughout most of the watershed.

Scenario #3 is assessing the time that would be required to clean the aquifer from nitrate by implying that no more nitrate is leaching to the aquifer after 2000. The simulation indicates that a time of about 20 yrs (around 2020) would be necessary to reach nitrate concentrations lower than 1 mg/L in the first four layers of the model. In layer 5, there is a different pattern, nitrate concentrations reach a maximum of 1 mg/L around 2035 to slowly decrease thereafter. The deeper the layer, the longer it takes to clean nitrate due to the longer GW flow path through deeper layers from recharge to discharge to the river. Actually, the model probably underestimates the lag time required for GW quality to recover after the cease in nitrate loading, because the model does not consider the delay caused by diffusion of nitrate from the porous matrix into the fracture system. The model only represents the average nitrate mass transport velocity in a porous matrix. On long-term basis however, considering fractured-porous or porous equivalent media will result in similar nitrate concentrations in the aquifer.

The simulation scenarios indicate that it would be necessary to reduce nitrate loading under present-day values in order to maintain nitrate concentrations at their average present-day concentration of 6.6 mg/L. Even totally curbing nitrate loadings would lead to continued increase in nitrate concentrations over the next 25 years.

5.5 Conclusion

In the Wilmot River Watershed, GW withdrawn from the fractured porous sandstone aquifer is the sole source of potable water. This aquifer is vulnerable to surface contamination as most of the watershed is covered only by a thin layer of sandy glacial till. Water quality surveys over the past decades have recorded important increases in nitrate concentrations in ground and surface water. These increases are mostly associated with the intensification of agricultural activities, especially the potato acreage increase in the last 25 years.

Numerical simulation was used in this project as a tool to predict potential future trends in nitrate concentrations in ground and surface water in the Wilmot watershed. Simulated predictions are deemed representative due to the use of known aquifer properties based on previous field work and well understood flow and transport processes that were integrated in the numerical model. Furthermore, a major effort was dedicated to model parameter calibration to make the model reproduce existing records. The calibrated numerical model can reproduce the hydraulic behaviour of the aquifer as well as observed present-day nitrate concentrations in surface and GW. The model can thus be used to make representative predictions about potential future evolutions of nitrate concentrations in the Wilmot Watershed. These predictions were made for three scenarios involving different hypotheses on the future evolution of nitrate loadings to GW over the watershed.

Simulation results show that major changes in agricultural practices would be required in the short term and needed to be maintained in the future to see improvements in GW quality over the

Wilmot Watershed. It would even be necessary to reduce nitrate loading under the present-day value just to maintain nitrate concentrations at their average present-day concentration of 6.6 mg/L. A further reduction in nitrate loading under present-day value would be required to substantially decrease the number of wells that exceed the 10 mg/L $\text{NO}_3\text{-N}$ drinking water guideline.

The numerical model developed for this project aimed at providing representative average nitrate concentrations in ground and surface water over the Wilmot Watershed. Limitations of the model are mainly related to its lack of representation of the variability in nitrate loadings over the watershed. Another study focussed on that aspect and thus provides another perspective on nitrate transport through the watershed that is complementary to this work (see Chapter 4). Improvements in the estimation of historical nitrate loadings would deserve further work as it would both improve the modelling of nitrate transport in the watershed and potentially indicate ways to avoid further increases in nitrate loading in the future.

6 Modelling four Climate Change scenarios for Prince Edward Island

Budong Qiang & Reinder De Jong

ABSTRACT

Daily climate data are required to evaluate the effect of climate change on possible contamination of drinking water by nitrogen from agricultural sources on Prince Edward Island. The objective of this chapter is to generate a continuous daily weather record for the historic period 1971 to 2000 and to develop daily future climate scenarios based on Global Climate Models (GCM). After calibrating the stochastic weather generator AAFC-WG with the historic climate data, daily maximum and minimum air temperatures and precipitation were generated for the period 2040-2069 using four climate change scenarios. The latter are taken from climate change simulations conducted by two GCMs (CGCM2 and HadCM3) with forcings of greenhouse gas under emission scenarios IPCC SRES A2 and B2. The four scenarios are used to represent uncertainties from the greenhouse gas emission scenarios, as well as uncertainties from the GCMs themselves. The most notable change in the future climate is substantial warming as indicated by all four scenarios. Non-growing season precipitation may change slightly, either increasing or decreasing; however, such changes tend to be insignificant and more uncertain compared to the expected warming trend.

6.1 Introduction

Daily climate data are required to evaluate the effect of climate change on the potential for contamination of drinking water by nitrogen from agricultural sources on Prince Edward Island (PEI). These data, including maximum and minimum air temperatures and precipitation, are necessary inputs to the so-called ‘impact’ models that simulate, for example, crop yields and nitrogen leaching under current and potential future climate change scenarios. Daily climate data are also required as input to GW models

Coupled atmosphere and ocean general circulation models (GCMs or Global Climate Models) are currently the most reliable tools for projecting future climate changes from greenhouse gas (GHG) emissions. However, it is well known (IPCC 2001) that daily climate scenarios from GCMs are usually not suitable as direct input into impact models, because of the coarse resolution of the GCMs. Subgrid processes in the atmosphere are parameterized in the GCMs and detailed topography is not included either. These deficiencies can result in unrealistic climate characteristics, especially at the local scale at which the impact models operate.

Historical daily climate data observed at meteorological stations are also required for the impact models to simulate the baseline conditions (i.e. the current situation) to which the future scenario is to be compared. The impact models need a continuous climatic record without missing values, but unfortunately the historical weather record is often incomplete. In this study, we used the stochastic weather generating technique (Wilks and Wilby 1999) to fulfill two major objectives: (i) generating a continuous daily weather record for the current/historic (baseline) period 1971 to 2000, and (ii) developing daily future climate scenarios based on GCM-simulated climate change.

6.2 Data and Methodology

6.2.1 Data bases – sources of weather data

Two different types of weather data are used in this study: (i) historical weather data observed at meteorological stations and (ii) daily output from climate change experiments conducted by GCMs. A total of eleven meteorological stations are selected, covering PEI fairly evenly and having the best available historical weather data for 1971-2000 (Fig. 6.1). The 23 agricultural Soil Landscape of Canada (SLC) polygons, employed as base units for modelling of soil nitrogen leaching, are also depicted on this map.

Historical weather data for 1971-2000, including daily maximum and minimum air temperatures and daily precipitation, are extracted from a database archived at the Eastern Cereal and Oilseed Research Centre (ECORC) of Agriculture and Agri-Food Canada (AAFC) in Ottawa. The historical weather data, originally provided by Environment Canada, are partly modified at AAFC to reduce missing values. However, missing data are still present. Climate normals (30-year mean of 1971-2000) for January and July monthly mean maximum temperature (Tmax), monthly mean minimum temperature (Tmin), monthly precipitation totals (P) and the number of days with precipitation (PD) are shown in Table 6.1. Since PEI is a relatively small island near the east coast of a large continent, spatial differences in temperature and precipitation are relatively small under the current climate. It is therefore reasonable to assume that any climate change will also be fairly uniform over the entire island.

Table 6.1. Climate normals (1971-2000 means) for 11 PEI stations*.

Station	Tmax (°C)		Tmin (°C)		P (mm)		PD (days)	
	January	July	January	July	January	July	January	July
Alberton	-3.9	23.2	-12.8	13.8	97.0	91.9	12.5	11.7
Alliston	-2.0	24.0	-11.3	13.7	94.4	96.7	13.4	12.2
Bangor	-2.8	23.2	-12.3	13.3	112.8	85.4	15.9	11.8
Charlottetown A	-3.3	23.2	-12.6	13.7	106.1	87.3	18.8	12.2
East Baltic	-2.9	22.3	-10.5	13.9	106.3	90.1	17.2	13.3
Monticello	-2.6	22.9	-11.3	13.7	105.2	82.2	13.2	12.1
New Glasgow	-3.1	23.4	-12.3	14.0	117.8	87.8	15.7	12.2
New London	-3.5	23.3	-12.3	13.5	86.1	92.6	11.8	11.0
Oleary	-4.4	23.2	-12.7	13.8	97.1	100.1	11.4	12.4
Stanhope	-2.7	23.2	-11.3	14.9	105.8	72.9	12.5	9.8
Summerside	-3.4	23.6	-12.3	14.5	100.1	84.8	17.2	12.7

*Tmax – monthly mean daily maximum temperature; Tmin – monthly mean minimum temperature; P – monthly precipitation total; PD – number of days with precipitation.

Daily outputs from two climate change scenarios conducted by two different GCMs are used in this study. The two GCMs are the CGCM2 (Flato and Boer 2001) developed at the Canadian Centre for Climate Modelling and Analysis (CCCma) and the HadCM3 (Gordon *et al.*, 2000) developed at the Hadley Centre for Climate Prediction and Research of the UK Meteorological Office. The CGCM2 is the second version of the coupled general circulation model at CCCma.

The HadCM3 is the third generation of Hadley Centre's coupled atmosphere-ocean general circulation model.

The Intergovernmental Panel on Climate Change Special Report on Emission Scenarios (IPCC SRES) (Nakicenovic and Swart, 2000) provides 40 different scenarios which are all deemed 'equally likely', but two scenarios (A2 and B2) have been widely adopted in climate change experiments and impact studies (IPCC 2001). The A2 scenario envisions a population growth to 15 billion by the year 2100 with rather slow economic growth and development. Consequently, the projected equivalent CO₂ concentration rises from 476 ppm in 1990 to 1320 ppm in 2100. The B2 scenario envisions slower population growth (10.4 billion by 2100) with a more rapidly evolving economy, but with more emphasis on environmental protection. It therefore produces lower emissions (CO₂ concentration of 915 ppm by 2100) and less future warming than scenario A2.

Daily outputs of maximum air temperature, minimum air temperature and precipitation are obtained electronically from CCCma and the Hadley Centre through the Climate Impacts LINK project (Viner, 1996) for the four climate change simulations. The data sets are labelled according to the GCM and the scenario used: CGCM2 A2, CGCM2 B2, HadCM3 A2 and HadCM3 B2. Climate change simulations CGCM2 A2 and CGCM2 B2 are the model runs of the CGCM2 forced by emission scenarios A2 and B2. Similarly, climate change simulations HadCM3 A2 and HadCM3 B2 are model runs of the HadCM3 forced by emission scenarios A2 and B2.

6.2.2 Stochastic weather generation

Missing values in input data are always a concern in modelling continuous processes like nitrogen leaching through the soil profile. Stochastic weather generators (Wilks and Wilby 1999) are statistical models that can generate synthetic daily weather series without missing values. Long synthetic weather series can facilitate risk analyses because the essential statistical characteristics of the observed weather data are preserved. In the past decade, stochastic weather generators have also attracted attention as a convenient tool for producing daily scenarios in climate change impact studies. The technique is based on modifying, or perturbing, weather generator parameters with statistics from climate change scenarios generated by GCMs at monthly or daily time scales (Mearns *et al.* 1997; Semenov and Barrow 1997). The weather generator AAFC-WG (Hayhoe 2000), was developed for, and evaluated in diverse Canadian climates. Compared to the LARS-WG weather generator (Racsko *et al.*, 1991; Semenov *et al.* 1998), AAFC-WG performed better in simulating temperature related statistics, while it did almost as well for statistics associated with daily precipitation (Qian *et al.* 2004). Qian *et al.* (2005) concluded that 'daily climate scenarios developed by weather generators can be reasonably reliable for agricultural impact studies, provided that the changes in the statistics of daily weather variables from daily GCM output are reliable'. Therefore, the stochastic weather generator AAFC-WG is employed in this study to generate both synthetic weather data for the present climate and for the future climate scenarios CGCM2 A2, CGCM2 B2, HadCM3 A2 and HadCM3 B2.

6.3 Development of daily climate scenarios

Daily maximum and minimum air temperatures and precipitation observed at each of the 11 stations (Fig. 6.1) for 1971-2000 are used to calibrate and validate the AAFC-WG. The locally calibrated model is then employed to generate a 300-year long daily synthetic weather series (daily Tmax, Tmin and P) for each station. Because of the stochastic properties of weather, a 300-year long weather series was generated by the weather generator instead of 30-year long. However, the 300-year long weather series represents the climate of the 30-year time period, i.e., 1971-2000 for the baseline climate and 2040-2069 for the future climate. For example, statistical characteristics of the 300-year long weather series for the baseline climate resemble those from the observed weather series for the time period 1971-2000. Similarly, the statistical characteristics of the 300-year long weather series for period 2040-2069 represent a climate of that time period only. In other words, any 30-year long weather series can be extracted from the 300-year long series to represent the climate of the same 30-year time period; however, the statistical analysis, especially the risk analysis, may be more reliable when the 300-year long series is used. Using both 300-year long synthetic data for the present and future climates may be of help for eliminating possible biases introduced by the weather generator, as the synthetic weather data are not exactly the same as the observed weather data. Besides, the 300-year synthetic data provide a good sample size for risk analysis. Using synthetic data for the present climate also provides the modelling procedure with the convenience of no missing in input data.

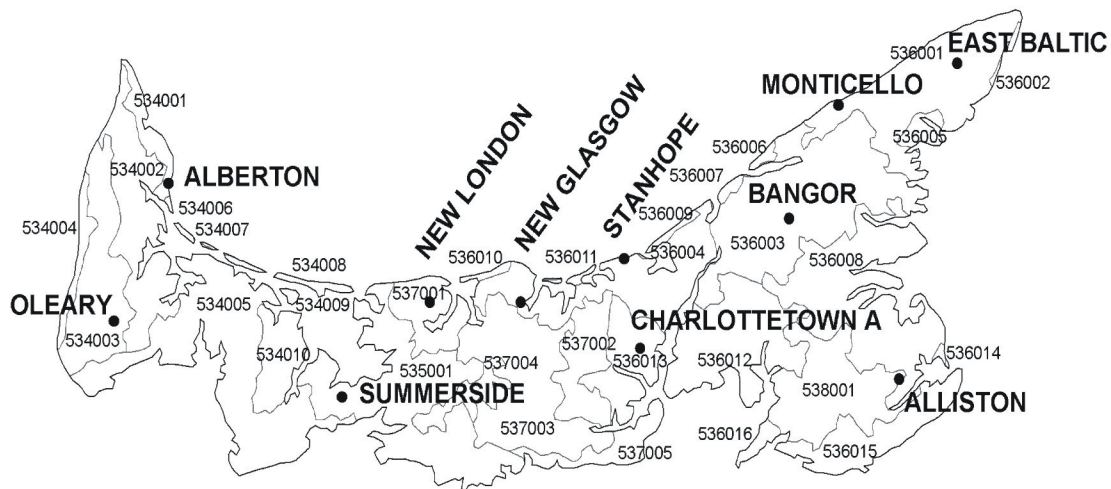


Figure. 6.1. Eleven meteorological stations and 23 Soil Landscape of Canada (SLC) polygons on PEI.

The calibrated station model is also used to generate a 300-year long weather series for 2040-2069. This involves the following steps: (1) from the daily outputs of the climate change scenario under consideration (CGCM2 A2, CGCM2 B2, HadCM3 A2 or HadCM3 B2), we compute statistics for daily Tmax, Tmin and P for each of the four GCM gridpoints surrounding the station under consideration for the time period 1971-2000 and for the time period 2040-2069; (2) changes in these statistics between the two time periods are calculated either as ratios

(precipitation-related variables) or as differences (temperature-related variables); (3) the ratios and differences are interpolated from the GCM grid points to the station using the nearest neighbour approach, weighing each neighbour by the inverse distance squared; (4) the interpolated ratios and differences are applied to the 1971-2000 calibrated weather generator parameters to form a new set of parameters for 2040-2069; and (5) a 300-year long daily weather series for 2040-2069 is generated, using the new set of parameters for the station.

6.4 Projected changes in future climate scenarios

The generated future climate scenarios show considerable warming from both GCMs and GHG emission scenarios, although warming under scenario A2 is more noticeable than under B2. As PEI is relatively small, coherent climate change is expected throughout the province. Therefore, projected climate changes at Charlottetown are presented here as an example. Climate change simulated by the two GCMs at Charlottetown is listed in [Table 6.2](#) for the two GHG emission scenarios (A2 and B2). Minimum temperatures seem to increase more markedly than maximum temperatures, but the range is large among the four scenarios. For example, the increase in January mean daily minimum temperature varies from 1.5°C (HadCM3 B2) to 4.6°C (CGCM2 A2). For this region, CGCM2 projected much greater warming than HadCM3. Warming is expected throughout the entire year, but changes in precipitation appear more uncertain. CGCM2 projects a slight decrease, but HadCM3 simulates a slight increase, for January precipitation. The projected July precipitation for 2040-2069 from all four scenarios shows a slight increase or no change from the 1971-2000 average. It is projected that, based on all four scenarios, the number of days with precipitation decreases slightly in January.

Table 6.2. Climate change scenarios for 2040-2069 compared to the 1971-2000 means at Charlottetown (PEI).*

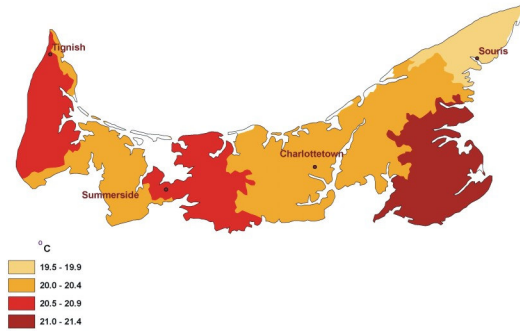
Scenarios	Tmax (°C)		Tmin (°C)		P (%)		PD (%)	
	January	July	January	July	January	July	January	July
CGCM2 A2	1.7	2.5	4.6	3.1	-5.3	0.0	-2.1	5.0
CGCM2 B2	1.1	1.8	4.0	2.2	-8.1	5.0	-3.8	1.8
HadCM3 A2	1.4	1.8	1.7	2.0	4.1	7.7	-5.0	-4.6
HadCM3 B2	1.2	1.4	1.5	1.5	5.1	1.4	-3.0	-1.9

*Tmax – monthly mean daily maximum temperature; Tmin – monthly mean minimum temperature; P – monthly precipitation total; PD – number of days with precipitation.

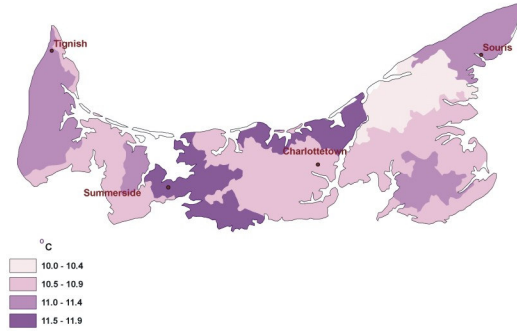
Modelling nitrogen leaching in PEI, at the SLC polygon scale, is limited to the non-growing season (refer to Chapter 7 for details) but the water budget calculations are carried out throughout the entire year, i.e. during both the growing season (GS) and the non-growing season (NGS). The spatial variability in GS and NGS mean, maximum and minimum air temperatures under the current/historic climate are generally less than 2 °C ([Fig. 6.2](#)) across PEI. Because the results from the two GCMs are very similar, we will now discuss only the results from CGCM2. Under the CGCM2 A2 2040-2069 climate scenario, both the GS and the NGS maximum air temperature are projected to increase by approximately 1.8 to 2.1 °C, while the minimum air temperatures are projected to increase by slightly larger values: minimum GS temperatures may increase by 1.8 to 2.5 °C (lowest increases in the eastern section of the island, see [Fig. 6.3](#)) and minimum NGS

temperatures may increase by 2.2 to 2.9 °C (again with the lowest increases in the eastern section of PEI, [Fig. 6.4](#)). Hence, most of the warming (up to 2.9 °C) is projected for the NGS minimum temperatures in the central and western part of PEI. Under the CGCM2 B2 2040 - 2069 climate scenario, the GS and NGS maximum temperatures are projected to increase by approximately 1.0 to 1.7 °C, slightly less than under the CGCM2 A2 scenario. The GS minimum temperatures are projected to increase by 1.4 to 1.7 °C, and the NGS minimums by 1.8 to 2.5 °C, with the lowest increases occurring again in the eastern section of the island.

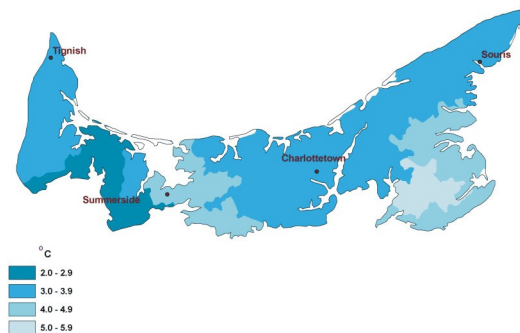
a) GS Tmax (historic)



b) GS Tmin (historic)



c) NGS Tmax (historic)



d) NGS Tmin (historic)

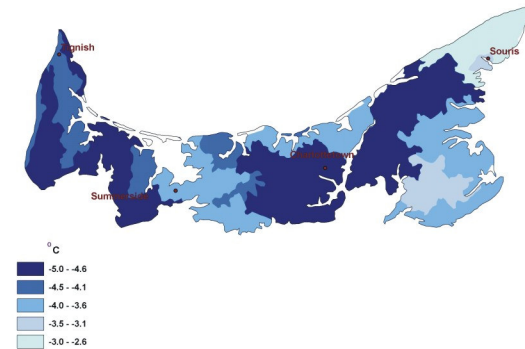
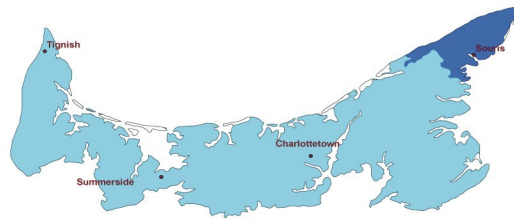


Figure 6.2. Historical/current (1971-2000) growing season mean Tmax (upper left), Tmin (upper right) and non-growing season mean Tmax (lower left) and Tmin (lower right).

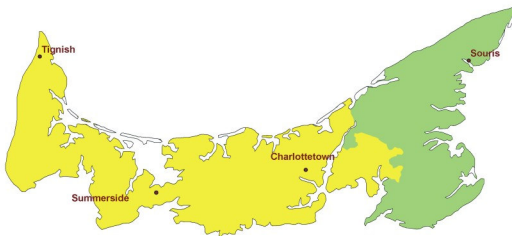
a) GS Tmax (CGCM2 A2)



b) GS Tmax (CGCM2 B2)



c) GS Tmin (CGCM2 A2)



d) GS Tmin (CGCM2 B2)

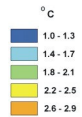
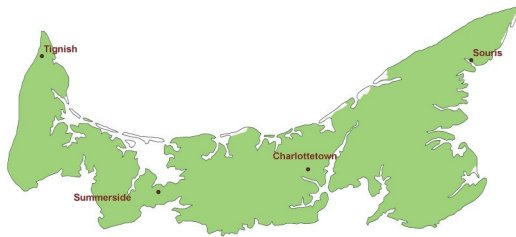
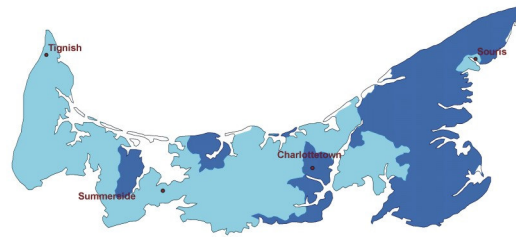


Figure 6.3. Changes in growing season mean Tmax (upper panels) and Tmin (lower panels) for 2040-2069 to the present (1971-2000), projected by CGCM2 A2 (left panels) and CGCM2 B2 (right panels).

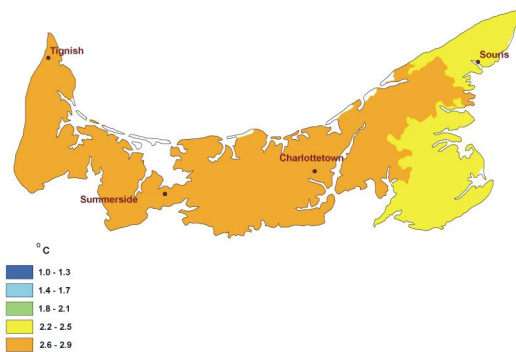
a) NGS Tmax (CGCM2 A2)



b) NGS Tmax (CGCM2 B2)



c) NGS Tmin (CGCM2 A2)



d) NGS Tmin (CGCM2 B2)

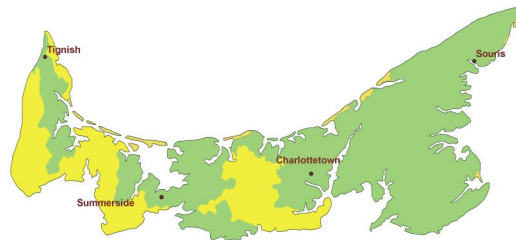


Figure 6.4. Changes in non-growing season mean Tmax (upper panels) and Tmin (lower panels) for 2040-2069 to the present (1971-2000), projected by CGCM2 A2 (left panels) and CGCM2 B2 (right panels).

NGS precipitation is the most important component in the water budget to calculate nitrogen leaching (refer to Chapter 7 for details). Current NGS precipitation (657–835mm) is approximately twice as high as GS precipitation (333–426mm) (Fig. 6.5). During the growing season, the western part of PEI receives slightly more precipitation than the eastern part, while the eastern part receives more during non-growing season. Under the projected CGCM2 A2 climate, both GS and NGS precipitation are slightly less than under the current/historic climate; in contrast, under the CGCM2 B2 climate, both GS and NGS precipitation are slightly higher than under the current/historic climate, although some polygons are projected to receive less GS precipitation. The projected precipitation under the HadCM3 A2 scenario is similar to CGCM2 B2, while the HadCM3 B2 scenario appears more like CGCM2 A2. Unlike the projected temperature change, the projected precipitation change appears more uncertain, depending upon the different GCMs and the different GHG forcing scenarios.

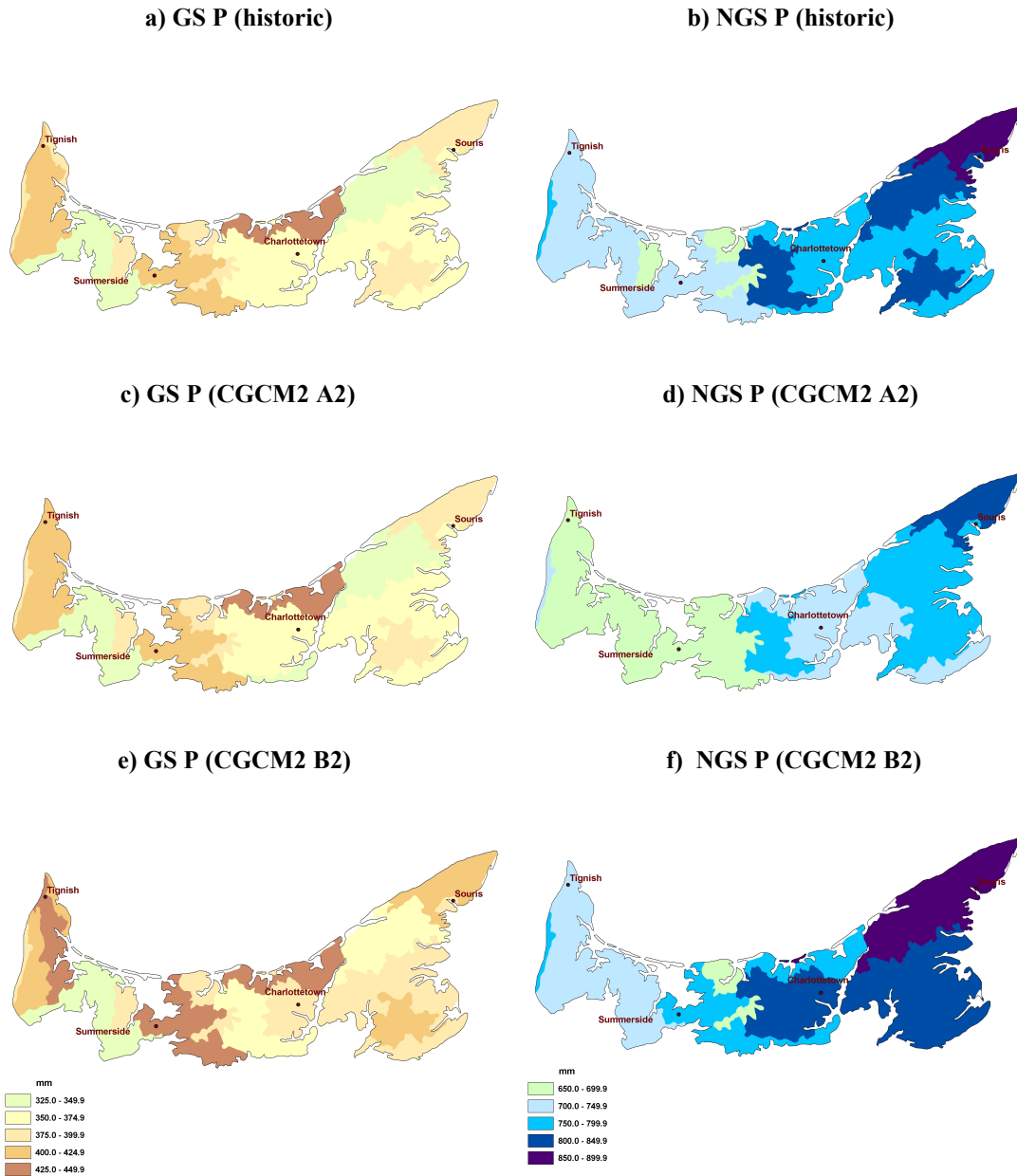


Figure 6.5. Historic (upper panels) and 2040-2069 growing season (left panels) and non-growing season (right panels) precipitation totals projected by CGCM2 A2 (middle panels) and CGCM2 B2 (lower panels).

6.5 Summary

Using the stochastic weather generator AAFC-WG, daily maximum and minimum air temperatures and daily precipitation data for 2040-2069 (the time span for an approximate doubling of the atmospheric CO₂ concentration) under four climate change scenarios are generated for impact modelling. The four climate change scenarios are taken from climate change simulations conducted by two global climate models (CGCM2 and HadCM3) with forcings of

greenhouse gases under emission scenarios SRES A2 and B2, respectively. The four scenarios are used to present uncertainties from the greenhouse-gas emission scenarios, as well as from the GCMs. The generated daily weather data for 2040-2069, as well as the synthetic weather data for 1971-2000, are suitable input to nitrogen leaching and GW simulation models.

The most notable change in the future climate is substantial warming as indicated by all four scenarios. This projected warming is more significant with the CGCM2 than with the HadCM3 model (refer to [Table 6.2](#) for Charlottetown as an example). Non-growing season precipitation may change slightly; either increasing or decreasing; however, such changes tend to be insignificant and more uncertain compared to the expected warming trend.

7 Modelling of Nitrogen leaching in Prince Edward Island under Climate Change scenarios

Reinder De Jong, Budong Qiang & Jingyi Y. Yang

ABSTRACT

Projected climate change in Canada and its impact on crop yield and production has been previously documented, but the impacts on soil and water quality are less well known. The objective of this study is to model and evaluate the potential impacts of climate change on soil nitrogen (N) leaching in Prince Edward Island. Residual Soil Nitrogen, the quantity of inorganic soil N at the time of harvest, is calculated from an annual N budget, based on the Census of Agriculture data. RSN is ‘added’ to the soil in the fall and subject to leaching until the start of the next growing season. Water and N movement in and through the soil is calculated with a modified version of the Versatile Soil Moisture Budget. With no changes in agricultural practices, N leaching for four climate change (2040-2069) scenarios remains similar to that simulated under historic (1970-2000) climatic conditions. If agricultural intensification takes place in response to climate change and economic conditions, estimates of soil N leaching increase from 5 to 30% beyond historic levels.

7.1 Introduction

Nitrogen is an essential nutrient required by all crops. Legumes (e.g. soybean, alfalfa, clover) fix nitrogen from the atmosphere but non-leguminous crops (e.g. potatoes, corn, cereal) require applied nitrogen to optimize their growth and yield. Nitrogen is added to these non-leguminous crops through fertilizer, manure, atmospheric deposition and through mineralization of crop residues and soil organic nitrogen.

The addition of nitrogen is not always without risks. Losses occur because not all of the applied nitrogen is used by the crop, and some inorganic nitrogen inevitably remains in the soil at the end of the growing season, i.e., Residual Soil Nitrogen (RSN). Environmental risks may be associated with unduly large surpluses of nitrogen in the soil, particularly in humid regions. Most of the residual inorganic nitrogen, in the form of nitrate, is water soluble and is susceptible to leaching through the soil into groundwater (GW) or to loss through tile drainage into ditches, streams and lakes (Drury *et al.*, 1996; Tan *et al.*, 2002). High nitrate levels in surface waters contribute to algae growth and eutrophication; high nitrate levels in drinking waters may also lead to methaemoglobinemia (blue baby syndrome) and have also been implicated in increased risk of stomach cancer (Chambers *et al.*, 2001; see also Chapter 1). Climatic conditions (drought, excess rain, frost, etc) and various soil physical and chemical factors can limit crop growth and nitrogen uptake, which can further increase the amount of residual soil nitrogen at the end of the growing season, leading to increased nitrogen leaching through the soil profile.

Concern over climate change has reached global dimensions, and concerted international efforts have been initiated to address this problem. Based on climate records, the average global surface

temperature has increased over the 20th century by about 0.6 °C. Based on a wide range of scenarios and several current Global Change Models (GCMs), the mean annual global surface temperature is projected to increase by 1.4 to 5.8 °C over the period 1990 to 2100, with likely precipitation increases over northern mid- to high latitudes and in the Antarctica (IPPC, 2001). However, regional changes could be quite different from the global ones. For example, Hengeveld (2000), discussing the simulations made with a Canadian GCM, suggests temperature increases for most of Canada in the order of 2 to 4 °C by the middle-, and 5 to 10 °C by the end of this century, except in the High Arctic where the temperatures could soar by more than 15 °C. Projected changes in annual precipitation over Canada remain within 10% of present levels until after 2050, when the precipitation would increase by 10 to 20%, with most of the increases occurring during the winter months. Bootsma *et al.* (2005a), using projections from the Canadian GCM (version 1) found that maximum and minimum air temperature changes, averaged over all GCM grid points in Atlantic Canada, were 1.3 and 1.6°C, respectively, for the 2040-2069 period. Changes in precipitation were generally small.

The variability of the climate has been a topic of recent interest. The consequences of changes in variability may be as important as those that arise due to changes in mean values of climatic variables (Hulme *et al.*, 1999; Carnell and Senior, 1998). Most studies of climate change impacts on agriculture have analyzed the effects of mean changes of climatic variables on crop production, but the impacts of changes in climate variability have been studied to a much lesser extent (Alexandrov and Hoogenboom, 2000).

Global and regional climate change will affect many economic sectors to some degree, but the agricultural sector is perhaps the most sensitive and vulnerable, because sustainable agricultural production remains very dependent on climate resources. The combined effects of increased temperatures, elevated atmospheric CO₂ concentrations, increased probability of extreme events and reduced crop-water availability are expected to cause significant changes in crop yields (e.g. McGinn *et al.*, 1999; Olesen and Bindi, 2002; Izaurrealde *et al.*, 2003; Lemmen and Warren, 2004; Bootsma *et al.*, 2005b). However, climate change impacts on the soil and water quality of agro-ecosystems has been less well documented (Ineson *et al.*, 1998). The purpose of this study is to model and evaluate the potential impacts of climate change on soil nitrogen leaching in PEI.

7.2 Methology

Because of the complexity of agro-ecosystems, computer simulation techniques are among the most practical approaches available to make assessments of climate change impacts on agriculture and soil and water resources. In this study we employed the Residual Soil Nitrogen indicator (Drury *et al.*, 2007), coupled with a modified version of the Versatile Soil Moisture Budget Model (VSMB; Akinremi *et al.*, 1996) to compute long-term nitrogen leaching in PEI under a historic baseline climate and four climate change scenarios. Further details on the methods, assumptions and data are given below. A schematic diagram of the water and nitrogen modelling system as described in sections 7.2.1 to 7.2.3 is shown in [Figure 7.1](#).

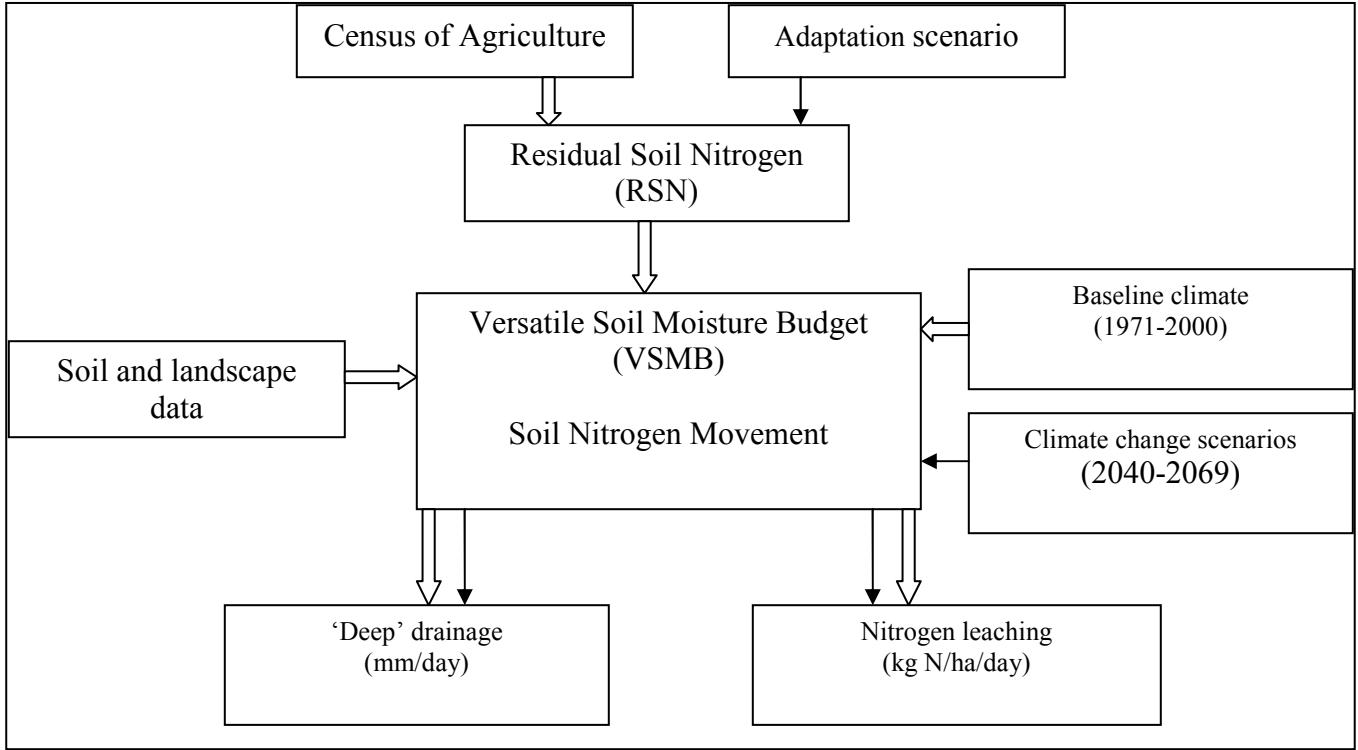


Figure 7.1. Flow chart of the RSN modeling system. Block arrows refer to present/historic conditions; solid arrows refer to climate change scenarios.

7.2.1 Residual Soil Nitrogen (RSN)

The Residual Soil Nitrogen indicator is part of the CANB model (Canadian Agricultural Nitrogen Budget; Yang *et al.*, 2007) which estimates, at the Soil Landscape of Canada (SLC) polygon level (Soil Landscapes of Canada Working Group, 2006), the quantity of inorganic soil nitrogen at the time of harvest. It is the difference between nitrogen inputs from chemical fertilizers, manure, biological nitrogen fixation and atmospheric deposition and outputs in the form of nitrogen in the harvested portion of the crops and gaseous losses to the atmosphere. Although soil mineralization and immobilization also occur on a seasonal basis, it is assumed that the soils are in a steady state situation, with no net change in soil organic nitrogen from one year to the next.

The following annual N budget equations are a summary of the nitrogen budget.

Calculation of total RSN (kg N ha^{-1}) is shown in Eq. (1):

$$RSN = (N_{input} - N_{output}) / FARMLAND_{SLC} \quad (1)$$

where N_{input} is the total nitrogen added to farmland during the growing season (Eq. 2), N_{output} is total nitrogen removed from farmland annually by crop uptake, ammonia volatilization and denitrification (Eq 3) and $FARMLAND_{SLC}$ (ha) is the total area of farmland in the SLC polygon.

$$N_{input} = N_{fertilizer} + N_{manure} + N_{fixation} + N_{deposition} \quad (2)$$

where $N_{fertilizer}$ is the total amount of N fertilizer applied to the crops (kg N SLC⁻¹), N_{manure} is the total amount of available manure N applied to crops and pasture (kg N SLC⁻¹), $N_{fixation}$ is the amount of N fixed by leguminous crops (kg N SLC⁻¹), and $N_{deposition}$ (kg N SLC⁻¹) is the total amount of wet and dry deposition.

$$N_{output} = N_{crop} + N_{gas} \quad (3)$$

where N_{crop} is the amount of N removed in the harvested portions of crops and pastures (kg N SLC⁻¹) and N_{gas} (kg N SLC⁻¹) is the amount of gaseous N loss to the atmosphere, mainly via denitrification and volatilization.

Nitrogen losses during manure storage, and therefore the amount of available N for land application, vary with manure source, storage methods and manure form (liquid, solid, compost). It is estimated that 15% of the N in the manure is lost during storage and handling (Burton and Beauchamp, 1986), 35% is added to the soil as organic N (Ontario Ministry of Agriculture and Food, 2003), and consequently 50% of the N in the manure is inorganic N which would be available to crops in the year of application. Nitrous oxide emissions reduce 1.25% of this available N and an equal portion is assumed to be lost via N₂ production.

7.2.2 Water balance calculations and nitrogen leaching

Because RSN is computed at the SLC polygon scale, the soil water balance and nitrogen leaching calculations must also be made at the same scale. This assumes that a single, composite, soil- and crop type will represent the entire SLC. The details of constructing the composite soil- and crop type for each SLC polygon are described in the input data section.

The VSMB (Baier and Robertson, 1966; Baier *et al.*, 1979) calculates the soil water budget resulting from precipitation, evapotranspiration, surface runoff and deep drainage. Each day of the year, the net loss or gain is added to the water already in the soil. For infiltration and soil water redistribution, Akinremi *et al.* (1996) incorporated the simple cascading algorithm of the Ceres-Wheat model (Ritchie and Otter, 1985). As in previous versions of the VSMB, the new algorithm uses field capacity to determine flow between layers (called a capacity based approach), but it is also linked to an empirical subroutine that accounts for both upward- and downward redistribution of soil water by unsaturated flow. Furthermore, Akinremi *et al.* (1996) improved the surface runoff subroutine from rainfall and snowmelt.

Actual evapotranspiration (AET) is calculated in terms of potential evapotranspiration, reduced according to the prevailing soil water conditions via a set of soil and root coefficients:

$$AET_i = PET_i \cdot \sum K_{ij} \cdot S_{ij} / C_j \cdot Z_j \quad (4)$$

Where the subscripts i and j refer to time (day) and depth (layer number). K is a set of crop specific root coefficients (dimensionless; Table 7.2), S is available water in layer j (mm), C is the available water holding capacity of layer j (mm), Z is a specific soil coefficient (dimensionless) and PET is the daily potential evapotranspiration (mm), calculated from maximum and minimum air temperatures and radiation received at the top of the atmosphere (Baier and Robertson, 1965).

The crop coefficients reflect crop cover and root distribution patterns that change over time and with depth. The Z coefficients represent empirical drying curves, relating the ratio AET/PET to the amount of available soil water (Baier *et al.*, 1979).

Table 7.1. Aggregated crop coefficients (K_{ij}) at the SLC polygon scale for different phenological periods.

Phenological period	Layer ¹						% of GSL
	1	2	3	4	5	6	
GSE ² to GSS ³	0.45	0.17	0.11	0.07	0.02	0.01	
GSS to emergence	0.45	0.20	0.13	0.12	0.03	0.02	10
Emergence to full cover	0.45	0.25	0.15	0.12	0.10	0.03	30
Full cover to senescence	0.45	0.30	0.20	0.15	0.10	0.05	40
Senescence to GSE	0.45	0.30	0.20	0.15	0.07	0.03	20

¹Layer 1, 2, 3, 4, 5 and 6 represent 5.0, 7.5, 12.5, 25.0, 25.0 and 25.0% of the maximum rooting depth; ² Growing season end; ³ Growing season start.

The VSMB has been further modified by including rainfall interception calculations according to the procedures documented by Feddes *et al.* (1978) where interception is a function of daily rainfall and degree of soil cover. The latter varies with the distribution of annual and perennial crops in the SLC polygon and with the progression of the crop growing season.

In order to simulate N leaching during winter, we added a new subroutine, adapted from the Ceres-Maize model (Jones and Kiniry, 1986) in which N movement in the soil profile is dependent upon water movement. As described above in the capacity based approach, the volume of water moving from layer j to the layer below it, $j+1$, is calculated as $FLUX_j$ (mm). The volume of water present in the layer before drainage occurred is also calculated from its volumetric water content, SW_j ($\text{cm}^3 \text{ cm}^{-3}$) and the thickness of the layer, $DLAYR_j$ (mm). Nitrogen lost from each layer, including that from the lowest layer, (N_{out} in kg N ha^{-1}) is then calculated as:

$$N_{out} = SN_j \bullet FLUX_j / [SW_j \bullet + FLUX_j] \quad (5)$$

where SN_j is the quantity of N present in layer j (kg N ha^{-1}). Thus a fraction of the mass of N present in each layer moves with each drainage event. The implicit assumption is that all the N present in a layer is uniformly and instantaneously in solution in all of the water in the layer (Burns, 1974). The same procedure is also employed to model upward or downward movement of N during redistribution of soil water via unsaturated flow. Generally, the latter redistribution of N in the soil profile will be small due to the small volume of moving water.

In contrast to ‘deep’ drainage of water that is calculated throughout the entire year, leaching of N will only be calculated during the non-growing season. Residual Soil Nitrogen is ‘added’ to the soil in the fall and subject to leaching until the start of the next growing season. Fertilizer- and manure N additions, N transformations in the soil, gaseous N losses and N uptake by crops during the growing season are considered in the calculation of RSN (Yang *et al.*, 2007), but these processes are not considered in the modified VSMB. Nitrogen leaching from the soil profile is

thought to be relatively small during the growing season because of the summer precipitation deficit (i.e. potential evapotranspiration exceeds precipitation).

7.2.3 *Input data*

a) *Baseline climate and climate change scenarios.* As described in Chapter 6, 300 years synthetic weather data (daily maximum and minimum air temperature and precipitation) are generated for the present climate (1971-2000) and for four climate change scenarios (CGCM2 A2, CGCM2 B2, HadCM3 A2 and HadCM3 B2) projected for 2040 -2069 at eleven meteorological stations in PEI. It is assumed that the weather at these stations is representative of that in the 23 agricultural SLC polygons of PEI (Table 7.1).

b) *Census data.* The main inputs of the RSN model consist of acreages for all major agricultural crops and their associated crop yields, as well as the type and number of livestock. This data is collected every five years through the Census of Agriculture and is allocated to SLC polygons (scale 1:1 million) based on the methodology described by Huffman *et al.* (2006).

c) *Adaptation scenario.* Many different climate change adaptation scenarios can be devised, either with increased or decreased production intensity as compared to the present level. Because none of these scenarios is verifiable, it was decided to go with a likely scenario. Based on consensus expert opinion of Agriculture and Agri-Food Canada (AAFC) staff of the Research- and Policy Branch, it is assumed that agricultural production in PEI will intensify over the next 50 years or so. Hence, relative to the 2001 Census of Agriculture provincial totals, the following sequential agricultural land use scenario is devised for 2040 - 2069:

1. The area of alfalfa, improved pasture, tame hay and other grain cereals reduces by 40, 30, 30 and 15%, respectively (total 'freed-up' area: 29,794 ha);
2. The berries and vegetable area increases by 100% (remaining 'freed-up' area: 25,179 ha);
3. Of the remaining 'freed-up' area, 20, 40 and 40% is allocated to potatoes, grain corn and soybeans, respectively;
4. Buffer strips, a legislative requirement, reduce the increased total area of potatoes by 5%, with this area going into the 'other land' category;
5. For SLCs 538001, 537002 and 537003, the total area of potatoes decreases by 6%, because these SLCs contain fields with steep slopes, and the 'freed-up' area is allocated equally to tame hay and spring wheat;
6. As a consequence of the decrease in perennial forages, the number of cattle decreases by 10%; and
7. The number of poultry and pigs increases by 30%.

In order to calculate RSN, we need data on nitrogen fertilizer recommendations and estimated crop yields. Based on CGCM-A scenarios for the years 2040 – 2069, Bootsma *et al.* (2001) report that in PEI crop heat units will increase to 3000–3200 and effective growing degree days will increase to 1800–2000. Because these numbers are similar to those currently in Ontario, we use the 1996 crop yields of Ontario (2001 was a drought year) for the PEI climate change scenario 2040-2069. To properly balance future crop N demands with fertilizer N supplies, we also use the Ontario nitrogen fertilization recommendations for the PEI climate change scenario.

d) *Soil and landscape data.* Soil profile data required as input to the VSMB, including bulk density and water content at field capacity and the wilting point, are obtained from the CanSIS Soil Layer File (Soil Landscapes of Canada Working Group, 2006). Because natural soil horizons do not fit the discrete divisions of the soil profile in the model, the value of the parameters for each layer are computed using an interpolation routine (Onofrei, 1987). The data are then area weighted averaged for all agricultural soils within an SLC polygon to form a single, composite, soil type. Curve numbers, used to estimate surface runoff, are calculated based upon area-weighted drainage classes, rooting depths and land use characteristics of the component soils within an SLC polygon.

e) *Crop management.* The perennial forage growing season begins on the day when the 5-day running mean air temperature reaches and stays above 5.5 °C and ends the day it drops below 5.5 °C. Planting and harvest dates of annual crops are based on air temperatures and are calculated using the methodology described by De Jong *et al.* (2001). Based on the area extent of these two crop types within an SLC, average growing season start/planting dates (GSS) and average growing season end/harvest dates (GSE) are determined for each of the 300 simulation years. The growing season length (GSL) is the difference between GSS and GSE dates. It is assumed that the periods between GSS and ‘emergence’, between ‘emergence’ and ‘full cover’, between ‘full cover’ and ‘senescence’ and between ‘senescence’ and GSE constitute 10%, 30%, 40% and 20% respectively of the growing season length. For each of these aggregated growth stages we have a set of crop coefficients (K_{ij} values in Eq. 4), as shown in [Table 7.2](#).

7.2.4 *Simulation runs*

The RSN model is run for all five census years (1981, 1986, 1991, 1996 and 2001) and the output is averaged to obtain a ‘baseline’ residual soil nitrogen value for each of the 23 SLC polygons (for trends in province-wide averages during the census period 1981 to 2001, see Drury *et al.*, 2007). The model is also run with the ‘adaptation scenario’ (see above) to obtain 23 projected RSN values for the climate change scenario.

The VSMB is run for all 23 SLC polygons in the province with the 300 years synthetic baseline (1971-2000) weather data and with the 300 years climate change (2040-2069) weather data, for all four scenarios. In these model runs, residual soil nitrogen is distributed linearly between the soil surface and the upper 30% of the rooting depth at the growing season end/harvest date (GSE) of each year. At the start of the next growing season/planting date (GSS), the soil nitrogen calculations, including nitrogen leaching, are stopped. The output files contain cumulative growing season and non-growing season variables such as precipitation, surface runoff, soil water content at the GSS and GSE, potential and actual evapotranspiration, drainage and nitrogen

leaching (the latter only for the non-growing season). For each output variable we calculate means, standard deviations and probability values ranging from 5 to 95% (Spiegel, 1961).

Table 7.2. Meteorological stations and their associated SLC polygons (see Chapter 6 for station and SLC polygon locations).

Station	SLC polygon
Alborton	534001, 534002, 534003
O’Leary	534004, 534005
Summerside	534010, 535001
New London	537001, 537004
New Glasgow	536011, 537003
Stanhope	536004
Charlottetown	536012, 536013, 537002, 537005
Alliston	536008, 536015, 536016, 538001
Bangor	536003
Monticello	536005
East Baltic	536001

7.3 Results and discussion

7.3.1 Baseline (1971 - 2000) scenario

The components of the nitrogen balance (see Eq. 1, 2 and 3) are averaged over the 23 SLC polygons in PEI (Table 7.3). The total amount of nitrogen input from fertilizer ($N_{fertilizer}$), manure (N_{manure}), leguminous crops ($N_{fixation}$) and atmospheric deposition ($N_{deposition}$) is 102.3kg N ha⁻¹. The outputs consist of nitrogen removed by the crop (N_{crop}) and gaseous losses (N_{gas}) which totals 71.5kg N ha⁻¹. The province-wide average of RSN is therefore 30.8kg N ha⁻¹.

Table 7.3. Province-wide average components of the nitrogen balance (kg N ha⁻¹) as simulated with historic crop and animal husbandry practices and with an adapted agricultural management scenario.

	Inputs				Outputs		RSN
	$N_{fertilizer}$	N_{manure}	$N_{fixation}$	$N_{deposition}$	N_{crop}	N_{gas}	
Historic	52.8	17.4	29.6	2.5	70.3	1.2	30.8
Adapted	61.2	16.8	30.1	2.5	73.2	1.6	35.7

As shown in Fig. 7.2a, the spatial variability of RSN ranges from less than 25kg N ha⁻¹ to approximately 40kg N ha⁻¹ (SLC polygon numbers are displayed in Chapter 6, Fig. 6.1). Agricultural management practices are responsible for this spatial variability. For example compare SLC polygon 536001 with adjoining SLC polygon 536003: in SLC 536003 there is more animal manure available than in SLC 536001 (17.0kg N ha⁻¹ vs. 7.3 kg N ha⁻¹ in SLC 536001)

and more N is fixed by leguminous crops like alfalfa (32.3kg N ha⁻¹ vs. 25.2kg N ha⁻¹). However, the amount of fertilizer N used and sold in SLC 536001 exceeds the amount used in SLC 536003 by 30kg N ha⁻¹ (76.9kg N ha⁻¹ in SLC 536001 vs. 46.6kg N ha⁻¹ in SLC 536003). Since the N output is fairly similar for both SLCs (approximately 70kg N ha⁻¹), the balance shows an average RSN of 39.8kg N ha⁻¹ in SLC 536001 and an average RSN of ‘only’ 28.7kg N ha⁻¹ in SLC 536003 (28% less).

The components of the soil water balance are also averaged over the 23 SLC polygons for both the growing season and the non-growing season (Table 7.4). During the growing season, 86 % of the precipitation infiltrates the soil, with the remainder being lost as either interception and/or surface runoff. Actual evapotranspiration accounts for 359mm, while 35mm drains through the soil profile; this leaves 141mm at the end of the growing season. During the non-growing season, precipitation is almost twice that of the growing season (767 vs. 393mm), but potential evapotranspiration is only 17 % of that simulated for the growing season (Table 7.4, bottom part). Snow blowing off the fields (88mm) and surface runoff (91mm) during the early spring period become more important components of the non-growing season water balance than actual evapotranspiration (48mm). Under this baseline climate, a large proportion of the non-growing season precipitation (61 %, i.e. 471mm) is lost via drainage.

Province-wide, the average amount of nitrogen lost via leaching is 27.9kg N ha⁻¹, i.e., 91 % of the RSN. The differences in nitrogen losses among SLC polygons (Fig. 7.2) are caused by agricultural practices (i.e. differences in RSN) and, to a lesser degree, by spatial climatic variability as is evidenced by the ‘percent of RSN lost’ which varies only from 87 to 96 (Table 7.4).

The temporal (i.e., year-to-year or inter-annual) variability in nitrogen leaching is small: coefficients of variation for nitrogen leaching (CV_{NL}) are mostly less than 3 %, with 4 SLC polygons having 3.0% < CV_{NL} < 7.5%. The province-wide average CV_{NL} equals 2.2 %. Some nitrogen leaching probability curves are shown in Figure 7.3. For a typical SLC polygon (# 536013, CV_{NL} = 2.5 %) there is a 90% probability that nitrogen leaching falls within the narrow range between 25.1 and 26.8kg N ha⁻¹. On the other hand, nitrogen leaching is more variable in SLC polygon 535001 (CV_{NL} = 4.4 %): there is a 90% probability that nitrogen leaching falls in the range from 32.9 to 37.5kg N ha⁻¹. Moreover, Figure 7.3 shows that there is a 5 % chance (1 year in 20) that nitrogen leaching exceeds 26.8 and 37.5kg N ha⁻¹ in polygons 536013 and 535001, respectively.

7.3.2 *Climate change (2040 - 2069) scenarios*

In this section, the agricultural management practices are kept to those described for the baseline situation, i.e. RSN values are the same as those depicted in Figure 7.2a. As discussed in Chapter 6, growing season precipitation of the four climate scenarios varies by less than 4 % from the 1970 -2000 baseline climate. However, potential evapotranspiration which is calculated as a function of maximum and minimum air temperatures (Baier and Robertson 1965), is projected to increase from a baseline value of 424mm to 471mm (+ 11%) with CGCM2 A2 and to 455mm (+ 7 %) with HadCM3 B2 (Table 7.4). This leads to a relatively small increase (approximately 5 %) in growing season actual evapotranspiration and to significantly less drainage (varying from 69 to 83 % of the baseline situation).

Table 7.4. Province-wide average components of the soil water balance and nitrogen leaching as simulated with baseline climate data and with climate change scenario data, with no changes in crop and animal husbandry practices (top half of the table refers to growing-season conditions, bottom half to non-growing season conditions).

Practice: Parameter	Baseline	CGCM2		HadCM3	
	current / historic	A2 current / historic	B2 current / historic	A2 current / historic	B2 current / historic
GSS ¹	131	124	128	128	129
SW-GSS ²	196	195	195	196	196
Precipitation	393	381	394	398	379
PET ³	424	471	456	464	455
Interception	45	47	46	45	44
Runoff	8	5	9	9	7
Infiltration	339	329	340	344	328
AET ⁴	359	379	378	382	372
Drainage	35	24	26	29	26
GSE ⁵	264	261	262	263	263
SW-GSE ⁶	141	120	131	129	124
Precipitation	767	724	788	765	725
PET	74	99	86	81	79
Blowoff	88	67	77	71	72
Runoff	91	80	101	90	79
Infiltration	574	560	597	589	562
AET	48	65	57	52	51
Drainage	471	420	477	471	439
RSN ⁷	30.8	30.8	30.8	30.8	30.8
N leaching	27.9	27.5	28.0	27.9	27.7
CV of N	2.2	3.5	2.1	2.4	3.1
leaching (%) ⁸					
% N lost	90.7	89.4	90.9	90.7	90.0

¹ Growing season start; ² Soil water content at the start of the growing season; ³ Potential evapotranspiration; ⁴ Actual evapotranspiration; ⁵ Growing season end; ⁶ Soil water content at the end of the growing season; ⁷ Residual Soil Nitrogen; ⁸ Coefficient of variation of N leaching.

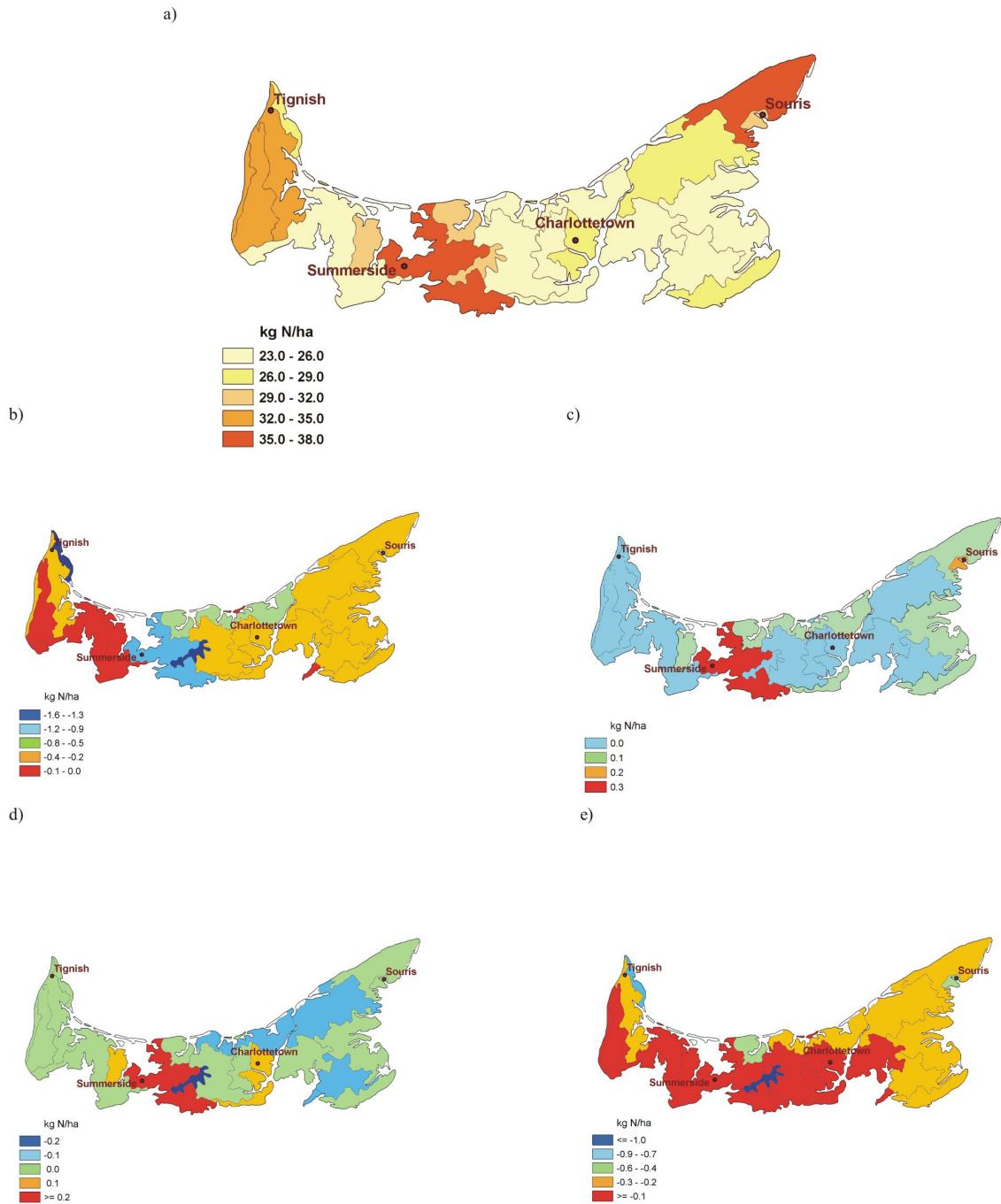


Figure 7.2. Simulated nitrogen leaching with historic management and the baseline climate (a) and projected changes with CGCM2 A2 (b), CGCM2 B2 (c), HadCM3 A2 (d) and HadCM3 B2 (e).

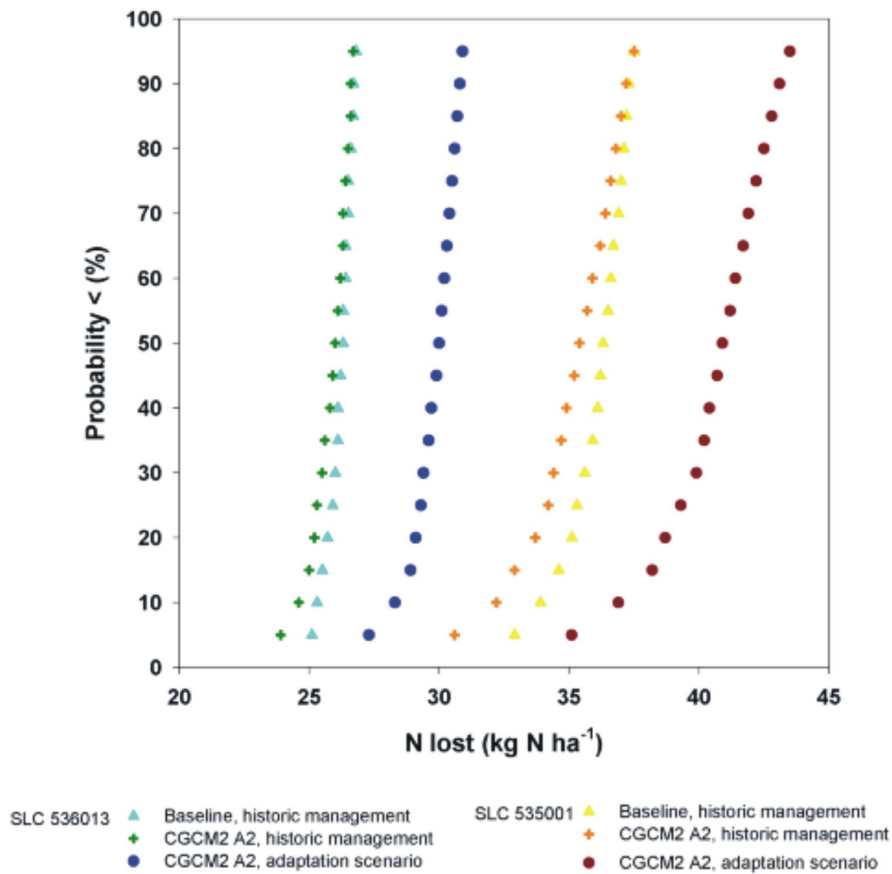


Figure 7.3. Probability curves of estimated nitrogen leaching in SLC polygons 535001 and 536013.

Although nitrogen leaching was not simulated during the growing season, based on the reduced drainage of water through the soil profile, it is conceivable that less growing season nitrogen leaching will take place under warmer future climates. The increased evapotranspiration of the climate change scenarios is also the cause of lower soil water contents at the end of the growing season.

Among the four climate scenarios, the non-growing season precipitation varies considerably: scenarios CGCM2 A2 and HadCM3 B2 project a 6 % decrease compared to the baseline climate; on the other hand, scenario CGCM2 B2 projects a 3 % increase, while with scenario HadCM3 A2 there is little change. Snow blowoff is reduced by 11 (CGCM2 B2) to 21 (CGCM2 A2) mm under the climate change scenarios because more precipitation will come in the form as rain rather than as snow under warmer conditions. Compared to the baseline climate, changes in

runoff and drainage are coupled to changes in precipitation: under scenarios CGCM2 A2 and HadCM3 B2 runoff and drainage decrease, under scenario CGCM2 B2 they increase and with scenario HadCM3 A2 there is no change. While the amounts of drainage vary considerably (from 420mm under scenario CGCM2 A2 to 477mm under scenario CGCM2 B2, the drainage as a proportion of the total non-growing season precipitation is relatively constant (58 to 62 %) among the climate scenarios and practically the same as that under the baseline climate.

The province-wide averages of nitrogen lost via leaching under the four climate scenarios are very similar to the one calculated with the baseline climate (Table 7.4). Even for scenarios CGCM2 A2 and HadCM3 B2, for which we calculated 51 and 32mm less non-growing season drainage, the accumulated non-growing season nitrogen losses are less than 1 % different from the one calculated with the baseline climate. This suggests that unless future climate change is much more dramatic (i.e. primarily significantly reduced over-winter precipitation) than what is used in our simulations, nitrogen leaching will remain near current levels.

Compared to the baseline climate, the spatial variability in nitrogen leaching does not change under scenarios CGCM2 B2 (Fig. 7.2c) and HadCM3 A2 (Fig. 7.2d): for each SLC polygon nitrogen leaching changes by less than 1 %. For scenario CGCM2 A2 (Fig. 7.2b) there are 4 polygons (534001, 535001, 536004 and 537004) in which nitrogen leaching increases by 2 to 5 %, and for scenario HadCM3 B2 (Fig. 7.2e), there are 2 of these polygons (534001 and 537004). All the remaining polygons change by less than 2 %.

With the exception of scenario CGCM2 B2, the inter-annual temporal variability in nitrogen leaching increases under the climate change scenarios as compared to the baseline scenario (Table 7.4), with scenario CGCM2 A2 being the most variable (province wide average $CV_{NL} = 3.5 \%$), followed by HadCM3 B2 (province wide average $CV_{NL} = 3.1 \%$). The increase in nitrogen leaching variability is also displayed in Figure 7.3. Both SLCs show that the 5 % chance of nitrogen leaching *exceeding* 26.8 and 37.5kg N ha⁻¹ in polygons 536013 and 535001 changes by less than 0.5kg N ha⁻¹ (does not change significantly) under climate scenario CGCM2 A2 as compared to the baseline climate. However, the 5 % chance of nitrogen leaching being less than 25.1kg N ha⁻¹ in polygon 536013 decreases by 1.2kg N ha⁻¹ (5 % decrease) to 23.9kg N ha⁻¹, while in polygon 535001 it decreases from 32.9 to 30.6 kg N ha⁻¹ (a 7 % decrease). In other words, nitrogen leaching variability increases primarily because the lower nitrogen leaching values become more variable; the larger nitrogen leaching values do not change.

7.3.3 *Climate change coupled with agricultural management change*

With the agricultural adaptation scenario, described in the methodology section under input data, nitrogen inputs from fertilizer increased by 8.4kg N ha⁻¹ over the historic simulated inputs (Table 7.3). The other inputs from manure, fixation and deposition remained relatively constant. Nitrogen removal by crop uptake increased by 3.1kg N ha⁻¹, and consequently residual soil nitrogen at the end of the growing season increased significantly from 30.8kg N ha⁻¹ under the historic management conditions to 35.7kg N ha⁻¹ (i.e. a 16 % increase) with the simulated adaptation scenario.

The spatial variability of RSN under the adaptation scenario ranges from 28.3kg N ha⁻¹ in SLC polygon 536016 to close to 46.1kg N ha⁻¹ in polygon 536001 (Fig. 7.4b). The relative increase in

RSN over the historic data ranges from 10 to 22.5 % (Fig. 7.4c). There is a strong positive correlation $r = 0.98$) between RSN simulated with historic management data and RSN simulated with the adaptation scenario.

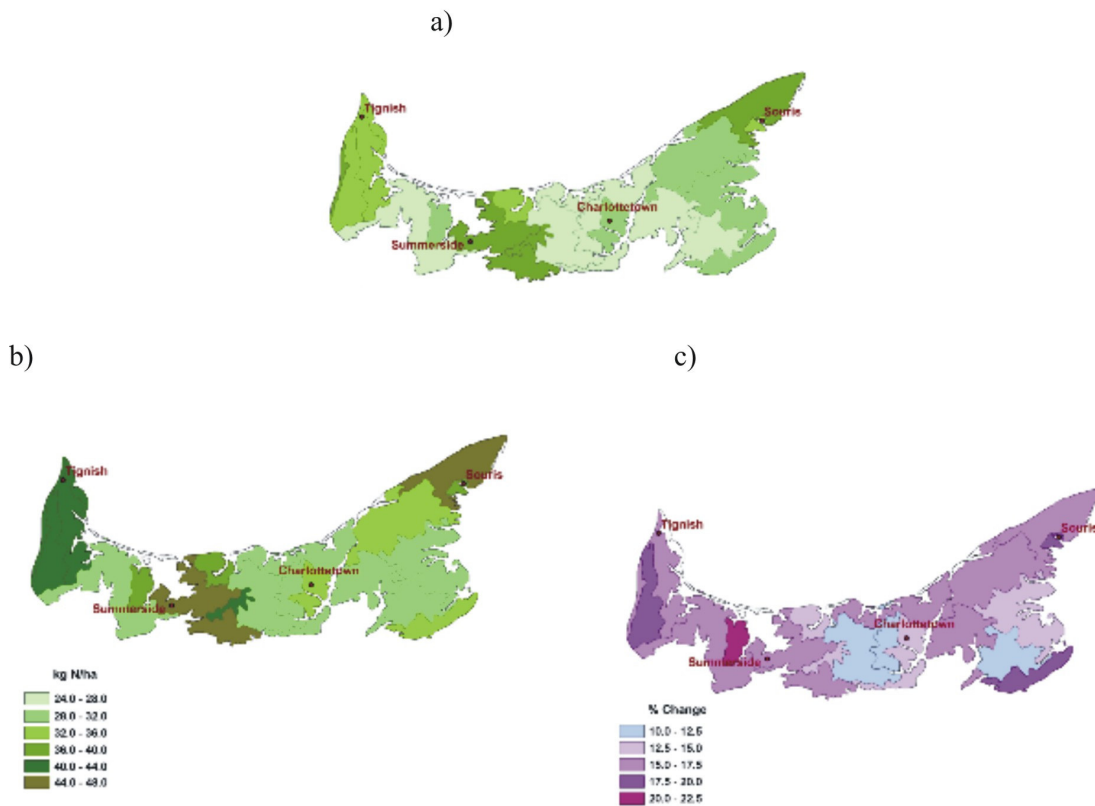


Figure 7.4. Simulated residual soil nitrogen (300 yr averages) using (a) historic management practices and (b) the adaptation scenario; (c) relative differences between historic management and the adaptation scenario.

The adaptation scenario has little effect (changes are smaller than 2mm) on the components of the soil water balance, with the exception of increased non-growing season surface runoff and consequently reduced drainage (13mm or 2.9% less than when simulated with the historic management data). With the adaptation scenario there is a shift towards increased annual cropping, at the expense of perennial forage crops, leading to more bare soil during the winter which causes the increased surface runoff.

A summary of the province-wide averages of residual soil nitrogen and nitrogen lost via deep drainage under different climate and different agricultural management scenarios is given in (Table 7.5). Under historic management conditions RSN is estimated to be $30.8 \text{ kg N ha}^{-1}$, while under the adaptation scenario it increases by 4.9 kg N ha^{-1} . N leaching is a function of the climatic scenario, as discussed in the section ‘climate change (2040 - 2069) scenarios, and the amount of RSN at the end of the growing season. The four climatic scenarios (CGCM2 A2, CGCM2 B2, HadCM3 A2 and HadCM3 B2) have little influence on nitrogen leaching in PEI, with the difference in the amount of nitrogen lost via deep drainage always being less than 0.5 kg N ha^{-1} as

compared to the baseline climate. However, there is a direct positive correlation ($r > 0.95$) between RSN and nitrogen leaching. With the adaptation scenario, RSN increases by 4.9kg N/ha, and under all four climate scenarios nitrogen leaching increases by an almost similar amount: 4.7kg N ha⁻¹, i.e. a 15 % increase over that estimated with the baseline climate and historic management. Under each scenario approximately 90 % of the RSN is lost during the non-growing season.

Table 7.5. Summary of province-wide averages of nitrogen related parameters under different climate and different agricultural management scenarios.

Climate	Management	RSN (kg N ha ⁻¹)	Nitrogen leaching (kg N ha ⁻¹)	% of RSN lost
Baseline	Historic	30.8	27.9	90.7
	Adaptation	35.7	32.6	91.3
CGCM2 A2	Historic	30.8	27.5	89.4
	Adaptation	35.7	32.1	90.0
CGCM2 B2	Historic	30.8	28.0	90.9
	Adaptation	35.7	32.7	91.5
HadCM3 A2	Historic	30.8	27.9	90.7
	Adaptation	35.7	32.6	91.4
Had CM3 B2	Historic	30.8	27.7	89.9
	Adaptation	35.7	32.3	90.6

The spatial variability in nitrogen leaching with the adaptation scenario is very similar for all four future climate scenarios (Fig. 7.5), and not unlike that displayed in Figure 7.4a. Estimated nitrogen leaching in excess of 35kg N ha⁻¹ takes place in SLC polygons south of Tignish, around Summerside and at the northeastern tip of PEI. The changes in nitrogen leaching compared to the values simulated with the baseline climate and historic management vary from 5 to 30 % (see Figs. 7.5b,d,f,h).

Compared to the baseline simulations, the provincial average temporal inter-annual variability of nitrogen leaching increased from 2.2 % to 3.7, 2.4, 2.6 and 3.3 % with scenarios CGCM2 A2, CGCM2 B2, HadCM3 A2 and HadCM3 B2, respectively (Table 7.3). This is slightly higher as compared to the simulations with current/historic management practices (Table 7.4, Fig. 7.3).

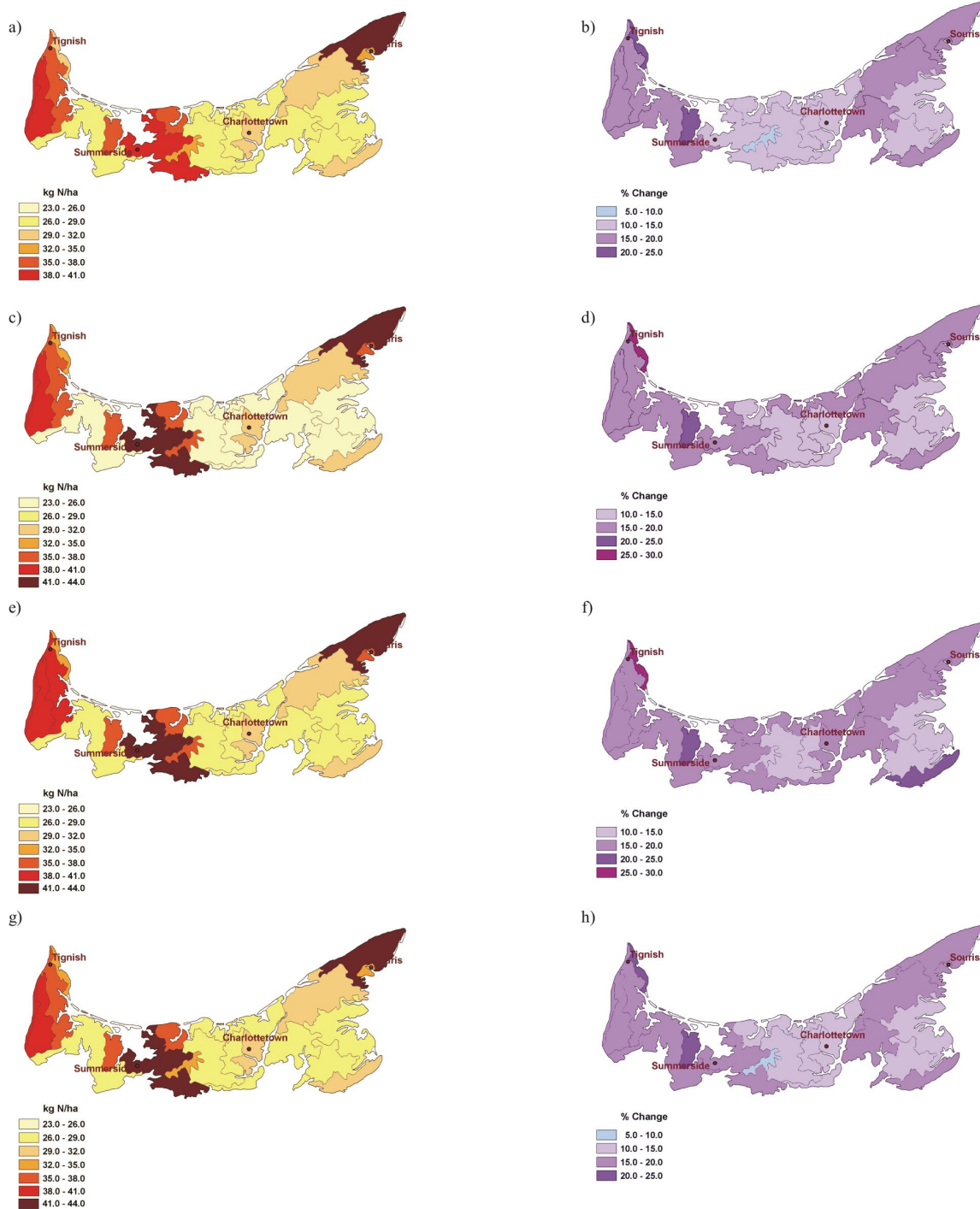


Figure 7.5. Simulated nitrogen leaching with the adaptation and climate-change scenarios: CGCM2 A2 (a), CGCM2 B2 (c), HadCM3 A2 (e) and HadCM3 B2 (g) and their respective changes as related to the baseline climate with historic management (b, d, e and f).

7.4 Conclusion

Projected climate change in Canada and its impact on crop yield and production has been documented, but the impacts on soil- and water quality are less well known. With four climate change scenarios, projected air temperatures for the period 2040 - 2069 in PEI increase by 1 to 3 °C, while precipitation varies from -5 % to +2 % as compared to the baseline (1970 - 2000) climate. As a result of the increased temperatures, growing season evapotranspiration increases by 7 to 11 %, and drainage of water through the soil profile decreases by 17 to 31 %. Consequently, although not simulated in this study, nitrogen leaching may be reduced during the growing season. During the non-growing season and with no changes in crop and animal husbandry practices, nitrogen leaching under all four climate scenarios remains similar to that simulated using the baseline climate, i.e. 28kg N ha⁻¹. The spatial distribution of nitrogen leaching is projected not to change, but the temporal inter-annual variability is projected to increase slightly from 2.2% under the baseline scenario to 3.5 % under the CGCM2 A2 scenario.

Under the defined adaptation scenario, the components of the soil water balance remain relatively constant (with the exception of non-growing season surface runoff which increases by approximately 14 mm), but the residual soil nitrogen increase from 10 to 23 % across PEI. This leads to non-growing season nitrogen leaching increases of 5 to 30 %. The temporal variability in nitrogen leaching increases slightly by less than 2%.

The direct impact of the projected climate change on nitrogen leaching appears to be small. Only when agricultural intensification takes place, in response to climate change and economic conditions, will soil nitrogen leaching increase beyond historic levels.

8 Numerical modelling of the evolution of groundwater nitrate concentrations under various Climate Change scenarios and agricultural practices for Prince Edward Island

Harold Vigneault, Daniel Paradis, Jean-Marc Ballard & René Lefebvre

ABSTRACT

Groundwater in 4 to 5% of domestic wells in Prince Edward Island currently exceeds the 10mg/L (N-NO₃) nitrate maximum concentration for drinking water. Such high concentrations seem related to agricultural practices. The objective of this study was thus to evaluate how nitrate concentrations in the aquifer could evolve in the future due to climate change as well as potential changes in agricultural practices. To meet this objective, an infiltration model was first used to evaluate how groundwater recharge could evolve due to climate change. Three out of the four climate change scenarios used showed that groundwater recharge could be reduced by 2050 due to an increase in evapotranspiration related to higher mean temperatures. A numerical model of groundwater flow and nitrate mass transport was then developed for the entire Island, based on available field data. Simulations involving the effect of CC used a constant nitrate loading corresponding to the 2001 estimated value and predicted an increase in nitrate concentration in 2050 that would be largely due to reaching steady-state conditions of aquifer concentrations generated by present-day loading. Simulations considering a potential increase in nitrate loading related to changes in agricultural practices predicted more important nitrate concentration increases, especially in watersheds with intense agricultural activities. The predicted increases in nitrate concentrations imply that in 2050, a proportion of domestic wells larger than the current percentage would not meet the nitrate drinking water criteria.

8.1 Introduction

Global warming due to the increase in greenhouse gases has led to considerable research around the world. Global average temperature is predicted to increase by 1.4 to 5.8°C in 2100 relative to 1990 (IPCC 1997). Since global warming is expected to impact the hydrologic cycle as well as future agricultural practices, it could also affect the evolution of nitrate concentrations in groundwater (GW).

The objective of this project is to make a global assessment of the potential impact of climate change as well as the resulting agricultural practice changes (APC) on nitrate concentrations in GW over the entire Province of Prince Edward Island (PEI). This project extends the work carried out on aquifer characterization and modelling done on the Wilmot River watershed (Chapters 2 to 5), to the whole Prince Edward Island.

Nitrate concentrations (mass of nitrate per volume of water, i.e. mg/L) found in aquifers depend on the loading (mass) of nitrate available for leaching in soils and the volume of water that infiltrates (recharge) through the soil to carry the nitrate to aquifers. An assessment of the potential impact of CC on nitrate concentration must consider the effect of CC both on nitrate loading and GW recharge. CC is itself predicted on the basis of meteorological models that have a

degree of uncertainty requiring that different climate scenarios be considered in order to represent the potential range of changes, especially regarding temperature and precipitation. To meet the objective of the project, the following steps are undertaken:

- 1) Selection of four climate scenarios that would provide daily weather conditions for the future (obtained from the Canadian Climate Center General Circulation Model described in Chapter 6);
- 2) Evaluation of nitrogen leaching to the aquifer under present-day conditions as well as considering APC scenarios; these nitrate loadings were determined on the basis of the Residual Soil Nitrogen (RSN) evaluated in Chapter 7;
- 3) Estimation of GW recharge with an infiltration model (HELP) which uses daily climate conditions and soil properties as input; the results obtained by this model are calibrated using present-day climate conditions, so that future recharge could then be estimated using the four climate scenarios;
- 4) Development and calibration with present-day recharge and nitrate loadings of a three-dimensional numerical model (FEFLOW) of GW flow and nitrate transport over the entire PEI; and
- 5) FEFLOW modelling to simulate PEI potential evolution of nitrate concentrations under different CC and APC scenarios.

8.2 Conditions representative of Prince Edward Island

8.2.1 Land use

PEI is located in eastern Canada and is one of the three Maritime Provinces ([Fig. 8.1](#)). The Island covers close to 5 660 km² and it is about 225km long by 3 to 65km wide ([Table 8.1](#)). Topographic elevation ranges from sea level to 140 masl (meter above sea level). PEI is predominantly rural with 39% of its surface dedicated to agricultural activities and 45% covered by forest ([Table 8.1](#)). Generally, forest cover is dominant in the eastern and western portions of the Island, whereas agricultural activities are mostly concentrated in central PEI. The largest cities on PEI are Charlottetown and Summerside with respective populations of 32,245 and 14,654 (2001 Census). Residential, urban and industrial activities use less than 6% of the territory.

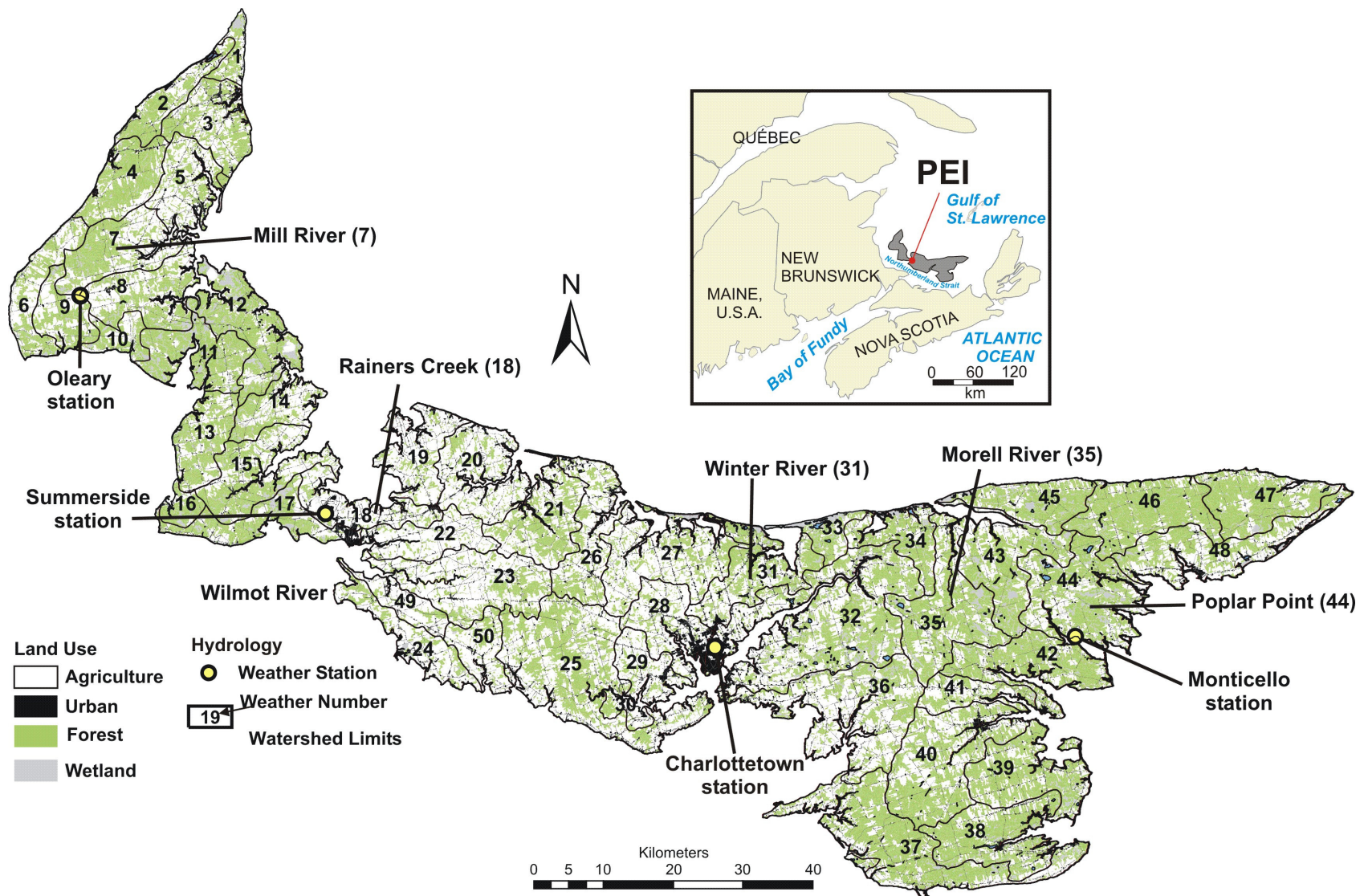


Figure 8.1. Location of Prince Edward Island (inset map) and distribution of its 48 main watersheds.

Table 8.1. Main characteristics of Prince Edward Island (land uses are based on a LANDSAT image for year 2000).

Physiography	
Area	5 660km ²
Width	3-65km
Length	225km
Elevation (above sea level)	0-140m
Land Use	
Forest	45 %
Agriculture	39 %
Wetland	7 %
Residential, urban, industrial	5.9 %
Recreational	0.3%
Miscellaneous	2.8 %

8.2.2 Climate and hydrology

The climate of PEI is humid-continental, with long, fairly cold winters and warm summers. Data selected from four meteorological stations distributed geographically across the Island that show fairly similar meteorological conditions (Fig. 8.1 and Table 8.2). As an example of the climatic conditions found on the Island, the mean annual precipitation at the Charlottetown meteorological station (8300300) is 1173mm (1971-2000), most of which falls as rain (75%). The mean annual temperature is about 5.3°C and means for monthly temperature range from minus 8°C in January to 18.5°C in July.

Table 8.2. Weather for Prince Edward Island (meteorological data are for the period 1971-2000).

Weather characteristics	O'Leary (8300525)	Summerside (8300700)	Charlottetown (8300300)	Monticello (8300447)
Mean annual total precipitation (mm)	1141	1078	1173	1164
Mean annual rain (mm)	860	806	880	903
Mean annual snow (mm)	281	282	311	261
Mean annual temperature (°C)	5.2	5.6	5.3	5.5
Minimum mean monthly temperature (°C)	-8.6	-7.9	-8.0	-7.4
Maximum mean monthly temperature (°C)	18.5	19.1	18.5	18.4

The Island can be divided into fifty main watersheds that can be further subdivided into 241 sub-watersheds. River basins are typically small, and the main rivers are estuarial over a significant

portion of their length (Fig. 8.1). Mean annual streamflow for typical river systems ranges from less than 0.66 to 2.88 m³/s (Table 8.3). Francis (1989) reported that the pumping withdrawal in the Winter River watershed reduced the river flow implying that the values shown in Table 8.3 is lower than natural conditions.

Table 8.3. Streamflow characteristics of selected rivers in Prince Edward Island (records are for the following periods: Wilmot, 1972-2005; Morell, 1961-1995; Winter, 1965-1991).

Streamflow characteristics	Morell 133 km ² (01CD003)	Wilmot 45.4 km ² (01CB004)	Winter 37.5 km ² (01CC002)
Mean annual (m ³ /s)	2.88	0.92	0.66
Minimum monthly mean (Sept.) (m ³ /s)	1.10	0.44	0.24
Maximum monthly mean (April) (m ³ /s)	6.77	1.89	1.61

Figure 8.2 illustrates a schematic representation of the water balance for PEI. Each process is represented in percentage of total precipitation.

8.2.3 Hydrogeology

PEI is a crescent-shaped cuesta of continental red beds, Upper Pennsylvanian to Middle Permian in age, dipping to the northeast at about one to three degrees (Van de Poll, 1983). The constituent mineral grains of these sedimentary rocks were carried by streams and rivers from highlands in present-day New-Brunswick and Nova Scotia and deposited under oxidizing conditions in the low-lying area which is now PEI (Prest, 1973). van de Poll (1983) mapped the red bed units as an upward-fining series of cyclic deposits containing four “megacycles”. These sequences consist of conglomerate, sandstone and siltstone red beds. These units exhibit rapid lateral and vertical facies changes and strong cross-bedding features. The continuity of lithological units is difficult to establish, even over short distances. The bedrock sequence of PEI is almost entirely covered by a layer of unconsolidated glacial material from a few centimetres to several meters in thickness (Prest, 1973). These deposits are generally derived from local sedimentary rock and include both unsorted tills and water-worked glacio-fluvial and glacio-marine deposits. With few exceptions these surficial deposits are not saturated, and do not represent significant aquifers.

In most parts of the Island the rock aquifer is unconfined. The potentiometric map representing the water levels was interpolated using more than 17,243 wells, and it shows that the water table in the sandstone follows the topography (not shown). The definition of the conceptual model (Fig. 8.2) for the Island is based on works of Francis (1989) in the Winter River watershed and on Paradis *et al.* (2006) in the Wilmot River watershed (see also Chapter 5).

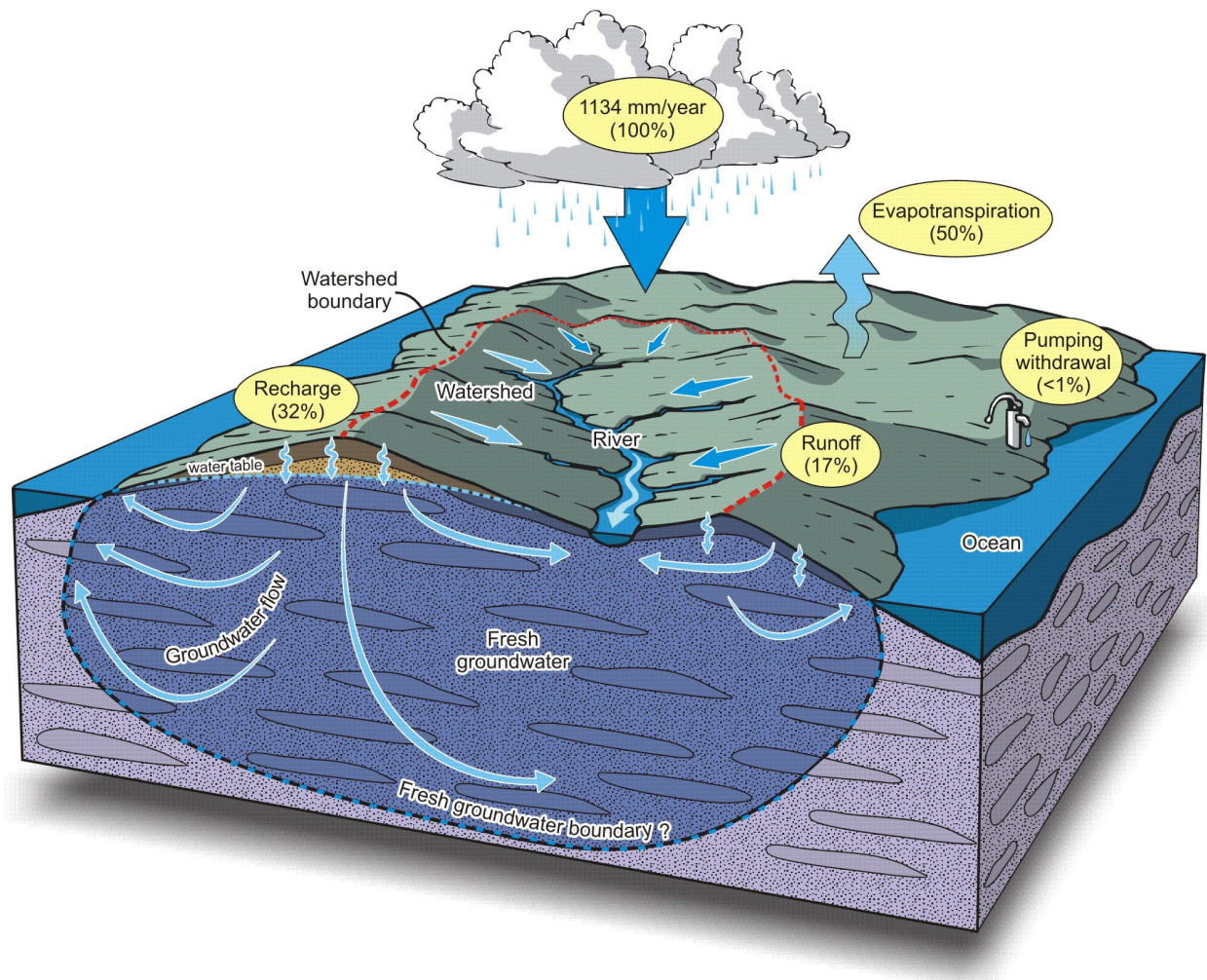


Figure 8.2. Schematic representation of the water balance in PEI and conceptual model for the numerical simulation.

8.2.4 Climate change scenarios

Four future climatic scenarios were selected to run predictive modelling. These scenarios are based on the two times carbon dioxide ($2\times\text{CO}_2$) assumption that is expected to be reached by 2050. The four climatic scenarios were provided by the Canadian Climate Center General Circulation Model (Chapter 6). To summarize these scenarios, average temperature and precipitation for 2050 and their percentage change relative to the 2001 conditions are presented in [Table 8.4](#). These climatic scenarios were mainly used as inputs for the HELP infiltration model (see Section 8.3.1) to represent the impact of CC on GW recharge. For a better spatial resolution of the weather data, the Island was divided into four zones corresponding to the weather stations: O’Leary, Summerside, Charlottetown and Monticello ([Fig. 8.1](#)).

Table 8.4. Summary of the change in temperature, precipitation, evapotranspiration, runoff and recharge for the historical period and the four CC scenarios for Prince Edward Island. Values provided in brackets are the change in % for the 2040-2069 period with respect to historical conditions (1959-2001).

Scenario	Precipitation (mm)	Temperature (°C)	Evapo- transpiration (mm)	Runoff (mm)	Recharge (mm)
Historic	1173	5.3	583	197	369
CGCM2 A1	1109 (-5)	8 (+1)	618 (+6)	131 (-33)	336 (-9)
CGCM2 B1	1223 (+4)	7 (+0.6)	620 (+6)	190 (-4)	394 (+7)
HadCMA2a	1141 (-3)	6.7 (+0.5)	616 (+6)	163 (-17)	323 (-12)
HadCMB2a	1197 (+2)	7.1 (+0.6)	615 (+5)	172 (-13)	361 (-2)

8.2.5 Residual Soil Nitrogen

Residual Soil Nitrogen (RSN) is an indicator that estimates, at the Soil Landscape of Canada (SLC) polygon level, the quantity of inorganic soil nitrogen at the time of harvest. RSN includes inputs in the form of nitrogen fertilizer, manure and nitrogen fixation, and outputs in the form of nitrogen in harvested crops (Chapter 7). There are 23 SLC polygons covering the island.

For the period of 2040-2069 the average RSN value was estimated to increase by 15% (5% to 30% depending on the SLC polygon). Since RSN values are estimated over entire SLC polygons, the nitrogen load was also applied on these polygons. RSN units are provided in kg of nitrogen per hectare of farmland area but farmlands are not defined within the SLC polygon. Hence, to be compatible with our numerical model, the nitrogen load applied at the surface was estimated by multiplying the RSN values by the ratio of farmland used over SLC polygon areas. This operation maintains the total nitrogen mass over the SLC polygon but reduces the applied rate. For modelling purposes, it was assumed, as a first approximation, that the total RSN was nitrified and leached to the aquifer within the year.

8.3 Model description and calibration

The general procedure followed to assess the impact of CC and APC was first to estimate the GW recharge and leaching of nitrate to the aquifer. Then a numerical GW flow and mass transport model was constructed from the existing conceptual model, calibrated with available records and used to simulate future nitrate concentrations.

We used HELP to estimate GW recharge (Schroeder *et al.*, 1994). The main objective was to reproduce the hydrological cycle on PEI and then assess how the different CC scenarios would affect the GW component. It is assumed that nitrate is highly soluble in water and that all nitrate in contact with water will be transported by water. Hence, the amount of GW recharge has an important diluting effect and for the same mass of nitrate in contact with a different quantity of water, the resulting nitrate concentrations would vary. The amount of nitrate leaching to aquifer was based on RSN values provided in Chapter 7. It was assumed that all RSN was nitrified and leached to the aquifer within the year. Finally, to reproduce the GW flow system and to simulate nitrate transport under various scenarios of CC, we used the three-dimensional finite element numerical simulator FEFLOW (Diersch, 2004).

8.3.1 *HELP model*

Groundwater recharge simulations were carried out with the quasi-two-dimensional deterministic, hydrologic model HELP (Schroeder *et al.*, 1994). This model was developed to simulate water infiltration in landfills but it has been extensively used to estimate GW recharge (Jyrkama *et al.*, 2002; Allen *et al.*, 2003; Croteau *et al.*, 2005). The model simulates daily movement of water in the ground and accounts for the effects of surface storage, snowmelt, runoff, infiltration, evapotranspiration, vegetative growth, soil-moisture storage and lateral subsurface drainage.

The spatial estimation of GW recharge over PEI was obtained by dividing the Island into cells of 500x500 m for a total number of 21,168 cells. Surface information needed for the analysis was retrieved with GIS software and a code was developed to automate the construction of the input files and to run the model in batch mode.

The model was first run with the historical records of temperature and precipitation (1960-2001) and calibrated with the average seasonal distribution of recharge and the runoff estimated from streamflow records. The calibration of the seasonal distribution of recharge was based on well hydrographs that follow water level changes through time and show that GW recharges all year long in PEI, including winter. To simulate winter recharge, the frozen soil condition in the HELP code was modified. The runoff was estimated by filter analysis using Furey and Gupta (2001) approach and the calibration of the total annual runoff was carried out using three gauged streamflow stations (Wilmot, Mill and Morell). Results of the calibration show that the seasonal recharge and runoff calibrations are respectively within 4-17% and 5-12% (not shown). The average recharge over the entire PEI was estimated at 369 mm/yr for the 1960-2001 period (Table 8.4). The recharge values can vary from 0 mm/yr in the wetland area to 704 mm/yr in areas with coarse sandy sediments.

Afterwards, the four climatic scenarios were used to estimate GW recharge for the 2040-2069 period. Values of evapotranspiration, runoff and recharge for 2045-2055 and relative change by respect to 1960-2001 are presented in Table 8.4. This table shows that, on average, scenarios CGCM2 A1 and HadCMA2a are the dryer whereas scenario CGCM2 B1 is the wetter and HadCMB2a has an intermediate behaviour. Moreover, the mean temperature is higher for all the scenarios implying an increase of the evapotranspiration and a decrease of the runoff. The recharge is higher for the scenario CGCM2 B1 (wetter condition) and lower for the three others.

8.3.2 *FEFLOW model*

To represent the GW flow system and to simulate nitrate transport under various scenarios of CC for the entire Province, the three-dimensional finite element numerical simulator FEFLOW (Diersch, 2004) was used. The finite element grid design is based on the conceptual model referred to in section 8.2.3. Table 8.5 presents the properties of the model according to this conceptual model. The boundary conditions are constant heads all around the Island. Moreover, since rivers are known to be connected to the aquifer (Francis, 1989; Paradis *et al.*, 2006), constant heads were also applied on main rivers and streams (Fig. 8.3).

Numerical model

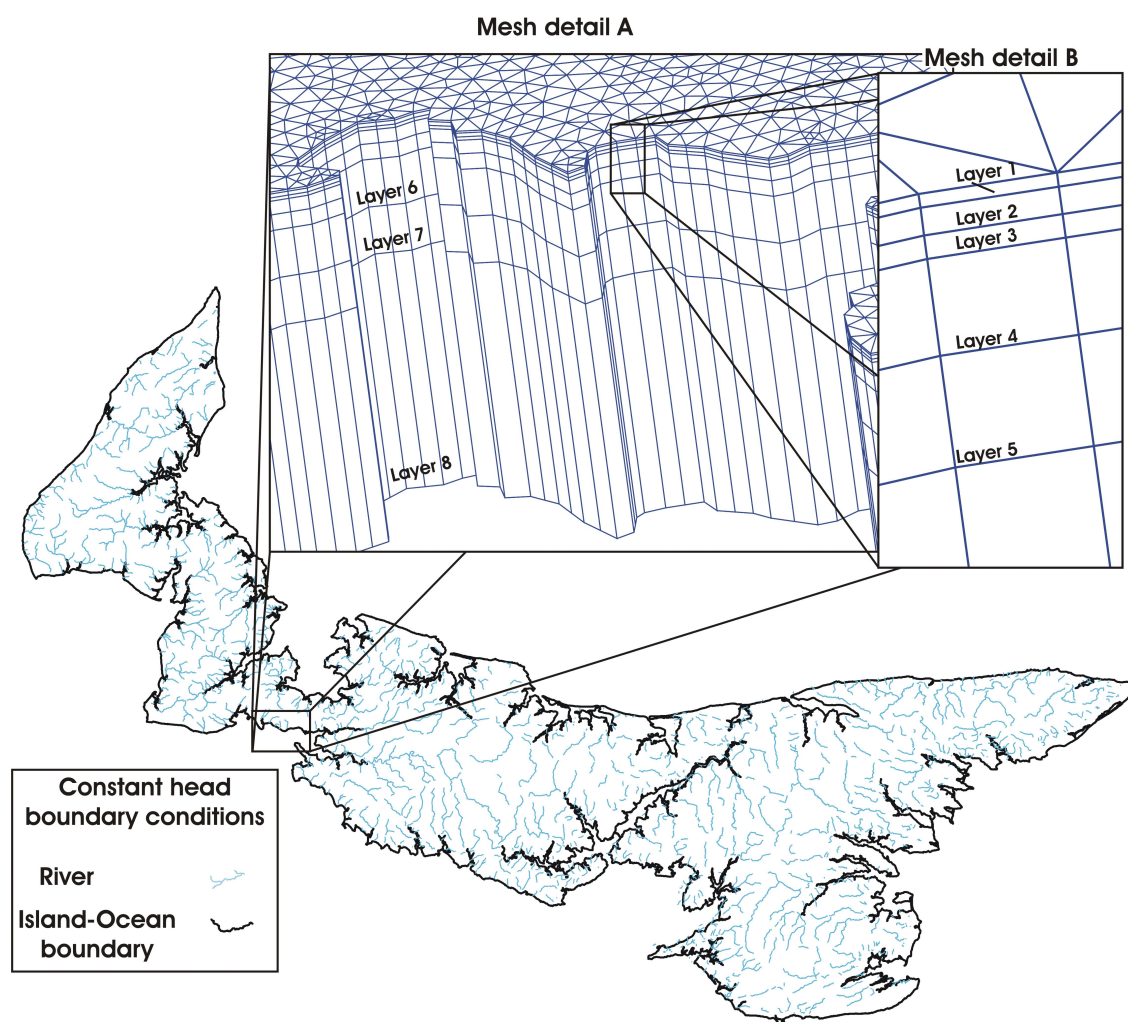


Figure 8.3. FEFLOW model for Prince Edward Island with mesh detail showing the eight layers, the triangular surface elements and the boundary conditions. The upper limit of the first layer corresponds to the top of the aquifer because the unsaturated zone is not represented in the model.

Given that the $2\times\text{CO}_2$ in atmosphere is expected to be reached in 2050, the future climate scenarios for temperature and precipitations are provided for the 2040-2069 period only. The gap between the last year of the calibration period (2001) and the beginning of the scenarios (2040) was filled with mean recharge and gradually increasing RSN input values to provide meaningful nitrate concentrations in the future (Fig. 8.4). For modelling purposes, a linear interpolation between values established for 2001 and 2040 was applied. Figure 8.4 shows the nitrogen concentrations that were applied on three different watersheds (Rainers Creek, Mill and Poplar Point) over the entire modelling period (historical, gap and 2040-2069).

Table 8.5. Field-based and calibrated hydraulic properties of the Prince Edward Island aquifer model (K_h and K_v are respectively horizontal and vertical hydraulic conductivity and n is total porosity). The effective diffusion coefficient used in the model is $1 \times 10^{-9} \text{ m}^2/\text{s}$ and longitudinal and transverse dispersivities are respectively 5 and 0.5 m.

Layer # (Depth in m)	Field K (m/s)	Numerical model		
		K (m/s)	K_h/K_v	n (%)
1 (0-5)	4.5×10^{-4} to 8.1×10^{-5}	3×10^{-4}	10	17
2 (5-10)		1×10^{-4}	10	17
3 (10-15))		5×10^{-5}	10	17
4 (15-30)		1×10^{-5}	100	17
(30-80)	1.7×10^{-4} to 8.4×10^{-7}	1×10^{-5}	1000	17
6 (80-180)		1×10^{-6}	100	17
7 (180-380)	n.d.	1×10^{-7}	10	17
8 (380-880)	n.d.	1×10^{-8}	1	17

The model was first calibrated prior to use for predictions. In the calibration process, model parameters were adjusted until simulation results were consistent with the understanding of the GW system and all the available observations. The present model was calibrated with three types of data: (1) the measured heads in domestic wells; (2) the mean base flow recession (MBR) curve for rivers and; (3) the GW nitrate concentration records in domestic wells for 2000-2005. More details on the calibration process are found in Paradis *et al.* (2006) and results of the calibration for the nitrate concentrations are shown on [Figure 8.5](#), where average measured nitrate concentrations are compared to simulated concentrations per SLC polygon. The difference between measured and simulated concentrations is 0.5 mg/L, meaning that the mass of nitrate on average is somehow under estimated. However, we should note that nitrate concentrations are distributed randomly around the 1:1 line. This stresses the fact that the model represents well the average conditions found on the Island but did not represent perfectly the concentrations within each watershed. Hence, model predictions should be used only to predict general trends and not to represent specific local conditions. 100% of the initial RSN estimates on each SLC polygon were used for the calibration. Resulting simulated nitrate concentrations in GW for 2001 are presented on [Figures 8.6a](#) and [8.7a](#). This simulation will be used as a reference to assess the impact of CC and APC.

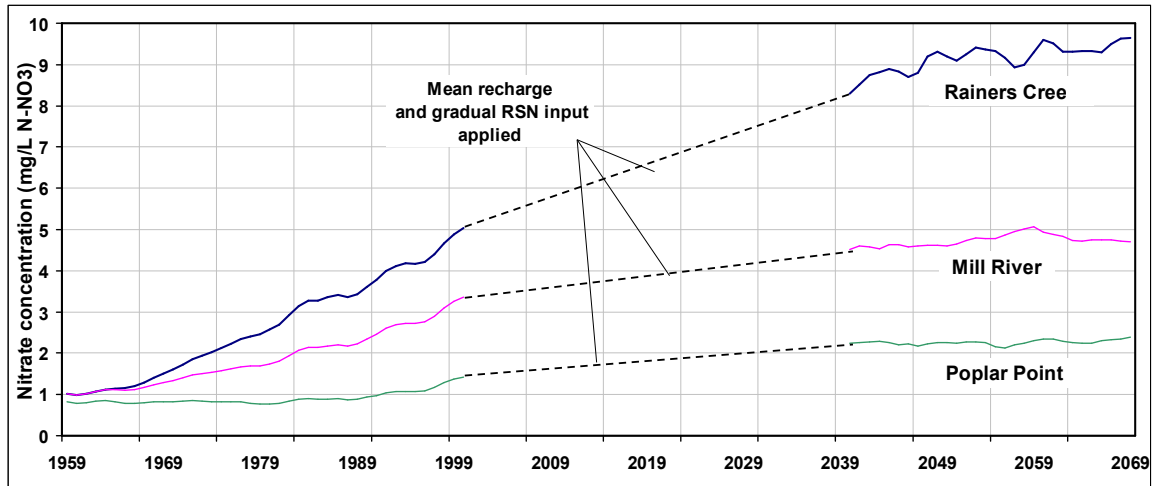


Figure 8.4. Evolution of nitrate concentrations applied at the model surface for the Rainer Creek, the Mill River and the Poplar Point River watersheds from 1959 to 2069. The dotted lines represent gaps in the meteorological (recharge) and RSN data used to estimate nitrate concentrations.

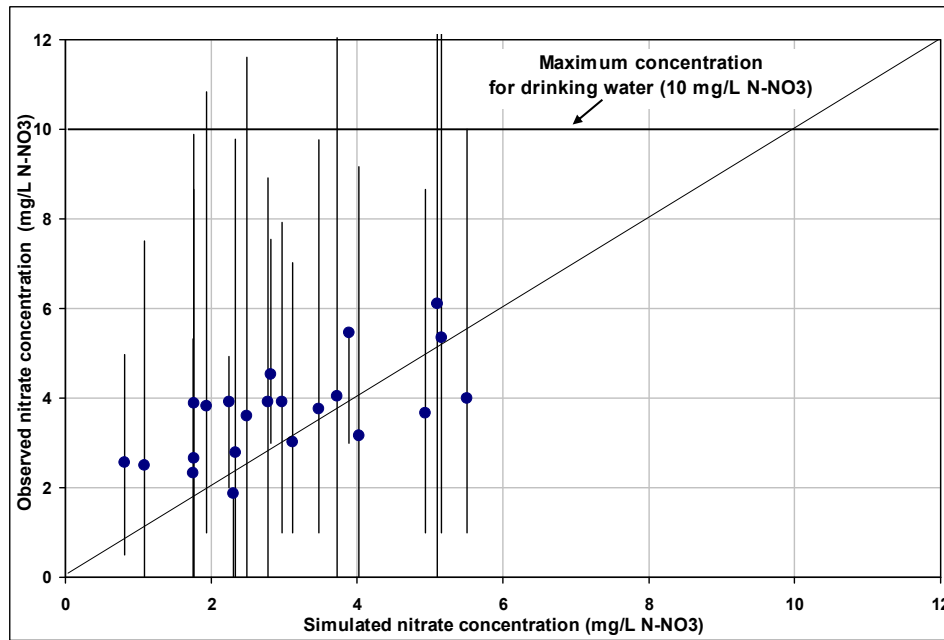


Figure 8.5. Model calibration with the average groundwater nitrate concentrations measured in domestic wells for 2002-2005. Each point on the figure represents the average nitrate concentration in each SLC polygon, whereas the bars span the interval between the 25 and 75 percentiles of concentrations within each watershed showing the large spatial variability of the measures. More than 17,000 measurements in domestic wells were used. The 45° perfect-fit line is presented as a reference.

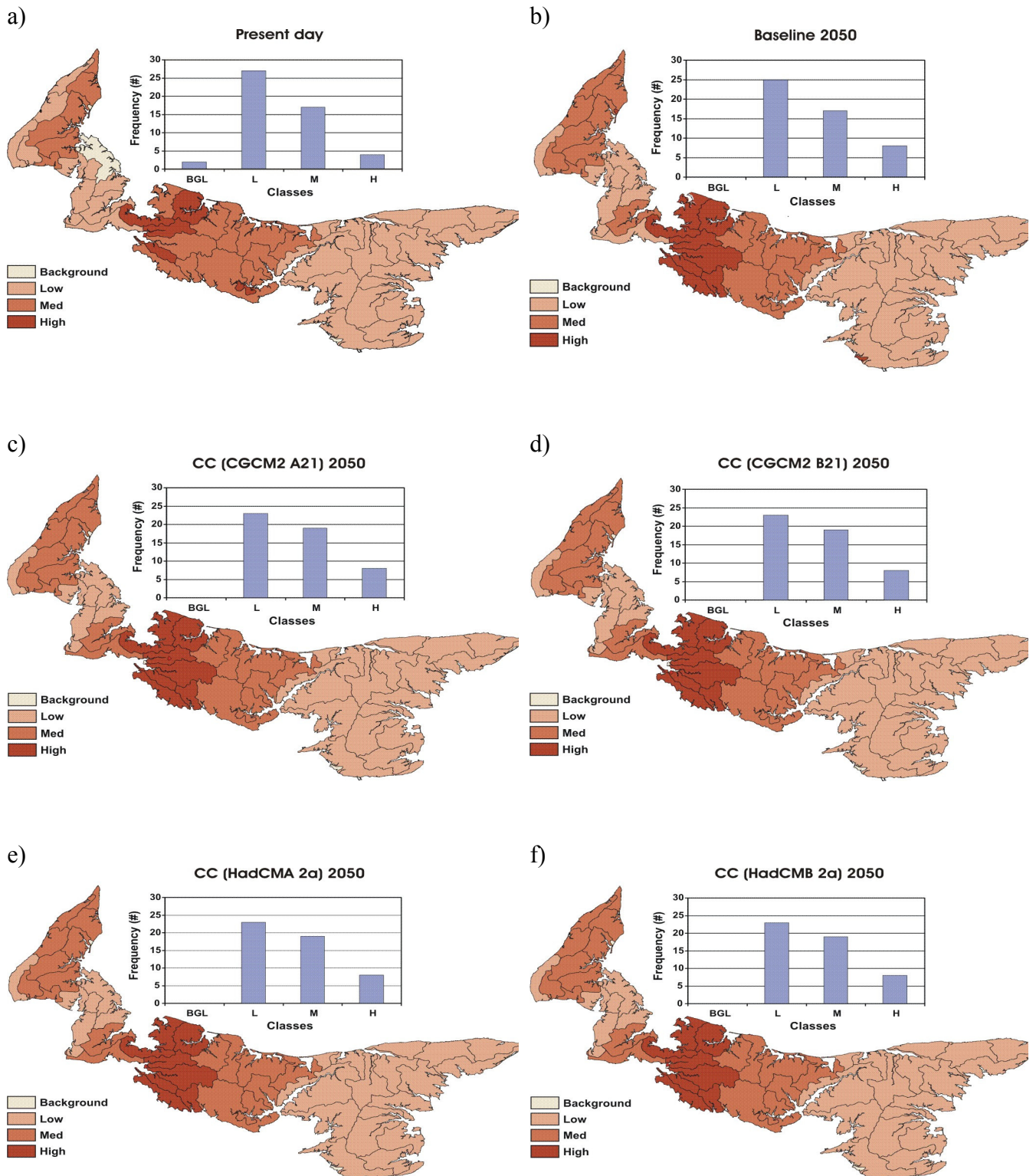


Figure 8.6. Class distribution of simulated mean nitrate concentrations per watershed and histogram of the number of watersheds in each class for present day (2001) (a), year 2050 with today's nitrate loading (b), and the four CC scenarios (c, d, e, f).

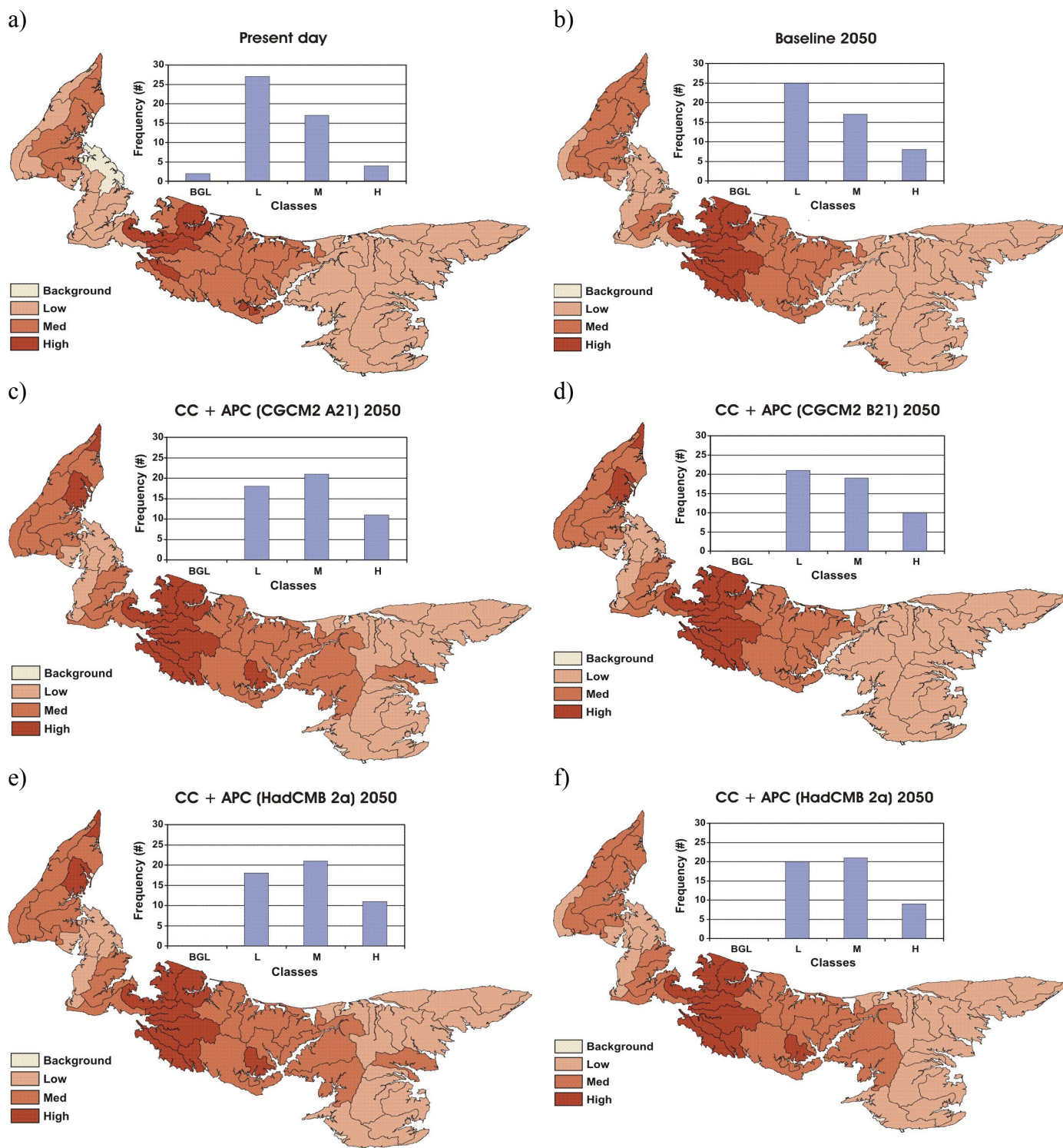


Figure 8.7. Class distribution of simulated mean nitrate concentrations per watershed and histogram of the number of watersheds in each class for present day (2001) (a), year 2050 with today's nitrate loading (b), and the four CC scenarios involving APC (c, d, e, f).

8.4 Assessment of the impact of climatic changes (CC) and agricultural practice changes (APC)

To assess the potential impact of CC and APC in the future, nine GW flow and mass transport simulation scenarios were defined:

Scenario #1: Maintain the current recharge conditions and the current agricultural practices until 2069. This scenario (baseline) is used to assess when aquifer concentrations are reaching steady-state conditions using present-day nitrate loadings (equilibrium between N input and N output from the aquifer)¹.

Scenarios #2-5: Maintain the current agricultural practices in the SLC polygon but change GW recharge based on the values obtained from the four CC scenarios. The mass of nitrate applied over the watershed is kept constant for the 23 SLC polygons until 2069. This mass represents the mean RSN value from the 5 past censuses (1981, 1986, 1991, 1996 and 2001). These scenarios compared to scenario #1 are used to assess the impact of CC alone (i.e. without APC).

Scenarios #6-9: Use the RSN values modelled for the 2040-2069 period with the four CC scenarios associated with APC along with the GW recharge based on the values obtained from these CC scenarios. These scenarios thus assess the combined impact of CC and APC.

Nitrate concentrations presented in the tables and figures of this discussion are the average nitrate concentrations for the first four layers of the numerical model that represent the aquifer zone that is mostly exploited by domestic wells. For comparison purposes, we define four classes of nitrate contamination based on nitrate concentrations obtained from the numerical model: background (0-1 mg/L), low (1-3 mg/L), medium (3-5 mg/L) and high (greater than 5 mg/L). These classes of nitrate concentrations are used instead of absolute concentrations to emphasize that the model can indicate the sense of potential evolution of nitrate concentrations but not an exact value for a specific watershed.

8.4.1 CC impact assessment

For comparison purposes, [Figures 8.6a,b](#) and [8.7a,b](#) show the spatial distribution of nitrate concentration classes for all watersheds and the histogram of nitrate concentrations classes resulting respectively from present-day conditions and the 2050 Baseline scenario (#1). When compared to the present-day (2001) simulation, the average increase in nitrate concentrations on the Island is about 11% by 2050 even when maintaining present-day nitrate loading ([Table 8.6](#)). No CC or APC are taken into account at this stage. Under the 2050 Baseline scenario, the 3 watersheds that were in the *Background* class have now moved to the *Low* class. In 2001, 26 watersheds were in the *Low* class, 17 in the *Medium* and 4 in the *High*. In 2050, 25 watersheds are in the *Low* class, 17 in the *Medium* and 8 in the *High*. Moreover, in the Western part of the Island, more watersheds have changed class than in the Eastern part. That is explained by the fact that more significant decrease in recharge is predicted in the western part relative to the rest of

¹ After model calibration based on SLC polygon means, only 4 watersheds in PEI have a modelled average nitrate concentration exceeding 5 mg/L. This is lower than the current 9 watersheds found through monitoring GW quality (see Chapter 1, [Fig. 1.2](#)).

the Province, thus leading FEFLOW to calculate higher nitrate concentrations in that area (not shown).

Figures 8.6c-f show the spatial distribution of nitrate concentrations for the four CC scenarios (scenario #2-5). When compared to the present-day (2001) simulation (Fig. 8.6a), the average nitrate concentrations for the 4 CC scenarios increase by 11% (CGCM2 B1), 15% (HadCMB2a) and 17% (CGCM2 A1 and HadCMA2a) (Table 8.6). The impact of CC minus the effect of scenario 1 is in the order of 0% for CGCM2 B1, 4% for HadCMB2a and 6% for CGCM2 A1 and HadCMA2a. On a class basis, there is no significant change of class between each CC scenarios. Compared to the 2050 Baseline scenario, only 2 watersheds move from the *Low* to the *Medium* class for all CC scenarios.

These observations shows that the impact of the CC scenarios #2 -5 is not very important compared to the effect of scenario #1 were the present-day loading in nitrate and the present day mean recharge are used in the model.

8.4.2 APC impact assessment

Figures 8.7c-f show the spatial distribution of nitrate concentrations for the four CC scenarios with APC (scenario #6-9). When compared to the present-day (2001) simulation (Fig. 8.7a), the average nitrate concentrations increase by 25% (CGCM2 B1), 29% (HadCMB2a) and 32% (CGCM2 A1 and HadCMA2a) (Table 8.6). The impact of APC minus the effect of scenario 1 and CC is in the order of 14% for CGCM2 B1, 18% for HadCMB2a and 21% for CGCM2 A1 and HadCMA2a.

On Figures 8.7c-f, the class distribution shows no significant change between CGCM2 A1 and HadCMA2a. These scenarios are the more impacted by the APC and the distribution of the watersheds in each class is 18 in the *Low*, 21 in the *Medium* and 11 in the *High* (Table 8.6). Scenarios CGCM2 B1 and HadCMB2a are the less impacted and their class distribution is respectively 21 and 20 in the *Low*, 19 and 21 in the *Medium* and 10 and 9 for the *High*. It is also shown that the center area of the Island is more affected by the APC because this is were the most intensive agriculture takes place.

On an individual basis, some of the watersheds show a slight decrease in nitrate concentrations (Table 8.6). This is caused by the fact that the RSN used to model the 2040-2069 GW concentrations was defined on the basis of the average RSN of the last 5 Census (1981, 1986, 1991, 1996 and 2001), whereas the GW model reproducing the 2001 concentrations was calibrated using individual Census. This difference in RSN values creates an artificial decrease in the future average GW nitrate concentrations relative to the 2001 RSN in each SLC polygon. Hence, in some watersheds, the RSN value for the 2040-2069 period is lower than the calibrated RSN value for 2001 (Figs. 8.6, 8.7).

Table 8.6. Classification of nitrate concentrations for each watershed and % change compared to 2001 in mean nitrate concentration for the entire PEI for scenarios 1 to 9 (BGL is for Background Level and L, M and H stand for Low, Medium and High nitrate concentrations, respectively).

#	Watershed Name	Present Day	Baseline 2050		CC								CC + APC							
					CGCM2 A1		CGCM2 B1		HadCM A2a		HadCM B2a		CGCM2 A1		CGCM2 2 A1		HadCM A2a		HadCM B2a	
			Class	%/2001	Class	%/2001	Class	%/2001	Class	%/2001	Class	%/2001	Class	%/2001	Class	%/2001	Class	%/2001	Class	%/2001
1	Sea Cow Pond	M	M	17	M	18	M	18	M	18	M	18	H	33	H	33	H	36	M	23
2	Cape Gage	L	M	27	M	27	M	27	M	27	M	31	M	45	M	45	M	45	M	45
3	Tignish River	M	M	15	M	15	M	15	M	15	M	19	M	35	M	31	M	35	M	38
4	Little Miminegash Riv.	L	M	19	M	20	M	20	M	20	M	20	M	38	M	38	M	38	M	38
5	Hills River	M	M	15	M	15	M	15	M	15	M	15	H	34	H	34	H	34	M	32
6	Whites Cove	L	L	25	L	24	L	29	L	24	L	24	M	43	M	43	M	43	L	38
7	Mill River	M	M	18	M	19	M	19	M	19	M	19	M	37	M	37	M	37	M	37
8	Trout River (Roxbury)	M	M	14	M	15	M	13	M	15	M	13	M	33	M	30	M	33	M	30
9	Little Pierre Jacques Riv.	L	M	23	M	24	M	24	M	24	M	24	M	40	M	40	M	40	M	40
10	Brae River	M	M	23	M	22	M	22	M	25	M	28	M	39	M	39	M	42	M	42
11	Enmore River	BGL	L	11	L	11	L	11	L	11	L	21	L	31	L	31	L	31	L	31
12	Cranberry Point	BGL	L	10	L	16	L	16	L	16	L	16	L	37	L	26	L	37	L	37
13	St. Phillip	BGL	L	12	L	14	L	14	L	14	L	14	L	25	L	25	L	25	L	35
14	Browns Creek	L	L	6	L	23	L	14	L	23	L	19	M	44	M	36	M	44	M	36
15	Little Trout River	L	M	16	M	31	M	24	M	31	M	24	M	54	M	46	M	54	M	42
16	Haldiman River	L	L	12	L	12	L	12	L	12	L	12	L	31	L	31	L	31	L	31
17	Sunbury Cove	L	L	26	M	44	M	35	M	44	M	35	M	62	M	53	M	62	M	53
18	Rainers Creek	H	H	21	H	40	H	31	H	40	H	33	H	59	H	50	H	59	H	50
19	Baltic River	M	H	21	H	39	H	31	H	39	H	24	H	57	H	49	H	57	H	41
20	Mackies Pond	M	H	20	H	37	H	29	H	37	H	31	H	55	H	47	H	55	H	45
21	Grahams Crrek	L	L	1	M	14	M	8	M	14	M	11	M	25	M	18	M	25	M	21
22	Schurman's Point	H	H	22	H	39	H	31	H	41	H	31	H	59	H	49	H	59	H	47
23	Dunk River	M	H	35	H	55	H	46	H	55	H	46	H	76	H	65	H	74	H	63
24	Prevost Cove	M	H	29	H	45	H	38	H	47	H	29	H	65	H	56	H	65	H	45
25	McPhee Creek	M	M	-18	M	-16	M	-18	M	-16	M	-16	M	-9	M	-13	M	-9	M	-11
26	Hunter River	M	M	1	M	5	M	-1	M	5	M	5	M	15	M	8	M	15	M	15
27	Cymbria	M	M	4	M	3	M	-6	M	3	M	3	M	12	M	3	M	12	M	12
28	North River	M	M	10	M	8	M	2	M	8	M	8	M	18	M	10	M	18	M	15
29	Hyde Creek	M	M	1	M	2	M	-5	M	2	M	2	H	10	M	2	H	10	H	8
30	Long Creek	H	M	-30	M	-31	M	-33	M	-29	M	-24	M	-23	M	-28	M	-23	M	-21
31	Winter River	M	M	15	M	12	M	2	M	12	M	12	M	24	M	15	M	24	M	24
32	Appletree Creek	L	L	16	L	13	L	1	L	13	L	13	M	30	L	18	M	26	M	26
33	Feehans Shore	L	L	15	L	7	L	-7	L	7	L	13	L	20	L	7	L	20	L	27
34	St. Peters Harbour	L	L	11	L	7	L	-4	L	7	L	7	L	24	L	7	L	18	L	24
35	Morell River	L	L	10	L	13	L	3	L	13	L	13	L	24	L	8	L	24	L	29
36	Orwell Cove	L	L	12	L	8	L	0	L	8	L	12	M	24	L	12	M	24	M	24
37	Little Sands Shore	L	L	-6	L	-4	L	-13	L	-4	L	-4	L	5	L	-4	L	5	L	5
38	Nicolle Point	L	L	-15	L	-11	L	-16	L	-11	L	-7	L	-3	L	-11	L	-3	L	1
39	Albion	L	L	8	L	9	L	-2	L	9	L	15	L	21	L	9	L	21	L	26
40	Montague-Valleyfield	L	L	-20	L	-15	L	-22	L	-15	L	-12	L	-9	L	-19	L	-9	L	-5
41	Brudenell River	L	L	9	L	9	L	3	L	9	L	14	L	19	L	9	L	25	L	30
42	Narrows Creek	L	L	12	L	23	L	9	L	23	L	14	M	36	L	23	M	36	L	27
43	Marie River	L	L	5	L	7	L	1	L	7	L	12	L	18	L	7	L	18	L	24
44	Poplar Point	L	L	7	L	8	L	-3	L	8	L	13	L	24	L	8	L	24	L	24
45	Shipwreck Point	L	L	13	L	14	L	4	L	14	L	20	L	30	L	14	L	30	L	35
46	St. Margarets Shore	L	L	14	L	13	L	3	L	13	L	18	L	28	L	13	L	28	L	33
47	Surveyor Point	L	L	15	L	13	L	2	L	13	L	19	L	29	L	13	L	29	L	35
48	MacKinnon Point	L	L	18	L	19	L	9	L	19	L	19	L	36	L	19	L	36	L	30
49	Bradshaw River	H	H	21	H	38	H	31	H	38	H	23	H	57	H	49	H	58	H	40
50	Victoria	M	H	7	H	23	H	15	H	23	H	17	H	40	H	31	H	40	H	29
%2001 mean concentrations PEI.			11		17		11		17		15		32		25		32		29	

Overall, the general trend for scenarios 1 to 9 is a significant increase in the number of watersheds that move to the *High* concentration class. Furthermore, if scenarios 6-9 are compared with scenarios 2-5 and 1, it is apparent that the APC (14-21%) has more impact on nitrate concentrations than the baseline condition (scenario 1, 11%) and CC (scenario 2-5, 0-6%).

8.5 Conclusion

To assess the potential impact of CC as well as the resulting APC on future nitrate concentrations in GW over PEI, we defined nine different GW flow and mass transport simulation scenarios. The analysis of these scenarios shows that reaching steady-state conditions of aquifer concentrations under present-day loading accounts for an 11% increase, that CC alone accounts for an increase of only 0 to 6%, and that the APC is responsible for a 14 to 21% increase expected for 2050. The combined effect of all the above variables (equilibration, CC and APC) shows a relative increase in nitrate concentration in the PEI aquifers between 25 to 32%, CC contributing the least to that increase. Moreover, the general trend from 2001 to 2050 is that a significant number of watersheds are predicted to move to the highly impacted group having a nitrate concentration between 5 and 10 mg/L. In 2001, 4 watersheds were in this group compared to 8 predicted for 2050 after reaching steady-state conditions and considering CC impacts, and compared to 9 to 11 if CC plus APC are considered together. The situations described here could be avoided if agricultural practices were managed to decrease nitrate loadings instead of progressively increase them.

9 Impacts of Climate Change on the water supply infrastructure in Prince Edward Island

George Somers, Martine M. Savard & Odile Pantako

ABSTRACT

Prince Edward Island relies entirely on groundwater and its water supply is delivered by infrastructure developed under current climatic conditions. With the possible implications of climate change, it is essential to assess the vulnerability of this infrastructure under future groundwater nitrate levels. Toward this end, the general characteristics of water supply infrastructure have been examined. A first order evaluation suggests that municipal water supply infrastructure plus domestic and industrial wells have an estimated “book value” in the range of \$100 million, with replacement costs likely to be 2 to 3 times higher. However existing municipal water supply infrastructures has not been designed to accommodate water treatment, and if nitrate removal becomes necessary as a result of climate change or other factors, the costs associated with the production of water (i.e., excluding distribution) could as much as double. With potential effects of climate change, regulators and water managers need to consider the possible financial impacts on the water supply infrastructure of the Province.

9.1 Introduction

In Prince Edward Island (PEI), the overall availability of groundwater (GW) exceeds demand by a significant margin. While locally, GW extraction has had a negative impact on base-flow to surface water resources, depletion of GW resources has not been an issue. Key water supply issues concern the capacity of existing water supply infrastructure to meet demand, and GW quality. Bacterial contamination and elevated nitrate concentrations are the most common water quality issues in the province, however the bacterial quality largely reflects the condition of water supply and wastewater treatment infrastructure and is not discussed further here. In contrast, nitrate contamination represents a widespread threat to GW resources, a problem that is becoming severe in some areas of the Province.

The purpose of this chapter is to document the nature of current water supply infrastructure in PEI for an evaluation of vulnerability to the consequences of climate change under projected 2xCO₂ climate scenarios. Its specific goals are to: 1) characterize and inventory the state of current water supply infrastructure; 2) document current GW use (municipal, domestic, and commercial water use); and 3) estimate the value of the infrastructure in financial terms. Sources of information and methods of aggregation of data are described in detail in “The current water supply infrastructure in Prince Edward Island” (Pantako *et al.*, 2006). It should be noted that the evaluation undertaken in this work is intended to provide only a first approximation of the current state and value of water supply infrastructure in PEI, and its potential vulnerability to changes in the extent of nitrate contamination as a result of climate change.

9.2 Water supply infrastructure in PEI

9.2.1 Current Infrastructure

Source of supply. Water supply infrastructure in PEI consists of central water supply systems that serve approximately 45% of the population, and “stand-alone” private water supplies serving rural residences and some larger industrial consumers. Virtually all wells are completed in a fractured sandstone aquifer and are of simple “open hole” construction (i.e., no well screens or gravel packs are used). Current construction standards require a minimum of 12 m of casing with mandatory grouting of casing and pitless well completion. Some older wells are completed in well pits and may have as little as 6m of casing, while in other instances as much as 30m of casing has been installed, usually in response to site specific water quality problems (Table 9.1). It is estimated that there are some 21,000 to 25,000 wells in operation in PEI (Table 9.2; Young *et al.*, 2002). Almost all municipal systems are supplied by one or more well fields, with each well field extracting water from several wells (Table 9.2).

Table 9.1. The Main Characteristics of Wells in the PEI.

Characteristics	Domestics Wells	Municipal Wells
Rock type	Sandstone	Sandstone
Type of well	Open hole	Open hole
Depths	25 to 50 m	75 to 100 m
Yields	0.023 to 0.046 m ³ /min	0.455 to 2.273 m ³ /min

Information provided by Water Management Department of PEI-FEE.

Table 9.2. The Current Water Supply Infrastructure of the main PEI Municipalities.

Municipality	No of Well Fields	Total No Well	Population Served
Charlottetown	3	12	31 955
Summerside	1	8	14 565
Kensington	1	3	1 383
Souris	1	5	1 300
Stratford	2	5	660
Montague	2	4	1 200
Cornwall	2	6	3 000
Borden	1	5	800
North Rustico	1	3	650
Victoria	1	2	175
Georgetown	1	3	500
Tignish	1	3	300-400

Information provided by Water Management Department of PEI-FEE;
EC 2001; No. Number.

Transmission & storage. With exception of Charlottetown and Summerside, well fields are relatively close to the distribution systems so that there is little need for extensive water transmission mains. Storage facilities for municipal systems vary considerably, depending principally on the size of the system, and whether it was designed to deliver fire flows or simply to meet average daily demand. They range from standpipes capable of storing several days' worth of water to small pneumatic tanks used by smaller systems. In all cases, storage capacity, in relation to average daily demand is low, and aside from fire protection and maintenance purposes, storage is used to even out the short term peaks in water demand that typically occur during normal daily use cycles.

Water treatment. Natural GW quality on PEI is generally good, and normally requires no treatment beyond disinfection prior to use (Fleury, 2003). The microbiological characteristics of waters are generally good and most bacteria problems relate to well construction or maintenance issues. Where natural GW quality has been compromised, elevated nitrate levels are the most widespread GW quality problem. For private wells, point of entry devices are used to treat for hardness, iron & manganese, nitrate and barium. There are no municipal water treatment plants in the traditional sense and on the few occasions where sources of municipal GW supply have been compromised, utilities have opted to develop new sources of supply rather than employ water treatment.

9.2.2 Water Use

Estimated water use by central water supply systems and stand alone facilities has been aggregated to estimate total consumption per water use sector, including residential, commercial, industrial, irrigation (agricultural and recreational facilities) and livestock operations. The importance of assessing water demand by geographic region (i.e. watershed) is recognized, but was beyond the scope of the current work. Salt water wells used by the aquaculture sector, the non-consumptive use of freshwater for heat pump or cooling applications, and water used by fish plants located essentially at the shore, have been excluded from the present compilation because they have no direct impact on availability of GW to other water users. Average per capita residential water use for PEI is 218 L/day (EC 2004), compared with a Canadian average of 335 L/day for the same period. The greater part of water demand in PEI is for domestic use ([Table 9.3](#), [Fig. 9.1](#)).

Estimated residential demand is based on an assumed population of 140,000 and a per capita daily consumption rate of 0.218m^3 per person. When additional demand associated with tourism is factored in, residential water use is estimated to be $11,875,000\text{m}^3/\text{year}$. Residential water use accounts for the greatest percentage of municipal water use in all communities but Charlottetown where industrial, commercial and institutional customers account for slightly more than half of total water flow.

Industrial water demand is met by both municipal sources and private stand-alone water supplies. Non-municipal commercial/industrial supplies collectively use approximately $4,124,500\text{m}^3/\text{year}$. Combined with the industrial demand met by municipal water supplies, total industrial/commercial water use is estimated to be $8,665,100\text{m}^3/\text{year}$. Approximately 90 % of this water is consumed for industrial purposes, the remaining 10%, mostly supplied by municipal systems, represents commercial water use. The greatest proportion of industrial water use is by the food

processing sector, and typical large food processing plants use a daily average GW quantity ranging between 2 and 8 million liters per day (Info PEI, 2005).

Table 9.3. Estimated Annual Water Use by Sector in PEI.

Sector	Water Use (m ³ /year)
Permanent Residential	11,140,000
Tourism	735,000
TOTAL RESIDENTIAL	11,875,000
Commercial	670,870
Industrial	7,994,230
TOTAL INDUSTRIAL/COMMERCIAL	8,665,100
Agricultural irrigation	212,540
Recreational irrigation	208,800
TOTAL IRRIGATION	421,340
TOTAL LIVESTOCK	3,501,102
TOTAL WATER USE	24,462,542

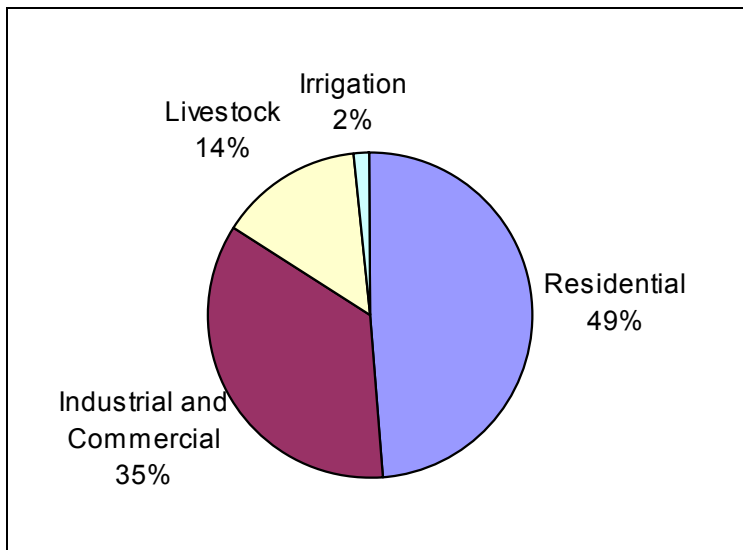


Figure 9.1. The percentage of PEI water use by sector of activities.

Water use by the agricultural sector is comprised of use in livestock production and for irrigation. Very little direct information is available on the consumption of water for livestock operations, however a crude estimate had been made, based on the number of livestock and their respective consumption rates, resulting in an estimated consumption of 3,501,102 m³/year. There are about 36 active “agricultural” irrigation wells in the province with instantaneous pumping rates in the range of 0.909 m³/min. Based on measured water use for selected irrigation wells in 1997 (Somers and Mutch 1999) and 2004, average annual water use for an individual irrigation wells is about 5,903 m³/year, and total demand by agricultural irrigation is in the range of 212,540 m³/year. Irrigation water use by golf courses and other recreational sports facilities is incomplete; but crude estimates place it in the same range as for agricultural irrigation wells at 208,800

m³/year. Total water use estimation for irrigation, combining agricultural and recreational applications is therefore 421,340m³/year. Overall, it is estimated that total consumptive water use in the Province is slightly less than 25 million m³/year.

Trends in water demand are affected by changes in population, level of industrial activity, per capita consumption rates, the influence of voluntary water reduction strategies and government regulation. These trends are most easily tracked for municipal users; however, several factors need to be considered. As in most regions, PEI is experiencing progressive “urbanization” of the population. While many water utilities have experienced considerable growth, this expansion usually includes some combination of “green field development” representing new demand, and the replacement of existing “on-site” supplies by central service. The latter case does not represent any increase in demand on GW resources, simply a change in the way the water is delivered. Furthermore, even for green field development, a significant portion of increased demand may represent a concentration of existing demand in more localized urban areas, rather than an overall increase in demand provincially.

Historical population growth and projected trends (simple linear regression) for representative urban areas of the province highlight the uneven growth in PEI, with rapid growth in the capital region of Charlottetown (and neighboring Stratford), much more modest growth in the Summerside area and a virtually static population in the eastern end of the province (Souris; Fig. 9.2). This trend reflects the ongoing migration of the population to larger urban centers, at the expense of smaller rural communities. For the Province as a whole, the population growth has been 12.5% over the last 25 years, and if this trend continues, it could lead in comparable increases in demand. However, increased activity by the industrial sector (including food processing or irrigation) which could generate significant increases in demand is impossible to predict with certainty (Environment Canada, 2001b).

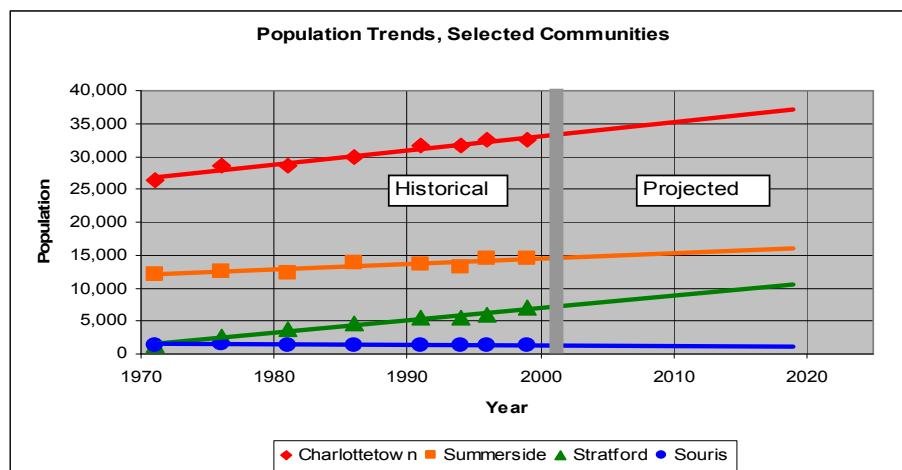


Figure 9.2. Population trends for selected communities with central water infrastructure.

9.3 Value of water supply infrastructure

9.3.1 Value of the current water supply infrastructure

At the outset, it should be noted that it is difficult to place an accurate value on water supply infrastructure with solid quantitative significance in the context of this discussion. First, only some of the components that make up a water systems may be vulnerable to climate change impacts (i.e. sources of supply, treatment facilities), yet information on the value of individual system components is difficult to obtain. Secondly, the value of infrastructure can be measured several ways; original construction costs, the book values or replacement costs, thus even two systems of identical design, but differing ages will have different “values”. Book values have been used here, as they are more easily obtainable and form a better basis for comparison, taking into account the remaining useful life of individual system components (Table 9.4). An estimate of replacement costs for just the specific system components vulnerable to nitrate contamination would be useful, but such estimates would require detailed, case by case evaluations, a task beyond the scope of the current work.

Table 9.4. Book value and estimated replacement costs of municipal water supply infrastructure.

Utility	“Book value” of water supply infrastructure (\$)	Estimated replacement costs
Charlottetown	31,652,000	102,802,000
Summerside	16,378,332	
Cornwall	3,442,804	9,116,500
Stratford	3,961,670	
Souris	1,010,396	
Montague	2,516,610	
Georgetown	N/A (estimate 400,000)	
Kensington	1,507,377	
Victoria	207,445	
North Rustico	394,227	
Borden-Carleton	3,194,014	
Tignish	448,903	
Total	65,113,778	

The book values presented provide a “first order” sense of the financial investment in water supply infrastructure in the Province, with a suggested total value of approximately \$100 million. The contribution of municipal water supply systems is almost 65% of this total. The costs of water supply infrastructure of the two largest urban centers (Charlottetown and Summerside) dominate the municipal share and represent 74% of the total for municipal systems. The book value for water supply infrastructure for the Province as a whole is based on the assumption that stand alone industrial and private wells values can be estimated using current replacement costs, with a suggested “book value” derived on an assumed useful life (Table 9.5).

Table 9.5. Estimated overall value of the water supply infrastructure.

Sector	Book Value (millions \$)
Private Domestic Wells	29.0
Municipal Water Systems	65.1
Private Industrial/Commercial Systems	4.0
Irrigation	2.7
TOTAL ESTIMATED VALUE	100.8

The estimate of average replacement costs for private wells in the province is in the range of \$60 million. Previous estimates, based on the method of Lebedin *et al.* (2000) suggest costs closer to \$100 million; however this discrepancy may reflect differences in local well construction practices as the relatively high yields and favorable drilling conditions in PEI enable the use of wells with simple open-hole construction and modest depth. While the exact replacement value of water supply infrastructure in the province is difficult to estimate, based on the observation that the ratio of book value to replacement costs are in the vicinity of 2:1 and 3:1 for domestic wells and municipal supplies respectively, it could be suggested that a global “replacement cost” for water supply infrastructure would be in the order of \$250 million.

It is important to note that the foregoing analyses do not make any allowance for the value of water treatment facilities. As noted in section 9.2.1, the municipal water supply infrastructure currently does not include conventional water treatment facilities. For domestic water supplies, the use of point of use devices such as sediment filters, ultra-violet disinfection, water softeners or other ion exchange devices is not uncommon. There is presently no way to estimate their prevalence and global value at this point. The cost implications of water treatment are discussed briefly in section 9.3.2 below.

9.3.2 Cost implications of elevated nitrate levels

The ultimate financial impact of nitrate contamination can be measured in terms of the treatment of contaminated drinking water, impacts on the fisheries and tourism sectors, and other ecological effects; the magnitude of each depending on current land use practices, the direct influence of climate change and potential changes in agronomic practices in response to climate change. Because of the complexity of these factors, here we discuss only the relative costs of nitrate contamination on drinking water supplies, based on the current situation.

For private wells with elevated nitrate concentrations, homeowners are generally faced with two options—(1) replacement/reconstruction of the well with additional casing to avoid shallower, high nitrate water, or (2) the installation of a treatment device for the removal of nitrate. Well replacement costs, based on typical current prices are in the order of \$3,000, assuming that the original pumping equipment can be re-installed in the new well. The cost of water treatment devices using ion-exchange processes are in the vicinity of \$1,500. Based on the PEI-FEE past 5 years data, tests from 133 private wells each year show average nitrate concentrations in excess of the drinking water guideline. It is impossible to know how many homeowners actually purchase treatment devices, or reconstruct their wells, as a response to high nitrate levels. However, if it were assumed that all affected homeowners chose to address their nitrate problems, this would represent a net cost to homeowners of the Province of \$200,000 to

\$400,000 per year depending on the manner they selected to reduce nitrate levels. This is a worst case scenario as it is not likely that in fact all well owners that have tested their well water and found nitrate levels above 10 mg/L will in fact invest in the corrective measures noted above.

To date, only a few municipal wells have been affected by elevated nitrate levels, and in each case, utilities have opted to relocate or reconstruct their production wells rather than treat the water for nitrate removal. This is no doubt due to the absence of existing water treatment plants that can be modified or upgraded and the costs of constructing water treatment facilities, complete with storage reservoirs, auxiliary pumping equipment etc, would be prohibitive. However, the availability of affordable, alternate sources of water cannot always be guaranteed, and it is instructive to examine the approximate magnitude of costs that might be incurred to treat water for nitrate removal.

Because there are no existing, local examples upon which to draw in developing such estimates, general information has been sought from industry and government officials in other jurisdictions. It is assumed that ion exchange would be the most cost effective treatment technology, and because most systems on PEI have limited storage capacity, it is further assumed that treatment plant size would be based on peak flows, rather than average daily flows. In the absence of existing water treatment plants in the conventional sense, it is also assumed that there would be additional costs associated with building construction, plumbing and electrical work for the installation of nitrate treatment capability. The resulting estimates are therefore purely theoretical and intended only to provide an “order of magnitude” indication of costs of adopting such treatment technology. With these assumptions capital costs for a relatively small utility with a peak flow in the range of 1000m³/day is estimated to be in the vicinity of \$150,000. For a system of intermediate size with peak flows in the range of 4500 m³/day, or for a single well field serving a larger municipal system, capital costs might be expected to range anywhere from \$500,000 to \$1,500,000 depending on the specific nature of the system infrastructure (D. French, Kinetico Canada Inc., pers. comm. 2006; F. Lemieux, Health Canada, pers. comm. 2006). For comparison, recent replacement costs for well field of Charlottetown were in the vicinity of \$250,000 per well (Walker, 2005, pers. comm.); with 5 wells and associated engineering costs, a total of \$1.25 million, thus any requirement to treat water for nitrate removal would essentially double the costs of producing water for distribution.

9.4 Discussion

The foregoing discussion describes the general characteristics of water supply infrastructure in PEI, places crude boundaries around water demand and the value of water supply infrastructure, as well as briefly addresses water treatment issues. Data on current nitrate levels in the province are well established and considered reliable. Data on water use and on the value of specific components of water supply infrastructure vulnerable to nitrate contamination are much weaker and merit further work.

To date, the majority of costs associated with increased nitrate levels in GW have fallen principally on private well owners, and while it is impossible to know what actual expenses are incurred in addressing this issue, theoretically, they could be as high as \$200,000 to \$400,000 at the provincial scale. Because this burden is shouldered by individual homeowners, and because

solutions are readily available, the problem has much less visibility than if these costs were borne by a municipal utility.

With the prospect of increased nitrate concentrations either as a result of current practices (Chapters 4 & 5) or as a result of adaptation to climate change (Chapters 7 & 8), the economic impact on private well owners could be substantial. Chapter 7 suggests Island-wide mean nitrate concentrations could increase by 15%, and by as much as 30% in some regions, in response to adaptations to climate change by the agricultural community. A province-wide increase in mean nitrate levels from the current 3.8 mg/L to 4.3 mg/L may not seem alarming, but it is important to recognize, that assuming a normal distribution of nitrate values, this potentially represents a 24 % increase in the number of wells with nitrate levels exceeding the drinking water guideline of 10 mg/L (Fig. 9.3). If one wishes to extrapolate this to a dollar value, and assuming the suggested current expenses borne by private well owners, this represents an increased cost of nearly \$50,000 to \$100,000 per year. More significant still are possible consequences in high impact areas. If for example, nitrate levels in a high impact region such as the area surrounding the Wilnot study area, increased by as much as 30%, the predicted number of wells exceeding the drinking water guideline would increase from the current 11.2% to 21%, an increase of 87.5%.

In general it is noted that municipal water supply systems in the province have evolved with little accommodation of future water treatment requirements. In the absence of water treatment plants in the conventional sense, any requirement for treatment will result in substantially increased costs at the source of supply, and it may not be unreasonable to suggest that the cost of supplying water to the distribution system might double, at least in some instances. At the same time, given the close relationship between land use and GW nitrate levels, it is unrealistic to assume all water utilities are equally vulnerable to nitrate contamination. Thus global estimates assuming a need for nitrate removal for all systems might simplify calculations but not be realistic. Nonetheless, any need for treatment is likely to require significant adjustments to prevailing water rates.

A more intangible element is the cost associated with well field protection measures intended to reduce nitrate losses from agricultural lands in sensitive water supply areas. Here the economic burden is not up-front capital costs borne by a water supply utility, but on-going opportunity costs associated with alteration to existing land use practices. At this point, it is not possible to quantify these impacts financially.

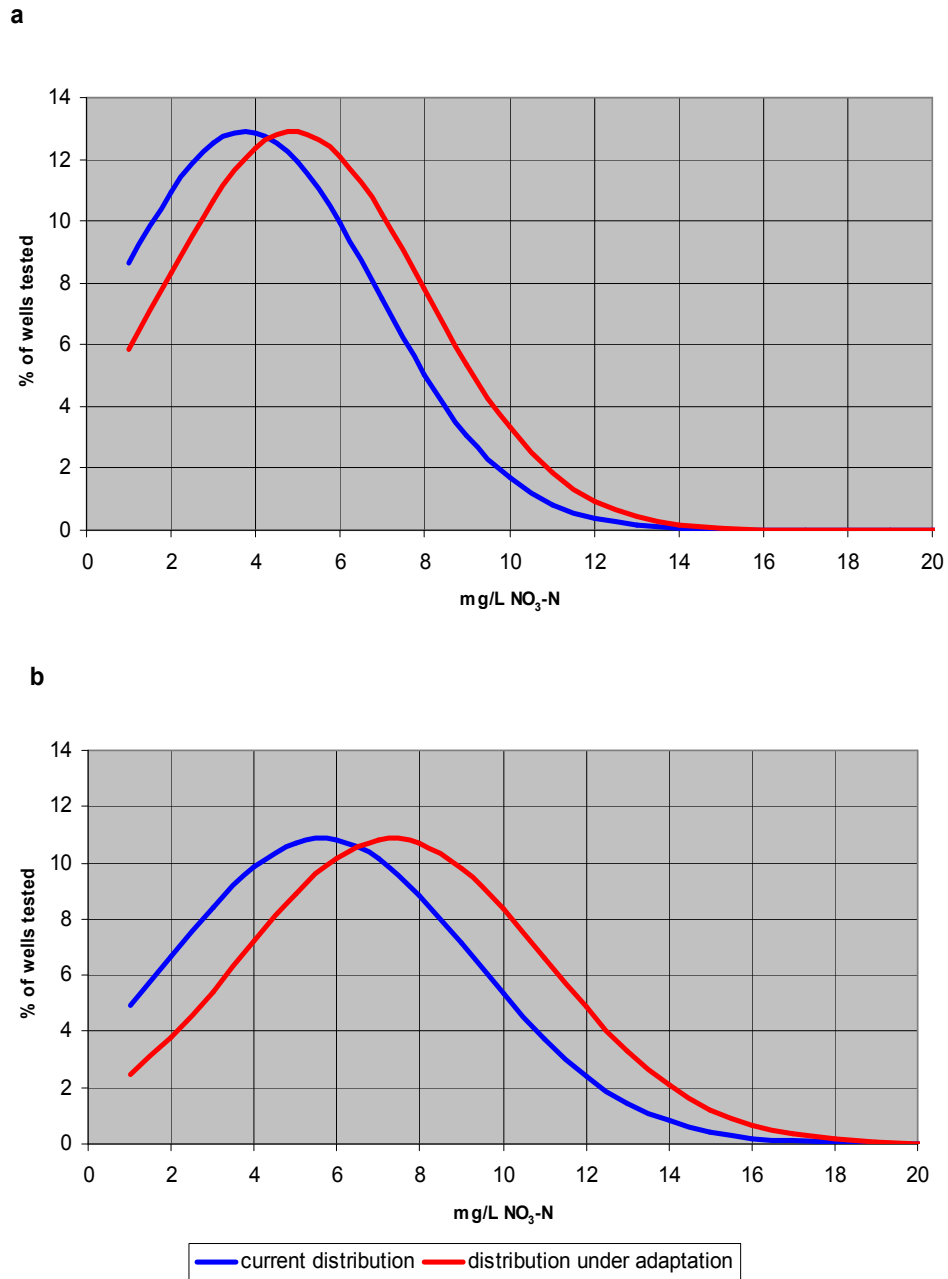


Figure 9.3. Current distribution of nitrate concentrations in domestic wells and distribution predicted under climate change adaptation scenarios: a) Island-wide statistics (n= 14552), b) Wilmot watershed and surrounding area (n=2878).

9.5 Conclusion

In PEI, approximately 55% of the population relies on private wells, with the remaining 45% being serviced by central (municipal) water supply systems. Industrial demand is met by a combination of municipal supply and stand alone water systems. Consumptive GW use in the Province is estimated to be in the range of 25 million m³/yr. Nearly half of water use is for domestic purposes; the remaining water used being accounted for by the industrial/commercial sector (35%) and the agricultural sector (16%). Industrial demand is dominated by the food processing sector, and the agricultural sector is dominated by livestock production. Water use for irrigation represents only a few percent of total water use. Total water use represents only a small fraction of annual GW recharge, and while there is a trend toward increasing GW extraction in the vicinity of major urban centres, GW quality issues, particularly relating to nitrate contamination, pose the greatest concern.

Elevated nitrate levels in GW are already creating a substantial financial burden on private well owners. Any increases in nitrate levels, and thus the number of wells requiring treatment, will only add to this burden. Nitrate contamination has also resulted in financial impacts to some municipal water suppliers, but to date have not involved excessive costs, due to the availability of other water sources. Should the extent of nitrate contamination increase to the point where such availability of alternate sources cannot be taken for granted, the cost implications to utilities will potentially be severe.

More detailed assessment of water demand and the economics of water supply would aid in a final evaluation. The magnitude of costs associated with increased levels of nitrate contamination also highlight the importance of investing in strategies such as nutrient management and well field protection to minimize impacts on source water quality.

10 General implications of Climate Change on contamination of groundwater by nitrate on Prince Edward Island

Martine M. Savard, George Somers, René Lefebvre, Eric van Bochove, Daniel Paradis & Reinder De Jong

ABSTRACT

Nitrate originating from agricultural activities is a contaminant of concern impacting groundwater quality on Prince Edward Island. The objective of this research was to understand the processes involved in the transfer of nitrate from soils to underlying aquifers and to estimate the impact of climate change (CC) on groundwater. To meet this objective, an NRCan/AAFC/PEI-EEF multi-disciplinary research group integrated expertise in soil and agricultural sciences, geology, hydrogeology, hydrogeochemistry and numerical modelling. Following the approach described in Chapter 1 and based on the main findings documented in chapters 2 to 8, we conclude that continuation of existing practices would lead to further degradation of the resource but that the impact of CC alone on the N cycle would not be significant. However, under some predicted scenarios for adaptation of agricultural practices to climate change, significant negative effects on groundwater quality could be expected. These potential impacts on water quality could create significant costs in terms of infrastructure replacement as well (Chapter 9). Thus, we recommend continued efforts to reduce the impact of agricultural sources of N on groundwater resources in watersheds where cropping activities are intense.

10.1 Introduction

During the 20th century, annual precipitation has increased by 5 to 10 % in most regions of mid and high latitudes of the Northern Hemisphere (IPCC, 2002). In the future, increasing mean temperature related to climate change (CC) will likely generate further increases in precipitation because a more dynamic hydrological cycle will exist, changes in atmospheric circulation will take place and the water holding capacity of the atmosphere will increase. The entire population of Prince Edward Island (PEI) relies on groundwater (GW) as a source of potable water, and this GW is renewed by the infiltration of precipitation to aquifers. Locally, PEI authorities are facing a problem of water quality degradation due to increasing nitrate concentrations. Nearly one 5th of all watersheds in the Province exhibit high impacts, i.e., their mean GW nitrate concentrations ranging between 5 and 10 mg/L (Somers *et al.*, 1999). Potential ecological impacts due to nitrate export from land via GW to estuaries exist as well in PEI, and they might have economic consequences on fishing as well as tourism. What should be expected to happen to the hydrological cycle on Prince Edward Island due to CC? Is CC likely to lead to a faster degradation of water quality? Several questions stemming from CC, GW availability and quality need to be answered in order for PEI authorities to have the information base necessary to address the issues of sustainability of GW resources.

This project was designed to provide key pieces of information, both at the watershed scale, as it corresponds to the boundaries of individual GW and surface water flow systems, and at the Island scale, for broader aspects related to CC impacts on GW quantity and quality. In a focussed study

of the Wilmot River watershed, we (1) estimated the soil-to-aquifer rate of nitrate transfer on a seasonal basis, (2) quantified the seasonal nitrate loads and evaluated the proportions of nitrate originating from chemical fertilizers, manures and residual crop material for summer-fall and winter-spring periods and (3) modelled the transport of nitrate under current land use practices and for nitrate-loading rates associated with potential changes in agricultural practices. The Wilmot watershed, located in the central part of the Province, was chosen because: a) land use practices, principally potato production systems, are typical of most agricultural regions in the Province; b) there is a significant base of information from previous studies on local hydrology, hydrogeology and land use for this watershed; and c) the soils and physiography of the region are typical of most other regions of PEI. The intensity of potato cultivation in the Wilmot is among the highest in the Province, thus we believe the general conclusions drawn from the Wilmot to be valid provincially, while the exact nature and magnitude of projected impacts can be expected to differ somewhat according to local variations in the proportion of specific land uses and agricultural intensity.

At the island scale, we (1) evaluated the impact of doubling atmospheric CO₂ (2xCO₂) on the climate of PEI; (2) estimated the impact of climate conditions on the soil nitrogen available for leaching under four predetermined CC scenarios (see chapter 1); (3) modelled the contamination of drinking water by nitrate (NO₃⁻) from agricultural sources under the four scenarios; and (4) evaluated the adequacy of the current drinking water supply infrastructure in PEI relative to the consequences of CC.

To support decision making related to the protection and sustainable use of GW on PEI, this final chapter aims at: (1) discussing the key pieces of information provided by the eight specific studies which were conducted during the course of this project, and (2) highlighting the main findings that are of consequence in the formulation of recommendations regarding land use practices in zones of intense agricultural activity. The particular questions related to watershed-scale issues concerning the processes responsible for the transfer of nitrate from soils to aquifers, the sources of nitrate during the course of the yearly N-cycle and modelling the impact of changes in practices are first summarized. Then questions dealt with at the scale of the Island such as predicting the regional changes in climate, quantifying the soil nitrate available for leaching, modelling the changes in nitrate concentrations in GW under 4 CC scenarios, and evaluating the adequacy of the current drinking water systems with regard to the consequences of CC are summarized. Lastly, the highlights and key findings to consider for the protection and sustainability of GW resources are summarized.

10.2 Principle factors to consider in relation to the N cycle at the watershed scale

At the watershed scale, the amount of N available for leaching from soils was estimated from the modelling of the Wilmot N soil system as well as from drainage water and analyses of exchange anionic and cationic membranes from the controlled agricultural fields of the Harrington Farm (Chapter 2). The annual estimation of N leaching indicates that substantial amounts of nitrate are present in agricultural soils at the end of the crop season and are available to contaminate aquifers afterwards (December to March; Chapter 2). At the Harrington Farm, the measured amounts of nitrate from forested lots yield N-NO₃⁻ concentrations (from undetected to 1.3mg/L) that are much lower than the controlled experimental fields (from 6.7 to 29.4mg/L). These wide differences for the distinct land uses show that the forest-litter microflora uses readily available

natural nitrogen whereas in an agricultural ecosystem excess N is potentially available for leaching.

The interpretations inferred from the soil study are corroborated by the GW-nitrate isotope investigation of two yearly cycles, which shows that nitrate having a specific cold weather isotopic pattern is leached to the Wilmot aquifer during winter months (Chapter 3). We estimate that this significant winter nitrate production releases 0.90 to 2.46 tonnes/day (38 to 103 kg/ha/year), which represents the highest N-loads for the two-year investigation of the Wilmot watershed. This winter load is mostly derived from the degradation of crop residues (62%), whereas the summer loads are dominated by chemical fertilizer (64%; Chapter 3). The field-based, watershed-scale, soil and aquifer research therefore reveals that soil microbial activity produces nitrate all year long, either by nitrification of ammonia based fertilizers or decomposition of plant residues or soil N mineralization, and that nitrate transfer from soils to the aquifers takes place whenever recharge is occurring. The direct correlation between recharge rates and fluxes of nitrate to the aquifer stresses the importance of considering recharge as a key parameter for the study of climate change impact on the N cycle (Chapter 3).

Two types of numerical simulations; ModFlow, a common finite difference model (Chapter 4) and FEFLOW, a finite element model (Chapter 5), were used independently to predict future trends in nitrate concentrations of GW and river water of the Wilmot watershed under current climate conditions. Both models used broadly similar approaches and assumptions, and were calibrated by reproducing observed hydraulic heads and base flow contributions to the Wilmot River as well as present day nitrate concentrations in the river and the aquifer. The two modelling approaches varied in some specifics relating to input values, calibration technique, and treatment, as well as the selection of some model parameters and method for the discretization of the watershed area.

For the ModFlow simulations, the model domain encompassed the Wilmot and adjacent watersheds, allowing the model to determine GW flow system boundaries, and the aquifer divided vertically into 15 layers. Landuse was discretized into individual polygons, representing specific crop types present throughout the watershed, with N input rates assigned on an annual basis to each specific crop within the overall crop rotation in that polygon.

For the finite element FEFLOW simulations, the model domain was determined from topographic contours and the aquifer was divided into 3 main zones vertically, with each zone subsequently subdivided into multiple layers. Nitrogen inputs were assigned for the watershed as a whole, using a calculation of soil nitrogen available for leaching (SNAL) based on the method of Cherif *et al.* (2004).

Both series of simulations (ModFlow and FEFLOW) reached generally similar conclusions and in each case predict:

- A continuation of current land use practices would generate a progressive increase in nitrate concentration likely to result in a mean value of 8 to 8.5mg/L by the year 2050;
- If all anthropogenic sources of nitrogen were to be eliminated immediately, it would take in the order of 15 to 20 years for nitrate concentrations in the shallow and intermediate portions of

the aquifer (representing base flow to streams and GW tapped by domestic wells respectively) to return to essentially pristine conditions (1 or 2 mg/L, depending on model assumptions); for deeper GW, nitrate contents are predicted to decrease much more gradually, only approaching pristine conditions by 2035 to 2045, depending on the model chosen.

Simulations using both models were also conducted for nitrate inputs 20% higher than current rates, with resulting ultimate GW nitrate concentrations in the range of 9.5 to 10 mg/L. It is important to note that even if neither model predicts mean nitrate concentrations in excess of the 10 mg/L drinking water guideline, at the predicted values nearly half of domestic wells would exceed the drinking water guideline, and indeed both models clearly show, that very substantial reductions in nitrogen inputs would be required to reverse the current trend in increasing nitrate concentrations. By way of example, a ModFlow simulation, assuming an immediate reduction in nitrate inputs to 1965 levels (approximately ½ current levels) predicts a gradual reduction of typical nitrate concentrations in the range of 4 to 5 mg/L by 2021. Even if these levels may be of some comfort from a drinking water perspective, they could still represent a significant loading of N to rivers through base flow transport and a threat to the health of ecosystems. As a second example, a FEFLOW simulation shows that about 15 years would be necessary to reduce average nitrate concentrations from 6.6 to 2 mg/L if loadings were to cease completely.

Regardless of the modelling approach used, it is clear that N loadings would need to be reduced substantially below current rates over a significant period before important changes in corresponding GW nitrate concentrations could be expected. The implications are that substantial reductions of source inputs by land use changes would be required to significantly reduce nitrate levels in GW tapped by wells, and in associated streams, and gradually reverse the trend of increasing nitrate levels in the aquifer.

10.3 Main aspects to consider in relation to climate change and its impacts on the N cycle at the Island scale

The most notable change in the potential future climate of PEI is substantial warming as indicated by all four scenarios modelled over the region (Chapter 6). This projected warming is more significant with one model (CGCM2) than with the other models (e.g. HadCM3). Non-growing season precipitation may change slightly; either increasing or decreasing. However, such changes tend to be insignificant and more uncertain compared to the expected warming trend.

As a result of the increased temperatures, growing season evapotranspiration is predicted to increase by 7 to 11 % and drainage of water through the soil profile should decrease by 17 to 31 % (Chapter 7). During the non-growing season, and with no changes in crop and animal husbandry practices, nitrogen leaching under all four climate scenarios remains similar to that simulated using the baseline climate, i.e. 28kg N ha⁻¹. In contrast if, as modelled in the adaptation scenario considered here, agricultural activities intensify as a consequence of adaptation to CC, soil nitrogen available for leaching may increase on average by 15% for the entire Island, ranging from 5 to 30% beyond historic levels in individual watersheds (Chapter 7). There are many uncertainties regarding the adaptation of agriculture to CC (Chapter 7), and not all CC impacts may be negative. It is recognized that cold weather conditions during late fall are a significant limitation in the effective establishment of cover crops (MacLeod *et al.*, 2002a, 2002b), an important strategy in the reduction of fall leaching of N following harvest. It has also been shown

that delaying fall tillage can reduce N leaching after harvest (Sanderson *et al.*, 2002). Although beyond the scope of the research described here, climatic changes such as a longer growing season could facilitate the implementation of such strategies for the reduction of N leaching.

The numerical modelling of the concentration of nitrate in GW, for the selected CC scenarios, used residual soil nitrate as input (Chapter 7) combined with modelled recharge at the scale of the island (Chapter 8). These model simulations corroborate the conclusions reached by the watershed scale modeling and highlight the fact that even in the absence of climate change, current nitrogen loading rates are predicted to result in increasing GW nitrate levels until a steady state is reached between N inputs to and outputs from the aquifer. The island scale modelling also demonstrates how the magnitude of these responses are expected to vary between individual watersheds according to their specific land use characteristics.

The results of predictions of N leaching are presented for both Soil Landscape of Canada (SLC) polygons and for discrete watersheds, representing individual GW flow systems. They clearly demonstrate that changes in climate and in agricultural practices generate increased concentrations of nitrate in the aquifers (Chapter 8). The simulations which used the loading generated by current agricultural practice as input over the next 50 years, suggest an average increase in the order of 11% in 2050 for the 4 scenarios. Under these conditions, mean nitrate concentrations in 16% of watersheds would reach the high impact group (with mean nitrate concentrations greater than 5 mg/L), a figure which is significantly higher than the current 10%. Considering the changes in agricultural practices which potentially could occur in the future (Chapter 7), the simulations predict that the increase in nitrate concentrations for the four CC scenarios in 2050 relative to 2001 would be 28% on average for the entire island, and 22% of the total number of watersheds would reach the high impact group having a GW nitrate concentration between 5 to 10 mg/L (Chapter 8). It is worth noting that none of the numerous numerical simulations dealing with the CC scenarios predict average concentrations above 10 mg/L in individual watersheds. However, for watersheds with intense agricultural activities, the increase in concentration is significantly higher (~55%) than for the others, a critical factor in terms of sustainability of the GW resource. Indeed, the modelled nitrate concentrations and their relative increase imply that many more wells than the current 4.2% would reach or exceed the recommended maximum concentration for drinking water of 10 mg/L.

In terms of impacts on drinking water-supply infrastructure, elevated nitrate concentrations in GW are already creating a substantial financial burden on private well owners. PEI-EEF records indicate that each year on average, water tests from over 130 private wells show nitrate levels exceeding the drinking water guideline of 10 mg/L. If it were assumed that all of these affected homeowners chose to address this issue, and assuming an approximate cost of \$1,500 or \$3,000 to either install treatment equipment or invest in a new well respectively, the potential net annual cost to Island homeowners associated with these nitrate problems would range from \$200,000 to \$400,000 per year. Any additional increases as a result of, or adaptations to climate change will only increase this burden. For example, a 15 % increase in mean nitrate concentration island-wide is predicted to result in 28% increase in the number of wells having concentration in excess of the 10 mg/L drinking water guideline (Chapter 9). In high impact regions, such as typified by the Wilmot area where more substantial increases in mean nitrate concentrations may occur (Chapters 4 & 5), up to 21% of wells would exceed the guideline, which corresponds to an 85%

increase over the currently estimated 12% of wells exceeding the guideline. Again the cost impact would echo this increase.

Nitrate contamination has also resulted in financial impacts to some municipal water suppliers, but to date these cases have not involved excessive costs, due to the current availability of other water sources. It is difficult to assess statistically the probability of an individual municipal well field being adversely impacted, however in cases where alternate water sources are not available, the additional cost associated with treatment for nitrate removal is likely to essentially double the cost of producing water for distribution, with associated impacts on water rates of municipal water customers.

10.4 Conclusions & Recommendations

The purpose of this project was to improve the understanding of the nitrate cycle and predict the potential future evolution of GW and surface water quality related to CC in PEI. The diagnosis following the investigation is meant to alert decision makers of the seriousness of the situation. The conclusions presented here support conventional thinking relative to agricultural practices in PEI, but emphasize the importance of considering all potential sources of N, particularly chemical fertilizers and residual crop material. Most importantly, this scientific report underlines the need for immediate actions. In essence, the multidisciplinary approach covering the entire hydrological cycle at the level of detail presented here, and the discussion of potential impacts for the future, aim at supporting GW-management decisions needed to maintain PEI's sole water supply.

This investigation carried out in PEI provides new data and a better understanding of the N-cycle. The results and conclusions drawn from this investigation have limitations that have been stated in each of the chapters describing the various specific studies. Such limitations include the restricted time period of the study, incompleteness of some data, uncertainty about parameters, and the use of models that must make simplifying assumptions about natural systems and processes. One such important simplification concerns the variability in time and space of conditions (especially nitrate loadings). It follows that study results mostly provide representative average nitrate amounts in soil, GW and surface water, without capturing the full variability of the natural system. Despite these limitations, the data available and results obtained strongly indicate an increasing nitrate trend in GW and surface water, especially in watersheds where intensive agricultural activities take place. Simulation results show that changes in agricultural practices that would be maintained in the long term are required in the near future in order to see improvements in GW quality over the Wilmot Watershed. Just to maintain GW at its present-day concentrations, it will be necessary to reduce soil nitrate loading under the present-day rates. A substantial further reduction in nitrate loading under present-day values would be required to reduce the number of wells exceeding the 10 mg/L guideline concentration for drinking water. We believe that our general conclusions about the future increase in these concentrations if no major changes in agricultural practices or eventually in cropping intensity are made, are firmly based, although the actual magnitude and duration of this trend could depart from predictions. The study of the Wilmot watershed shows the value and importance of detailed studies to understand the processes involved during nitrate export from soil to aquifer. Other watersheds should be investigated in a similar manner to validate the conclusions drawn for the Wilmot area.

The main implication of our research results is that alternative agricultural practices to mitigate nitrate GW contamination and sustain drinking water supply in PEI have to be developed. Decisions regarding future strategies, policies and specific actions needed for the implementation of sustainable fertilization practices must be made by local agricultural experts and water managers who have the required understanding of the current situation. Finally, we make three general recommendations concerning improvements that would lead to sustainable conditions where GW and surface water quality would no longer degrade with time.

1) Any strategy for reducing nitrate concentration in GW must take into account the seasonal behavior and potential sources of this nitrate. In watersheds of intense agricultural activities as exemplified by the Wilmot watershed, chemical fertilizers represent the dominant source of nitrate during summer and fall, whereas crop and other organic residues may constitute the main source of nitrate during winter. Strategies for reducing nitrate concentration in GW should also consider the impact that climate change may have on the modification of yearly agricultural practices.

2) Existing GW and surface monitoring activities should be maintained, and further characterization of key nitrogen sources and transfer processes should be conducted in other geographic and land-use settings in the Province. This is suggested to allow for continued assessment of nitrate concentrations in GW and surface waters, as well as establishing a sound baseline against which to evaluate potential remedial strategies. It is recommended to investigate other watersheds where agricultural activities are not as intensive as in the Wilmot area in order to cover a wider spectrum of nitrate concentrations and hydrogeological contexts.

3) The Province should continue to work towards reducing nitrate outputs from agricultural soils to GW. We recommend that PEI involves all stakeholders in the development of an integrated agricultural strategic plan using the ecosystem approach² in the near future as postponing actions could only make matters worse. We suggest investigating not just current land use practices (e.g. agriculture intensity, livestock operations and forestry), but also alternative crops (e.g. leguminous, cover crops, cash crops) and cropping practices (e.g. fertilization, crop rotations).

The scientific information we have provided in this report has advanced the body of knowledge regarding the complex processes of climate change and nitrate contamination of GW in PEI, and it has identified specific avenues upon which to focus remedial measures. This work will likely stimulate further examination of the many dimensions of the problem by the research community, but more significantly, we sincerely hope it will provide directions toward more immediate and concrete actions by decision makers and agricultural stakeholders in addressing this important issue.

² The International Joint Commission (IJC) actually recommends using the ecosystem approach in a new Great Lakes Water Quality Agreement between Canada and United States. The ecosystem approach is a strategy for the integrated management of land, water and living resources that promotes conservation and sustainability. It is a comprehensive management framework already used by different levels of government throughout the Great Lakes basin.

11 References

Aber, J. D., Goodale, C.L., Ollinger S.V., Smith, M.L., Magill A.H., Martin, M.E., Hallett, R.A., Stoddard, J. 2003. Is nitrogen deposition altering the nitrogen status of northeastern forests? *Biosc.* 53, 375-388.

Agriculture and Agri-Food Canada - AAFC 2004. Census of Agriculture: Soil Landscapes of Canada (SLC)-v.3 and Water Survey of Canada sub-sub drainage area (WSCSSDA)-v.5 (Unpublished research data)

Akinremi, O.O., McGinn, S.M., Barr, A.G. 1996. Simulation of soil moisture and other components of the hydrological cycle using a water budget approach. *Can. J. Soil Sci.* 76, 133-142.

Alexander, M. 1977. Chapter 15: Mineralization and Immobilization of Nitrogen. Pages 225-250 and Chapter 16: Nitrification. Pages 251-271 in *Introduction to Soil Microbiology*, 2nd Edition. John Wiley & Sons, Inc.

Alexandrov, V.A., Hoogenboom, G. 2000. The impact of climate variability and change on crop yield in Bulgaria. *Agric. For. Meteorol.* 104, 315-327.

Allen, D.M., Mackie D.C, Wei, M. 2003. Groundwater and climate change: a sensitivity analysis for the Grand Forks aquifer, southern British Columbia, Canada. *Hydrogeology Journal* 10.1007/s10040-003-0261-9, 40 pp.

Andersson, K.K., Hooper, A.B. 1983. O₂ and H₂O are each the source of one O in NO₂⁻ produced from NH₃ by *Nitrosomonas*: ¹⁵N-NMR evidence. *Federation of European Biochemical Societies Letters*, 164, 236-240.

Aravena, R., Evans, M.L., Cherry J.A. 1993. Stable isotopes of oxygen and nitrogen in source identification of nitrate from septic systems. *Groundwater*, 31, 180-186.

Atlantic AgriTech 2006. Report to the PEI Department of Environment, Energy and Forestry on Agricultural land use practices in the Wilmot River watershed area of PEI. February 2006 Atlantic AgriTech Inc., Hunter River RR#3, Prince Edward Island.

Atlantic AgriTech - AAT 2005. Agricultural land use practices in the Wilmot River watershed area of PEI. (Unpublished data for research purposes)

Baier, W., Robertson, G.W. 1965. Estimation of latent evaporation from simple weather observations. *Can. J. Plant Sci.* 45, 276-284.

Baier, W., Robertson, G.W. 1966. A new versatile soil moisture budget. *Can. J. Plant Sci.* 46, 299-315.

Baier, W., Dyer, J.A., Sharp, W.R. 1979. The versatile soil moisture budget. *Tech. Bull.* 87, Agrometeorology Section, Research Branch, Agric. Canada, Ottawa, ON, 52 pp.

Bootsma, A., Gameda, S., McKenney, D.W. 2001. Adaptation of agricultural production to climate change in Atlantic Canada. Final report for Climate Change Action Fund Project A214, 30 pp.

Bootsma, A., Gameda, S., McKenney, D.W. 2005a. Impacts of climate change on selected agroclimatic indices in Atlantic Canada. *Can. J. Soil Sci.* 85, 329-343.

Bootsma, A., Gameda, S., McKenney, D.W. 2005b. Potential impacts of climate change on corn, soybeans and barley yields in Atlantic Canada. *Can. J. Soil Sci.* 85, 345-357.

Burns, I.G. 1974. A model for predicting the redistribution of salts applied to fallow soils after excess rainfall or evaporation. *J. Soil Sci.* 25, 165-178.

Burton, D.L., Beauchamp, E.G. 1986. Nitrogen losses from swine housings. *Agric. Waste* 15, 59-74.

Canadian Council of Ministers of the Environment (CCME) 2006. Canadian Water Quality Guidelines for the Protection of Aquatic Life, Inland Waters Directorate, http://www.ccme.ca/publications/ceqg_rcqe.html

Canadian Fertilizer Institute - CFI 2001. Nutrient uptake and removal by field crops. Eastern Canada 2001 [Online]. http://www.cfi.ca/files/publications/archive/d160_NU_E_01.pdf [2006 October 15].

Carnell, R.E., Senior, C.A. 1998. Changes in mid-latitude variability due to increasing greenhouse gases and sulphate aerosols. *Clim. Dynamics* 14, 369-383.

Caron, J., Ben Jemia, S., Gallichand, J., Trépanier, L. 1999. Field Bromide Transport under Transient-State: Monitoring with Time Domain Reflectometry and Porous Cup. *Soil Sci. Soc. Am. J.* 63, 1544-1553.

Chambers, P.A., Guy, M., Roberts, E.S., Charlton, M.N., Kent, R., Gagnon, C., Grove, G., Foster, N. 2001. Nutrients and their impact on the Canadian environment. Agriculture and Agri-Food Canada, Environment Canada, Fisheries and Oceans Canada, Health Canada and Natural Resources Canada, Ottawa, Ontario, Canada.

- Chang, C.C.Y., Langston, J., Riggs, M., Campbell, D.H., Silva, S.R., Kendall, C. 1999. A method for nitrate collection for $\delta^{15}\text{N}$ and $\delta^{18}\text{O}$ analysis from waters with low nitrate concentrations. *Canadian Journal of Fisheries and Aquatic Sciences*, 56, 1856-1864.
- Chantigny, M.H., Angers, D.A., Rochette, P. 2002. Fate of carbon and nitrogen from animal manure and crop residues in wet and cold soils. *Soil Biology & Biochemistry*, 34, 509-517.
- Choi, W.-J., Lee, S.-M., Ro, H.-M., Kim, K.-C., Yoo, S.-H. 2002. Natural ^{15}N abundances of maize and soil amended with urea and composed pig manure. *Plant and Soil*, 245, p. 223-232.
- Cookson, W.R., Cornforth, I.S., Rowarth, J.S. 2002. Winter soil temperature (2-15°C) effects on nitrogen transformations in clover green manure amended or unamended soils; a laboratory and field study. *Soil Biology & Biochemistry*, 34, 1401-1415.
- Croteau, A., Nastev, M., Lefebvre, R., Lamontagne, L., Lamontagne, C., Lavigne, M.A., Blanchette, D. 2005. Estimation of spatial and temporal distribution of recharge to des Anglais River aquifer system, Québec. 6th Joint IAH-CNC and CGS Groundwater Specialty Conference, Saskatoon 2005, 8 p., CD version.
- De Jong, R., Li, K.Y., Bootsma, A., Huffman, T., Roloff, G., Gameda, S. 2001. Crop yield and variability under climate change and adaptive crop management scenarios. Final report for Climate Change Action Fund Project A080, 50 pp.
- De Jong, R., Yang, J.Y., Drury, C.F., Huffman, E., Kirkwood, V., Yang, X.M. 2007. The indicator of risk of water contamination by nitrate-nitrogen. *Can. J. Soil Sci.* (in press).
- Delgado, J., Riggensbach, R., Sparks, M., Dillon, L.K., Ristau, R. 2001. Evaluation of Nitrate-nitrogen transport in a potato-barley rotation. *Soil Sci. Soc. Am. J.* 657, 878-883.
- Diersch, H.-J.G. 2004. FEFLOW: Finite Element Subsurface Flow and Transport Simulation System – Reference Manual. WASY Institute for Water Resources Planning and System Research Ltd. 277 p.
- Domenico, P.A., Schwartz, F.W. 1990. *Physical and Chemical Hydrogeology* (2nd edition). John Wiley and Sons, New York, 506 p.
- Drury, C.F., Tan, C.S., Gaynor, J.D., Oloya, T.O., Welacky, T.W. 1996. Influence of controlled drainage-subirrigation on surface and tile drainage nitrate loss. *J. Environ. Qual.* 25, 317-324.
- Drury, C.F., Yang, J.Y., De Jong, R., Yang, X.M., Huffman, E., Kirkwood, V., Reid, K. 2007. Residual soil nitrogen indicator for Canada. *Can. J. Soil Sci.* (in press).

Environment Canada - EC 2001a. Municipal water use database (MUD). MUD2001 Municipal Aggregations Imputed Database, http://www.ec.gc.ca/water/en/manage/use/e_data.htm; accessed on March 2005.

Environment Canada - EC 2001b. National Environmental Indicators Series. Urban water indicators: Municipal water use and wastewater treatment SOE Bulletin No. 2001-1. Available at <http://www.ec.gc.ca/water/en/manage/data/MUD> (accessed on February 2005).

Environment Canada – EC 2004. Water; available at <http://www.ec.gc.ca/water> (accessed on January 2005).

Feddes, R.A., Kowalik, P.J., Zaradny, H. 1978. Simulation of field water use and crop yield. Centre for Agricultural Publishing and Documentation, Wageningen, The Netherlands, 189 pp.

Flato, G.M., Boer, G.J. 2001. Warming Asymmetry in Climate Change Simulations. *Geoph. Res. Let.* 28, 195-198.

Fleury, M.A. 2003. Unearthing Montreal's municipal water system amalgamating and harmonizing urban water services. Volume 8, number 7. FES outstanding graduate student paper series, June 2003. Faculty of Environmental Studies, York University. Toronto (Ontario), M3J 1P3.

Francis, R.M. 1989. Hydrogeology of the Winter River Basin, Prince Edward Island; PEI Department of the Environment, Water Resources Branch, 117 p.

Fukada, T., Hiscock, K. M., Dennis, P. 2004. A dual-isotope approach to the nitrogen hydrogeochemistry of an urban aquifer. *Applied Geochemistry*, 19, 709-719.

Furey, P.R., Gupta, V.K. 2001. A physically based filter for separating base flow from streamflow time series. *Wat. Res. Res.* 37, 2709-2722.

Galloway, J.N., Aber, J.D., Erisman, J.W., Seitzinger, S.P., Howarth, R.W., Cowling E.B., Cosby, B.J. 2003. The Nitrogen Cascade. *BioSci.* 53, 341-356.

Galloway, J.N., Cowling, E.B. 2002. Reactive Nitrogen and the World: 200 years of change. *Ambio* 11, 64-71.

Gburek, W.J., Folmar, G.J., Urban, J.B. 1999. Field data and groundwater modelling in a layered fractured aquifer. *Groundwater* 37, 175-184.

Gelhar, L., Welty, C., Rehfeldt, K. 1992. A critical review of data on field-scale dispersion in aquifers. *Wat. Res. Res.* 28, 1955-1974.

Gelhar, L.W., Wilson, J.L. 1974. Ground-water quality modelling. *Groundwater* 12, 399-408.

Gordon, C., Cooper, C., Senior, C.A., Banks, H., Gregory, J.M., Johns, T.C., Mitchell, J.F.B., Wood, R.A. 2000. The simulation of SST, sea ice extents and ocean heat transports in a version of the Hadley Centre coupled model without flux adjustments. *Climate Dynamics* 16, 147-168.

Hayhoe, H.N. 2000. Improvements of stochastic weather data generators for diverse climates. *Climate Res.* 14, 75-87.

Health Canada – HC 1987. Guidelines for Canadian Drinking Water Quality, Supporting Documentation, http://www.hc-sc.gc.ca/ewh-semt/pubs/water-eau/doc_sup-appui/nitrate_nitrite/index_e.html.

Health Canada – HC 2004. Summary of guidelines for Canadian drinking water quality; Prepared by the Federal–Provincial-Territorial Committee on Drinking Water of the Federal–Provincial-Territorial Committee on Health and the Environment, April 2004, <http://www.hc-sc.gc.ca/waterquality>.

Heaton, T.H.E. 1986. Isotopic studies of Nitrogen pollution in the Hydrosphere and Atmosphere: a review. *Chemical Geology*, 59, 87-102.

Hengeveld, H.G. 2000. Projections for Canada's climate future. A discussion of recent simulations with the Canadian global climate model. Science Assessment and Integration Branch, Meteorological Service of Canada, Downsview, ON., 27 pp.

Hollocher, T.C. 1984. Source of the Oxygen atoms of nitrate in oxidation of nitrite by *Nitrobacter agilis* and evidence against a P-O-N anhydride mechanism in oxydative phosphorylation. *Archives of Biogeochemistry and Biophysics*, 233, 721-727.

Huffman, T., Ogston, R., Fisette, T., Daneshfar, B., Gasser, P.Y., White, L., Maloley, M., Chenier, R. 2006. Canadian agricultural land-use and land management data for Kyoto reporting. *Can. J. Soil Sci.* 86, 431-439.

Hulme, M., Barrow, E.M., Arnell, N.W., Harrisson, P.A., Johns, T.C., Downing, T.E. 1999. Relative impacts of human induced climate change and natural climate variability. *Nature* 397, 688-691.

Ineson, P., Taylor, K., Harrison, A.F., Poskitt, J., Benham, D.G., Tipping, E., Woof, C. 1998. Effects of climate change on nitrogen dynamics in upland soils. 1. A transplant approach. *Glob. Change Biol.* 4, 143-152.

Info PEI 2005. Island Information Service, Government of Prince Edward Island. <http://iis.peigov/index.jsp>

International Panel on Climate Change – IPCC 1997. Organization for Economic Cooperative Development, IPCC Guidelines for National Greenhouse Gas Inventories, OCDE, Paris.

International Panel on Climate Change - IPCC 2001. Impacts, adaptations and vulnerability. Contribution of Working Group II, 3rd assessment report. Houghton, JT, Ding, Y., Griggs, D.J., Noguer, M., van, P.J. der Linden *et al.* (eds.). Cambridge University Press, UK.

International Panel on Climate Change – IPCC 2001. Climate Change 2001 - Working Group I: the Scientific Basis. Electronic version at http://www.grida.no/climate/ipcc_tar/wg1/index.htm.

International Panel on Climate Change – IPCC 2002. Technical report V prepared under the auspices of the IPCC Chair, Dr. Robert T. Watson, and administered by the IPCC Working Group II Technical Support Unit, <http://www.ipcc.ch/pub/tpbiodiv.pdf>.

Izaurrealde, R.C., Rosenberg, N.J., Brown, R.A., Thomson, A.M. 2003. Integrated assessment of Hadley Center (HadCM2) climate-change impacts on agricultural productivity and irrigation water supply in the conterminous United States. Part II. Regional agricultural production in 2030 and 2095. *Agric. For. Meteorol.* 117, 97-122.

Jackson, R.E., Mutch, J.P., Priddle, M.W. 1990. Persistence of aldicarb residues in the sandstone aquifer of Prince Edward Island, Canada. *J. Cont. Hydr.* 6, 21-35.

Jacques Whitford Environment Ltd 2001. Nutrient management strategy -Technical and policy options for nutrient management planning in PEI. Project No. PEC80450 prepared for PEI department of Agriculture and Forestry, produced in partnership with LJM Environmental Consulting and Atlantic Agritech Inc., 76 p+appendices.

Jiang, Y., Woodbury, A., Painter, S. 2004. Full-Bayesian inversion of the Edwards Aquifer. *Groundwater* 42, 724-733.

Jiang, Y., Somers, G., Mutch, J. 2004. Application of numerical modelling to groundwater assessment and management in Prince Edward Island. In *Proc. from the 57th Canadian Geotechnical Conference and the 5th Joint CGS/IAH-CNC Conference*, Quebec, Canada.

Jiang, Y., Somers, G., Paradis, D. *et al.* 2006. Modelling basin-scale nitrate transport in the Wilmot River watershed of Prince Edward Island (PEI), Canada. In *Proc. from 34th Congress of International Association of Hydrogeologists*, Beijing, China

Jones, C.A., Kiniry, J.R., eds. 1986. CERES-Maize: a simulation model of maize growth and development. Texas A&M Univ. Press, College Station, TX., 193 pp.

Jyrkama, M.I., Sykes, J.F., Normani, S.D. 2002. Recharge estimation for transient groundwater modeling, *Groundwater* 40, 638-648.

Kampbell, D.H., Wilson, J.T., Vandegrift, S.A. 1989. Dissolved oxygen and methane in water by a GC headspace equilibration technique. Intern. J. Environ. Anal. Chem. 36, 249-257.

Kendall, C., Aravena, R. 2000. Nitrate isotopes in groundwater systems - Chapter 9. In: Peter G. Cook and Andrew L. Herczeg editors, Environmental Tracers in subsurface hydrology, Kluwer Academic Publishers, Boston, 261-297.

Kraft, G., Stites, W. 2003. Nitrate impacts on groundwater from irrigated-vegetable systems in a humid north-central US sand plain. Agric., Ecos. Envir. 100, 63-74.

Kumar, S., Nicholas, D.J.D., Williams, E.H. 1983. Definitive ^{15}N NMR evidence that water serves as a source of 'O' during nitrite oxidation by *Nitrobacter agilis*. Fed. Eur. Bioch. Soc. Letters, 152, 71-74.

Lebedin, J., Rohde, H., Jacques, D., Hammer, M. 2000. Rural water well infrastructure assessment on the Prairies: An overview of groundwater development and reliance trends. Agriculture and Agri-Food Canada, Prairie Farm Rehabilitation Administration, Technical Service Earth Sciences Unit, March, 31, 2000. 14 p.

Lemmen, D.S., Warren, F.J., eds. 2004. Climate change impacts and adaptation: a Canadian perspective, 174 pages. Available from Climate Change Impacts and Adaptation Directorate, Natural Resources Canada, 601 Booth Street, Ottawa, Ontario K1A 0E8 or email to adaptation@nrcan.gc.ca.

Levallois, P., Thériault, M., Rouffignat, J., Tessier, S., Landry, R., Ayotte, P., Girard, M., Gingras, S., Gauvin, D., Chiasson, C. 1998. Groundwater contamination by nitrates associated with intensive potato culture in Québec. The Sci. Total Envir. 217, 91-101.

Mackenzie, F.T. 1998. Our changing planet. Second edition, Prentice Hall, 486 p.

MacLeod, J.A., Sanderson, J.B., Campbell, A.J, Somers, G.H. 2002a. Potato production in relation to concentrations of nitrate in groundwater: current trends in PEI and potential management changes to minimize risk. In National Conference on Agricultural Nutrients and Their Impact on Rural Water Quality, April 29 to 30, 2002, the Waterloo Inn, Waterloo, Ontario. Volume of proceedings, Agricultural Institute of Canada, Ottawa, ON., 15-21.

MacLeod, J.A. and Sanderson, J.B. 2002b. Fall Cover Crops for Reducing Nitrate Loss. National Conference on Agriculture Nutrients and their impact on Rural Water Quality, April 29 to 30, 2002, The Waterloo In, Ontario. Proceeding volume, Agricultural Institute of Canada Foundation 283-292.

McCulloch, M., Forbes, D.L., Parkes, G., Thompson, K., Chagnon, R. *et al.* 2001. Coastal impacts of climate change and sea level rise on Prince Edward Island. Project A041 of CCAF. Natural Resources Canada.

McFarlane, N.A., Boer, G.J., Blanchet, J.P., Lazare, M. 1992. The Canadian Climate Centre Second Generation General Circulation Model and its equilibrium climate. *J. Climate* 5, 1013-1044.

McGinn, S.M., Toure, A., Akinremi, O.O., Major, D.J., Barr, A.G. 1999. Agroclimate and crop response to climate change in Alberta, Canada. *Outl. Agric.* 28, 19-28.

Mearns, L.O., Rosenzweig, C., Goldberg, R. 1997. Mean and variance change in climate scenarios: methods, agricultural applications, and measures of uncertainty. *Climatic Change* 35, 367-396.

Milburn, P., MacLeod, J. 1991. Considerations for tile drainage-water quality studies in temperate regions. *Ap. Agric. Eng.* 7, 209-215.

Milburn, P., Mosher, A., MacLeod, J. 1992. A 32 -channel event interface for commercial portable data acquisition systems. *Can. Agric. Eng.* 36, 69-78.

Millington, R.J., Quirk, J.P. 1961. Permeability of porous solids. *Trans. Faraday Soc.* 57, 1200-1206.

Mitchell, R.J., Babcock, R.S., Gelinas, S., Nanus, L., Stasney, D.E. 2003. Nitrate Distributions and Source Identification in the Abbotsford-Sumas Aquifer, Northwestern Washington State. *J. Environ. Qual.* 32, 789-800.

Moore, K.B., Ekwurzel, B., Esser, B.K., Hudson, G.B., Moran, J.E. 2006. Sources of groundwater nitrate revealed using residence time and isotope methods. *Applied Geochemistry*, 21, 1016-1029.

Mutch, J.P., Jackson, R.E., Priddle, M.W. *et al.* 1992. The fate and simulation of Aldicarb in the soil and groundwater of Prince Edward Island, Scientific Series NO. 194, National Water Research Institute, Burlington, Ontario.

Nakicenovic, N., Swart, R., eds. 2000. Special Report on Emissions Scenarios-A special report of Working Group III of the Intergovernmental Panel on Climate Change. Cambridge University Press, Cambridge, UK, 612pp.

Natural Resources Canada – NRCAN 2005a. The Atlas of Canada. Groundwater. Available at <http://atlas.gc.ca/site/english/maps/freshwater/distribution/groundwater> (accessed on January 2005).

Natural Resources Canada – NRCan 2005b. The Atlas of Canada. Commercial and institutional water consumption, 1999. Available at http://atlas.gc.ca/site/english/maps/fresh_water/

Olesen, J.E., Bindi, M. 2002. Consequences of climate change for European agricultural productivity, land use and policy. *Eur. J. of Agron.* 16, 239-262.

Onofrei, C. 1987. A method of land evaluation using crop simulation techniques. Ph. D. thesis, Univ. of Man., Winnipeg, MN. 314 pp.

Ontario Ministry of Agriculture and Food 2003. Soil fertility handbook. Publication 611, Ontario Ministry of Agriculture and Food, Ontario Government.

Pantako, O., Savard, M.M., Somers, G. 2006. The Current Water Supply Infrastructure in Prince Edward Island Geological Survey of Canada, open file report.

Paradis, D., Ballard, J.-M., Savard, M.M., Lefebvre, R., Jiang, Y., Somers, G., Liao, S., Rivard, C. 2006. Impact of agricultural activities on nitrate levels in groundwater and surface water of the Wilmot River watershed, Prince-Edward Island, Canada. Proceeding of 59th Canadian Geotechnical Conference and the 7th joint CGS/IAH-CNC Conference, Victoria, CD, 8 pages.

Parker, J.C., Gillham, R.W., Cherry, J.A. 1994. Diffusive disappearance of immiscible-phase organic liquids in fractured geologic media. *Groundwater* 32, 805-820.

Piggott, A., Brown, D., Moin, S., Mills, B. 2001. Exploring the dynamics of groundwater and climate interaction; report prepared for the Climate Change Action Fund, 8 p.

Prest, V.K. 1973. Surficial deposits of Prince Edward Island; Geological Survey of Canada, "A" Series Map 1366A.

Qian, B., Gameda, S., Hayhoe, H., De Jong, R., Bootsma, A. 2004. Comparison of LARS-WG and AAFC-WG stochastic weather generators for diverse Canadian climates. *Climate Res.* 26, 175-191.

Qian, B., Hayhoe, H., Gameda, S. 2005. Evaluation of the stochastic weather generators LARS-WG and AAFC-WG for climate change impact studies. *Climate Research* 29, 3-21.

Qian, P., Schoenau, J., Ziadi, N. 2007. Ion Supply Rates Using Resins, *in* M. R. Carter, ed., Soil sampling and methods of analysis. 2nd edition, Canadian Society of Soil Science, Lewis Publishers, Boca Raton, Fl. (in press).

Racsko, P., Szeidl, L., Semenov, M. 1991. A serial approach to local stochastic weather models. *Ecol. Mod.* 57, 27-41.

Richardson, C.W. 1981. Stochastic simulation of daily precipitation, temperature, and solar radiation. *Wat. Res. Res.* 17, 182-190.

Richardson, C.W., Wright, D.A. 1984. WGEN: a model for generating daily weather variables. US Department of Agriculture, Agricultural Research Service, ARS-8. USDA, Washington, DC.

Ritchie, J.T., Otter, S. 1985. Description and performance of Ceres-Wheat: a user oriented wheat yield model. USDA-ARS, ARS 38, 159-170.

Sanderson, J.B. MacLeod, J.A. 2002. Maximizing Legume Nitrogen Use and Minimizing Nitrate Leaching. National Conference on Agriculture Nutrients and their impact on Rural Water Quality, April 29 to 30, 2002, The Waterloo In, Ontario. Proceeding volume, Agricultural Institute of Canada Foundation, 302-309.

Savard, M.M., Liao, S., Smirnoff, A., Paradis, D., Somers, G., van Bochove, E. 2005. Year-long Nitrification contributing to excess N in an agricultural watershed as revealed by a Dual Isotope Study of Nitrates in Aquifer and Surface Waters. Sixth International Conference on Applied Isotope Geochemistry, September 11 to 18, Prague, Czech Republic. AIG-6 Abstracts, F. Buzek & M. Novak (editors), p. 208.

Savard, M. M., Paradis, D., Somers, G., Liao, S. 2006. Deciphering seasonal nitrification in an agricultural watershed using nitrate oxygen isotopes of aquifer and surface waters. *Proceedings of the International Perspective on Environmental and Water Resources*, December 18-20, 2006 in New Delhi, India.

Savard, M. M., Paradis, D., Somers, G., Liao, S., van Bochove, E., 2007. Winter nitrification contributes to excess NO_3^- in groundwater of an agricultural region - A dual isotope study. *Water Resource Research*, manuscript 2006wr005469 (in press).

Savard, M.M., Simpson, S., Smirnoff, A., Paradis, D., Somers, G., Bochove E. V., Thériault, G. 2004. A study of the Nitrogen cycle in the Wilmot River Watershed, Prince Edward Island: Initial Results. In *Proc. from the 57th Canadian Geotechnical Conference and the 5th Joint CGS/IAH-CNC Conference*, Quebec, Canada, session 4A on water quality, 20-27.

Schroeder, P.R., Aziz, N.M., Lloyd, C.M., Zappi, P.A. 1994. The Hydrologic Evaluation of landfill Performance (HELP) Model: Engineering Documentation for Version EPA/600/R-94/168b, 116 pp.

Schulze-Makuch, D. 2005. Longitudinal dispersivity data and implications for scaling behavior. *Groundwater* 43, 443-456.

Semenov, M.A., Barrow, E.M. 1997. Use of a stochastic weather generator in the development of climate change scenarios. *Climatic Change* 35, 397-414.

Semenov, M.A., Brooks, R.J., Barrow, E.M., Richardson, C.W. 1998. Comparison of the WGEN and LARS-WG stochastic weather generators for diverse climates. *Climate Res.* 10, 95-107.

Silva, S.R., Kendall, C., Wilkinson, D.H., Ziegler, A.C., Chang, C.C.Y., Avanzino, R.J. 2000. A new method for collection of nitrate from fresh water and the analysis of nitrogen and oxygen isotope ratios. *Journal of Hydrology*, 228, 22-36.

Soil Landscapes of Canada Working Group 2006. Soil Landscapes of Canada v3.1. Agriculture and Agri-Food Canada (digital map and database at 1:1 million scale).

Somers, G. 1998. Distribution and trends for occurrence of nitrate in PEI groundwater. In *Proc. from nitrate-agricultural sources and fate in the Environment-Perspectives and Direction*, Grand Falls, Canada.

Somers, G., Mutch, J. 1999. Results of an Investigation into the Impact of Irrigation Wells on the Availability of Groundwater in the Baltic area. Available at <http://res.agr.ca/cansis/nsdb/slc/v3.1/intro.html>

Somers, G.H., Raymond, B., Uhlman, W. 1999. PEI water quality interpretative report 99. Prepared for Canada-Prince Edward Island Water Annex to the Federal/Provincial Framework Agreement for Environmental Cooperation in Atlantic Canada, 67 p.

Spiegel, M.R. 1961. *Schaum's outline of theory and problems of statistics*. Schaum's Publishing Co., New York, 359 pp.

Spoelstra, J., Schiff, S.L., Elgood, R.J., Semkin, R.G., Jeffries, D.S. 2001. Tracing the sources of exported nitrate in the Turkey Lakes watershed using $^{15}\text{N}/^{14}\text{N}$ and $^{18}\text{O}/^{16}\text{O}$ isotopic ratios. *Ecosystems*, 4, 536-544.

Tan, C.S., Drury, C.F., Reynolds, W.D., Groenevelt, P.H., Dadfra, H. 2002. Water and nitrate loss through tiles under a clay loam soil in Ontario after 42 years of consistent fertilization and crop rotation. *Agric. Ecosyst. Environ.* 93, 121-130.

Van Bochove, E., Jones, H.G., Bertrand, N., Prévost, D. 2000. Winter fluxes of greenhouse gases from snow-covered agricultural soil: Intra-annual and interannual variations. *Global Biogeochem. Cycles* 14, 113-125.

Van de Poll, H.W. 1981. Report on the Geology of Prince Edward Island. Department of Tourism, Industry and Energy, PEI.

Van de Poll, H.W. 1983. Geology of Prince Edward Island; Report 83-1, PEI Department of Energy and Forestry, Energy and Minerals Branch, Charlottetown, 66 p.

Viner, D. 1996. The Climate Impacts LINK Project. *Climate Monitor* 23, 3-5.

Vitousek, P.M., Aber, J.D., Howarth, R.W., Likens, G.E., Matson, P.A., Schindler, D.W., Schlesinger, W.H., Tilman, D.G. 1997. Human alteration of the global nitrogen cycle: Sources and consequences. *Ecolog. Appl.* 7, 737-750.

Wagner-Riddle, C., Thurtell, G.W. 1998. Nitrous oxide emissions from agricultural fields during winter and spring thaw as affected by management practices. *Nutrient Cycling in Agroeco.* 52, 151-163.

Wassenaar, L. 1995. Evaluation of the origin and fate of nitrate in the Abbotsford aquifer using the isotopes of ^{15}N and ^{18}O in NO_3^- . *App. Geoch.*, 10, 391-405.

Waterloo Hydrogeologic Inc. 2004. Visual MODFLOW v4.0 users manual, copyright Waterloo Hydrogeologic Inc. 2004.

Wilks, D.S, Wilby, R.L. 1999. The weather generator game: A review of stochastic weather models. *Prog. in Phys. Geogr.* 23, 329-358.

Yang, J.Y., De Jong, R., Drury, C.F., Huffman, E.C., Kirkwood, V., Yang, X.M. 2007. Development of a Canadian agricultural nitrogen budget model (CANB v2.0): simulation of the nitrogen indicators and integrated modelling for policy scenarios. *Can. J. Soil Sci.* 87 (in press).

Young, J., Somers, G.H., Raymond, G.B. 2002. Distribution and trends for nitrate in PEI groundwater and surface waters. National Conference on Agriculture Nutrients and their impact on Rural Water Quality, April 29 to 30, 2002, The Waterloo In, Ontario. Proceeding volume, Agricultural Institute of Canada Foundation 313-319.

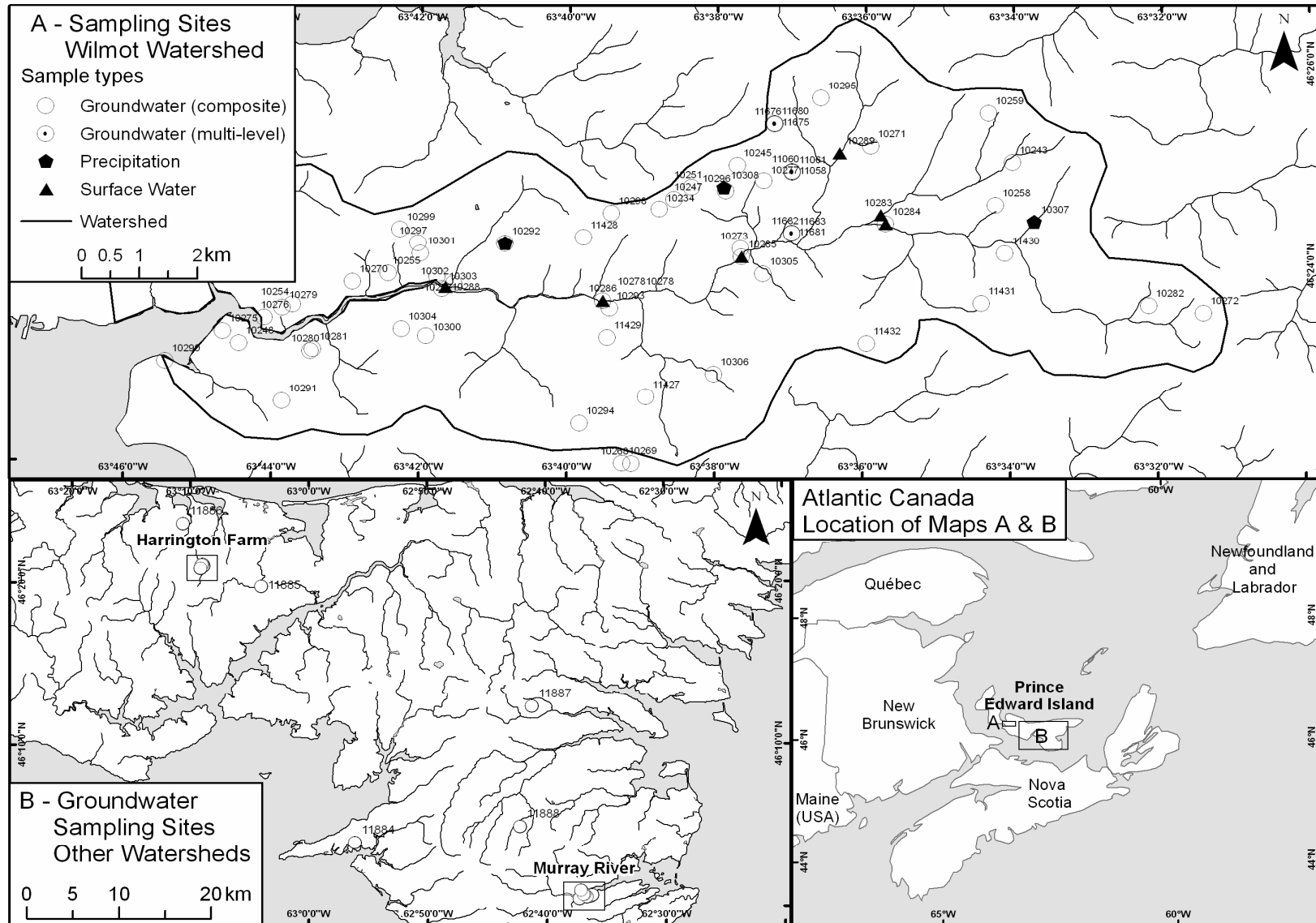
Zak, D.R., Groffman, P.M., Pregitzer, K.S., Christensen, S., Tiedje, J.M. 1990. The vernal dam: plant-microbe competition for nitrogen in northern hardwood forests. *Ecology* 71, 651-656.

Zheng, C., Wang, P. 1998. MT3DMS documentation and User's Guide. Waterloo Hydrogeologic, Inc.

Ziadi, N., Cambouris, A.N., Nolin, M.C. 2006. Anionic exchange membranes as a soil test for N availability. *Commun. Soil Sci. Plant Anal.* 37, 2411-2422.

Ziadi, N., Simard, R.R., Allard, G., Lafond, J. 1999. Field evaluation of anion exchange membranes as a N soil testing method for grasslands. *Can. J. Soil Sci.* 79, 281-294.

ANNEX – Map of sample location for the nitrate characterization and Tables of analytical results.



Wilmot River watershed - Groundwater samples

Site	$\delta^{18}\text{O}-\text{H}_2\text{O}$ (‰, VSMOW)								δD in H_2O (‰, VSMOW)								$\delta^{18}\text{O}$ in NO_3^- (‰, VSMOW)								$\delta^{15}\text{N}$ in NO_3^- (‰)								N in NO_3^- (mg/L)													
	1	2	3	4	5	6	7	8	1	2	3	4	5	6	7	8	1	2	3	4	5	6	7	8	1	2	3	4	5	6	7	8	1	2	3	4	5	6	7	8						
10234	-12.7				-11.4				-62.5				-77.9				11.7				2.8				5.3															8.10						
10243	-10.9				-10.6				-63.4				-70.9				9.8				1.3				4.9																4.29					
10245	-11.8	-12.8	-10.9	-11.1	-11.5	-11.2		-11.4	-68.9	-71.4	-76.0	-69.7	-77.1	-68.1	-74.2	-73.4	11.8	9.1	1.1	2.5	3.1	3.4	1.8	3.5	5.5	4.1	5.9	6.1	4.7	5.5	5.3	6.3	3.86	8.61	9.21	8.11	7.06	9.83	10.23	9.42						
10247	-11.3				-10.3				-62.1				-54.9				11.6				3.0				3.6																					
10248	-10.0	-10.3	-10.6	-10.4	-10.3	-9.9		-10.3	-67.1	-62.6	-63.7	-66.5	-65.4	-67.3		-68.3	11.1	10.7	0.5	4.1				4.5	4.4	5.7	6.2																0.71			
10251	-10.2				-11.3				-79.8				-61.1				12.0				3.3				5.7																					
10254	-10.4				-11.2				-67.1				-69.2				10.8				2.4				3.4																					
10255	-11.3	-11.7	-11.4	-10.8	-11.2	-11.0	-11.5	-11.0	-75.5	-73.8	-80.7	-62.1	-75.8	-75.5	-71.9	-70.9	6.5	7.8	-2.1	-1.3	0.9	1.1	-3.7	2.1	-3.0	0.5	1.6	3.4	0.6	2.6	2.1	3.4	0.48	0.38	0.54	3.13	0.33	0.64	0.62	7.69						
10257	-10.9	-11.0	-10.7	-11.3	-11.6	-11.0	-10.3	-11.3	-71.7	-69.6	-67.6	-76.9	-79.5	-68.6	-73.4	-77.0	11.3	8.5	-1.5	-2.4	2.2	1.9	0.4	1.9	2.2	3.2	4.1	3.2	3.4	3.2	3.6	10.96	10.39	10.60	7.07	10.47	11.97	14.23	10.12							
10257					-10.4								-73.1								3.1				3.7																					
10258	-12.9				-10.9				-71.3				-76.6				11.5				3.2				4.1																					
10259	-12.4	-10.7	-11.0	-11.2	-11.2	-11.4	-10.8	-11.0	-63.6	-71.0	-77.0	-74.9	-80.2	-66.0	-74.7	-76.2	-0.1	7.0	0.5	-2.6	0.9	0.9	0.5	1.2	1.0	2.2	3.8	3.4	3.8	4.1	3.4	4.0	6.21	4.45	4.71	5.35	6.95	8.26	8.40	9.19						
10268	-10.5	-11.4	-11.1	-11.6	-11.2	-10.5	-10.5	-11.6	-71.2	-71.6	-66.0	-77.1	-66.0	-74.1	-69.3	-73.0	11.7	8.7	-1.1	0.1	2.8	3.1	-2.3	4.0	2.8	2.3	3.0	3.6	2.8	3.5	2.8	3.6	9.06	8.27	8.36	7.64	9.17	9.68	6.47	11.63						
10269	-10.4				-11.4				-67.2				-68.8				13.0				3.5				3.5																					
10270	-12.7				-11.4				-72.5				-76.0				10.5				1.0				1.5																					
10271	-10.4	-10.1	-10.8	-11.2	-11.0	-11.5	-10.4	-11.5	-72.1	-67.6	-66.8	-76.3	-69.5	-69.3	-68.7	-74.0	7.0	9.0	-1.7	-0.9	2.5	2.0	-3.9	2.4	0.7	2.1	2.6	3.7	3.1	3.3	2.6	4.1	8.95	9.03	9.40	7.98	0.01	12.79	11.79	21.42						
10272	-11.6	-10.5	-11.2	-11.3	-11.5	-14.8	-11.2	-11.7	-70.8	-67.6	-76.6	-81.2	-79.4	-81.0	-76.4	-75.4	8.7	8.9	-0.2	-1.1	1.8	2.0	1.2	2.0	6.1	6.6	8.3	8.1	7.2	8.5	7.2	4.7	3.34	2.71	3.73	3.14	3.15	4.35	2.81	2.98						
10273	-10.7	-11.1	-11.6	-11.4	-11.2	-12.0	-10.8	-11.3	-76.0	-74.7	-99.5	-74.1	-80.6	-74.7	-76.6	-76.0	10.6	9.0	-1.3	1.0	2.7	2.8	1.1	2.3	2.6	2.2	3.5	3.8	23.3	3.6	3.3	3.9	0.91	0.84	0.59	0.68	5.65	1.07	0.94	0.89						
10275	-10.4				-10.8				-67.1				-75.5				11.6				2.2				7.5																					
10276	-11.5				-11.4				-54.1				-67.8				10.5				0.9				5.1																					
10277	-10.5	-10.0	-10.6	-10.6	-11.1	-10.7	-10.1	-10.7	-66.0	-75.0	-70.1	-66.1	-70.4	-68.3	-67.3	-67.6	7.5	7.2	-1.3	0.3	1.5	1.7	-1.4	1.9	1.6	3.9	6.7	6.5	5.6	6.3	5.9	6.7	2.46													
10279	-10.1	-11.0	-10.4	-10.6	-11.1	-9.7	-9.8	-9.9	-62.0	-70.4	-71.6	-70.5	-72.7	-68.8	-68.1	-72.3	9.3	9.5	-0.4	-1.2	2.7	3.2	2.0	3.6	3.8	3.4	4.7	5.5	4.5	4.8	4.4	4.0	12.20	11.59	12.28	10.39	37.10	12.89	15.29	11.87						
10280	-10.8				-11.0				-70.7				-66.3				12.2				2.3				4.0																					
10281	-10.0				-11.3				-74.1				-66.1				12.6				7.4				3.6																					
10282	-12.2				-10.5				-71.9				-76.9				13.0								3.9																					
10284					-11.1																																									
10285					-10.8				-73.3																																					
10286					-10.9				-75.5																																					
10290	-11.0				-11.8				-74.7				-73.5				11.9				2.4				2.6																					
10291	-11.0				-11.7				-74.8				-81.6				12.5				3.4				3.1																					
10292	-11.4	-10.2	-11.1	-11.1	-11.1		-11.4	-11.2	-71.4	-69.4	-66.3	-74.3	-64.6		-71.1	-72.1	11.2	6.9	-3.2	0.3	0.7		1.0	1.0	3.4	2.0	3.6	3.9	3.2		3.7	4.0	5.17	5.06	5.03	2.99	4.46		3.71	3.54						
10293	-10.4	-11.8	-11.4	-11.4	-11.3	-10.3	-11.4	-11.3	-67.8	-83.6	-68.7	-88.6	-64.4	-93.5	-72.1	-72.7	9.7	6.6	-2.8	-0.6	-0.4	0.6	-0.7	0.7	3.3	2.5	4.2	4.2	3.9	4.6	4.1	4.2	3.84	3.05	2.18	3.66	3.83	4.55	4.14	4.13						
10294	-10.7				-11.0				-68.1				-75.3				3.1				1.3				0.8																					
10295	-10.7				-11.0				-68.9				-77.4				11.3								2.6																					
10296	-10.8	-10.7	-10.9	-11.1	-11.0	-10.8	-10.9	-11.3	-73.2	-65.8	-64.9	-76.6	-77.4	-65.5	-70.7	-71.3	12.3	10.1	-0.2	-0.2	3.3	4.3	-2.5	3.6	3.3	2.1	3.5	4.4	3.2	3.6	3.3	4.0	8.72	9.06	5.99	6.99	9.50	12.04	9.66	8.13						
10297	-10.4	-11.8	-10.8	-11.4	-11.2	-11.1	-10.0	-10.9	-72.4	-80.5	-74.3	-75.7	-77.0	-64.8	-72.1	-69.7	12.1	9.8	-0.5	2.0	2.7	3.7	-4.4	3.8	4.2	3.7	4.9	5.1	4.5	4.8	4.5	5.2	10.23	11.66	13.19	6.73	33.76	14.98	16.04	14.51						
10298	-11.1	-13.8	-11.1	-11.9	-11.9	-12.1	-11.7	-11.4	-72.5	-80.5	-66.3	-76.1	-73.3	-102.3	-76.9	-79.6	4.3	5.8	-3.6	-0.1	-0.2	1.1	-0.7	-0.2	4.5	3.7	4.8	4.4	4.3	4.6	3.6	4.5</														

Wilmot River watershed - Surface water samples

Site	$\delta^{18}\text{O}\text{-H}_2\text{O}$ (‰, VSMOW)								δD in H_2O (‰, VSMOW)								$\delta^{18}\text{O}$ in NO_3^- (‰, VSMOW)								$\delta^{15}\text{N}$ in NO_3^- (‰)								N in NO_3^- (mg/L)								
	1	2	3	4	5	6	7	8	1	2	3	4	5	6	7	8	1	2	3	4	5	6	7	8	1	2	3	4	5	6	7	8	1	2	3	4	5	6	7	8	
10283	-12.5				-11.0				-72.5				-75.4				12.7				3.4				5.1				4.2				7.03				7.48				
10284	-10.2	-10.0			-11.6	-11.0	-11.2	-12.6	-11.7	-70.9	-66.7		-92.8	-77.5	-83.0	-84.9	-75.3	13.3	9.6		2.4	4.1	3.5		3.9	3.9	3.8		4.5	5.3	4.2		4.0	7.28	6.36		5.56	7.64	5.96	4.71	5.70
10284									-11.1				-73.4											3.8									4.8								7.17
10285	-10.7	-12.1	-12.0	-11.3	-10.8	-13.9	-13.5	-12.1	-73.4	-67.3	-74.2	-74.1	-79.0	-90.8	-87.3	-79.9	14.2	9.4	0.2	2.1	3.8	4.3	0.1	3.7	5.3	3.8	4.6	4.5	5.5	3.9		4.5	5.58	5.69	5.85	5.12	6.51	2.72	2.84	3.40	
10285									-11.2				-70.3											4.6									4.7								6.92
10286	-10.9	-10.9	-11.7	-11.4	-10.4	-12.6	-13.0	-11.7	-68.7	-68.2	-74.0	-64.1	-74.3	-89.1	-88.8	-78.2	13.6	9.5	0.0	2.2	3.8	4.0	-0.3	4.0	4.7	2.9	4.2	4.6	5.2	3.8		4.5	6.42	6.24	6.53	5.63	7.10	3.59	3.25	3.81	
10286									-11.3				-74.4											4.0									4.9								7.47
10288	-10.4	-9.6	-11.7	-11.5	-10.5	-11.2	-13.2	-12.0	-73.2	-68.6	-72.3	-72.2	-71.5	-80.7	-88.8	-80.0	13.0	8.9	0.1	2.7	7.2	4.5	-0.4	4.1	3.4	3.5	4.1	4.6	5.6	4.4	3.8	4.6	6.12	7.68	6.28	5.47	6.74	4.44	2.66	2.82	
10288									-11.0				-72.9											4.3									4.8								7.14
10289	-10.7				-11.0								-74.8				13.9							3.4					4.9				7.39				2.10				

Wilmot River watershed - Precipitation samples

Site	$\delta^{18}\text{O}$ -H ₂ O (‰, VSMOW)								δD in H ₂ O (‰, VSMOW)							
	1	2	3	4	5	6	7	8	1	2	3	4	5	6	7	8
10292	-8.4	-6.2			-15.7				-46.7	-35.6						
10292					-14.5											
10307	-5.4	-5.9			-12.9	-9.2	-11.3	-12.4	-9.0	-40.2	-34.9					
10307					-26.0	-6.6		-14.3	-10.7							
10307					-7.8	-9.3		-11.3								
10307					-6.5											
10308	-6.7				-13.3			-14.1		-43.6	-37.3					
10308					-26.4											

Murray River watershed - Groundwater samples (Spring 2005)

Site	$\delta^{18}\text{O}$ -H ₂ O	δD in H ₂ O	$\delta^{18}\text{O}$ in NO ₃ ⁻	$\delta^{15}\text{N}$ in NO ₃ ⁻	N in NO ₃ ⁻
11889	-10.2	-63.6	-5.9	4.9	1.82
11890	-10.4	-66.6	-6.5	3.0	1.49
11891	-10.4	-63.2	-8.5	6.2	2.87
11892	-10.1	-62.7			0.78
11893	-10.5	-66.6	-6.4	3.2	1.85
11894	-10.1	-66.3			2.51
11895	-10.4	-69.7			6.78
11896	-10.1	-67.9			3.44
11897	-10.4	-67.4			0.31
11897	-10.3	-66.3			
11898	-10.3	-68.7			3.06

Other watersheds - Groundwater samples (Spring 2005)

Site	Area	$\delta^{18}\text{O}$ -H ₂ O	δD in H ₂ O	$\delta^{18}\text{O}$ in NO ₃ ⁻	$\delta^{15}\text{N}$ in NO ₃ ⁻	N in NO ₃ ⁻
11884	Buchanan	-10.4	-63.4			
11885	Suffolk	-10.3	-67.9	4.1	20.1	3.62
11886	Beach	-10.5	-70.4	-6.2	7.0	8.99
11887	New Perth	-10.4	-66.8	-3.2	6.6	2.77
11888	Brooklyn	-10.4	-69.2	-6.5	5.1	7.04

Harrington farm - Lysimetre samples

Site	$\delta^{18}\text{O}$ in NO ₃ ⁻ (‰, VSMOW)			$\delta^{15}\text{N}$ in NO ₃ ⁻ (‰)			N in NO ₃ ⁻ (mg/L)		
	6	7	8	6	7	8	6	7	8
12098			1.8			-0.8			0.16
12098			0.6			-0.5			0.23
12098			-0.6			-0.1			1.25
12098			-0.9						1.00
12098			1.0			3.4			0.77
12099			4.5			0.5			0.52
12099			4.2			0.8			0.78
12099			2.0			0.6			1.03
12099			2.9			1.2			1.31
12099			4.0			1.6			1.20
12100			4.3			-0.9	6.90		1.33
12100			3.9			-0.5			1.34
12100			7.2			-0.9			0.02
12100			7.1			0.3			3.95

Harrington farm - Tile drain samples

Site	$\delta^{18}\text{O}$ in NO ₃ ⁻ (‰, VSMOW)			$\delta^{15}\text{N}$ in NO ₃ ⁻ (‰)			N in NO ₃ ⁻ (mg/L)		
	6	7	8	6	7	8	6	7	8
12085	3.5		0.3	8.6		8.1	25.48		7.30
12085	3.1		0.6	8.6		7.1	47.99		9.41
12085	3		0.4	8.3		8.1	49.30		11.59
12085			1.5			8.8			34.44
12085			2.6			8.6			33.52
12085			1.7			8.3			31.77
12085			3.2			8.6			34.24
12085			2.2			8.5			28.04
12085			2.3			8.3			8.14
12087	0.3		5.3	7.3		16.4	17.00		3.94
12087	0.3		1.1	8		6.6	19.25		6.24
12087	0.9		0.4	6.7		7.9	8.35		10.61
12087			0.6			7			10.72
12087			-0.2			7.8			15.92
12087			-0.4			8.3			16.77
12087			1.3			7.3			
12087			0.5			7.6			14.54
12087			-0.2			7.9			16.89
12088	0.4		4	8.7		15.7	21.31		6.52
12088	0.4		3.7	8.7		13.8	21.95		7.86
12088	0		3.8	7.9		14.4	20.74		8.95
12088			-1.3			8.6			17.80
12088			-1.4			8.9			17.54
12088			-0.8			9.2			16.36
12088			1			9			16.92
12088			-0.4			9.2			17.02
12088			1.2			9.3			17.13

Site	$\delta^{18}\text{O}$ in NO ₃ ⁻ (‰, VSMOW)			$\delta^{15}\text{N}$ in NO ₃ ⁻ (‰)			N in NO ₃ ⁻ (mg/L)		
	6	7	8	6	7	8	6	7	8
12089	4.9		5.6	7.4		11.7	40.42		8.67
12089	4.7		4.4	7.3		8.5	38.92		
12089	5.1			7.1			41.76		11.74
12089			3			7			21.10
12089			2.3			6.9			20.85
12089			2.4			7.3			19.08
12089			0.6			6.9			20.54
12089			2.9			7.2			19.77
12089			3.4			7.4			18.60
12090	1.2		3.7	6.5		11.4	14.72		3.51
12090	0.8		1.6	6.8		6.9	15.75		9.77
12090	0.9		0.9	6		6.8	12.15		10.46
12090			-1.5			7.3			13.53
12090			-1.3			6.9			14.62
12090			-0.03			7.1			12.84
12090			0.4			6.6			12.64
12090			-0.6			6.4			13.84
12090			1.2			6.9			14.70
12091	-0.6		2.8	7.5		12.7	20.11		10.01
12091	-0.8		0.9	7.5		9	20.27		10.90
12091	-0.9			7.3			20.59		12.83
12091			-1.8			8.1			
12091			-1.8			7.9			9.57
12091						8			16.66
12091			3.7			7.8			17.18
12091			-1			7.8			15.52
12091			0			7.9			15.07

Site	$\delta^{18}\text{O}$ in NO_3^- (‰, VSMOW)			$\delta^{15}\text{N}$ in NO_3^- (‰)			N in NO_3^- (mg/L)		
	6	7	8	6	7	8	6	7	8
12093	4.2		5.9	6.5		12.5	37.39		7.76
12093	4.2		6.7	6.3		11.9	35.75		11.35
12093	3.5		6.9	5.8		12.5	35.56		13.27
12093			3.4			6.7			25.65
12093			2.5			6.7			26.34
12093			2.3			6.8			21.10
12093			0.6			6.7			22.73
12093			3.4			6.6			21.88
12093			7.1			6.8			22.52
12096	5.7		5.5	6.2		12.5	38.00		7.20
12096	5			6.1			40.20		9.68
12096	4.8		5.2	5.8		10.2	40.78		10.75
12096			4.3			6.4			15.77
12096			3.2			6.4			21.79
12096			4			6.4			20.26
12096			4.8			6.3			21.62
12096			5.1			6.3			21.41
12096			5			6.9			19.42
12097	2.3		4.5	7.2		11.1	36.32		5.51
12097	2.1		3.8	6.8		9.2	33.33		8.13
12097	2.2		3	7		8.7	41.00		9.08
12097			0.7			7			18.21
12097			2.2			7			21.11
12097			1.1			6.8			18.86
12097			2.8			7.5			22.47
12097			2.1			6.9			21.17
12097			2.2			6.8			17.32